



United States Nuclear Regulatory Commission

Protecting People and the Environment

NUREG/CR-7288

Volume 2

Evaluation of In-Service Radon Barriers over Uranium Mill Tailings Disposal Facilities

Appendices

AVAILABILITY OF REFERENCE MATERIALS IN NRC PUBLICATIONS

NRC Reference Material

As of November 1999, you may electronically access NUREG-series publications and other NRC records at the NRC's Library at www.nrc.gov/reading-rm.html. Publicly released records include, to name a few, NUREG-series publications; *Federal Register* notices; applicant, licensee, and vendor documents and correspondence; NRC correspondence and internal memoranda; bulletins and information notices; inspection and investigative reports; licensee event reports; and Commission papers and their attachments.

NRC publications in the NUREG series, NRC regulations, and Title 10, "Energy," in the *Code of Federal Regulations* may also be purchased from one of these two sources:

1. The Superintendent of Documents

U.S. Government Publishing Office
Washington, DC 20402-0001
Internet: www.bookstore.gpo.gov
Telephone: (202) 512-1800
Fax: (202) 512-2104

2. The National Technical Information Service

5301 Shawnee Road
Alexandria, VA 22312-0002
Internet: www.ntis.gov
1-800-553-6847 or, locally, (703) 605-6000

A single copy of each NRC draft report for comment is available free, to the extent of supply, upon written request as follows:

Address: **U.S. Nuclear Regulatory Commission**
Office of Administration
Digital Communications and Administrative
Services Branch
Washington, DC 20555-0001
E-mail: distribution.resource@nrc.gov
Facsimile: (301) 415-2289

Some publications in the NUREG series that are posted at the NRC's Web site address www.nrc.gov/reading-rm/doc-collections/nuregs are updated periodically and may differ from the last printed version. Although references to material found on a Web site bear the date the material was accessed, the material available on the date cited may subsequently be removed from the site.

Non-NRC Reference Material

Documents available from public and special technical libraries include all open literature items, such as books, journal articles, transactions, *Federal Register* notices, Federal and State legislation, and congressional reports. Such documents as theses, dissertations, foreign reports and translations, and non-NRC conference proceedings may be purchased from their sponsoring organization.

Copies of industry codes and standards used in a substantive manner in the NRC regulatory process are maintained at—

The NRC Technical Library

Two White Flint North
11545 Rockville Pike
Rockville, MD 20852-2738

These standards are available in the library for reference use by the public. Codes and standards are usually copyrighted and may be purchased from the originating organization or, if they are American National Standards, from—

American National Standards Institute

11 West 42nd Street
New York, NY 10036-8002
Internet: www.ansi.org
(212) 642-4900

Legally binding regulatory requirements are stated only in laws; NRC regulations; licenses, including technical specifications; or orders, not in NUREG-series publications. The views expressed in contractor prepared publications in this series are not necessarily those of the NRC.

The NUREG series comprises (1) technical and administrative reports and books prepared by the staff (NUREG-XXXX) or agency contractors (NUREG/CR-XXXX), (2) proceedings of conferences (NUREG/CP-XXXX), (3) reports resulting from international agreements (NUREG/IA-XXXX), (4) brochures (NUREG/BR-XXXX), and (5) compilations of legal decisions and orders of the Commission and the Atomic and Safety Licensing Boards and of Directors' decisions under Section 2.206 of the NRC's regulations (NUREG-0750).

DISCLAIMER: This report was prepared as an account of work sponsored by an agency of the U.S. Government. Neither the U.S. Government nor any agency thereof, nor any employee, makes any warranty, expressed or implied, or assumes any legal liability or responsibility for any third party's use, or the results of such use, of any information, apparatus, product, or process disclosed in this publication, or represents that its use by such third party would not infringe privately owned rights.

Evaluation of In-Service Radon Barriers over Uranium Mill Tailings Disposal Facilities

Appendices

Manuscript Completed: November 2021

Date Published: March 2022

Prepared by:

M. Williams²

M. Fuhrmann³

M. Stefani¹

A. Michaud¹

W. Likos¹

C. Benson¹

W. Waugh²

¹Geological Engineering, University of Wisconsin-Madison

1415 Engineering Drive

Madison, WI 53706 USA

²RSI EnTech, LLC

Grand Junction CO 81503

³U.S. Nuclear Regulatory Commission

Mark Fuhrmann, NRC Project Manager

Office of Nuclear Regulatory Research

ABSTRACT

Earthen final covers over uranium mill tailings and associated wastes were investigated at four sites that had been in service for approximately 20 years: Falls City in Texas, Bluewater in New Mexico, Shirley Basin South in Wyoming, and Lakeview in Oregon. Test pits were excavated, radon fluxes were measured, soil morphological observations made, and samples were collected to determine saturated hydraulic conductivity, soil water characteristic curves, Pb-210 concentrations, and related properties. Similar procedures were conducted at natural analogue sites – nearby locations of undisturbed natural ground used as an indicator of the very long-term state of the covers. Saturated hydraulic conductivity of the Rn barriers at three of the four sites typically fell within the range recommended to represent long-term in-service conditions (1.0×10^{-7} to 5.0×10^{-6} m/s), regardless of depth or thickness of the cover or radon barrier. These saturated hydraulic conductivities are 2 to 3 orders of magnitude higher than the common 1.0×10^{-9} m/s design criterion established for low-conductivity Rn barriers. One Rn barrier was an exception, with some hydraulic conductivities as low as 10^{-11} m/s. A slight increase over the as-built Rn flux was evident for some of the barriers. However, the intentionally biased sampling procedure and differences between the methods used in this study for measuring Rn flux relative to those used in the as-built condition precluded making inferences regarding sitewide in-service Rn fluxes. Rn fluxes were higher in regions where woody vegetation (mesquite, salt bush, and bitterbrush) or aggressive insects had established on the cover, suggesting that the vegetation and insects affected the performance of the barrier in these locations. These higher fluxes are attributed to soil structure induced by root activity and insect burrowing in the Rn barrier, as well as higher Rn diffusion coefficients associated with lower water saturation in areas influenced by root water uptake. A method to use Pb-210 concentration profiles to quantify long-term (decades) Rn-222 fluxes was developed. Soil morphology within the covers is evolving toward a more structured condition, and in some places appears to be approaching a state comparable to the natural analogues.

TABLE OF CONTENTS

ABSTRACT	iii
LIST OF FIGURES.....	ix
LIST OF TABLES	xv
EXECUTIVE SUMMARY	xvii
ACKNOWLEDGMENTS	xxi
ABBREVIATIONS AND ACRONYMS.....	xxiii
1 INTRODUCTION	1-1
1.1 Regulations.....	1-1
1.2 Overview of the Radon Barriers Project	1-2
1.2.1 Drivers and Objectives	1-2
1.2.2 Radon Barriers Project Sites.....	1-3
1.3 References.....	1-4
2 BACKGROUND INFORMATION, STUDY SITE SELECTION, AND PLANT ECOLOGY.....	2-1
2.1 Introduction.....	2-1
2.2 Background	2-1
2.2.1 UMTRCA Disposal Sites and Engineered Covers	2-1
2.2.2 Long-Term Surveillance and Maintenance Activities	2-3
2.2.3 Site Inspections.....	2-4
2.2.4 Study Site Selection Objectives and Bias	2-5
2.3 Disposal Site Selection	2-5
2.3.1 Phase I Methods: Initial Ranking.....	2-5
2.3.2 Phase II Methods: Contrasting Designs and Environments.....	2-6
2.3.3 Attributes of Selected Sites	2-6
2.4 Selection of Test Conditions	2-16
2.4.1 Selection Methods for Test Pits on Covers	2-16
2.4.2 Selection Methods for Analogue Sites	2-17
2.4.3 Bluewater, New Mexico.....	2-21
2.4.4 Falls City, Texas.....	2-23
2.4.5 Shirley Basin South, Wyoming.....	2-24
2.4.6 Lakeview, Oregon	2-26
2.5 Plant Ecology of Disposal Cells and Analogue Sites.....	2-28
2.5.1 Methods	2-28
2.5.2 Results and Discussion.....	2-29
2.6 References	2-33
3 HYDRAULIC PROPERTIES OF BARRIER MATERIALS.....	3-1
3.1 Introduction.....	3-1

3.2 Methods.....	3-1
3.2.1 Block Sampling	3-1
3.2.2 Hydraulic Properties	3-4
3.2.3 Other Properties	3-5
3.3 Results.....	3-5
3.3.1 Saturated Hydraulic Conductivity	3-6
3.3.2 Soil Water Characteristic Curve	3-11
3.4 Summary.....	3-12
3.5 References.....	3-13
4 RADON FLUX	4-1
4.1 Introduction.....	4-1
4.2 Methods	4-1
4.2.1 Site Selection and Survey Design.....	4-2
4.2.2 Field Test Pits	4-2
4.2.3 Surface Radon Flux Measurements (“Top” Flux).....	4-3
4.2.4 Radon Flux Measurements from the Waste (“Bottom” Flux).....	4-4
4.2.5 Flux Measurement and Uncertainty	4-5
4.3 Background Fluxes.....	4-6
4.3.1 Falls City	4-6
4.3.2 Bluewater	4-7
4.3.3 Shirley Basin South.....	4-7
4.3.4 Lakeview	4-7
4.4 Measured Radon Fluxes	4-8
4.4.1 Falls City, TX.....	4-8
4.4.2 Bluewater, NM.....	4-10
4.4.3 Shirley Basin South, WY (Petrotomics).....	4-11
4.4.4 Lakeview, OR.....	4-13
4.5 Radon Flux Discussion	4-14
4.5.1 Radon Flux Overview.....	4-14
4.5.2 Current Fluxes vs. As-built Radon Fluxes.....	4-14
4.5.3 Effects of Surface Features.....	4-21
4.6 Diffusion Modeling	4-28
4.6.1 RAECOM 2-Flux Calculations.....	4-28
4.6.2 Empirical Correlations to Estimate D	4-28
4.6.3 Comparison of Diffusion Coefficients by Several Methods	4-30
4.6.4 Site Specific Diffusion Coefficients and Rn Travel Times	4-31
4.6.5 Laboratory Diffusion Coefficients and Comparison to Field D	4-38
4.6.6 Comparison of Moisture Saturation Flux Correlation to Field Measurements of D	4-40
4.7 Summary and Conclusions	4-42
4.8 References	4-44
5 LEAD-210 PROFILES IN RADON BARRIERS, INDICATORS OF LONG- TERM RADON-222 TRANSPORT	5-1
5.1 Introduction.....	5-1
5.2 Radon Decay and Progeny	5-2
5.3 Methods	5-3

5.4	Results	5-4
5.4.1	Falls City	5-4
5.4.2	Bluewater	5-8
5.4.3	Shirley Basin South	5-11
5.4.4	Lakeview	5-15
5.5	Discussion	5-18
5.5.1	Modeling.....	5-19
5.5.2	Complexities in Radon Transport.....	5-21
5.5.3	Relationship Between Rn Flux at the Barrier Top and Excess Pb-210.....	5-24
5.6	Summary and Application.....	5-26
5.7	References	5-27
6	SOIL MORPHOLOGY OF FOUR IN-SERVICE UMTRCA WASTE COVERS AND CORRESPONDING NATURAL ANALOGUES	6-1
6.1	Introduction.....	6-1
6.2	Soil-Forming Factors and Pedogenic Process in Waste Covers	6-1
6.3	Methods.....	6-3
6.3.1	Soil Morphological Characterization.....	6-4
6.3.2	Laboratory Analysis.....	6-6
6.4	Field Observations and Results.....	6-6
6.4.1	Falls City, Texas.....	6-9
6.4.2	Bluewater, New Mexico.....	6-15
6.4.3	Shirley Basin South, Wyoming.....	6-23
6.4.4	Lakeview, Oregon	6-28
6.4.5	Physical and Chemical Characteristics of UMTRCA Covers and Analogues.....	6-36
6.4.6	Reduction and Oxidation.....	6-42
6.5	Conceptual Models of Decadal Cover Evolution and Soil Morphology	6-43
6.6	Section Summary and Conclusions	6-50
6.1	References	6-52
7	DETERMINATION OF LONG-TERM PERFORMANCE CONDITION OF FOUR WASTE COVERS THROUGH SOIL MORPHOLOGICAL COMPARISON TO NATURAL ANALOGUES	7-1
7.1	Introduction.....	7-1
7.2	Methods.....	7-1
7.2.1	Radon Diffusion Coefficients.....	7-2
7.2.2	Saturated Hydraulic Conductivity	7-2
7.2.3	Soil Morphological Development Score	7-3
7.3	Results and Discussion	7-4
7.3.1	Comparison of tSMDS Between Sites.....	7-4
7.3.2	Soil Morphology, Radon Diffusion Coefficients, and Radon Travel-Time	7-10
7.3.3	Saturated Hydraulic Conductivity and Soil Morphology	7-16
7.3.4	Saturated Hydraulic Conductivity and Depth from Ground Surface.....	7-19
7.4	Summary and Implications	7-22
7.5	References	7-23
8	SUMMARY AND CONCLUSIONS	8-25

APPENDIX A DESCRIPTIONS AND CRITERIA OF SITE ATTRIBUTES FOR PHASE I RANKING OF SITES..... A-1

APPENDIX B PHASE II SELECTION OF SITES B-1

APPENDIX C COVER DESIGNS, CLIMATES, AND ECOLOGIES OF SITES CONSIDERED FOR PHASE II OF THE STUDY C-1

APPENDIX D HISTORIES OF DISPOSAL SITES SELECTED FOR STUDY D-1

APPENDIX E VEGETATION SUMMARY TABLESE-1

APPENDIX F METHODS TO MEASURE RADON FLUX FROM EARTHEN RADON BARRIERS OVER URANIUM MILL TAILINGS AND IMPACT OF VARIABLES..... F-1

APPENDIX G EFFECT OF CHAMBER SIZE ON RADON FLUX MEASUREMENTG-1

APPENDIX H FACTORS OF SOIL DEVELOPMENT AND PEDOGENIC PROCESS IN ENGINEERED SURFACE COVERS FOR WASTE CONTAINMENT H-1

APPENDIX I TABLES OF ROOTING CHARACTERISTICS AT UMTRCA SITES..... I-1

APPENDIX J MORPHOLOGICAL DEVELOPMENT SCORING SYSTEM VALUES J-1

LIST OF FIGURES

Figure 2-1	Map of Current and Anticipated Title I and Title II UMTRCA Sites.....	2-2
Figure 2-2	Cross Sections of Engineered Cover Designs at the Four Sites Selected for Study	2-10
Figure 2-3	Annual and Monthly Temperature and Precipitation Data for the Four Study Sites	2-12
Figure 2-4	Test Pit Locations on the Disposal Cells and at Analogue Sites for Bluewater, New Mexico	2-22
Figure 2-5	Test Pit Locations on the Disposal Cell Top Slope and Side Slopes and at an Analogue Site for Falls City, Texas.....	2-24
Figure 2-6	Test Pit Locations on the Disposal Cell Top-Deck Terraces, Interior Slope, and at an Analogue Site for Shirley Basin South, Wyoming.....	2-25
Figure 2-7	Test Pit Locations on the Disposal Cell Top-Deck, Side Slope, and at Analogue Sites for Lakeview, Oregon.....	2-27
Figure 2-8	Estimated Percent Foliar Cover by Seral Stage for Plant Communities.....	2-30
Figure 3-1	Cover Profiles from Which Block Samples were Collected: (a) Falls City, Texas and (b) Bluewater, New Mexico.....	3-2
Figure 3-2	Cover Profiles from Which Block Samples were Collected: (c) Shirley Basin, Wyoming and (d) Lakeview, Oregon	3-3
Figure 3-3	Block Samples from Radon Barriers to Characterize Hydraulic Properties.....	3-4
Figure 3-4	Soil Water Characteristic Curve for Radon Barrier at the Shirley Basin Site	3-5
Figure 3-5	Saturated Hydraulic Conductivity of Block Samples Removed from Radon Barriers and Analogue Sites.....	3-10
Figure 3-6	Soil Water Characteristic Curve Parameters for Block Samples Removed from the Bluewater and Shirley Basin Sites	3-11
Figure 3-7	Relationships Between (a) α Parameter and Saturated Hydraulic Conductivity and (b) n and α Parameter for Block Samples.....	3-12
Figure 4-1	Field Installation of Eight Flux Chambers of Four Sizes on the Top of the Radon Barrier at Shirley Basin South.....	4-4
Figure 4-2	Schematic of a “Bottom” Flux Measurement Taken Directly on the Tailings Underlying the Rn Barrier Layer.....	4-5
Figure 4-3	A Small Flux Chamber Installed Directly on the Tailings with a Rad7 Instrument to Obtain a “Bottom Flux” Measurement	4-6
Figure 4-4	Radon Fluxes Measured at the Falls City Site	4-9
Figure 4-5	Radon Fluxes Measured at the Bluewater Site	4-11
Figure 4-6	Radon Fluxes Measured at the Shirley Basin South Site.....	4-12
Figure 4-7	Radon Fluxes Measured at the Lakeview Site.....	4-13

Figure 4-8	All Rn Flux Measurements from the Tops of Rn Barriers at the Four Sites.....	4-16
Figure 4-9	Frequency of Falls City Radon Fluxes for As-Built and In-Service Conditions.....	4-17
Figure 4-10	Comparison of In-Service Fluxes to As-Built Fluxes from Near-by Measurement Locations	4-18
Figure 4-11	Frequency of Bluewater Main Tailings Pile Radon Fluxes for As-built and In-service Conditions.....	4-19
Figure 4-12	Comparison of Bluewater In-service Fluxes to As-built Fluxes from Near-by Measurement Locations	4-19
Figure 4-13	Frequency of Flux Values at Shirley Basin South (Petrotomics) Comparing As-built to 2016/2017 In-service Data.....	4-20
Figure 4-14	Comparison of In-Service Fluxes to As-Built Fluxes from Near-by Measurement Locations	4-21
Figure 4-15	Fluxes Measured from Test Pit Pairs Showing Results from Pits Containing Features (Numbered) that May Influence Flux and Their Controls	4-24
Figure 4-16	Small Roots Grow in Thin Structural Cracks in the Radon Barrier at Falls City TP-4	4-25
Figure 4-17	Root Structure in 70 mm Diameter Shelby Tube Sample from Bluewater Test Pit 5.....	4-26
Figure 4-18	Large Root in the Radon Barrier in a Shelby Tube Sample from Bluewater Test Pit 5 Where Fluxes were High and Exhibited a Wide Range	4-27
Figure 4-19	Schematic Showing the Approach to Determining Rn Diffusion Coefficients in Rn Barriers.....	4-29
Figure 4-20	Diffusion Coefficients Calculated in Several Ways for Test Pits at the Falls City Site.....	4-31
Figure 4-21	Schematic of Apparatus for Lab Measurements of Rn Diffusion Coefficients of Samples Taken from Shelby Tubes.....	4-38
Figure 4-22	Comparison of a Curve Calculated from Eq. 6 with Samples Taken from the Shirley Basin South Site	4-40
Figure 4-23	Rn Diffusion Coefficients Determined from Field Flux Measurements at All Four Sites Compared to an Empirical Relationship Between Moisture Saturation and Flux from Rogers and Nielson, 1991.....	4-42
Figure 5-1	Decay chain for U-238. (U.S. EPA).....	5-2
Figure 5-2	Pb-210 Sample Locations (Circles) and Concentrations within the Rn Barrier at Pit 2 at Falls City.....	5-5
Figure 5-3	Pb-210 Sample Locations (Circles) and Concentrations Within the Rn Barrier at Pit 3 at Falls City.....	5-6
Figure 5-4	Pb-210 Sample Locations (Circles) and Concentrations Within the Rn Barrier at Pit 6 at Falls City.....	5-7

Figure 5-5	Rn Fluxes Measured on the Top of the Rn Barrier at Falls City, for Pits where Pb-210 Samples were Taken	5-7
Figure 5-6	Pb-210 Sample Locations (Circles) and Concentrations Within the Rn Barrier at Pit 4 at Bluewater.	5-9
Figure 5-7	Pb-210 Sample Locations (Circles) and Concentrations Within the Rn Barrier at Pit 5 at Bluewater.	5-10
Figure 5-8	Rn Fluxes from the Top of the Rn Barrier at Bluewater. The 3 Background Fluxes Are All Below 0.005 Bq/m ² /s.....	5-10
Figure 5-9	Pb-210 Sample Locations (Circles) and Concentrations Within the Rn Barrier at Pit 2 at Shirley Basin South.	5-13
Figure 5-10	Pb-210 Sample Locations (Circles) and Concentrations Within the Rn Barrier at Pit 3 at Shirley Basin South.	5-13
Figure 5-11	Pb-210 Sample Locations (Circles) and Concentrations Within the Rn Barrier at Pit 5 at Shirley Basin South.	5-14
Figure 5-12	Pb-210 Sample Locations (Circles) and Concentrations Within the Rn Barrier at Pit 6 at a Rip-Rap Covered Slope at Shirley Basin South.	5-14
Figure 5-13	Radon Fluxes Measured at the Top of the Radon Barrier at Pits Where Pb-210 Was Measured.....	5-15
Figure 5-14	Pb-210 Sample Locations (Circles) and Concentrations Within the Rn Barrier at Pit 12 at Lakeview.	5-17
Figure 5-15	Measured and Modeled Pb-210 Profiles from Pit 3 at the Shirley Basin South Site.....	5-20
Figure 5-16	Pb-210 Measured at Lakeview and a Diffusion Model Using D = 6.5 x 10 ⁻⁸ m ² /s Which Was Calculated from Measured Fluxes at Pit 12.	5-21
Figure 5-17	Pb-210 Profile at the Rock Slope Pit 6 at Shirley Basin South Showing Zones Discussed in Text.	5-23
Figure 5-18	Relationship Between Excess Measured Pb-210 Concentrations in the Upper Part of the Barrier vs Rn Fluxes.....	5-25
Figure 6-1	Site Factors, Soil Process, and Morphological Development in Compacted Mineral Barriers ¹	6-3
Figure 6-2	Soil Structure of UMTRCA Covers and Natural Analogues Under Variable Surface Conditions	6-7
Figure 6-3	Root Structure of UMTRCA Covers and Natural Analogues Under Variable Surface Conditions	6-8
Figure 6-4	Representative Surface and Vegetation Condition on the Disposal Cell at Falls City, Texas.....	6-9
Figure 6-5	Remnant Soil Structure in the Radon Barrier at Falls City, Texas.....	6-10
Figure 6-6	Soil Profile Sections on the Disposal Cell at Falls City, Texas.....	6-11
Figure 6-7	Honey Mesquite Root Benching and Gleying Along the Top Boundary of the Radon Barrier at Falls City, Texas.....	6-12

Figure 6-8	Honey Mesquite Soil Morphology Impact Gradient (TP-1), Falls City, Texas.....	6-13
Figure 6-9	Natural Analogue Soil Profile at the Falls City Site.....	6-14
Figure 6-10	Surface and Vegetation Condition on the Main Disposal Cell at Bluewater, New Mexico.....	6-16
Figure 6-11	Soil Profile Sections on the Main Disposal Cell at Bluewater, New Mexico.....	6-17
Figure 6-12	Bioturbation by Harvester Ants, Bluewater, New Mexico Main Disposal Cell.....	6-18
Figure 6-13	Rooting Along Fractures Under Saltbush at the Bluewater, New Mexico, Disposal Cell.....	6-19
Figure 6-14	Fourwing Saltbush Soil Morphology Impact Gradient (TP-5), Bluewater, New Mexico.....	6-20
Figure 6-15	Squirreltail Grass Soil Morphology Impact Gradient (TP-2), Bluewater, New Mexico.....	6-21
Figure 6-16	Natural Analogue Soil Profiles at the Bluewater Site.....	6-22
Figure 6-17	Surface and Vegetation Condition on the Disposal Cell at Shirley Basin South, Wyoming.....	6-24
Figure 6-18	Soil Profile Sections on the Disposal Cell at Shirley Basin South, Wyoming.....	6-25
Figure 6-19	Pocket Gopher Mixing of Rock Riprap and Gravel Layers, Shirley Basin South, Wyoming.....	6-26
Figure 6-20	Natural Analogue Soil Profile at the Shirley Basin South Site.....	6-27
Figure 6-21	Representative Surface and Vegetation Condition on the Disposal Cell at Lakeview, Oregon.....	6-29
Figure 6-22	Soil Profile Sections on the Disposal Cell at Lakeview, Oregon.....	6-30
Figure 6-23	Great Basin Pocket Mouse Burrow Perched Above Rock Riprap (DC-5), Lakeview, Oregon.....	6-31
Figure 6-24	Rabbitbrush Soil Morphology Impact Gradient (DC-12), Lakeview, Oregon.....	6-32
Figure 6-25	Bitterbrush Soil Morphology Impact Gradient (DC-2), Lakeview, Oregon.....	6-34
Figure 6-26	Natural Analogue Soil Profile at the Lakeview Site.....	6-35
Figure 6-27	Soil Texture Found in Four UMTRCA Radon Barriers and Analogues.....	6-37
Figure 6-28	Clay Mineralogy Found in Four UMTRCA Radon Barriers and Analogues.....	6-37
Figure 6-29	Distribution of Soil Organic Matter in Four UMTRCA Covers and Analogues.....	6-38
Figure 6-30	Relationship Between Soil Organic Matter Percent and Soil Structural Unit Size.....	6-39
Figure 6-31	Distribution of pH in Four UMTRCA Covers and Analogues.....	6-40
Figure 6-32	Distribution of Soluble Salts (EC) in Four UMTRCA Covers and Analogues.....	6-41

Figure 6-33	Distribution of Calcium Carbonate (eq.%) in Two UMTRCA Covers and Analogues	6-42
Figure 6-34	Gleying in a Clay Lens Located Above the Radon Barrier at Shirley Basin South, Wyoming	6-43
Figure 6-35	Shirley Basin South, Wyoming, Cover Morphology and Soil Development Over Time.....	6-47
Figure 6-36	Falls City, Texas, Cover Morphology and Soil Development Over Time.....	6-48
Figure 6-37	Bluewater, New Mexico, Cover Morphology and Soil Development Over Time	6-49
Figure 7-1	ρ SMDS of the Radon Barrier in Each Test Pit at Each Site and for Horizons at Similar Depth in Natural Analogue Profiles	7-6
Figure 7-2	Radon Diffusion Coefficients and Radon Barrier tSMDS	7-11
Figure 7-3	Mean Travel Time (Radon Half-Lives) and tSMDS	7-12
Figure 7-4	Radon Diffusion, Moisture Saturation, and Radon Barrier ρ SMDS at Each Site	7-15
Figure 7-5	Saturated Hydraulic Conductivity and pSMDS	7-17
Figure 7-6	Relationship Between Depth from Ground Surface and Hydraulic Conductivity	7-20
Figure 7-7	Relationship Between Depth from Ground Surface and Hydraulic Conductivity at Each Site	7-21

LIST OF TABLES

Table 1-1	Radon Barriers Project Research Sites.....	1-3
Table 2-1	Attributes of UMTRCA Title I and Title II Sites Considered for Field Evaluation of Radon Flux from an In-Service Cover.	2-8
Table 2-2	Contrasting Cover Designs, Climates, and Ecologies of Uranium Mill Tailings Sites Selected for the Study.....	2-9
Table 2-3	Taxonomic Classification for Radon Barrier Borrow Soils at Disposal Sites Selected for Study.	2-13
Table 2-4	Soil Moisture Regimes ¹	2-13
Table 2-5	Soil Temperature Regimes ¹	2-14
Table 2-6	Potential Natural Vegetation Types and Associated Common Plants at Disposal Sites Selected for Study.	2-15
Table 2-7	Rooting Depths of Woody Plants Growing on Cell Covers Selected for Study.	2-16
Table 2-8	Test Conditions and Rationale for Selecting Test Pit Locations on Covers.	2-18
Table 2-9	Test Conditions and Rationale for Selecting Analogue Sites and Test Pit Locations.	2-19
Table 2-10	Summary of Soil-Forming Factors at Four Engineered Covers for Waste Containment and Natural Analogues	2-20
Table 2-11	Disposal Cell Cover Conditions at Test Locations, Bluewater, New Mexico.	2-22
Table 2-12	Disposal Cell Cover Conditions at Selected Test Locations, Falls City, Texas.....	2-23
Table 2-13	Disposal Cell Cover Conditions at Selected Test Locations, Shirley Basin South, Wyoming.	2-26
Table 2-14	Conditions for Test Pits on the Disposal Cell Cover at Lakeview, Oregon.....	2-27
Table 3-1	Summary of Physical Properties and Saturated Hydraulic Conductivities for Bluewater and Falls City. Sampling Location Corresponds to Fig. 3-1	3-7
Table 3-2	Summary of Physical Properties and Saturated Hydraulic Conductivities for Shirley Basin and Lakeview. Sampling Location Corresponds to Fig. 3-2	3-8
Table 3-3	Ranges of Index Properties of Radon Barriers and Enalogues at Each Site	3-9
Table 3-4	Ranges of Primary Minerals in Radon Barriers and Analogues at Each Site	3-9
Table 3-5	Summary of van Genuchten Parameters for SWCCs	3-9
Table 4-2	Ra-226 Concentration in Barrier Material and Fluxes Calculated from Ra-226 for Shirley Basin South.....	4-8
Table 4-3	Summary of Test Pit Characteristics at Falls City, TX Field Site.....	4-8

Table 4-4	Summary of Test Pit Characteristics at Bluewater Field Site.	4-10
Table 4-5	Summary of Test Pit Characteristics at Shirley Basin South Field Site.	4-12
Table 4-6	Summary of Test Pit Characteristics at the Lakeview Field Site.	4-14
Table 4-7	Description of Test Pit Pairs	4-22
Table 4-8	Summary of Test Pit Data	4-23
Table 4-9	Falls City: Rn Diffusion Coefficients and Transport Times.	4-33
Table 4-10	Bluewater: Rn Diffusion Coefficients and Transport Times.	4-34
Table 4-11	Shirley Basin South: Rn Diffusion Coefficients and Transport Times.	4-36
Table 4-12	Lakeview: Rn Diffusion Coefficients and Transport Times.	4-37
Table 4-13	Comparison of D for Samples from the Shirley Basin South Site.	4-39
Table 5-1	Falls City Samples	5-6
Table 5-2	Bluewater Samples	5-11
Table 5-3	Shirley Basin South Samples	5-16
Table 5-4	Lakeview Samples	5-17
Table 5-5	Pb-210 as an Indicator of Top Flux	5-26
Table 6-1	Soil Structure and Size Classifications	6-5
Table 6-2	Soil Grade Classifications	6-5
Table 6-3	Root Size	6-5
Table 6-4	Root Quantity	6-5
Table 6-5	Rupture Resistance	6-6
Table 6-6	Summary of Soil Condition at 1250–1500 mm from Ground Surface	6-15
Table 6-7	Summary of Soil Condition at 500–750 mm from Ground Surface	6-23
Table 6-8	Summary of Soil Condition at 1250–1500 mm from Ground Surface	6-28
Table 6-9	Summary of Soil Condition at 750–1000 mm from Ground Surface	6-36
Table 6-10	Summary of Soil-Forming Factors at Four Engineered Covers for Waste Containment and Natural Analogues	6-45
Table 6-11	Summary of Pedogenic Process in Four Radon Barriers in the UMTRCA Program	6-46
Table 7-1	Points for Soil Morphological Classes (Lin et al. 1999a)	7-5
Table 7-2	Relative Contribution of Individual Soil Morphological Features to ι SMDS	7-7
Table 7-3	Summary of Radon Diffusion Coefficients and Radon Barrier ι SMDS	7-13
Table 7-4	Summary of Saturated Hydraulic Conductivity and Block Sample ρ SMDS	7-18

EXECUTIVE SUMMARY

Compacted soil materials used to build covers over waste disposal cells do not retain 'as built' properties after being in service for time periods as short as 9 years. This observation resulted from an earlier NRC research project on engineered covers published in December 2011 as NUREG/CR-7028, "Engineered Covers for Waste Containment: Changes in Engineering Properties and Implications for Long-Term Performance Assessment." That report was limited in scope and did not conduct any radon (Rn) studies at uranium mill tailing disposal sites. The NRC subsequently formed the NRC Engineered Covers Technical Group (ECTG) to discuss and review the implications of the findings in NUREG/CR-7028. Following their recommendations, the current project expands upon this earlier research and investigates changes in cover soil properties and on Rn and water transport through engineered covers at uranium mill tailing disposal sites.

A study was conducted to evaluate changes in properties of radon (Rn) barriers in earthen final covers at four disposal facilities for uranium mill tailings that had been in service for approximately 20 yr: Falls City in Texas, Bluewater in New Mexico, Shirley Basin South in Wyoming, and Lakeview in Oregon. Rn barriers are engineered fine-textured earthen barriers placed within final covers that are used to control egress of gaseous Rn emitted from the waste and ingress of water from precipitation. The study was conducted to evaluate how abiotic and biotic processes (e.g., wet-dry cycling, freeze-thaw cycling, biota intrusion) occurring while the final covers were in service affected the saturated hydraulic conductivity and gaseous diffusivity of the Rn barriers, and how changes in these engineering properties are related to the development of soil structure. The anticipated very long-term naturalized condition was assessed by studying a natural analogue nearby each facility. Descriptions of the sites that were studied are in Section 2.

Test pits were excavated at each site to collect samples and to measure Rn flux. Overburden and protective layers above the Rn barrier were removed to expose the surface of the Rn barrier. Rn flux measurements were made on the surface of the Rn barrier using flux chambers, with the Rn concentration buildup curves measured with an electronic radon monitor (ERM). After the flux measurements on the Rn barrier were completed, samples were collected from the Rn barrier and soil morphological surveys were conducted. Large diameter (400 mm) block samples were collected for saturated hydraulic conductivity and soil water characteristic curve measurements. When possible, samples were collected in a vertical profile to capture conditions existing as a function of depth. Additional samples were collected to determine moisture content, dry unit weight, index properties, and root characteristics. After sampling, excavation into the Rn barrier continued until the surface of the tailings was exposed. Rn flux measurements were made directly on the surface of the tailings for comparison with fluxes measured on the surface of the Rn barrier. At least five test pits were excavated at each site, and as many as eight flux measurements were made in each test pit. After sampling and testing, the final cover was restored to the specifications employed at the time of construction.

Test pits were located in areas where greater change likely occurred to the Rn barrier while in service (e.g., in areas with woody vegetation or insect burrowing), which biased the findings. In some cases, pairs of nearby test pits were excavated to compare areas likely to have greater impact (e.g., areas with woody vegetation) to areas that with less impact (e.g., areas with mowed grass cover). A systematic survey was not conducted to determine a site-wide average Rn flux. Details on site selection, criteria used to select locations of the test pits, and the

conditions that were tested are in Section 2. The inferences made in this report reflect the biased sampling methodology, and may not reflect site-wide conditions.

Hydraulic properties of the Rn barriers are reported in Section 3. Saturated hydraulic conductivities of the Rn barriers ranged from 3.9×10^{-6} to 1.2×10^{-9} m/s for the Falls City site, 4.7×10^{-6} to 1.5×10^{-8} m/s for the Bluewater site, 1.1×10^{-7} to 2.4×10^{-11} m/s for the Shirley Basin site, and 3.2×10^{-6} to 1.1×10^{-7} m/s for the Lakeview site. A limited number of SWCCs were measured. For those that were measured, the saturated water content ranged from 0.29 to 0.50, van Genuchten's α ranged from 0.0018 to 0.30 kPa⁻¹, and van Genuchten's n ranged from 1.14 to 1.36. The saturated hydraulic conductivities for all but the Shirley Basin site fall within the range of 1×10^{-7} to 5×10^{-6} m/s recommended in NUREG/CR-7028 for use in performance assessments. The hydraulic conductivities at Shirley Basin are approximately one to four orders of magnitude lower than the lower bound recommended in NUREG CR-7028, with some approaching 10^{-11} m/s, which is comparable to sodium bentonite. For all sites, the saturated hydraulic conductivities generally are similar regardless of depth of sampling or type of surface (vegetated or rock armored). Saturated hydraulic conductivities of samples from the analogue sites were comparable to or modestly higher than saturated hydraulic conductivities of the blocks removed from each site, and generally were near the upper bound recommended in NUREG CR-7028. The analogue at Shirley Basin was an exception, with saturated hydraulic conductivities ranging from 1.4×10^{-9} to 9.8×10^{-9} m/s.

The Rn-222 fluxes and associated diffusion coefficients computed from the data are in Section 4. Rn-222 fluxes on the surface of the Rn barriers ranged from 0.005 to 1.28 Bq/m²/s at the Falls City site, 0.002 to 1.26 Bq/m²/s at the Bluewater site, 0.004 to 0.226 Bq/m²/s at the Shirley Basin site, and 0.002 to 0.040 Bq/m²/s at the Lakeview site. The fluxes at Shirley Basin were low despite very high fluxes from the surface of the underlying tailings (up to 397 Bq/m²-s). Fluxes from the surface of the Rn barrier at the Lakeview site were much lower than at the other sites because the underlying waste contains only a small quantity of Ra-226, and the waste closer to the Rn barrier had low activity.

Fluxes from the surface of the Rn barriers varied with surface treatment (e.g., riprap vs. vegetated) and the surface condition (e.g., woody species present, ephemeral ponding). For example, the geometric mean Rn fluxes on the top deck at the Falls City site was 0.254 Bq/m²/s, whereas geometric mean flux on the side slope was 0.011 Bq/m²/s (23 times lower). The Rn barrier beneath the apron and on the side slope at Falls City was moist and plastic, whereas the Rn barrier on the top deck was drier and more friable. Similarly, areas where woody and deep-rooted plants had established generally exhibited greater variability in fluxes. For example, in one test pit at the Bluewater site, the Rn-222 flux ranged from 0.11 to 1.26 Bq/m²/s at separation distances on the order of a meter, suggesting local zones of preferential Rn transport. Comparison of distributions of the in-service fluxes measured in this study relative to distributions of the as-built fluxes indicated that some in-service fluxes at the Falls City and Bluewater sites were higher than any as-built flux. In contrast, at the Shirley Basin site, the in-service and as-built distributions of flux were comparable. However, because the sampling method was deliberately biased, inferences cannot be made regarding the in-service condition relative to the as-built condition.

Diffusion coefficients were determined from the flux data using RAECOM, a 1-D model that calculates the Rn flux based on diffusive transport in the Rn barrier. Diffusion coefficients are computed from the Rn fluxes measured on the surface of the Rn barrier and the surface of the underlying waste. Steady-state gaseous diffusive transport is assumed. Diffusion coefficients for Rn barriers in RAECOM and other models used for design and analysis are assumed to vary

consistently with water saturation. The findings in this study suggest that this relationship is not valid if preferential pathways developed for Rn transport.

A method to determine the long-term average Rn-222 flux from activity profiles of Pb-210 in the Rn barrier is described in Section 5. Pb-210 is a progeny of Rn-222, with a half-life of 22.3 yr. The method provides a relatively simple technique to assess long-term average Rn fluxes based on Pb-210 present in the upper 100-200 mm of the Rn barrier. Samples for Pb-210 analysis could be collected by drilling and sampling, direct push techniques, or hand auger, precluding the need for disruptive test pits and flux chambers. Because the approach is sufficiently rapid and unobtrusive, the technique could be used for periodic assessment of Rn barriers.

Soil morphology and soil chemistry of the earthen materials in the test pits and at the analogue sites are described in Section 6. Morphological properties that were determined include horizon/material thickness, boundary, Munsell color, pedality/structure (size, shape and grade, consistence), root morphology per unit area (abundance, diameter, class), shape and size of void structures or animal excavations, rupture resistance, and descriptions of inclusions. Anomalous morphologies were also recorded. Gravimetric moisture content profiles were also determined. Soil samples were collected from each horizon from at least five locations for measurements of organic matter content, total carbon, nitrogen, hydrogen, macro- and micronutrients, nitrogen speciation, calcium carbonate, electrical conductivity (EC), pH, and particle size.

Soil structure developed in all of the Rn barriers in response to plant root growth, volume change due to root water uptake, and biota intrusion (e.g., insect burrowing). With few exceptions, roots were observed throughout the depth of the Rn barriers. Roots were found near the bottom of the Rn barrier at each site. Deep-rooted woody plants and harvester ants contributed to greater structural development than other biota. For example, in the vegetated section of cover at the Falls City site, the Rn barrier was drier and friable, containing remnant soil structure from the borrow area with clods of mixed sizes delineated by hairline fractures that served as preferred sites for water flow, iron precipitation, and root mats. At the Shirley Basin site, the Rn barrier is composed of a montmorillonite rich clay with little structure. Although fine roots did penetrate the barrier, the root development was less extensive than at other sites, resulting in less soil structure, lower Rn flux, and lower saturated hydraulic conductivity. Root growth at Shirley Basin apparently was tempered by acidic conditions within the Rn barrier. Similar conditions were observed at the analogue sites.

Morphological characteristics at each site and each analogue were quantified using the soil morphological development score (SMDS), which incorporates texture, pedality, macroporosity, root density, and water content. The SMDS ranged from as low as 5 (Falls City site) to as high as 10,688 (Bluewater site), with higher SMDS corresponding to greater structure. The scoring system was used to assess the impact of soil morphology on the saturated hydraulic conductivity and Rn diffusion coefficients. Generally, as the SMDS increased, the hydraulic conductivities and Rn diffusion coefficients also increased.

ACKNOWLEDGMENTS

The authors are grateful for the many persons who contributed to this project. They include Joseph Kanney, Michael Salay, Hans Arlt, Sarah Tabatabai, and Karen Dickey (USNRC), Jiannan Chen (U. Central Florida), Xiaodong Wang (U. Wisconsin), Laurel Larsen (U. California Berkeley) David Dander, Ray Johnson, Anthony Martinez, Aaron Tigar, and Chris Holmes.

This report was peer reviewed by: Nicholas Kiusalaas (RSI Entech/DOE-Legacy Management Support), Stephen Dwyer (Dwyer Engineering, LLC) and William Albright (Desert Research Institute, emeritus). Peer review, by four anonymous reviewers, for the sections on Pb-210 and radon flux also resulted from the publication of two journal articles. We thank all those reviewers.

This research is a collaboration between the DOE Office of Legacy Management (LM) and the Nuclear Regulatory Commission with funds provided by both agencies. Investigators are from the University of Wisconsin, University of Virginia, University of California at Berkeley, Navarro Research and Engineering Inc. (the former DOE/LM contractor), RSI Entech/DOE-Legacy Management (the current DOE/LM contractor) and NRC. Additional support was provided by DOE/EM through the Consortium for Risk Evaluation with Stakeholder Participation (CRESP).

ABBREVIATIONS AND ACRONYMS

ASTM	American Society for Testing and Materials
Bq/g	becquerels per gram
Bq/m ² /s	becquerels per meter square per second
CFR	<i>Code of Federal Regulations</i>
cm	centimeters
cm/s	centimeters per second
CMB	compacted mineral barrier
D	diffusion coefficient (m ² /s)
D _{Rn}	diffusion coefficient for radon
DOE	U.S. Department of Energy
DOE/EM	U.S. Department of Energy/Environmental Management
DOE/LM	U.S. Department of Energy/Legacy Management
EC	electrical conductivity
ECTG	Engineered Covers Technical Group
EPA	U.S. Environmental Protection Agency
ET	evapotranspiration
K _{sat}	saturated hydraulic conductivity
LM	Office of Legacy Management
LTS&M	long-term surveillance and maintenance
LMS	Legacy Management Support
LTSP	long-term surveillance plan
MDA	minimum detectable activity
mm	millimeters
NRC	U.S. Nuclear Regulatory Commission
NRCS	Natural Resources Conservation Service
Pb	lead (isotope)
pCi/m ² /s	picocuries per square meter per second
PNV	potential natural vegetation
ρ _{SMDS}	partial soil morphological development score
Ra	radium (isotope)
RAECOM	Radiation Attenuation Effectiveness and Cover Optimization with Moisture Effects
RCRA	Resource Conservation and Recovery Act of 1976
Rn	radon (isotope)
SMDS	soil morphological development score
SWCC	soil water characteristic curve

t SMDS	total soil morphological development score
S_r	soil moisture saturation (%)
SOM	soil organic matter
UMTRCA	Uranium Mill Tailings Radiation Control Act
USDA	U.S. Department of Agriculture

APPENDIX A

DESCRIPTIONS AND CRITERIA OF SITE ATTRIBUTES FOR PHASE I RANKING OF SITES

Urban Proximity

Description

This attribute refers to the location of a site relative to an urban center that will allow access to the facility and can provide supplies. Urban is used in a general sense. For example, Grand Junction, Colorado, would be considered an urban center in proximity to the Grand Junction, Disposal Site.

Criterion

Priority was assigned based on the distance to a town with lodging and hardware supplies. High priority sites are within an hour (one way), medium priority sites are between 1–1.5 hours, and low priority sites are in remote locations greater than 1.5 hours' drive time to an urban area.

Climatic Influence: Aridity and Seasonality

Description

Radon diffusion and flux are greater for dry soil. Aridity is the overall aridity of the site on an annual basis. Seasonality describes the soil moisture condition expected during the summer months. Arid sites would have high opportunity whereas humid sites would have low opportunity. Sites that are wetter in the summer have lower opportunity whereas sites that are dry in the summer have high opportunity.

Criterion

Aridity was determined by average annual precipitation with less than 300 mm ranked high priority, 300 to 500 mm ranked medium, and more than 500 mm ranked low. Seasonality was based on whether or not there was a preponderance of summer precipitation, winter precipitation, or an even distribution of precipitation and the likely influences of rock and/or vegetation on seasonal soil moisture content.

Cover Vegetation

Description

Plants growing on covers may increase radon diffusion and flux by drying the soil and enhancing development of soil structure. The vegetation attribute includes the abundance of vegetation, management activities to limit vegetation on the site, and the presence of deep-rooted plants.

Criterion

High priority sites had abundant (>50% cover) deep-rooted vegetation and little or no management; medium priority sites had between 10 and 50% cover, fewer deep-rooted plants, and little or no management; and low priority sites had less than 10% total plant cover and frequent herbicide spraying to control vegetation on covers.

Barrier Vulnerability

Description

This attribute refers to the vulnerability of the cover design to soil-forming processes. Cover designs with thin, shallow radon barriers overlain by fine-textured soils that allow capillary conduction and support vegetation are most vulnerable. Covers with thicker, deeper radon barriers overlain by coarse gravel or cobble riprap and no vegetation would have low vulnerability.

Criterion

High priority was assigned to sites that have 0.3–0.91 meter of protection soil above the radon barrier and no rock riprap. Medium priority was assigned to sites that have riprap, sandy bedding, and 0.96–2.28 meter protection layers overlying radon barriers. Low priority sites had 2.28–5.49 meter protection layers overlying relatively thick (1.83–2.13 meters) radon barriers.

Source Activity

Description

Source activity refers to the radioactivity of the tailings and therefore the propensity to produce radon gas. Sites with high activity tailings would have high opportunity for an increase in radon flux and sites with low activity tailings would have low opportunity.

Criterion

Site completion reports were reviewed for information on radium activity. Information was missing in some reports and inconsistent in others. High priority was assigned to sites with tailings that had >18.5 becquerels per gram (Bq/g) radium, medium priority was assigned to sites with tailings that had between 18.5 Bq/g and 3.7 Bq/g radium, and low priority was assigned to sites with tailings that had <3.7 Bq/g radium.

Depth to Source

Description

Depth to source indicates the depth of the high activity tailings from base of the radon barrier. Sites with low-activity material (e.g., windblown tailings) placed over high activity tailings present a low opportunity for detecting an increase in radon flux. Tailings directly below the radon barrier present the highest opportunity for radon flux.

Criterion

High priority was assigned to sites with tailings located right below the radon barrier. A threshold of 1 meter was selected to separate medium and low priority. Low activity soil < 1 meter may prevent higher fluxes but not too significantly. Sites that have > 1 meter of lower activity soils between the radon barrier and high activity tailings should provide the lowest opportunity for higher radon fluxes.

Borrow Source

Description

Borrow sources for soils used to construct disposal cell covers, if undisturbed, are often the best location to characterize natural analogs of soil morphology and plant ecology. Natural analogs provide clues about possible future changes in cover soil morphology and engineering properties.

Criterion

Opportunity ratings afforded by sites for study of natural analogs were based on the following parameters: a) favorable for plant growth, b) favorable to shrink/swell, c) location of borrow source (natural analog site), d) access to natural analog site, e) reactivity of clay mineral fraction, and f) soil age.

NRC Priority

Description

This attribute reflects how NRC perceives the potential radon flux for the site based on an NRC evaluation methodology.

Criterion

NRC's evaluation of the potential radon flux for sites is described in the unpublished report, "Documentation of the Engineered Covers Technical Group (ECTG) Activities, October 2011."

APPENDIX B

PHASE II SELECTION OF SITES

Descriptions of site attributes and rationale for Phase II selection of sites with contrasting designs and environments.

UMTRCA Title

Description

Title I sites were inactive (milling had ceased) and their milling licenses had been terminated before 1978 when UMTRCA was passed. Title II sites had active milling licenses in 1978 or were issued a license after 1978.

Selection Rationale

Select both Title I and Title II sites. Title II disposal cells were largely constructed after Title I cells. The design process evolved over time. Title I disposal cell covers, constructed first, are generally more conservative designs.

Cover Designs

Description

All Title I and Title II designs have a low-permeability radon barrier designed to limit percolation and slow radon diffusion. Some have a protection layer overlying the radon barrier. Some are armored with rock. Others have topsoil and vegetation.

Selection Rationale

Compare covers with and without rock, with and without vegetation, and with and without a protection layer overlying the radon barrier. Rock riprap limits evaporation whereas vegetation enhances release of water to the atmosphere. Protection layers may isolate radon barriers from certain soil-forming processes. Also, compare covers with thick and thin radon barriers to evaluate depth-dependent changes in soil morphology and engineering properties.

Climate Classes and Data

Description

Climate data included mean monthly and annual maximum temperature, minimum temperature, precipitation amount, and snow accumulation. Climate classes and descriptions are from an updated Koppen-Geiger climate map (Peel et al., 2007).

Selection Rationale

Compare sites with contrasting climates: (e.g., warm/wet, warm/dry, cold/wet, cold/dry). Also select sites with contrasting seasonality of precipitation (e.g., dry summers versus summers with monsoon rains). Seasonality influences soil moisture, pedogenesis, and radon flux.

Soil Moisture/Temperature Regimes

Description

Soil moisture and temperature regimes are used as criteria for soil classification (www.nrcs.usda.gov). Soil moisture regimes are based on the depth, probable duration, and

seasonality of soil saturation and vegetation-induced soil dryness. Soil temperature regimes encompass mean annual and seasonal change in soil temperature.

Selection Rationale

Compare sites with contrasting soil moisture and temperature regimes (similar to the selection of contrasting climate types). Different soil moisture and temperature regimes may have different effects on plant ecology, soil morphology, and soil engineering properties.

Potential Natural Vegetation

Description

Potential natural vegetation (PNV) is the vegetation that would be expected in a given environment without human intervention or other disturbances. PNV species are considered to have optimum ecological resilience for their environment. PNV is retrospective; it doesn't take into account future invasive species or climate change. By comparing PNV with current vegetation on covers and with analog site vegetation, ecologists can infer the current seral stage and the future trajectory of plant succession on covers.

Selection Rationale

Select disposal sites with different types of PNV. These sites are likely to have contrasting soil morphologies. Also select disposal sites that have analog sites with undisturbed vegetation that is representative of the PNV.

Deep-rooted Plants

Description

Sites with deep-rooted plants likely have greater soil morphological development within the radon barrier. Sites with deeper-rooted plants may also have relatively drier radon barriers. Woody plants generally have deeper roots than herbaceous plants.

Selection Rationale

Select disposal sites with mid-to-late seral, deep-rooted woody plants growing on the cover. Sites with more deep rooted plants, more developed soil structure, and drier radon barriers may experience greater increases in radon diffusion and flux.

Vegetation Development Score

Description

This score is a combined measure of the change in plants species (e.g., grasses to woody shrubs) and change in plant abundance on a disposal cell since construction. Scores were calculated differently for planted and unplanted covers. Text, annotated maps, and photographs from annual inspection reports were used to interpret these changes.

Selection Rationale

Select sites with high and low vegetation development scores. The higher the score, the greater the change in plant species (plant succession) and plant abundance and a greater likelihood for change in subsurface conditions (soil morphology).

Tailings Activity and Amount

Description

Tailings activity refers to the total curries of ²²⁶Ra in the disposal cell. Amount is the tons of tailings and residual radioactive material (e.g., mix of windblown tailings and soil) in the disposal cell.

Selection Rationale

Select disposal sites with a high tailings activity to dry mass ratio.

APPENDIX C

COVER DESIGNS, CLIMATES, AND ECOLOGIES OF SITES CONSIDERED FOR PHASE II OF THE STUDY

Table C-1 Information for Sites Considered for this Study

Site	Title ¹	Top Deck Cover Designs ²	Climate Class ³	Ann Temp Max/Min (°C) Precip (mm) ⁴	Soil Regime ⁵	Potential Natural Vegetation ⁶	Deep-Rooted Plants ⁷	Vegetation Development Score ⁸	Tailings Activity/ Dry Tons ⁹
Ambrosia Lake, New Mexico	I 1995	Rock/Bedding/ Radon Barrier (30/15/76) NP	Arid, Cold Steppe (Semiarid)	21.3/1.4 267	Typic Aridic/ Mesic	Juniper/ Pinyon	ATCA TARA 0%	Low (3.0)	1850/ 6.9x10 ⁶
Bluewater, New Mexico	II 1995	Rock/ Radon Barrier (20/76) NP	Arid, Cold Steppe (Semiarid)	21.3/1.4 267	Aridic- Ustic/ Mesic	Grama/ Galleta Steppe	ATCA ULPU 3%	High (8.0)	11,200/ 2.3x10 ⁷
Burrell, Pennsylvania	I 1987	Rock/Bedding/ Radon Barrier (30/30/91) NP	Continental, Hot Summer No Dry Season	16.1/3.1 1181	Udic/ Mesic	Appalachian Oak	POCU AIAL ACSA 9%	High (11.0)	4/ 8.6x10 ⁴
Canonsburg, Pennsylvania	I 1985	Topsoil/Rock Radon Barrier (30/46/91) P	Continental, Hot Summer No Dry Season	15.5/3.3 986	Udic/ Mesic	Appalachian Oak	SEVA 1%	Medium (4.5)	100/ 2.6x10 ⁵
Durango, Colorado	I 1991	Rock-Soil Matrix/ Rooting/ Rock Biointrusion/ Sand Drainage & Bentonite Mat/ Radon Barrier (15/76/46/15/61) P	Continental, Warm Summer No Dry Season	18.1/-0.1 409	Aridic Ustic/ Frigid	Mountain Mahogany/ Oak scrub	GUSA MACA 1%	Low (3.5)	1400/ 3.4 x10 ⁶
Edgemont, South Dakota	II 1989	Topsoil/ Fill Layer/ Radon Barrier (30/152/91) P	Continental, Warm Summer Without Dry Season	16.9/0.5 414	Aridic Ustic/ Mesic	Wheatgrass/ Needlegrass	0%	Low (3.5)	527/ 4.0x10 ⁶
Falls City, Texas	I 1994	Soil/ Rooting/ Barrier (15/76/91) P	Temperate, Hot Summer No Dry Season	26.9/14.3 721	Udic- Ustic/ Hyper thermic	Mesquite/ Acacia Savanna	PRGL 2%	Low (3.5)	1277 7.1x10 ⁶

C-1

Table C-1 Information for Sites Considered for this Study (Continued)

Site	Title ¹	Top Deck Cover Designs ²	Climate Class ³	Ann Temp Max/Min (°C) Precip (mm) ⁴	Soil Regime ⁵	Potential Natural Vegetation ⁶	Deep-Rooted Plants ⁷	Vegetation Development Score ⁸	Tailings Activity/Dry Tons ⁹
Grand Junction, Colorado	I Open	Rock/Bedding/Protection/ Radon Barrier (30/15/61/61) NP	Arid, Cold Steppe (Semiarid)	18.6/4.3 239	Ustic Aridic/ Mesic	Saltbrush/ Greasewood	ATCA ERNA 2%	Medium (5.0)	?/ 5.9x10 ⁶
Green River, Utah	I 1989	Rock/Bedding/ Radon Barrier (30/15/91) NP	Arid, Hot Desert	20.8/3.1 181	Typic Ustic/ Aridic	Saltbrush/ Greasewood	0%	Low (1.0)	30/ 5.2x10 ⁵
Gunnison, Colorado	I 1995	Rock/Bedding/ Protection/ Bedding/ Radon Barrier (15/15/183/15/46) NP	Continental, Warm Summer No Dry Season	12/-6.4 270	Typic Ustic/ Cryic	Great Basin Sagebrush	0%	Low (2.0)	175/ 1.1x10 ⁶
L-Bar, New Mexico	II 2000	Fill Layer/ Radon Barrier (61-305/127) NP	Arid, Cold Steppe (Semiarid)	18.6/3.1 236	Ustic Aridic/ Mesic	Grama/ Galleta Steppe	ATCA ERNA 3%	Medium (4.5)	206/ 2.1x10 ⁷
Lakeview, Oregon	I 1988	Soil/Rock/ Bedding/ Barrier (15/30/15/46) P	Continental, Hot Dry Summer	15.5/0.8 374	Xeric/ Frigid	Sagebrush Steppe	PUTR ARTR ERNA 5%	High (8.5)	42 9.3x10 ⁵
Lowman, Idaho	I 1992	Rock/Bedding/ Radon Barrier (30/15/46) NP	Continental, Warm Dry Summer	14.6/-1.4 663	Udic/ Cryic	Western Ponderosa	PIPO 8%	High (9.0)	12/ 2.2x10 ⁵
Maybell, Colorado	I 1998	Rock/Bedding/ Protection/ Radon Barrier (20/15/122/46) NP	Continental, Warm Summer No Dry Season	14.2/-1.9 425	Aridic Ustic/ Frigid	Sagebrush Steppe	0%	Low (2.0)	455/ 4.7x10 ⁶
Maybell West, Colorado	II 2005	Rock/ Radon Barrier (?/?) NP	Continental, Warm Summer No Dry Season	14.2/-1.9 425	Aridic Ustic/ Frigid	Sagebrush Steppe	0%	Low (2.0)	96/ ?
Mexican Hat, Utah	I 1995	Rock/Bedding/ Radon Barrier (20/15/61) NP	Arid, Hot Desert	22.3/6.0 171	Aridic Ustic/ Mesic	Blackbrush	0%	Low (0.0)	1800/ 1.3x10 ⁶

Table C-1 Information for Sites Considered for this Study (Continued)

Site	Title ¹	Top Deck Cover Designs ²	Climate Class ³	Ann Temp Max/Min (°C) Precip (mm) ⁴	Soil Regime ⁵	Potential Natural Vegetation ⁶	Deep-Rooted Plants ⁷	Vegetation Development Score ⁸	Tailings Activity/ Dry Tons ⁹
Naturita, Colorado	I 1995	Rock/Bedding/Protection/Radon Barrier (30/15/168/91) NP	Continental, Hot Summer Without Dry Season	20.9/3.3 329	Typic Ustic/Mesic	Great Basin Sagebrush	0%	Low (0.0)	79/ 1.1x10 ⁶
Rifle, Colorado	I 1996	Rock/Bedding/Protection/Radon Barrier (20/15/122/46) NP	Continental, Warm Summer No Dry Season	17.3/0.8 363	Typic Ustic/Frigid	Juniper/ Pinyon	0%	Low (3.0)	2738/ 4.7x10 ⁶
Salt Lake City, Utah	I 1989	Rock/Bedding/Radon Barrier (61/15/213) NP	Continental, Hot Summer No Dry Season	17.7/5.7 510	Xeric/Mesic	Saltbrush/ Greasewood	0%	Low (2.0)	1550\ ?
Sherwood, Washington	II 1996	Topsoil/Radon Barrier (15/366-610) P	Continental, Warm Dry Summer	14.6/2.6 500	Xeric/Frigid	Western Ponderosa	PIPO 5%	High (7.0)	470/ 2.9x10 ⁶

C.1 Footnotes for Appendix C

- ¹ Uranium Mill Tailings Radiation Control Act (UMTRCA) Title I or Title II and the year the disposal cell was completed.
- ² Cover layer types and thicknesses (cm) from the surface down to tailings: Rock = rock riprap layer, Bedding = course sand or gravel bedding for rock, Rooting = rooting medium or protection layer overlying the radon barrier, Barrier = low-permeability radon barrier. NP = not planted and P = planted. All four sites had two or more cover designs. The table shows top deck designs and the Main Tailings Cell cover for Bluewater. Other designs are listed below.
 - Bluewater Carbonate Cell: rock/barrier (20 cm/varying thickness up to 240 cm), NP.
 - Bluewater Acid Cell: soil/barrier (15/20), P
 - Falls City Side Slope: rock/bedding/barrier (41/15/61), NP
 - Shirley Basin Terrace Slope: rock/bedding/rooting/barrier (15/10/61/61), NP
 - Lakeview Side Slope: rock/bedding/barrier (30/15/46), NP
- ³ Climate classes are from an updated Koppen-Geiger climate map (Peel et al. 2007).
- ⁴ Mean annual maximum and minimum temperatures (°C) and mean annual precipitation (mm) (www.usclimatedata.com).
- ⁵ Soil moisture/temperature regimes (NRCS; www.nrcs.usda.gov).
- ⁶ Potential natural vegetation (PNV) types are from a 2000 version of the Kuchler (1964) PNV map (firelab.org/document/potential-natural-vegetation-groups-v2000).
- ⁷ Genus and species for potentially deep-rooted plants growing on disposal cell covers are from the USDA Plants Database (www.plants.usda.gov). Percent cover values are estimates from 2014 site inspection reports (www.lm.doe.gov). Plant acronyms are the first two letters of the genus followed by the first two letters of the species:
 - ACSA (*Acer saccharum*, sugar maple)
 - AIAL (*Ailanthus altissima*, tree of heaven)
 - ARTR (*Artemisia tridentata*, big sagebrush),
 - ASCI (*Astragalus cicer*, chickpea milkvetch),
 - ATCA (*Atriplex canescens*, fourwing saltbush),
 - ERNA (*Ericameria nauseosa*, rubber rabbitbrush)
 - GUSA (*Gutierrezia sarothrae*, broom snakeweed)
 - MACA (*Machaeranthera canescens*, hoary tansyaster)
 - PIPO (*Pinus ponderosa*, ponderosa pine)
 - POCU (*Polygonum cuspidatum*, Japanese knotweed)
 - PRGL (*Prosopis glandulosa*, honey mesquite),
 - PUTR (*Purshia tridentata*, antelope bitterbrush),
 - SEVA (*Securigera varia*, crownvetch)
 - TARA (*Tamarix ramosissima*, saltcedar)
 - ULPL (*Ulmus pumila*, Siberian elm)
- ⁸ The vegetation development score was calculated based on a combination of changes in plants species (e.g. grasses to shrubs) and changes in plant abundance on the cover, from the time of construction.
- ⁹ Total curries of ²²⁶Ra in the disposal cell and dry tons of tailings and other materials (e.g., mix of windblown tailings and soil).

APPENDIX D

HISTORIES OF DISPOSAL SITES SELECTED FOR STUDY

D.1 Selection Process

The study site selection process (Section 2.3) resulted in the selection of four UMTRCA disposal sites: Bluewater, New Mexico; Falls City, Texas; Shirley Basin South, Wyoming; and Lakeview, Oregon. Selection of these four sites (1) provided the greatest opportunities for evaluating effects of ecological and soil-forming process on cover engineering properties and performance, and (2) encompassed the broad range of cover designs and environments within the LM portfolio. Bluewater ranked highest with respect to opportunity to evaluate changes in the morphology and engineering properties of radon barriers. The other three sites ranked relatively high in this initial ranking and also provided the greatest opportunity to compare and contrast different cover designs, climates, and ecologies.

The selection process also identified test conditions and test pit locations on disposal cell covers and at analog sites (Section 2.5) where researchers anticipated the greatest changes in soil morphology and related engineering properties. Selection of test pit conditions provided opportunities to compare different cover designs at a site, to evaluate effects of different surface conditions on subsurface morphology and engineered properties, and to measure the highest (not the average) radon fluxes at a site.

This appendix provides brief histories of the four sites. Sources of information included fact sheets, LTSPs, and completion reports for the four sites (www.lm.doe.gov).

D.2 Bluewater, New Mexico

The Bluewater disposal site is in Cibola County approximately 9 miles northwest of Grants, New Mexico (Figure D-1). Carbonate-leach and acid-leach milling processes were both used at the site.

D.2.1 Uranium Ore Processing

Anaconda Copper Mining Company (a subsidiary of ARCO after 1977) constructed the original carbonate-leach mill in 1953 to process uranium ore mined from the Jurassic Todilto Limestone Formation in the vicinity of the site. The carbonate-leach mill initially had a production capacity of 300 tons of ore per day and a maximum capacity of 1200 tons per day in 1955. Tailings from the carbonate process were placed in a depression just northeast of the mill site; what is now the carbonate tailings pile. The carbonate leach mill closed in 1959. The carbonate pile and adjacent disposal areas include mill building debris and other rubble creating an undulated surface prior to construction of the final cover.

An acid-leach mill with an initial capacity of 2000 tons of ore per day was constructed in 1957 to process sandstone uranium ore from mines in the Jurassic Jackpile Sandstone member of the Morrison Formation and the Cretaceous Paguate member of Dakota Sandstone Formation, both

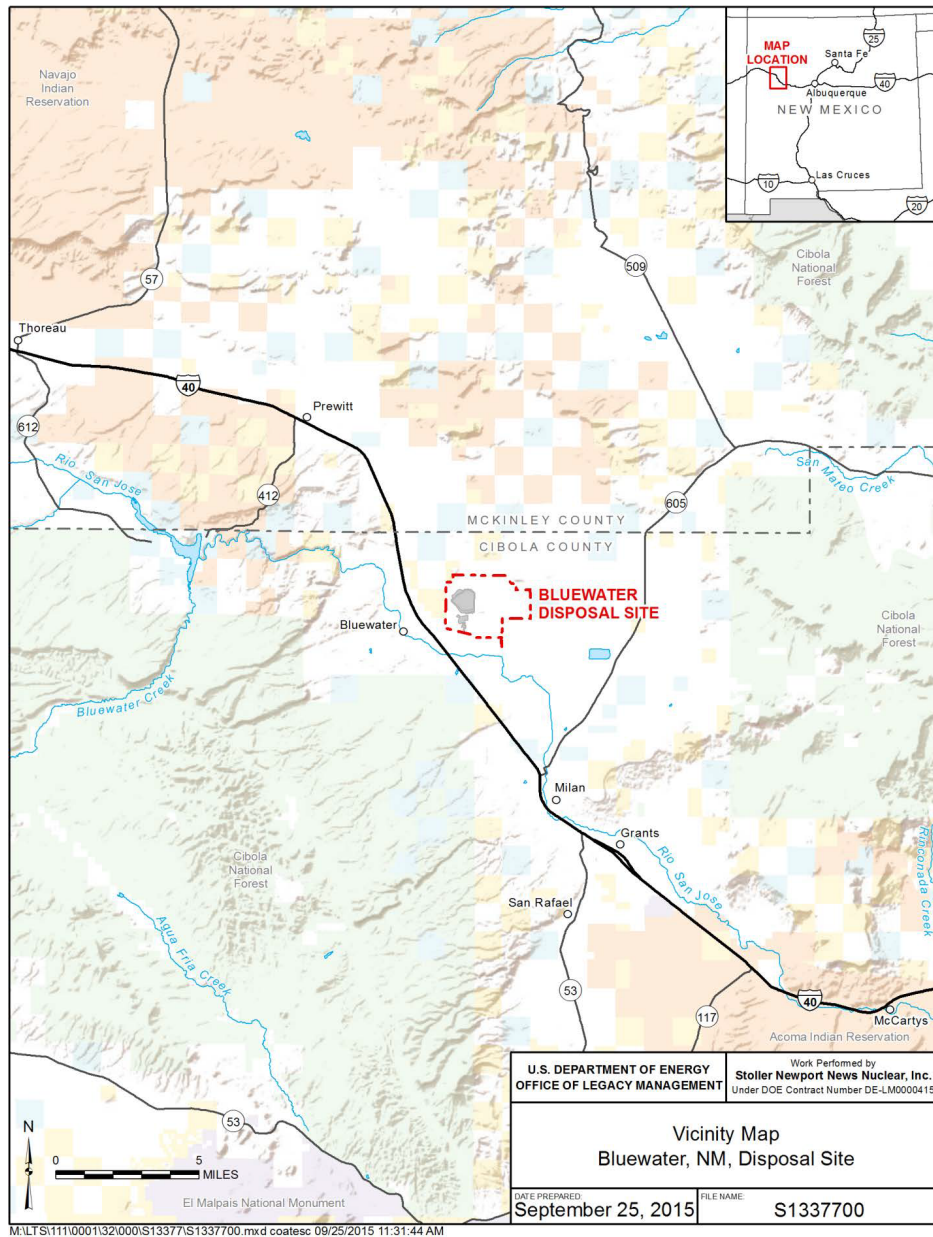


Figure D-1 Vicinity Map of the Bluewater, New Mexico, Disposal Site

located near the Laguna Pueblo, approximately 35 miles southeast of the mill. In 1967, the capacity of the acid-leach mill was increased and reached about 6000 tons of ore per day by 1978. Tailings from the acid leach process were conveyed in a slurry into another natural depression north of the carbonate tailings pile and segregated from the carbonate-leach tailings to prevent mixing of acidic and basic compounds. As the slurry spread over the pile, heavier, coarser sand tailings deposited near the south end, and liquids and finer tailings (slimes) flowed to the north end. Containment of acid-leach tailings in the depression was aided by dikes constructed on the northern, eastern, southern, and southwestern boundaries of what is now the main tailings pile. Between 1955 and 1957, acid tailings drained around the dikes to the northwest of the current main tailings pile. This area is now referred to as the acid tailings pile.

In 1957, a northwestern dike was constructed to fully contain tailings in the main tailings pile. Dikes were raised several times before milling operations at the site ended in 1982.

By the late 1950s, Anaconda Company became aware that process water in the tailings slurry was seeping into and contaminating groundwater in the underlying San Andres and Glorieta aquifers. In 1960, Anaconda began disposing of tailings effluent through an injection well 950 to 1423 feet deep in the Yeso Formation. Effluent injection continued at a rate of 200 to 400 gallons per minute until the practice ended in 1977. After deep injection ceased, 300 acres of lined evaporation ponds were constructed north and northeast of the main tailings pile to contain the liquid effluent. After milling operations ended, wells were installed to dewater the sands tailings in the southern portion of the main tailings pile. These tailings fluids were pumped back to the mill between 1982 and 1985 to extract dissolved uranium. Raffinate from this process was initially pumped back to the main tailings pile, but, from 1983 to 1985, it was pumped directly to the evaporation ponds.

D.2.2 Remedial Action

The licensee, ARCO, was responsible for reclamation of Bluewater, an UMTRCA Title II site. ARCO constructed disposal cells to contain tailings waste that satisfied NRC design requirements and reclamation standards in 10 CFR 40, Appendix A, and EPA standards in 40 CFR 192. The site was transferred from ARCO to DOE for long-term custody in 1997.

The main tailings disposal cell, the adjoining acid tailings disposal cell to the northwest, and a south bench disposal area have a total activity of about 11,200 curies of ^{226}Ra , occupy about 354 acres, and contain an estimated 23 million dry tons of tailings and other residual materials. A total of about 623,000 cubic yards of low-activity windblown tailings from surrounding areas and residues from the evaporation ponds were placed on the slimes portion of the main tailings pile.

The engineered cover consists of a low-permeability radon barrier placed over compacted tailings and a rock erosion protection layer. According to the Bluewater Fact Sheet (www.lm.doe.gov), the radon barrier is 1.7 – 2.6 feet thick overlying sand tailings and has a minimum thickness of 1.7 feet overlying relocated materials placed over the slime tailings and immediately below the radon barrier. The rock erosion protection layer averages 4.5 inches thick on the top deck with a D_{50} of 1.5 inches. The top deck of the engineered cover for the relatively flat acid disposal cell along the northwest edge of the main tailings cell has an 8-inch thick radon barrier covered with 8 inches of topsoil. The topsoil was seeded with native grasses for erosion protection (see Section 2.6 for current plant species composition and abundance data).

The carbonate tailings disposal cell covers about 54 acres and contains an estimated 1.3 million tons of contaminated materials having a total activity of about 1130 curies of ^{226}Ra . The radon barrier was constructed to fill and level the undulated surface resulting from the disposal of building debris and other rubble in the disposal cell. Therefore, the radon barrier varies in thickness from less than a foot thick overlying the highest points to greater than 10 feet thick overlying the deepest swales.

The borrow area for radon barrier soil for all disposal cells and for topsoil on the acid tailings disposal cell was east of the evaporation ponds. The material in the borrow area varied from a

low plastic clay (CL) to a silty sand (SM) with some small lenses of sand (SP). All of the material in the borrow area except the sand lenses was used to construct radon barriers. The design compaction requirement for the radon barrier was 95% of maximum dry density at $\pm 3\%$ of optimum moisture.

The source of rock riprap for erosion protection was quarried from the Bluewater flow of the Zuni-Bandera volcanic field approximately 1000 feet southeast of the main tailing pile. Rock cores were extracted from the quarry area and tested for specific gravity, absorption, soundness, abrasion, and tensile strength as required by NRC. All rock on the project was oversized a minimum of 15% to allow for inconsistencies within the rock properties and still meet the NRC design requirements.

Table D-1 is a compilation of cover materials parameters from a report on characterization of borrow soil (Rogers and Associates, 1987) and the Bluewater Completion Report (ARCO 1990).

Table D-1 Bluewater Barrier Material Parameters

Parameter	Value	Source
% passing #200 sieve (74 μm)	Ave. 33.9 (range 49.2 – 24.6)	4 tests, borrow area
Specific Gravity (g/cm^3)	2.68 ± 0.02	10 tests, borrow area
Original Dry density	1.68	n = 25 borrow area
Original Moisture Content (%) *	10.4	n = 25 borrow area p 5-3 fiche sheet 53420
Organic Matter	----	
Clay Content (< 2 μm) % *	Ave. 23.6 (range 30.8 – 18.9)	4 tests, borrow area
Clay Mineralogy	----	
Ra-226 (Bq/g) *	0.022 Mean	14 samples
Rn flux ($\text{Bq}/\text{m}^2\text{-s}$) (measured background)*	Mean 0.033 ± 0.022	n= 5 borrow area p 5-3 fiche sheet 53420
Estimated Design Diffusion Coefficient (m^2/s) *	1.8×10^{-6}	Table 5-2 p 5-5 fiche sheet 53420
Unit weight (kN/m^3)		
Moisture As-Built (%)	Main Tailings Pile 11.6 Carbonate Pile 12.4 Asbestos Pile 12.4	n = 605 n = 604 n = 47
Dry Density As-Built (g/cc)	Main Tailings Pile 1.858 Carbonate Pile 1.847 Asbestos Pile 1.868	n= 605 n = 604 n = 47
Radon Flux As-Built ($\text{Bq}/\text{m}^2\text{-s}$)	Main Tailings Pile 0.079 ± 0.112 Carbonate Pile 0.048	n = 125 Closure Report Vol 1 n = 100

D.3 Falls City, Texas

The Falls City, Texas, Disposal Site is in Karnes County, approximately 40 miles southeast of San Antonio and approximately 8 miles southwest of the town of Falls City (Figure D-2). Uranium discovered in 1954 in shallow sandstone units of the Eocene Whitsett Formation underlie the Falls City disposal site and surrounding area. Uranium was mined in open pits.

D.3.1 Uranium Ore Processing

Susquehanna-Western Inc. constructed and operated the first mill at the site from 1961 to 1973. More than 700 tons of uranium oxide was extracted from approximately 2.5 million tons of sandstone ore with a sulfuric acid leaching process, creating approximately 3.1 million tons of mill tailings. The sandy tailings and acid raffinate were placed in several unlined ponds and former open-pit mines at the site. Between 1978 and 1982, Solution Engineering Inc. conducted solution mining to extract additional uranium from some of the tailings using a system of injection and recovery wells. Fluid from this leaching process was pumped to one of the tailings ponds. By 1982, all ponds had dewatered through evaporation and recharge, and Solution Engineering recontoured and covered the remaining tailings piles with 1 to 2 feet of local clayey soil and planted native and introduced grasses.

D.3.2 Remedial Action

DOE remediated the Falls City site and contaminated vicinity properties, designated as a Title I UMTRCA site, between 1992 and 1994. Surface remediation consisted of consolidating contaminated material from the former mill site, the recontoured tailings piles, windblown material present on 388 acres surrounding the site, and vicinity properties where contaminated materials had been imported from the mill site, in a single engineered disposal cell.

The rectangular disposal cell contains over 7 million tons of dry tailings, has a total activity of about 1300 curies of ^{226}Ra , and occupies 127 acres. The cell measures 2600 feet by 2200 feet at the base and rises approximately 62 feet above the surrounding terrain. Tailings previously placed below grade in open pit mines are within the footprint of the cell. The material placement included mill building rubble above the preexisting tailings overlain by tailings from the other piles. Windblown material was placed above the tailings and just below the engineered cover to limit release of radon to the atmosphere.

A vegetated cover on the top deck and a rock-armored cover on the side slope were designed to withstand a probable maximum precipitation event (19.2 inches per hour), limit radon flux to less than the 20 pCi/m²s standard, and restrict percolation of rainwater into the tailings (DOE 1992). The top deck cover design consists of a 36-inch-thick highly-compacted clay soil that serves as a low-permeability radon barrier, a 30-inch-thick layer of soil suitable as a plant growth medium, and a 6-inch-thick layer of topsoil. The top of the disposal cell has a 100:1 slope designed to limit standing water while also minimizing runoff velocity.

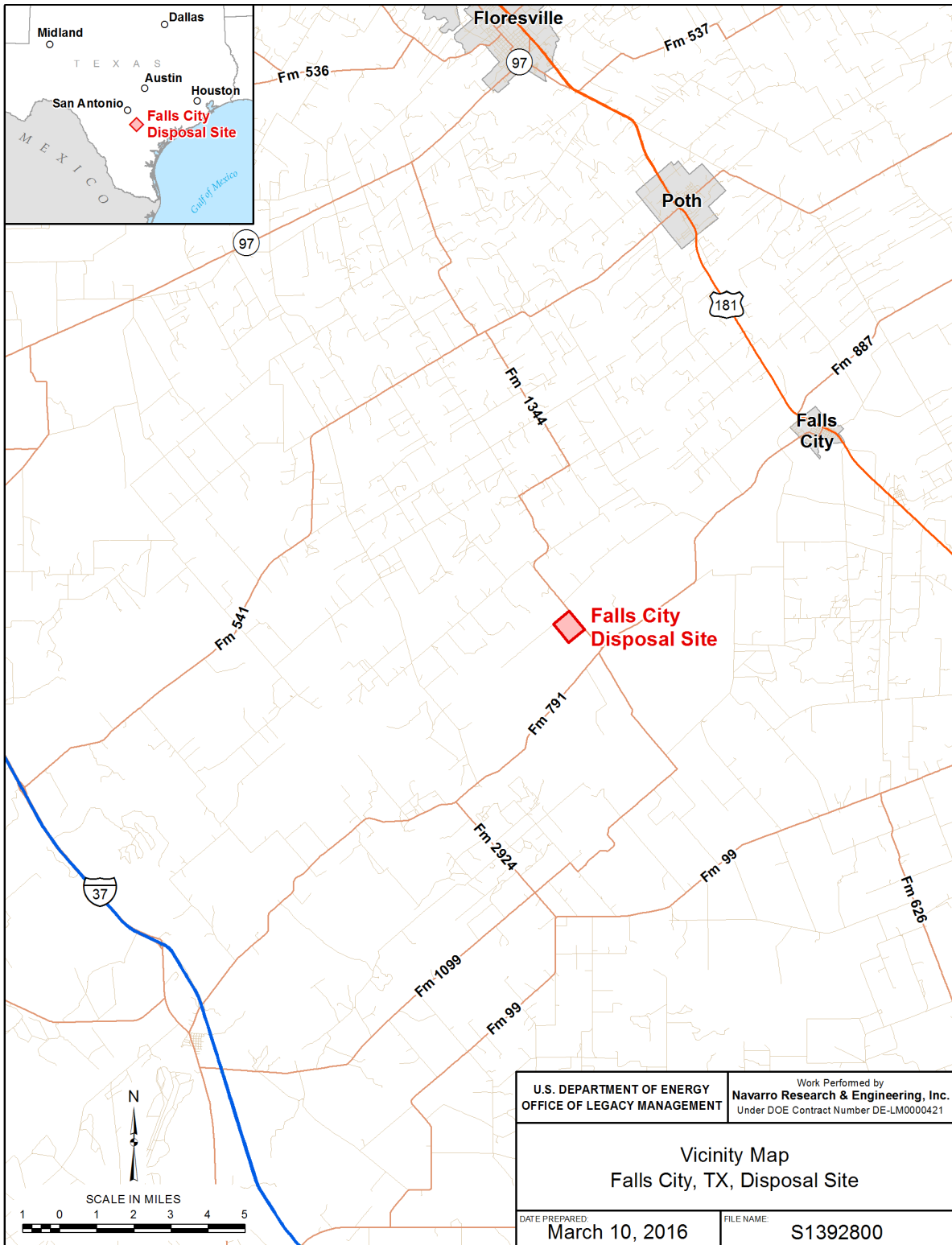


Figure D-2 Vicinity Map of the Falls City, Texas, Disposal Site

The side slope cover overlying tailings consists of a 24-inch-thick low-permeability radon barrier of the same highly-compacted clay soil used for the top deck. Overlying the radon barrier is a 6-inch layer of gravel bedding material and a 16-inch-thick layer of rock riprap. The 3-inch minus gravel bedding layer, designed to protect the radon barrier during placement of the riprap, is also designed to facilitate runoff following storm events. The riprap has a median D₅₀ of 7 inches on the side slope and a D₅₀ of 11 inches in a 6 to 10 foot deep rock apron that surrounds the base of the disposal cell. The side slopes of the disposal cell are 5:1.

The borrow area for radon barrier soil, growth medium layer, and topsoil layer was approximately 0.5 mile southwest of the disposal cell. During excavation, a minimum of three feet of topsoil material was removed and stockpiled. Material for the radon barrier and growth medium were removed in 1 foot depth increments. Radon barrier material was placed in four 12-inch loose lifts on the top deck and three 12-inch loose lifts on the side slope. The gradation requirement for the radon barrier material was a maximum of 10% retained on a #4 sieve with a minimum of 40% passing the #200 sieve. The radon barrier was compacted to 97% of maximum dry density at ±3% of optimum moisture content. The growth medium was placed in 12-inch loose lifts and compacted to 95% of maximum dry density at ±3% of optimum moisture content.

Topsoil on the top deck was placed in 6-inch loose lifts, fertilized with nitrogen and phosphorus, and seeded with a mixture of native and introduced grasses: kleingrass (*Panicum coloratum*), bermudagrass (*Cynodon dactylon*), sideoats grama (*Bouteloua curtipendula*), and green sprangletop (*Leptochloa dubia*). Limestone from a quarry near Marble Falls, Texas, 135 road miles north of the disposal site, was used for the bedding and rock riprap layers on the side slope.

Table D-2 is a compilation of barrier material parameters from the Falls City final completion report (DOE, 1996).

Table D-2 Falls City Barrier Material Parameters

Parameter	Value	Source
% passing #200 sieve (74 µm)	72%	9 tests, borrow area
Specific Gravity	2.61	9 tests, borrow area
Original Moisture Content	34.3 %	9 tests, borrow area
Organic Matter	4.5 – 13.2 %	3 tests, borrow area, varies with method
Clay Content (< 2 µm)	11.7 – 16.5 %	3 tests, borrow area
Clay Mineralogy	primarily smectite	3 tests, borrow area
Ra-226 (Bq/g)	0.148 Mean	15 samples (range: 0.067 – 0.35)
Cover Moisture as built (%)	42.0 Mean	n= 1377 range 43.5 – 29.8%* Completion Report Vol 3
Cover Porosity as built (%)	59.9 Mean	n = x Completion Report Vol 3
Cover Rn Flux as built (Bq/m ² -s)	0.024 Mean	n = 100 range 0.003 - 0.157 Completion Report Vol 4a

D.4 Shirley Basin South, Wyoming

The Shirley Basin South disposal site is located in rural Carbon County about 60 miles south of Casper and 35 miles north of Medicine Bow, Wyoming. The site is at an elevation of about 7100 feet (Figure D-3). Economically important uranium deposits are in the Wind River Formation underlying the site. Ore was extracted in open pit mines at a depth of 200–300 feet below the surface in the immediate vicinity of the site.

D.4.1 Uranium Ore Processing

Petrotoomics Company operated the mill from 1962 to 1974 and from 1978 to 1985. Production, 500 tons per day in 1962, expanded to 1000 tons per day in 1968, and expanded again to 1500 tons per day in 1970. The mill used a conventional acid leach process to extract uranium from the ore. Tailings and process solution from milling operations were pumped as a slurry to a tailings impoundment onsite. In 1977, an amendment to the NRC license allowed a new impoundment dam to be constructed over the original dam. The new dam, completed in 1979, raised the elevation of the tailings impoundment to a maximum height of 75 feet and a top width of 50 feet. Mining and milling operations ceased in 1985.

D.4.2 Remedial Action

Petrotoomics Company, the licensee, was responsible for reclamation of Shirley Basin South as an UMTRCA Title II site because it was operating under an active NRC license when UMTRCA was passed in 1978. Petrotoomics began decommissioning and reclamation in 1985; completed encapsulation of the tailings, contaminated site soils, and contaminated building materials in an engineered disposal cell in 2000; and completed site remediation in 2001. NRC included the site under a general license for long-term custody and transferred the title from Petrotoomics to DOE in 2005.

The tailings impoundment was recontoured and capped in place to form the disposal cell. The cell topography consists of two benched top decks, the original impoundment dam sloping below the lower top deck and an interior tailings slope separating the upper and lower top decks. The tops decks are sloped at about 20:1, and the side slope and interior slope are 5:1. The disposal cell contains about 6.3 million tons of tailings, contaminated soils, and rubble from site structures. The disposal cell has a 142-acre footprint. Tailings and other residual materials have a total activity of about 974 curies of ²²⁶Ra.

The engineered cover has vegetation on the two top decks and rock armor on the impoundment dam slope and on the interior tailings slope. The cover consists of a 24-inch compacted clay radon barrier and a 24-inch silty sand overburden or protection layer. The onsite source of the radon barrier material was a clay borrow area about 0.1 miles east of the disposal cell. The sandy overburden borrow source was a swale about 0.2 mile southwest of the disposal cell. Topsoil was stockpiled during excavation of clay and silty sand materials. The radon barrier and protection layer were both compacted to 95% of maximum dry density. Granite used for riprap was quarried in the foothills of the Laramie Mountains about 12 miles northeast of the disposal cell. Topsoil on top deck areas was seeded with a mixture of native and introduced grasses (see Appendix C for information on current species composition and abundance). See the Shirley

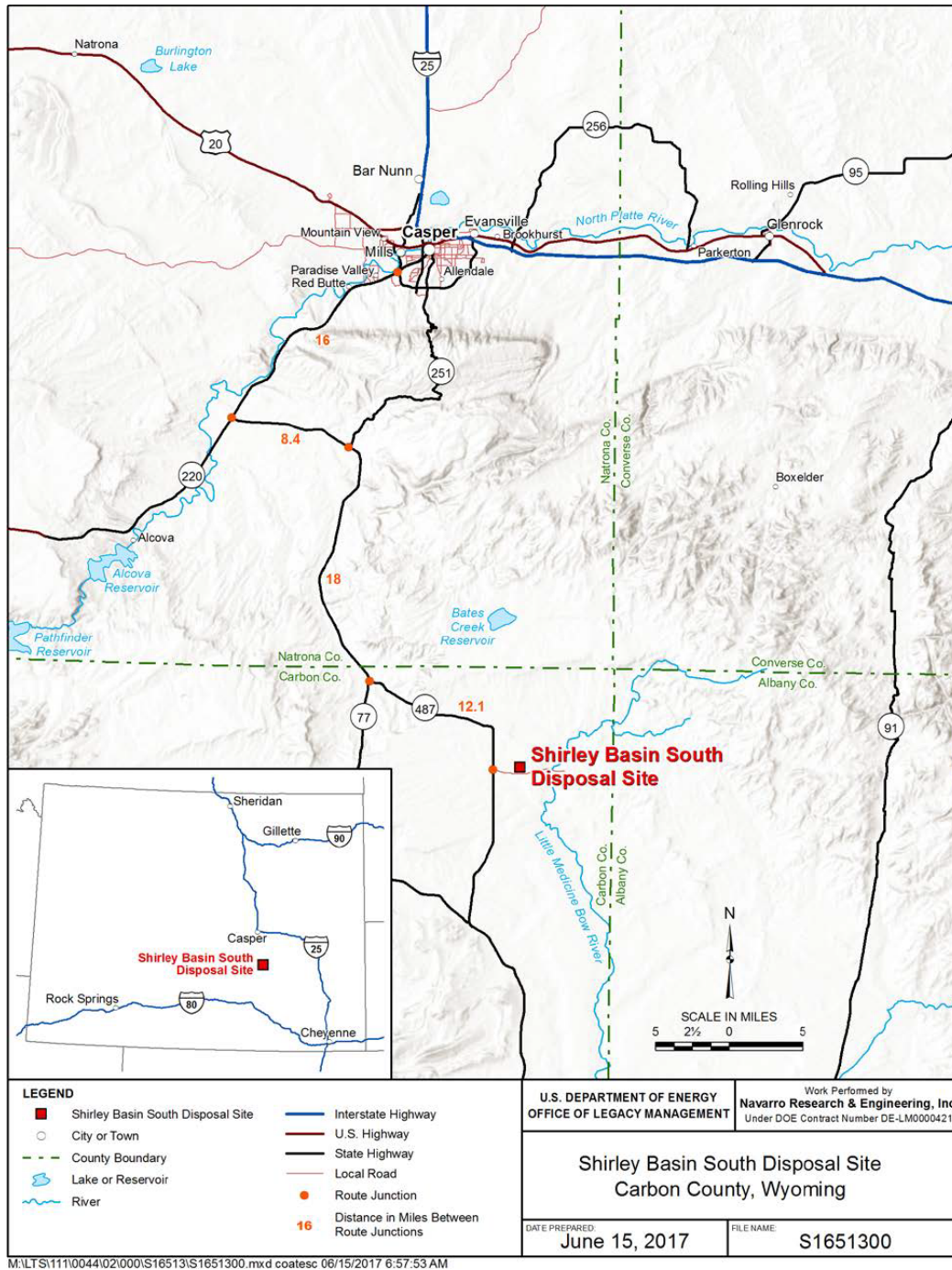


Figure D-3 Vicinity Map of the Shirley Basin South, Wyoming, Disposal Site

Basin South completion report (Petrotoomics 2001) for disposal cell design details, specifications, and testing results for all engineered cover materials. Table D-3 is a compilation of cover materials parameters drawn from the completion report (Petrotoomics, 2001).

Table D-3 Shirley Basin South Barrier Materials Parameters

Parameter	Value	Source
% passing #200 sieve (74 µm)	Mean 75.8	Petrotomics, 2001
Specific Gravity	Mean 2.74	n = 6
Dry density	96.0 lbs/ft ³ 1.54 g/cc	n = 1078
Clay Content (< 2 µm)		
Moisture as built (%)	Mean = 24.2%, Median = 23.6%, Range: 18 – 26%	n = 1078
Porosity as built (%)		
Rn Flux as built (Bq/m ² -s)	Mean = 0.049, range: 0.05 (DL) to 1.20	n = 130, Letter to NRC dated 1/16/2001

D.5 Lakeview, Oregon

The Lakeview disposal site is in Lake County at an elevation of about 4900 feet and approximately seven miles northwest of the town of Lakeview, Oregon (Figure D-4). Uranium was discovered in 1955 in the foothills about 17 miles northwest of town in low-temperature, Pliocene, hydrothermal volcanic deposits. The low-grade ore occurs in shallow uraninite and autunite lenses in a fault zone within volcanic tuff. Uranium was mined in underground and open pits at the White King and Lucky Lass mines from 1955 until 1965.

D.5.1 Uranium Ore Processing

The Lakeview Mining Company constructed and operated a mill 1.5 miles northwest of the town of Lakeview between 1958 and 1961. The mill processed approximately 130,000 tons of uranium ore, hauled from the White King and Lucky Lass mines, using a sodium chlorate and sulfuric acid leach process. When milling operations ceased in 1961, the processing site consisted of a 30-acre tailings pile, seven raffinate ponds that covered a total of 69 acres, and several mill buildings. A lumber company purchased the mill site property in 1978 and used some of the raffinate ponds and buildings in its operations. A lumber company continues to use some of the former mill buildings, and in 2016 a solar company purchased approximately 170 acres of the former processing site for a solar farm.

D.5.2 Remedial Action

DOE remediated the former mill site between 1986 and 1989 under Title I of UMTRCA. To reduce risks associated with contamination seeping into the alluvial aquifer, DOE trucked contaminated material from the tailings pile, evaporation ponds, buildings, and wind- and water-borne deposits from the mill site to the Lakeview disposal site on the Collins Ranch northwest of town. Windblown materials on property adjacent to the former mill site were included.

DOE excavated a hillside (Auger Hill) for the disposal cell, placed a portion of the tailings and other residual contaminated materials below the original grade, and used excavated materials to construct the engineered cover. Contaminated materials were placed on a 24-inch thick clay liner. Approximately 13 feet of low-activity contaminated material from evaporation ponds and windblown material at the mill site were placed above the tailings and immediately below the engineered cover. The disposal cell measures approximately 1050 feet by 800 feet, occupies an area of about 16 acres, and contains about 926,000 cubic yards of contaminated material with a total activity of 42 curies of ^{226}Ra .

The engineered cover consists of an 18-inch thick, low-permeability radon barrier placed over contaminated materials, a 6-inch thick sandy gravel bedding layer placed over the radon barrier, and a 12-inch thick rock riprap armor. DOE added a 6 inch layer of topsoil above the riprap layer on the top deck. Soil has since moved into rock interstices in some places. Topsoil and silt and clay for the radon barrier were excavated, processed, and stockpiled before tailings were placed in the disposal cell. Sand, gravel, and rock for the bedding and riprap layers were hauled from basalt quarries east of the disposal site. Some rock on the side slope has deteriorated since construction. Soil on the top deck was seeded with a mixture of native and introduced grasses (see Appendix E for current plant species composition and abundance data).

The low-permeability radon barrier was designed to limit release of radon to the atmosphere and water percolation into tailings. As with other sites, the radon barrier thickness was determined using the RAECOM code to limit radon flux to well below the NRC standard (see Section 2.2.1). The design compaction requirement for the radon barrier was 100% of maximum dry density and a moisture content of -1% to $+3\%$ of optimum. Three cover design attributes were intended to limit percolation into the tailings: (1) an average radon barrier saturated hydraulic conductivity less than 1×10^{-7} cm/s, (2) a high-conductivity bedding/drainage layer (>1.0 cm/s) to shed runoff, and (3) evapotranspiration of water stored in the grass-covered topsoil layer. Follow-up studies have shown that by 2003 the average saturated hydraulic conductivity had increased more than two orders of magnitude (Waugh et al, 2007).

See the Lakeview completion report (DOE 1991) for more information on disposal cell design specifications and testing results for all engineered cover materials.

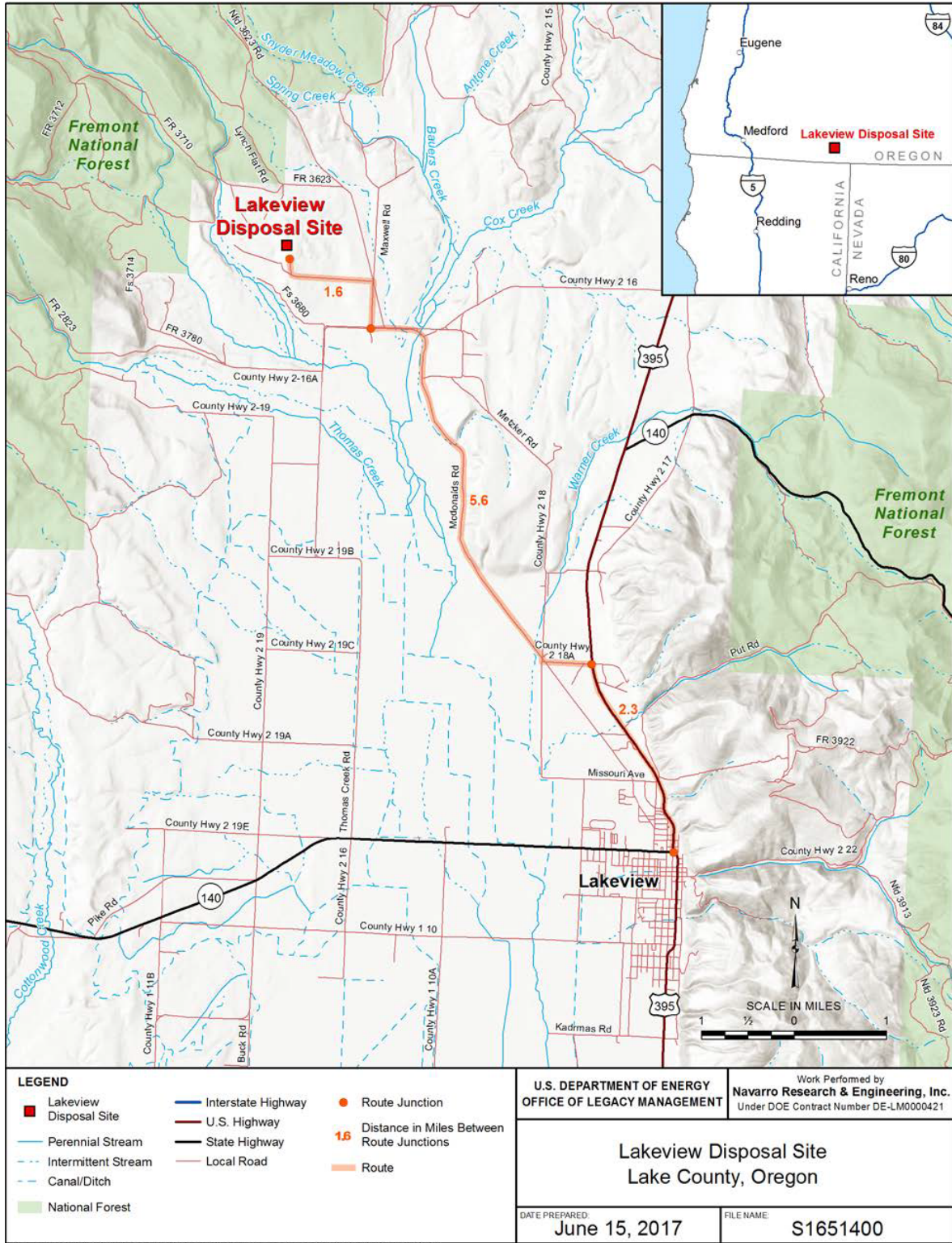


Figure D-4 Vicinity Map of Lakeview, Oregon, Disposal Site

D.6 References for Appendix D

- ARCO Coal Co Bluewater Mill Reclamation Plan, Volumes 1-3, 1990, 1099 pages, ADAMS Accession Number 9004050501, U.S. Nuclear Regulatory Commission, Washington DC.
- Atlantic Richfield Co., 1996, Completion Report for Reclamation of the Bluewater Mill Site, Vol. 1-4. ADAMS Accession Number ML16047A198, U.S. Nuclear Regulatory Commission, Washington DC.
- MK-Ferguson Company, (1991) Lakeview Oregon Final Completion Report, Volumes 1-6, Department of Energy Contract No. DE-AC04-83AL18796.
- MK-Ferguson Company, (1996) Falls City Texas Final Completion Report, Volumes 1-5, Department of Energy Contract No. DE-AC04-83AL18796.
- Petrotoomics Company (2001a), Tailings Reclamation Construction Completion Report, Volumes 1-3. USNRC ADAMS Accession Number ML020040278, U.S. Nuclear Regulatory Commission, Washington DC.
- Petrotoomics Company (2001b), Shirley Basin South letter report to NRC from Petrotoomics dated January 16, 2001, ADAMS Accession Number ML003774667, U.S. Nuclear Regulatory Commission, Washington DC.
- Rogers and Associates Engineering Corporation, (1987) Characterization of Borrow Soil at the Bluewater Uranium Mill Site, RAE-8721-1.
- U.S. Department of Energy, Legacy Management (accessed 2017a). Falls City, Texas, Disposal Site. Fact Sheet and other documents at <https://www.energy.gov/lm/falls-city-texas-disposal-site>
- U.S. Department of Energy, Legacy Management (accessed 2017b). Bluewater, New Mexico, Disposal Site. Fact Sheet and other documents at <https://www.energy.gov/lm/bluewater-new-mexico-disposal-site>
- U.S. Department of Energy, Legacy Management (accessed 2017c). Shirley Basin South, Wyoming, Disposal Site. Fact Sheet and other documents at <https://www.energy.gov/lm/shirley-basin-south-wyoming-disposal-site>
- U.S. Department of Energy, Legacy Management (accessed 2017d). Lakeview, Oregon, Disposal Site. Fact Sheet and other documents at <https://www.energy.gov/lm/lakeview-oregon-disposalprocessing-sites>

APPENDIX E

VEGETATION SUMMARY TABLES

Table E-1 Bluewater, New Mexico, Disposal Site Plant Species and Abundance¹

Genus Species ²	Common Name ²	Growth Form	Duration ³	Origin ⁴	Main Cell	Carbonate Cell	Acid Cell	RB ³ Analog	DP ³ Analog
<i>Achnatherum hymenoides</i>	Indian ricegrass	grass	P	N	T				
<i>Amaranthus polygonoides</i>	Tropical amaranth	forb	A	N				S	
<i>Amaranthus retroflexus</i>	Redroot pigweed	forb	A	NW					T
<i>Ambrosia artemisiifolia</i>	Ambrosia leaf bur ragweed	forb	A	NIW		T		T	
<i>Anemone tuberosa</i>	Tuber anemone	forb	P	N				T	T
<i>Aristida adscensionis</i>	Six-weeks threeawn	grass	A	N				T	T
<i>Aristida purpurea</i>	Purple threeawn	grass	P	N	S	T	T	S	
<i>Artemisia filifolia</i>	Sand sagebrush	subshrub/ shrub	P	N	T				
<i>Artemisia nova</i>	Black sagebrush	Subshrub/ shrub	P	N				S	S
<i>Artemisia tridentata</i>	Big sagebrush	shrub	P	N	T				
<i>Asclepias subverticillata</i>	Horsetail milkweed	forb	P	NW	T	T			
<i>Astragalus drummondii</i>	Drummond's milkvetch	forb	P	N			T		
<i>Atriplex canescens</i>	Fourwing saltbush	shrub	P	N	T	T	T	D	S
<i>Atriplex cuneata</i>	Valley saltbush	subshrub/ shrub	P	N	T		T	S	T
<i>Bassia scoparia</i>	Burningbush (kochia)	forb	A	IW	S	T			T
<i>Bouteloua curtipendula</i>	Sideoats grama	grass	P	N		T	T		
<i>Bouteloua eriopoda</i>	Black grama	grass	P	N	T	T			S
<i>Bouteloua gracilis</i>	Blue grama	grass	P	N	T	T	S	D	T
<i>Chamaesaracha coronopus</i>	Greenleaf five eyes	forb	P	N		T		T	
<i>Chamaesyce maculata</i>	Spotted sandmat	forb	A	N				T	
<i>Chamaesyce</i> sp.	Sandmat	forb	A	U				T	T

Table E-1 Bluewater, New Mexico, Disposal Site Plant Species and Abundance¹ (Continued)

Genus Species²	Common Name²	Growth Form	Duration³	Origin⁴	Main Cell	Carbonate Cell	Acid Cell	RB³ Analog	DP³ Analog
<i>Convolvulus arvensis</i>	Field bindweed	forb	P	IW	T				
<i>Conyza canadensis</i>	Canadian horseweed	forb	A	NW	T	T	T	T	
<i>Dasyochloa pulchella</i>	Low woollygrass	grass	P	N				T	T
<i>Descurainia pinnata</i>	Western tansymustard	forb	P	N					T
<i>Dimorphocarpa wislizeni</i>	Touristplant (spectaclepod)	forb	A	N	T			T	
<i>Elymus elymoides</i>	Bottlebrush squirreltail	grass	P	N	S	S			
<i>Eragrostis</i> sp.	Lovegrass	grass	A	U	T				
<i>Ericameria nauseosa</i>	Rubber rabbitbrush	shrub	P	N	T	T		S	
<i>Erigeron divergens</i>	Spreading fleabane	forb	B	N	T			S	T
<i>Eriogonum fasciculatum</i>	Eastern Mojave buckwheat	subshrub	P	N					T
<i>Glandularia bipinnatifida</i>	Dakota mock vervain	forb	P	N				T	
<i>Gutierrezia sarothrae</i>	Broom snakeweed	subshrub	P	N		T	T	S	S
<i>Helianthus annuus</i>	Annual sunflower	forb	A	NW	T			T	
<i>Hesperostipa comata</i>	Needle and thread	grass	P	N	T	T			
<i>Heterotheca villosa</i>	Hairy false goldenaster	forb	P	N	T			S	T
<i>Hordeum jubatum</i>	Foxtail barley	grass	P	NW	T				
<i>Juniperus osteosperma</i>	Utah juniper	tree	P	N				T	
<i>Kallstroemia parviflora</i>	Warty caltrop	forb	A	N				T	T
<i>Krascheninnikovia lanata</i>	Winterfat	subshrub/ shrub	P	N				S	S
<i>Lactuca serriola</i>	Prickly lettuce	forb	B	IW	S	T	T		
<i>Laennecia coulteri</i>	Coulter's horseweed	forb	A	N		T	T	T	T
<i>Lepidium</i> sp.	Pepperweed	forb	U	U			T		
<i>Leucelene ericoides</i>	Rose heath	forb	P	N				T	
<i>Lycium pallidum</i>	Pale desert-thorn	shrub	P	N				T	T

Table E-1 Bluewater, New Mexico, Disposal Site Plant Species and Abundance¹ (Continued)

Genus Species ²	Common Name ²	Growth Form	Duration ³	Origin ⁴	Main Cell	Carbonate Cell	Acid Cell	RB ³ Analog	DP ³ Analog
<i>Mirabilis multiflora</i>	Colorado four o'clock	forb	P	N	T	T			
<i>Monarda pectinata</i>	Pony beebalm	forb	A	N		T			T
<i>Muhlenbergia torreyi</i>	Ring muhly	grass	P	N			T	S	S
<i>Oenothera pallida</i>	Pale evening primrose	forb	P	N			T		
<i>Opuntia polyacantha</i>	Plains pricklypear	shrublike	P	N				S	
<i>Packera</i> sp.	Packera	forb	U	U		T			
<i>Pascopyrum smithii</i>	Western wheatgrass	grass	P	N		T			
<i>Phacelia integrifolia</i>	Gypsum phacelia	forb	P	N	T				
<i>Pleuraphis jamesii</i>	James' galleta	grass	P	N		T		S	S
<i>Portulaca oleracea</i>	Little hogweed	forb	A	IW				T	
<i>Psilostrophe</i> sp.	Paper flower	forb	U	U				T	
<i>Salsola tragus</i>	Russian thistle	forb	A	IW	S	S		T	T
<i>Senecio flaccidus</i>	Threadleaf ragwort	subshrub	P	N	T	T	T		
<i>Sphaeralcea coccinea</i>	Scarlet globemallow	forb	P	N	T		T	T	T
<i>Sporobolus cryptandrus</i>	Sand dropseed	grass	P	N	T		D	S	S
<i>Sporobolus giganteus</i>	Giant dropseed	grass	P	N	T	T		T	
<i>Stephanomeria exigua</i>	Small wire lettuce	forb	B	N	T				
<i>Symphotrichum ericoides</i>	White heath aster	forb	P	N			T	T	
<i>Tetradymia canescens</i>	Spineless horsebrush	subshrub/shrub	P	N					S
<i>Ulmus pumila</i>	Siberian elm	tree	P	IW	T				
<i>Xanthium strumarium</i>	Rough cocklebur	forb	A	NW				T	

¹ Data from DOE (2015) and researcher observations. Abundance classes and percentage foliar cover were D (dominant) >20% (25%); S (secondary) 5-20% (10%), T (trace) 0-5% (1%). Percentage values in parentheses were used to calculate foliar cover.

² Scientific and common names follow the U.S. Department of Agriculture (USDA) Natural Resources Conservation Service (NRCS) PLANTS Database (<https://plants.usda.gov/home>)

³ Indicates the duration of plant growth: P = perennial; A = annual; B = biennial; U = unknown; some species have several forms.

⁴ Indicates whether the plant is native to the region (N), introduced (I), both native and introduced (NI), and weedy or invasive (W). ⁵ RB = Radon Barrier, DP = Desert Pavement

Table E-2 Falls City, Texas, Disposal Site Plant Species and Abundance¹

Genus Species ²	Common Name ²	Growth Form	Duration ³	Origin ⁴	Topdeck Central	Topdeck Edges	Sideslope Rock	Adjacent Grassland	Borrow Area	Analog Site
<i>Ageratina herbacea</i>	Fragrant snakeroot	Forb	P	N			T			
<i>Amaranthus</i> sp.	Amaranth	Forb	A	U			T			
<i>Ambrosia artemisiifolia</i>	Annual ragweed	Forb	A	I		T	T			T
<i>Amblyolepis setigera</i>	Huisache daisy	Forb	A	N						
<i>Baccharis neglecta</i>	Dryland willow; Rooseveltweed	Shrub	P	N			T			
<i>Bothriochloa barbinodis</i>	Cane bluestem	Grass	P	N		T	T	T	C	C
<i>Bothriochloa ischaemum</i> var. <i>songarica</i>	King Ranch bluestem	Grass	P	IW	D	A		A		
<i>Bouteloua rigidisetata</i>	Texas grama	Grass	P	N				T		
<i>Bromus catharticus</i>	Rescuegrass	Grass	AP	IW						
<i>Calystegia macounii</i>	Macoun's false bindweed	Forb	P	N			T			
<i>Castilleja indivisa</i>	Texas paintbrush	Forb	A	N		T				
<i>Centaurium texense</i>	Lady Bird's centaury	Forb	A	N	T		T			
<i>Cirsium texanum</i>	Texas thistle	Forb	B	N		T		T	T	T
<i>Clematis</i> sp.	Clematis	Vine	P	U		T				
<i>Coreopsis lanceolata</i>	Lanceleaf tickseed; lance coreopsis	Forb	P	N	T	T		T		
<i>Coreopsis tinctoria</i>	Plains coreopsis	Forb	AP	N				T		
<i>Coronilla varia</i>	Crown vetch	Forb, Vine	P	IW						T
<i>Cynodon dactylon</i>	Bermuda grass	Grass	P	IW		T	T	T		O
<i>Daucus carota</i>	Queen Anne's lace	Forb	B	I	T	T		T	T	T
<i>Desmanthus leptolobus</i>	Prairie bundle flower	Forb	P	N					T	
<i>Diospyros texana</i>	Texas persimmon	Tree, Shrub	P	N		T				T
<i>Erigeron geiseri</i>	Geiser's fleabane	Forb	A	N					T	

E-4

Table E-2 Falls City, Texas, Disposal Site Plant Species and Abundance¹ (Continued)

Genus Species ²	Common Name ²	Growth Form	Duration ³	Origin ⁴	Topdeck Central	Topdeck Edges	Sideslope Rock	Adjacent Grassland	Borrow Area	Analog Site
<i>Eragrostis sessilispica</i>	Tumble lovegrass; windmill grass	Grass	P	N				T		
<i>Evax verna</i>	spring pygmy cudweed	Forb	A	N	T			T		
<i>Galium sp.</i>	Bedstraw	Forb	A	IW			T	T	O	O
<i>Gladularia bipinnatifida</i>	Prarie verbena	Forb	AP	N				T		T
<i>Helianthus annuus</i>	Common sunflower	Forb	A	N	T	T	T	T		T
<i>Herbertia lahue</i>	Prairienymph	Forb	P	N	T	T		T		
<i>Hordeum pusillum</i>	Little barley	Grass	A	N				T	O	
<i>Houstonia parviflora</i>	Greenman's bluet	Forb	A	N			T			
<i>Lesquerella gracilis</i>	Spreading bladderpod	Forb	AB	N	T			T		
<i>Limnodea arkansana</i>	Ozark grass	Grass	A	N	T			T	O	
<i>Linum rigidum</i>	Stiff flax	Forb	AP	N				T		T
<i>Lupinus texensis</i>	Bluebonnet; Texas lupine	Forb	A	N	T					
<i>Lygodesmia texana</i>	Texas skeletonplant	Forb	P	N			T			
<i>Melilotus officinalis</i>	Sweetclover	Forb	ABP	IW	T					
<i>Monarda punctata</i>	Spotted beebalm; horsemint	Forb	ABP	N						
<i>Nassella leucotricha</i>	Texas winter grass	Grass	P	N				T	O	O
<i>Oenothera speciosa</i>	Pinkladies	Forb	P	N	T	T		T	T	
<i>Oxalis sp.</i>	Wood sorrel	Forb	U	U						T
<i>Panicum coloratum</i>	Klein grass	Grass	P	I	T	T		T		
<i>Phalaris caroliniana</i>	Wild canary grass	Grass	A	N				T	O	
<i>Plantago virginica</i>	Pale-seed plantain	Forb	AB	N	T			T	O	T
<i>Prosopis glandulosa</i>	Honey mesquite	Tree, Shrub	P	N	T			T	T	
<i>Pyrrhopappus sp.</i>	False dandelion	Forb	U	U	T			T	T	

Table E-2 Falls City, Texas, Disposal Site Plant Species and Abundance¹ (Continued)

Genus Species ²	Common Name ²	Growth Form	Duration ³	Origin ⁴	Topdeck Central	Topdeck Edges	Sideslope Rock	Adjacent Grassland	Borrow Area	Analog Site
<i>Quercus</i> sp.	Live oak	Tree	P	N						T
<i>Ratibida columnifera</i>	Mexican hat; upright prairie coneflower	Forb	P	N					T	T
<i>Sabatia formosa</i>	Buckley's sabatia; rose-gentian	Forb	A	N	T			T		
<i>Sisyrinchium langloisii</i>	Roadside blue-eyed grass	Forb	P	N			T			T
<i>Solanum elaeagnifolium</i>	Trompillo; silver-leaf nightshade	Forb, Subshrub	P	N				T		
<i>Solanum ptychanthum</i>	West Indian nightshade	Forb	A	N			T			
<i>Sonchus arvensis</i>	Field sowthistle	Forb	P	I		T		T	T	T
<i>Sorghum halepense</i>	Johnson grass	Grass	P	IW		T				
<i>Sphaeralcea</i> sp.	Globemallow	Forb	P	Native						T
<i>Vachellia farnesiana</i>	Huisache; sweet acacia	Tree, Shrub	P	N				T	T	T
<i>Vachellia rigidula</i>	Blackbrush acacia	Tree, Shrub	P	N	T					O
<i>Verbena halei</i>	Slender vervain	Forb, Subshrub	P	N	T			T	T	T

E-10

¹ Data from DOE (2016a) and researcher observations. D (dominant) 75-95% (85%); A (abundant) 50-75% (62%); C (common) 25- 50% (38%); O (occasional) 5-25% (15%); T (trace) 0-5% (1%). Percentage values in parentheses were used to calculate foliar cover.

² Scientific and common names follow the U.S. Department of Agriculture (USDA) Natural Resources Conservation Service (NRCS) PLANTS Database (www.plants.usda.gov).

³ Indicates the duration of plant growth: P = perennial; A = annual; B = biennial; U = unknown; some species have several forms.

⁴ Indicates whether the plant is native to the region (N), introduced (I), both native and introduced (NI), and weedy or invasive (W).

Table E-3 Shirley Basin South, Wyoming, Disposal Site Plant Species and Abundance¹

Genus Species ²	Common Name ²	Growth Form	Duration ³	Origin ⁴	Seeded Cell	Wetland Cell	Rock Slope	Analog Site
<i>Agropyron cristatum</i>	Crested wheatgrass	Grass	P	I	S		S	T
<i>Agrostis stolonifera</i>	Creeping bentgrass	Grass	P	IW		S	T	
<i>Ambrosia artemisiifolia</i>	Annual ragweed	Forb	A	NIW				
<i>Antennaria microphylla</i>	Littleleaf pussytoes	Forb	P	N				T
<i>Artemisia frigida</i>	Prairie sagewort	Subshrub	P	NW				T
<i>Artemisia nova</i>	Black sagebrush	Shrub/subshrub	P	N				D
<i>Astragalus cicer</i>	Chickpea milkvetch	Forb	P	I	T		S	
<i>Atriplex canescens</i>	Fourwing saltbush	Shrub	P	N	T			
<i>Bromus inermis</i>	Smooth brome	Grass	P	I	S		T	
<i>Bromus arvensis</i>	Field brome	Grass	A	IW	T			
<i>Bromus tectorum</i>	Cheatgrass	Grass	A	IW	T	T	D	T
<i>Cardaria draba</i>	Hoary cress	Forb	P	I	T			
<i>Carex nebrascensis</i>	Nebraska sedge	Grasslike	P	N				
<i>Carex simulate</i>	Analog sedge	Grasslike	P	N		D		
<i>Carex vulpinoidea</i>	Fox sedge	Grasslike	P	N		T		
<i>Chenopodium album</i>	Lambsquarters	Forb	A	I	T			
<i>Cirsium arvense</i>	Canada thistle	Forb	P	IW	T	T		
<i>Cirsium ochrocentrum</i>	Yellowspine thistle	Forb	B/P	I	T			T

Table E-3 Shirley Basin South, Wyoming, Disposal Site Plant Species and Abundance¹ (Continued)

Genus Species ²	Common Name ²	Growth Form	Duration ³	Origin ⁴	Seeded Cell	Wetland Cell	Rock Slope	Analog Site
<i>Echinochloa crus-galli</i>	Barnyard grass	Grass	A	I				
<i>Eleocharis palustris</i>	Common spikerush	Grasslike	P	N		T		
<i>Elymus lanceolatus</i>	Thickspike wheatgrass	Grass	P	N	S			
<i>Elymus trachycaulus</i>	Slender wheatgrass	Grass	P	N		T		S
<i>Ericameria nauseosa</i>	Rubber rabbitbrush	Shrub/subshrub	P	N	T			
<i>Gnaphalium palustre</i>	Lowland cudweed	Forb	A	N				
<i>Grindelia squarrosa</i>	Curlycup gumweed	Forb	A/B/P	NW	T			
<i>Gutierrezia sarothrae</i>	Broom snakeweed	Subshrub/shrub/forb	P	N				T
<i>Heterotheca stenophylla</i>	Stiffleaf false goldenaster	Subshrub/forb	P	N				T
<i>Hordeum jubatum</i>	Foxtail barley	Grass	P	NW	T	S		
<i>Juncus arcticus</i> ssp. <i>littoralis</i>	Mountain rush	Grasslike	P	N		S		
<i>Juncus ensifolius</i>	Swordleaf rush	Grasslike	P	N		T		
<i>Koeleria macrantha</i>	Prairie Junegrass	Grass	P	N	T		T	S
<i>Machaeranthera canescens</i>	Hoary tansyaster	Forb	A/B/P	N	T			
<i>Medicago lupulina</i>	Black medick	Forb	A/P	IW	T	T		

Table E-3 Shirley Basin South, Wyoming, Disposal Site Plant Species and Abundance¹ (Continued)

Genus Species ²	Common Name ²	Growth Form	Duration ³	Origin ⁴	Seeded Cell	Wetland Cell	Rock Slope	Analog Site
<i>Medicago sativa</i>	Alfalfa	Forb	A/P	I	T			
<i>Melilotus officinalis</i>	Sweetclover	Forb	A/B/P	IW	T		T	
<i>Muhlenbergia filiformis</i>	Pullup muhly	Grass	A	N	T			D
<i>Nassella viridula</i>	Green needlegrass	Grass	P	N				T
<i>Opuntia polyacantha</i>	Plains prickly pear	Shrublike	P	NW				T
<i>Panicum dichotomiflorum</i>	Fall panicgrass	Grass	A	N	T			
<i>Pascopyrum smithii</i>	Western wheatgrass	Grass	P	N	S			T
<i>Phleum pratense</i>	Timothy	Grass	P	I		T		
<i>Phlox hoodii</i>	Spiny phlox	Forb	P	N				T
<i>Poa compressa</i>	Canada bluegrass	Grass	P	I			T	
<i>Poa secunda</i>	Sandberg bluegrass	Grass	P	N	T		T	S
<i>Polygonum aviculare</i>	Prostrate knotweed	Forb	A/P	I	T			
<i>Psathyrostachys juncea</i>	Russian wildrye	Grass	P	I	T			
<i>Puccinellia nuttalliana</i>	Nuttall's alkaligrass	Grass	P	N	T	T	T	
<i>Taraxacum officinale</i>	Dandelion	Forb	P	NIW	T			

Table E-3 Shirley Basin South, Wyoming, Disposal Site Plant Species and Abundance¹ (Continued)

Genus Species ²	Common Name ²	Growth Form	Duration ³	Origin ⁴	Seeded Cell	Wetland Cell	Rock Slope	Analog Site
<i>Thermopsis rhombifolia</i>	Prairie thermopsis	Forb	P	N	T			T
<i>Thinopyrum intermedium</i>	Intermediate wheatgrass	Grass	P	I	T			
<i>Thlaspi arvense</i>	Field pennycress	Forb	A	IW				

¹ Data from DOE (2013) and researcher observations. D (dominant) >20% (25%); S (secondary) 5-20% (10%), T (trace) 0-5% (1%). Percentage values in parentheses were used to calculate foliar cover.

² Scientific and common names follow the U.S. Department of Agriculture (USDA) Natural Resources Conservation Service (NRCS) PLANTS Database (<https://plants.usda.gov/home>)

³ Indicates the duration of plant growth: P = perennial; A = annual; B = biennial; U = unknown; some species have several forms.

⁴ Indicates whether the plant is native to the region (N), introduced (I), both native and introduced (NI), and weedy or invasive (W).

Table E-4 Lakeview, Oregon, Disposal Site Plant Species and Abundance¹

Genus Species²	Common Name²	Growth Form	Duration³	Origin⁴	North Top Slope	South Top Slope	Rock Side Slope	Analog Site
<i>Achillea millefolium</i>		forb	P	NI				T
<i>Agropyron cristatum</i>	Crested wheatgrass	Grass	P	I	T	T		T
<i>Allium acuminatum</i>	Wild onion	Forb	P	N	1	T		T
<i>Artemisia tridentata</i>	Big sagebrush	Shrub	P	N	S	T		S
<i>Balsamorhiza deltoidea</i>	Balsamroot	Forb	P	N				T
<i>Bromus tectorum</i>	Cheatgrass	Grass	A	IW	S	S		D
<i>Cirsium arvense</i>	Canada thistle	Forb	P	IW				T
<i>Crepis accuminata</i>	Hawksbeard	Forb	P	N	T	T		T
<i>Chrysothamnus viscidiflorus</i>	Green rabbitbrush	Shrub	P	N				S
<i>Elymus elymoides</i>	Squirreltail	Grass	P	N				T
<i>Elymus lanceolatus</i>	Thickspike wheatgrass	Grass	P	N	T	T	T	
<i>Elymus trachycaulus</i>	Slender wheatgrass	Grass	P	N	T	T	T	
<i>Ericameria nauseosa</i>	Rubber rabbitbrush	Shrub	P	N	S	T		
<i>Festuca idahoensis</i>	Idaho fescue	Grass	A	N	T	T		S
<i>Festuca ovina</i>	Sheep fescue	Forb	P	I	S	S		
<i>Juniperus occidentalis</i>	Western juniper	Tree	P	N				T
<i>Leymus cinereus</i>	Basin wildrye	Grass	P	N				T
<i>Lepidium ramosissimum</i>	Pepperweed	Forb	A	N	T	T		T

Table E-4 Lakeview, Oregon, Disposal Site Plant Species and Abundance¹ (Continued)

Genus Species ²	Common Name ²	Growth Form	Duration ³	Origin ⁴	North Top Slope	South Top Slope	Rock Side Slope	Analog Site
<i>Lupinus sp</i>	Lupine	Forb	P	N	S	S	T	T
<i>Purshia tridentata</i>	Antelope bitterbrush	Shrub	P	N	S	T	T	D
<i>Pascopyrum smithii</i>	Western wheatgrass	Grass	P	N	S	S		S
<i>Phleum pratense</i>	Timothy	Grass	P	I	T	T		
<i>Phacelia linearis</i>	Threadleaf phacelia	Forb	P	N				T
<i>Poa fendleriana</i>	Muttongrass	Grass	P	I	T	T		T
<i>Poa secunda</i>	Bluegrass	Grass	P	N	T	S		T
<i>Prunus virginiana</i>	Chokecherry	Tree	P	N				T
<i>Scenecio sp</i>	Groundsel	Forb	P	N	T	T		
<i>Tetradymia canescens</i>	Horsebrush	Shrub	P	N				T
<i>Zigadenus venenosus</i>	Deathcamas	Forb	P	N				T
<i>Tragopogon dubius</i>	Yellow salsify	Forb	A	I	T	T		

¹ Data from researcher observations. D (dominant) >20% (25%); S (secondary) 5-20% (10%), T (trace) 0-5% (1%). Percentage values in parentheses were used to calculate foliar cover.

² Scientific and common names follow the U.S. Department of Agriculture (USDA) Natural Resources Conservation Service (NRCS) PLANTS Database (<https://plants.usda.gov/home>)

³ Indicates the duration of plant growth: P = perennial; A = annual; B = biennial; U = unknown; some species have several forms.

⁴ Indicates whether the plant is native to the region (N), introduced (I), both native and introduced (NI), and weedy or invasive (W).

APPENDIX F

METHODS TO MEASURE RADON FLUX FROM EARTHEN RADON BARRIERS OVER URANIUM MILL TAILINGS AND IMPACT OF VARIABLES

F.1 INTRODUCTION

The Uranium Mill Tailings Radiation Control Act (UMTRCA) of 1978 requires disposal of residuals from beneficiation of uranium U-bearing ore (*aka* U mill tailings) in engineered disposal facilities with indefinite service life (UMTRCA 2013). UMTRCA disposal facilities employ a cover containing a radon (Rn) barrier – an engineered earthen barrier to control emission of gaseous radon, a radioactive decay product of U. Rn barriers are also expected to control percolation of water into the tailings in addition to Rn flux control. Radon barriers in UMTRCA covers are required to emit no more than 0.74 Bq/m²-s of ²²²Rn, and some Rn barriers have been required to have a saturated hydraulic conductivity no greater than 1x10⁻⁹ m/s. Measurements of Rn flux are made soon after construction of a Rn barrier to confirm that the flux criterion is met. However, radon fluxes are rarely measured for in-service Rn barriers. This paper focuses on the methods used to measure the Rn flux, with emphasis on evaluating the effectiveness of in-service Rn barriers.

Rn barriers typically are constructed from compacted fine-textured soil and generally have a thickness ranging from 0.4 m to 1.2 m (figure F-1). The Rn barrier in many disposal cells is overlain by a protection layer (0.3-0.6 m) intended to preclude damage by pedogenic processes (e.g., wet-dry and freeze-thaw cycling, biota intrusion). The protection layer may be covered with a vegetated surface layer or armored with an erosion layer (riprap) underlain by a bedding layer. Even with protective layers, pedogenic processes are known to induce macroscopic features (e.g., cracks, root structures, insect holes, etc.) that alter hydraulic properties (Benson and Othman 1993, Sutter et al. 1993, Othman et al. 1994, Benson et al. 1997, 2007, 2011; Khire et al. 1997, Albrecht and Benson 2001, Albright et al. 2006). This study was conducted as part of a larger project to evaluate if and how those same processes affect Rn fluxes from barriers in covers that have been in service two decades or more.

Radon flux typically is measured with a static flux chamber consisting of a polymeric or metallic chamber placed on the surface of the barrier. An activated carbon (AC) canister is placed within the chamber to measure the Rn concentration. Multiple measurements of Rn flux are made across the surface of the Rn barrier, and the average Rn flux is computed and compared to the flux criterion (EPA 1986, Stothoff 2012). A typical flux chamber is circular, with an inside diameter of 0.3-m (cross-sectional area, $A = 0.071 \text{ m}^2$). The AC in the canister typically is exposed to the gas within the chamber for 24 hr, and then sent to a laboratory for analysis of Rn concentration. However, other methods can be used to measure radon concentration in the flux chamber and to interpret the radon flux.

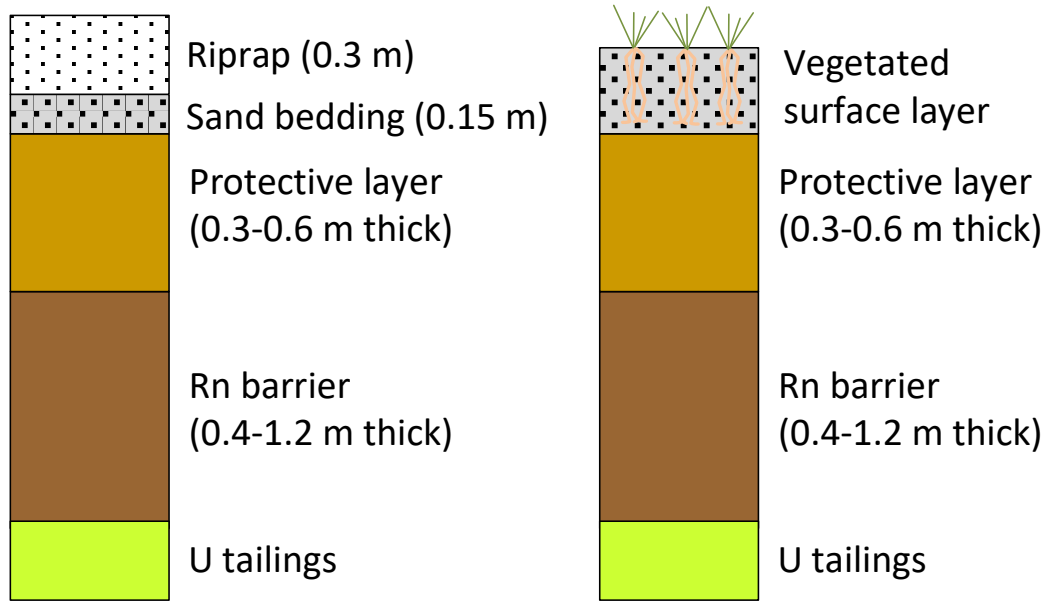


Figure F-1 Schematic of Cover Profiles used for Closure of Uranium Mill Tailings Disposal Facilities under UMTRCA

This Appendix describes the lab and field methods used for Rn flux measurements and a laboratory assessment of variables affecting Rn flux measurements, including flux chamber size, exposure time, relative humidity (RH) of the flux chamber, method to measure Rn concentration, and method to compute Rn flux. Field measurements of Rn flux made on the surface of an in-service Rn barrier at a U mill tailings disposal site in New Mexico are presented and compared to the laboratory observations. Recommendations are made for measuring Rn flux from earthen Rn barriers. A detailed assessment of accumulation chamber size is presented in Appendix G.

F.2 LABORATORY METHODS AND MATERIALS

F.2.1 Flux Chambers

Static flux chambers consist of an impermeable chamber sealed to the surface emitting Rn. The chamber is equipped with a device to measure Rn concentration in the headspace within the chamber (Fig. F-2) (Grossi et al. 2001, Gervino et al. 2004). Rn can be measured with an active or passive device. An active device provides a continuous record of Rn concentration within the chamber over time, generally by passing a sample of the gas through an electronic radon monitor (ERM) equipped with a solid-state alpha particle detector. A passive device accumulates Rn during the test and then is analyzed post testing, providing a single measurement of Rn concentration at the end of the test.

Four flux chambers with different cross-sectional areas were used in this study to evaluate the effect of chamber area on flux measurements. Cross-sectional area (A), internal volume (V), and volume-to-area ratio (V/A) for the chambers are summarized in Table F-1, which are designated as extra small, small, medium, and large. The extra small and small chambers were comprised of circular polyvinyl chloride (PVC) caps having a diameter of 0.15 m or 0.3 m. The area and volume of the “small” chamber were selected to be similar to flux chambers commonly

used in practice at UMTRCA sites. Two different medium chambers were used. The initial medium chamber was a rectangular (1.2 m × 0.5 m) polyethylene box used for laboratory experiments. The subsequent medium chamber, used in the field, was a rectangular (0.8 m × 0.4 m) fiberglass container. The “large” chamber was a fiberglass chamber with a square cross-section (1.2 m × 1.2 m). In select tests using the large chamber, a small battery-powered fan was placed inside the chamber to create a well-mixed internal environment. The fan had no measurable effect on Rn concentrations (Stefani 2016).

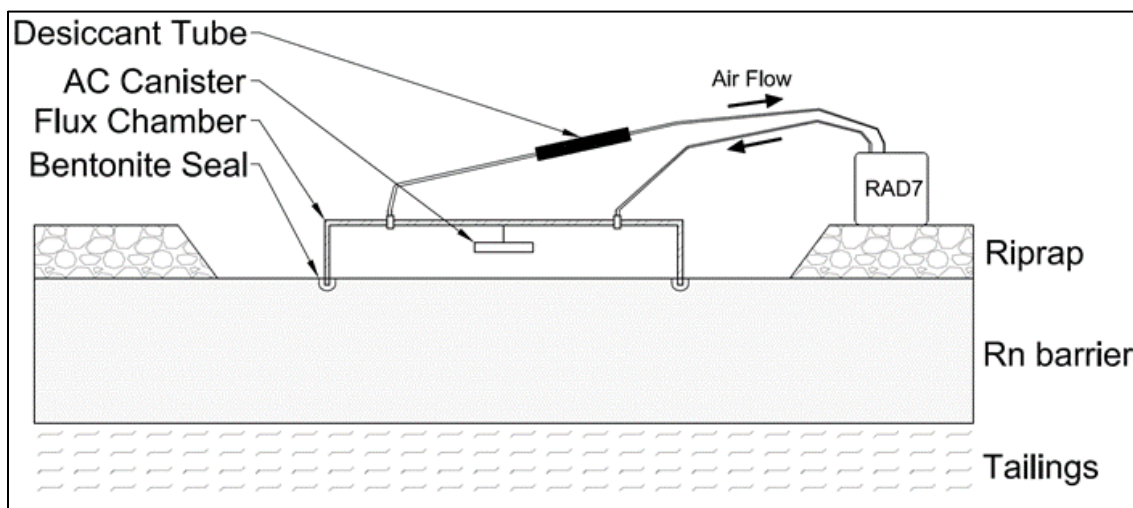


Figure F-2 Schematic of a Flux Chamber Installed on a Rn Barrier with an Activated Carbon (AC) Canister and a RAD7 Radon Monitor

Table F-1 Radon flux chambers used in laboratory and field testing program

Chamber	Area, A (m ²)	Volume, V (m ³)	V/A (m)
Extra Small	0.020	0.002	0.083
Small	0.071	0.011	0.155
Medium-Laboratory	0.590	0.204	0.347
Medium-Field	0.282	0.056	0.199
Large	2.320	0.352	0.152

F.2.2 Activated Carbon (AC) Canisters

Passive measurements of Rn concentration were made using activated carbon (AC) canisters from Radon Testing Corporation of America (RTCA, Elmsford, NY). These canisters, which are analogous to canisters used in residential Rn sensing applications (Countess 1976, Gervino et al. 2004), were 100-mm-diameter open-faced canisters containing 90 g of AC (National Radon Safety Board device code = 10331). Canisters exposed in the flux chambers were sealed and shipped to RTCA for analysis of adsorbed Rn concentration.

F.2.3 Electronic Radon Monitor (ERM)

Continuous ERMs contain a solid-state alpha detector to measure disintegrations of Rn alpha progenies over a designated time period. RAD7 ERMs (DurrIDGE Company, Inc. Billerica, MA) were used in this study. The RAD7 has been used extensively in Rn emanation rate studies for building materials (Chao et al. 1997, Tuccimei et al. 2006, Vargas and Ortega 2007, Ujic et al. 2008). A pump in the RAD7 continually cycles air from the sampling environment through the detector (Fig. F-2). The RAD7 distinguishes between different energy levels so that only Rn is accounted for in the alpha particle monitoring. A flow rate of 800 mL/min and a sampling frequency (cycle time) of 15 min to 1 h were used for the majority of the tests.

The RAD7 was connected to influent and effluent ports on the flux chambers to pump gas in a continuous circuit from the chamber, through the RAD7, and back into the chamber (Fig. F-2). Water vapor was removed from the gas prior to entering the RAD7 using a desiccant tube, and Rn progeny were removed from the influent air using a fine inlet filter. Alpha counts recorded by the RAD7 were converted to Rn concentration using a calibration provided by the manufacturer. The influent and effluent sampling ports for the ERM were placed at various locations on the flux chamber to determine if sampling location influenced the Rn measurement. Location of the sampling ports had no measurable effect on Rn concentration (Stefani 2016). All ERMs were calibrated by the manufacturer immediately prior to the study.

F.2.4 Rn Flux Computation

Computing Rn flux from Rn concentration measurements differs depending on whether an active or passive device is used to measure Rn concentration. An active device provides a time series of Rn concentration (C) measurements in the chamber, and the relationship between C and time (t) is known as a Rn “buildup” curve (Fig. F-3). Mass balance on the control volume within the chamber yields the following partial differential equation (Chao et al. 1997, Tuccimei et al. 2006, Ujic et al. 2008):

$$\frac{dC}{dt} = -\lambda C - DC + \frac{J_0 A}{V} + \frac{q(C_0 - C)}{V} \quad (1)$$

where C is Rn concentration, t is time, λ is the Rn decay coefficient, D is the radon diffusion coefficient, J_0 is the initial Rn flux, A (m^2) is the cross-sectional area of the flux chamber, V is the internal volume of the chamber and associated equipment including the analytical chamber in the RAD7 (800 cc), q is the chamber leakage rate, and C_0 is the background Rn concentration. The decay term ($-\lambda C$) accounts for the short half-life of ^{222}Rn (3.8 d) within the chamber. The back-diffusion term ($-DC$) accounts for the progressive reduction in radon flux as the Rn concentration increases (“builds up”) inside the chamber, and reduces the concentration gradient driving the Rn flux. The leakage term [$q(C_0 - C)/V$] accounts for potential exchange between the atmosphere inside the chamber and the external environment (Chao et al. 1997). The initial Rn flux (J_0) is reported as the Rn flux from the barrier and corresponds to the condition when back diffusion is negligible.

For an accumulation chamber initially purged of Rn ($C=0$ at $t=0$), the solution of Eq. 1 for a flux chamber is (Chao et al. 1997):

$$C(t) = \frac{J_0 A + qC_0}{V\lambda_{\text{eff}}} (1 - e^{-\lambda_{\text{eff}} t}) \quad (2)$$

where λ_{eff} is an effective decay constant that combines the effects of Rn decay, back diffusion, and chamber leakage:

$$\lambda_{eff} = \lambda + D + \frac{q}{V} \quad (3)$$

When back diffusion is insignificant early in the accumulation period, the initial slope (M_e) of the buildup curve can also be used to compute the Rn flux (J_0):

$$J_0 = \left(M_e - \frac{qC_0}{V} \right) \left(\frac{V}{A} \right) \quad (4)$$

For flux measurements with the ERM, the Rn flux was determined two ways: (1) by fitting Eq. 2 to a continuously measured buildup curve using multivariable non-linear least-squared regression to optimize the parameters J_0 and λ_{eff} and (2) by determining the initial slope M_e in the linear portion of the buildup curve and computing J_0 with Eq. 4. Examples of both methods are illustrated in Fig. F-3. The dashed line corresponds to the initial linear slope (M_e) and the solid line is the best fit of Eq. 2 obtained by non-linear least-squares regression.

Passive measurements of Rn concentration (e.g., AC canister) provide a single point of Rn concentration at the time when the canister is removed and sealed (the exposure time). For AC measurements, the flux is computed as:

$$J_0 = \left(\frac{C_{AC}}{t_e} \right) \left(\frac{V}{A} \right) \quad (5)$$

where C_{AC} is the concentration of Rn from the AC canister and t_e is the exposure time.

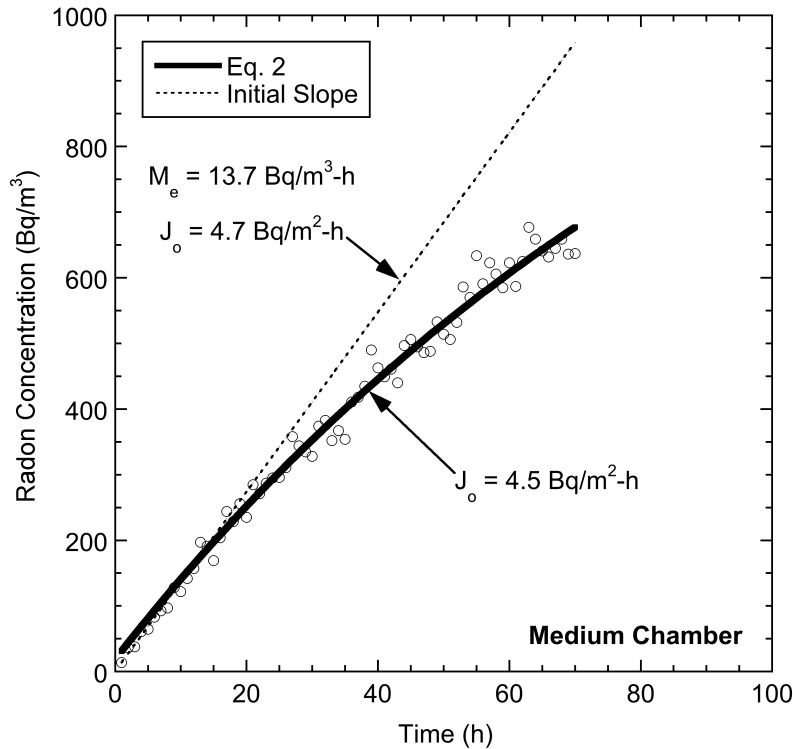


Figure F-3 Rn Buildup Curve with ERM and Granite Source. Rn Flux is Determined by Initial Slope (Dashed Line) and Fit of Eq. 2 (Heavy Solid Line)

F.2.5 Radon Source

Two materials were used as radon sources in the laboratory: Wisconsin Red Granite aggregate obtained from a mine near Wausau, Wisconsin and the reinforced concrete floor in the laboratory. The granite aggregate was washed to remove fines, dried, and sieved to remove particles passing the US No. 4 standard sieve (4.75 mm), resulting in particle sizes ranging from 4.75 mm to 40 mm. Both materials provided low levels of Rn emanation comparable to the low Rn fluxes typical of UMTRCA site conditions. Many common building and architectural materials, including concrete and granite, have consistent and measurable radon emanation rates (e.g., Chao et al. 1997, Daoud and Renken 1999).

F.3 RESULTS OF LABORATORY EXPERIMENTAL PROGRAM

Laboratory experiments were conducted to evaluate the effect of scale of flux chambers, to compare concentrations and fluxes measured using AC canisters and the ERM, and to evaluate the impact of relative humidity on AC measurements. In addition these tests allow a measurement of method reproducibility. Experiments were conducted directly on the concrete floor or on a layer of granite aggregate spread on the laboratory floor. The granite aggregate was separated from the concrete laboratory floor using a 25- μm polyethylene sheet. Flux chamber size, Rn source, time of exposure, and Rn measurement technique were varied to evaluate how they affected the flux measurement. The same mass-to-flux area (22.6 kg/m², ratio of granite aggregate mass to cross-sectional area of flux chamber) was used for all tests with granite as the Rn source. Because radon exhalation rates for granular materials depend on grain size (Tuccimei et al. 2006), the granite aggregate used in these experiments was washed to remove fines, dried, and sieved to remove particles passing the US No. 4 standard sieve (4.75 mm) so that a similar material would be used in all tests. The remaining material used for the experiments had particle sizes ranging from 40 mm to 4.75 mm.

Preliminary tests were conducted with the large flux chamber, a 30-mm-thick layer of granite aggregate, and a 48-h exposure time using the ERM for measuring Rn concentration. These tests indicated that the granite produced J_0 ranging from 1.7 – 8.0 Bq/m²-h, with an average of 3.3 Bq/m²-h. This range is consistent with emanation rates reported for similar materials (e.g., Chao et al. 1997, Chao and Tung 1999, Tuccimei et al. 2006). Subsequent tests were conducted using the extra small, small, medium, and large flux chambers using both the ERM and the AC to measure Rn concentration. AC canisters were placed directly on top of the Rn source (concrete slab or granite aggregate), whereas the ERM was placed outside the chamber with gas from the chamber circulated through the ERM continuously (Fig. F-2).

F.3.1 Concentration Build-Up Curves

Typical Rn build-up curves measured using the ERM are shown in Fig. F-4 for the extra small, small, medium, and large flux chambers placed on granite. Time for the concentration to reach a steady state and the ultimate concentration in the chamber increases with chamber size. Radon concentrations in the extra small and small chambers typically approached steady state in laboratory tests after about 60 h, whereas steady-state in the large chamber required as long as 7 days. However, reaching steady-state concentration is not needed to assess the initial Rn flux, and most tests were terminated before concentrations reached steady state.

F.3.2 Radon Flux from Initial Slope vs. Buildup Curve

Radon fluxes computed by fitting Eq. 2 to the build-up curve are compared to fluxes computed from the linear fit to the initial slope (Eq. 4) in Fig. F-5. Fluxes from the fit of Eq. 2 range from 73% (small chamber) to 98% (large chamber), on average, of the flux obtained from the initial slope of the build-up curve for the tests on granite. For the tests on concrete, fluxes obtained from the fit of Eq. 3 range from 74% (small chamber) to 101% (extra small chamber) of the flux obtained from the initial slope, on average. The most similar fluxes were obtained with the largest chambers (95% for tests on granite; 98% for tests on concrete, on average). The overall average was 86% for the tests on granite, and 90% for the tests on concrete, although for individual tests the range was from 43% (granite, small chamber) to 212% (one test on concrete small chamber, all others $\leq 124\%$). The Rn concentrations in the lab experiments were very low compared to typical concentrations in the field, as a result this comparison was repeated with field data and is discussed later.

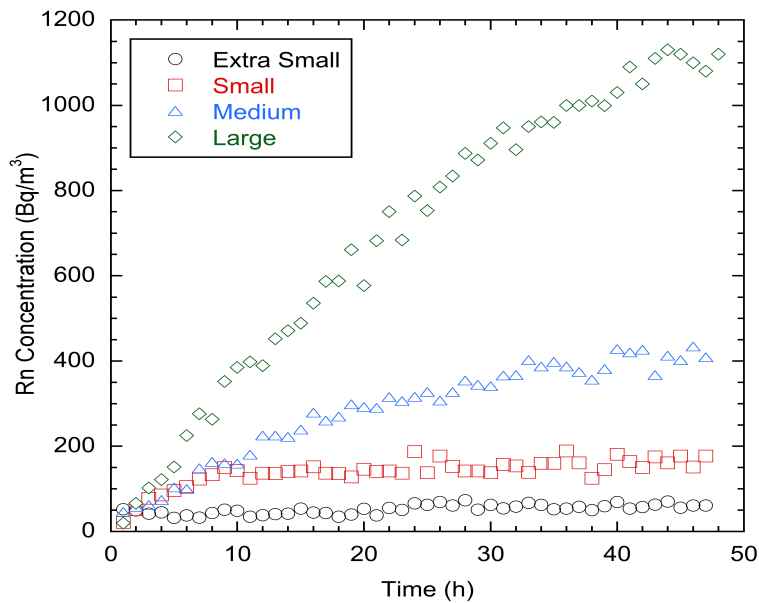


Figure F-4 Rn Buildup Curves from Granite Source Measured with ERM in Chambers of Four Sizes

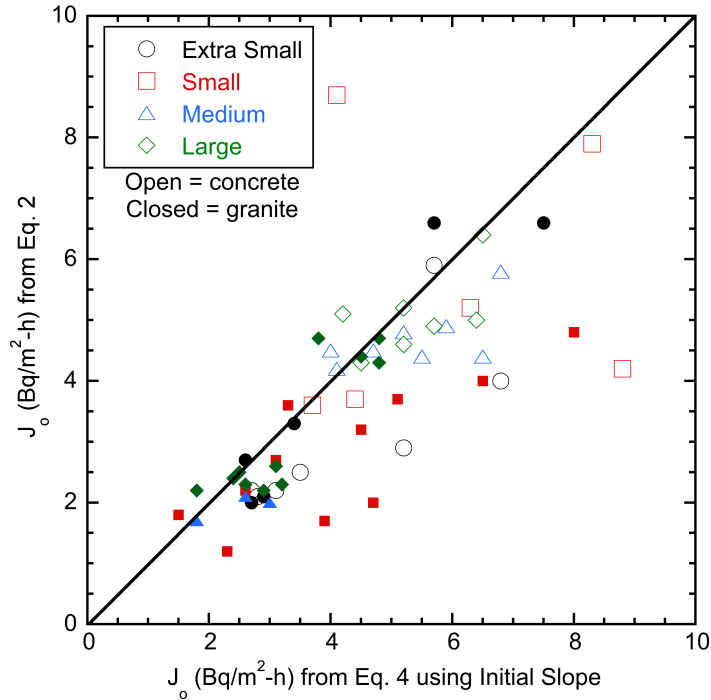


Figure F-5 Comparison of Rn Flux Computed from Fit of Eq. 2 to ERM data and by Eq. 4 Using Linear Fit to Initial Slope of ERM data

F.3.3 Measurement Variability and Chamber Size

A preliminary series of tests was conducted to assess reproducibility of measurements obtained using the RAD7 (Stefani et al., 2017). Wisconsin Red Granite and the concrete lab floor were used as Rn sources. Four different chamber sizes were used to quantify the effect of flux area (A) on the Rn flux measurement and measurement reproducibility. Test duration ranged from 18 to 96 h and a 1-h automatic cycle time was used to obtain readings from the RAD7.

Table F-2 summarize results obtained using the granite Rn source and by direct placement of flux chambers on the concrete laboratory floor. Mean flux is calculated from the average of (n) measurements with standard deviation 1-sigma. Results indicate that measurement reproducibility using the RAD7, Rn sources, and procedures described above is weakly chamber size dependent. While the average fluxes are similar for each chamber size, the measurement variability is larger for the extra small chambers, as indicated by higher 1-sigma values. Overall, these flux values are very low compared to the field measurements made at the four disposal sites in this study and in many cases are below the background field fluxes. This suggests that the reproducibility of the field measurements would be better than indicated in Table F-1 but additional factors such as temperature variation, wind, barometric pressure, and preferential pathways likely influence field measurements.

Table F-2 Reproducibility of Rn Flux Measurements at Low Fluxes

Chamber Size	Area m ²	Granite Mean Flux Bq/m ² /s (n)	1- Sigma	Concrete Mean Flux Bq/m ² /s (n)	1-Sigma
Extra Small	0.018	0.0011 (6)	0.00059 55%	0.0009 (7)	0.00039 45%
Small	0.071	0.0008 (11)	0.00032 40%	0.0015 (6)	0.00062 40%
Medium	0.590	NA	NA	0.0013 (7)	0.00014 11%
Large	2.323	0.0009 (12)	0.00030 36%	0.0014 (8)	0.00018 13%
All		0.0009 (29)	0.00039 44%	0.0013 (28)	0.00043 33%

Radon flux is shown vs. flux chamber size in Fig. F-6 for the tests on concrete (Fig. F-6a) and granite aggregate (Fig. F-6b). Each solid circle corresponds to a unique test, with replicates at each chamber size. The larger open squares are the arithmetic mean flux for each chamber size. Average fluxes measured for the concrete source were comparable for the small, medium, and large chambers (5.0 – 5.7 Bq/m²-h), with the smallest chamber yielding a lower flux (2.8 Bq/m²-h). For the granite, the average flux for all four chambers was comparable (2.2 - 3.4 Bq/m²-h).

Variability in the Rn flux decreased systematically with increasing chamber size, with standard deviations for the tests on concrete as large as 1.52 Bq/m²-h for the small chamber and 0.64 Bq/m²-h for the large chamber. Similarly, for the granite source, the standard deviations decreased from 1.45 Bq/m²-h for the extra small chamber to 0.32 Bq/m²-h for the medium chamber and 1.01 Bq/m²-h for the large chamber. This reduction in variability with increasing chamber size reflects greater spatial averaging in the larger chambers (Vanmarcke 1983). Fluxes with larger chambers may not reflect localized anomalies from macroscopic features that result in preferential pathways, but are anticipated to be more representative of the larger field-scale condition.

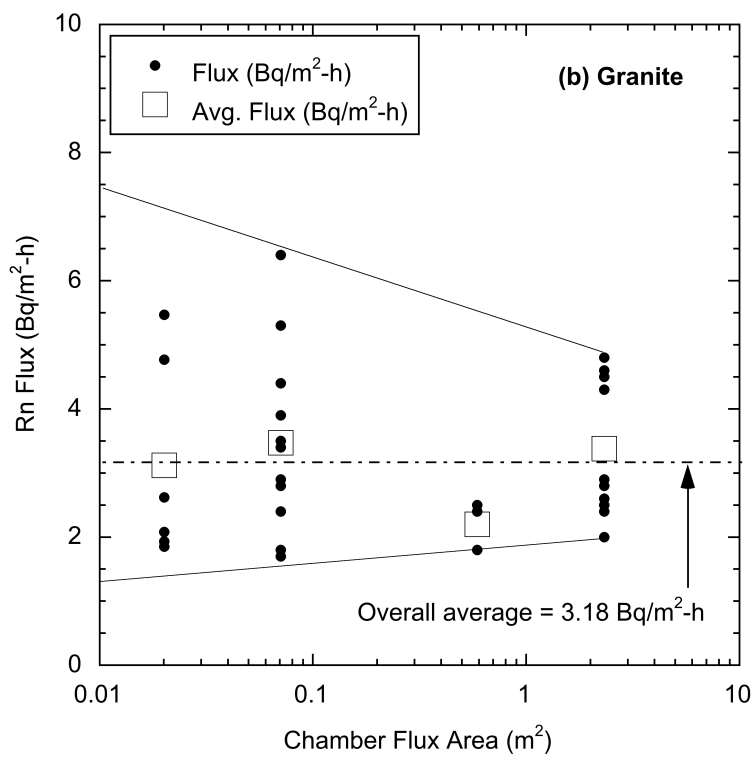
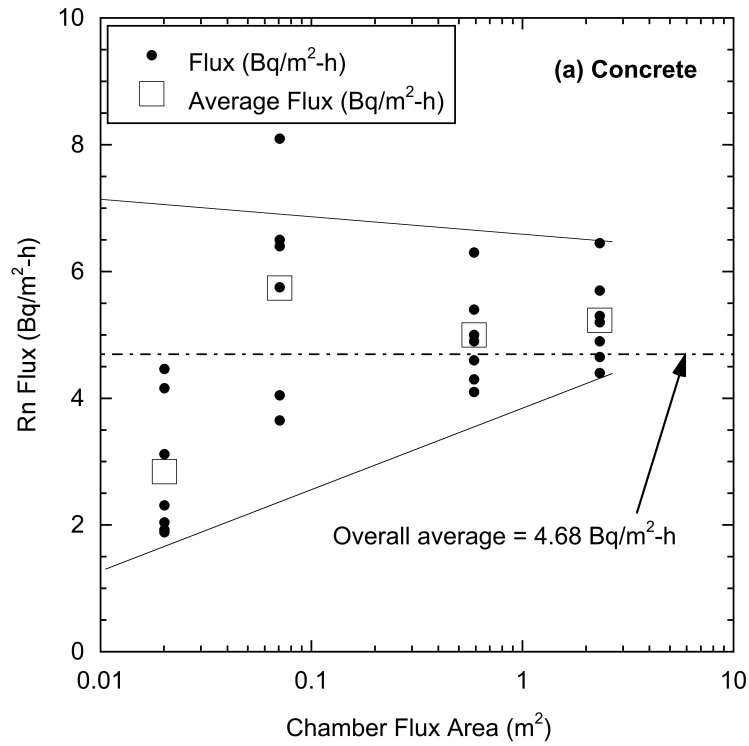


Figure F-6 Rn Flux Measurements Made Using Various Size Chambers with Source as (A) Concrete Floor and (B) Granite

F.3.4 Continuous vs. Passive Radon Measurement

Radon concentrations from five replicate tests are shown in Fig. F-7 that were recorded simultaneously with the ERM (continuous measurements) and an AC canister (single passive measurement) in a large flux chamber over granite. The exposure time was approximately 50 hr. All Rn concentrations measured with the AC canisters were corrected for relative humidity (average RH in the chamber during the tests was 47%) using the method in Stefani (2016). Good agreement generally was obtained between replicates made with the ERM and the replicates made with AC. However, the Rn concentrations measured with the AC canisters were consistently lower than Rn concentration measured at the same exposure time using the ERM. On average, Rn concentrations from the AC canisters were 59.4% of the concentration measured with the ERM.

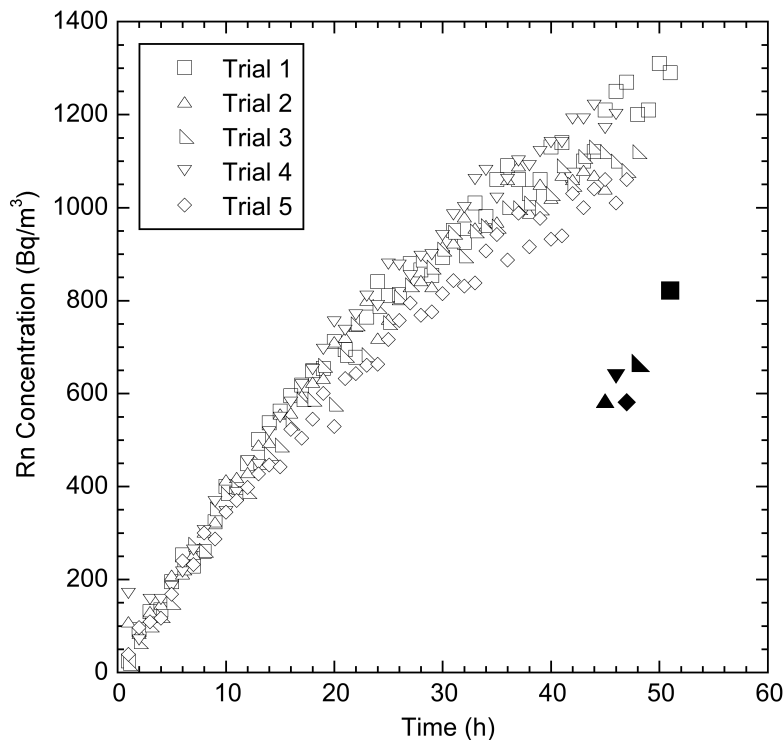


Figure F-7 Five Replicate Tests on Concrete Source with Large Flux Chamber with Radon Measured with ERM (Open Symbols) and AC (Closed Symbols)

Additional comparisons of Rn concentrations measured with the ERM and AC were made using different chamber sizes and different exposure times. Rn concentrations are shown in Fig. F-8 that were measured with the ERM and AC in the four chamber sizes (Fig. F-8a) for an exposure time of 48 h and in the large flux chamber for five different exposure times (12, 24, 48, 72 and 96 h) (Fig. F-8b). Granite was used as the source in each case. Regardless of chamber size, the Rn concentration measured at 48 hr exposure time using the AC canister was $58.0\% \pm 7.2\%$ of Rn concentrations measured using the ERM (Fig. F-9a). For different exposure times (Fig. F-8b), the Rn concentrations with AC were 55%, 47%, 58%, 59%, and 56% (short to long exposure time) of the Rn concentrations measured at the same time, with an average of 55%. These differences in concentration between the ERM and AC are all very similar, regardless of chamber size or exposure time.

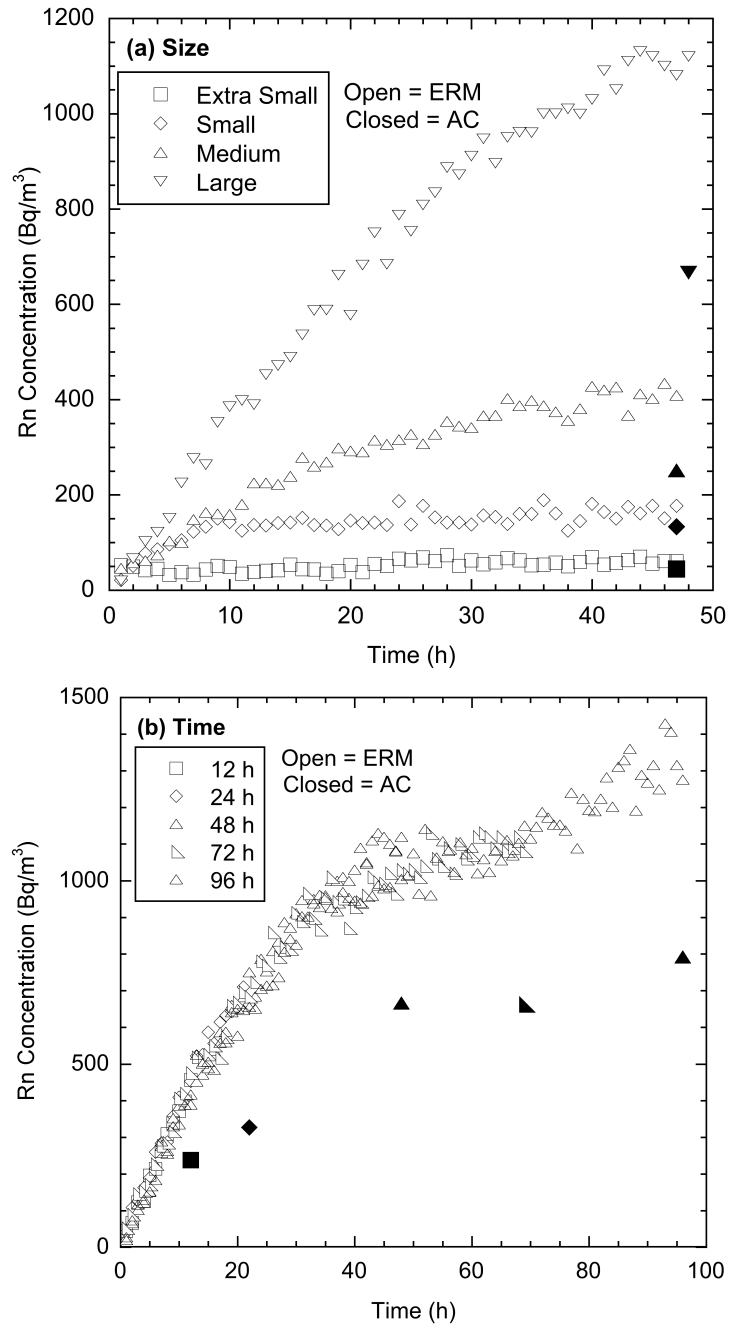


Figure F-8 Rn Concentrations from Concrete Source Measured with ERM (Open Symbols) and AC (Closed Symbols): Varying Chamber Size (A) and Exposure Time (B) with Large Flux Chamber

Fluxes from the concrete sources computed with the AC and ERM data are compared in Figure F-9a. Fluxes were computed from the ERM data using Eq. 2 and with Eq. 5 for the AC data. The data are from experiments conducted using chambers of different size and tests of different duration. In all cases, the flux computed from the AC data is lower than the flux computed from

the ERM data. On average, the flux is underestimated approximately three fold using the AC data.

The flux is underestimated from the AC data due to two factors: the underestimate of Rn concentration by the AC technique, and the non-linearity in the buildup curve that is not captured with the single Rn concentration measured with AC. These effects are illustrated in Fig. F-9b using data from the 72-h test conducted with the concrete source and a large flux chamber (reported in Fig. F-9b). In this example, not capturing the non-linearity in the slope of the buildup curve reduces the flux by a factor of 2.8 ($6.6 \div 2.4 = 2.8$) and the underestimate in Rn concentration reduces the flux by a factor of 1.7 ($2.4 \div 1.4 = 1.7$).

F.3.5 Effects of Water Vapor

The effect of water vapor on Rn concentration measured with AC was explored as a mechanism causing the underestimation of Rn concentration by the AC. AC canisters were equilibrated over a range of RH by placing the containers in the headspace over saturated salt solutions in sealed chambers. Salt solutions were used with corresponding RH ranging from 10 to 90%. Each AC canister was equilibrated in the headspace for 2 d, and then placed on top of a layer of granite in a large flux chamber. After 48 h of exposure in the flux chamber, the canister was sealed and shipped to the laboratory for analysis. Relative humidity inside the flux chamber was recorded using a solid-state RH sensor (Model 42275, Extech, Waltham, MA) placed in the chamber.

The AC gained moisture with increasing RH, which resulted in a reduction in counts (analogous to concentration) for the same exposure condition (Fig. F-10a). The Rn buildup curve measured with the ERM is shown in Fig. F-10b along with the Rn concentration measured by the AC after 48 hr of exposure. The error bars for the Rn concentration from AC represent the minimum and maximum Rn concentrations measured with AC, which corresponded to the highest and lowest RH. Rn concentrations from the AC were corrected for moisture gained using the method in Stefani (2016). Even with the correction, the average Rn concentration from the AC canister value (solid circle) was 59% of the Rn concentration measured with the ERM, regardless of the moisture gained by the AC. This suggests that factors other than water vapor are responsible for differences in Rn concentration measured with the ERM and AC, potentially including kinetic limitations to Rn transport and sorption in the AC, surficial moisture suppressing sorption, and sorption capacity limitations.

F.4 FIELD TESTS

Field tests were conducted on the Rn barrier in the final cover of the Bluewater uranium disposal facility, approximately 15 km northwest of Grants, New Mexico (Fig.F-11a). The disposal facility has four disposal areas. Data from flux chambers installed in a test pit at the main tailings pile (MTP) are presented here. The MTP has a surface area of 143 ha and contains 20.9 Tg of tailings with 414.4 TBq of ^{226}Ra (Atlantic 1996). A schematic of the cover profile at the MTP is in Fig. F-11b. The profile consists of a rip rap surface layer (200 mm) for erosion control underlain by a 750-mm-thick Rn barrier constructed from low plasticity clayey sand. The cover was completed in 1995; the tests described in the following were conducted in 2016 after 21 years of service.

The test pit was approximately 2 m × 4 m and was excavated to the surface of the Rn barrier. After flux measurements were obtained at the top of the Rn barrier, the excavation was extended downward so that flux measurements could be taken directly on the surface of the underlying waste. Rn buildup curves from the surface of the Rn barrier and from the surface of

the waste measured with the ERM are shown in Fig. F-12. The Rn concentration buildup from the flux chamber on the waste is significantly greater and faster than Rn buildup on the surface of the Rn barrier, indicating the Rn barrier reduces the Rn flux significantly. The buildup from the large chamber on the surface of the barrier is appreciably larger than the flux from the other three chamber sizes, suggesting that the large chamber captured a preferential pathway for Rn diffusion that was not captured by the other chambers.

Rn concentrations measured with AC are compared in Fig. F-14 with Rn data obtained with the ERM for the small and large chambers. As with the laboratory experiments, lower Rn concentrations were measured in the field with AC relative to the ERM. Rn concentrations from the AC are 90.7% (small chamber) and 69.6% (large chamber) of the Rn concentrations obtained from the ERM for the same exposure time (18 hr). Fluxes computed from the ERM data using Eq. 2 are approximately the same for both chambers (0.026 Bq/m²/s for the small chamber, 0.024 Bq/m²/s for the large chamber), whereas fluxes from the AC data computed with Eq. 4 vary with chamber size (0.006 Bq/m²/s for the small chamber, 0.013 Bq/m²/s for the large chamber). The ratio of the fluxes computed with the AC data to the flux computed with the ERM (J_{AC}/J_{ERM}) is 0.23 for the small chamber and 0.54 for the large chamber, which is comparable to the ratio of these fluxes observed in the laboratory experiments (Fig. F-10a). As observed in the laboratory experiments, the AC data from the field yield a lower flux because the Rn concentration is under estimated and the non-linearity of the buildup curve is not captured.

The underestimate of Rn flux using AC data can be reduced using a shorter test time and a larger chamber, which reduces the impact of non-linearity in the buildup curve and the deviation between Rn concentrations (Fig. F-9). This effect is illustrated in Fig. F-13b using field data from the Bluewater disposal facility and Rn concentrations measured at shorter and longer times with the ERM and AC canisters (two canisters per chamber). These findings indicate that field measurements of Rn flux measurements made using AC should be conducted in larger chambers ($A > 2 \text{ m}^2$ and $V/A > 0.15 \text{ m}$) and for shorter test times ($< 4 \text{ h}$) to minimize the underestimate in Rn flux.

As discussed above field measurements were made simultaneously using both methods in the same chamber. Fluxes determined by each method are compared in Figure F-14 for each of the sites. For Falls City and Bluewater the relationship is linear with R^2 values slightly greater than 0.8. However the slopes were very different, one is 13.4 while the other is 1.4. The Shirley Basin and Lakeview sites showed poor correlation. The fluxes at these sites were low, especially Lakeview and the poor correlation likely reflects a detection limit issue for the AC method which is estimated to be around 0.01 or 0.02 Bq/m²/s. AC provides only a single concentration data point and adsorption of Rn onto AC is sensitive to competition by moisture.

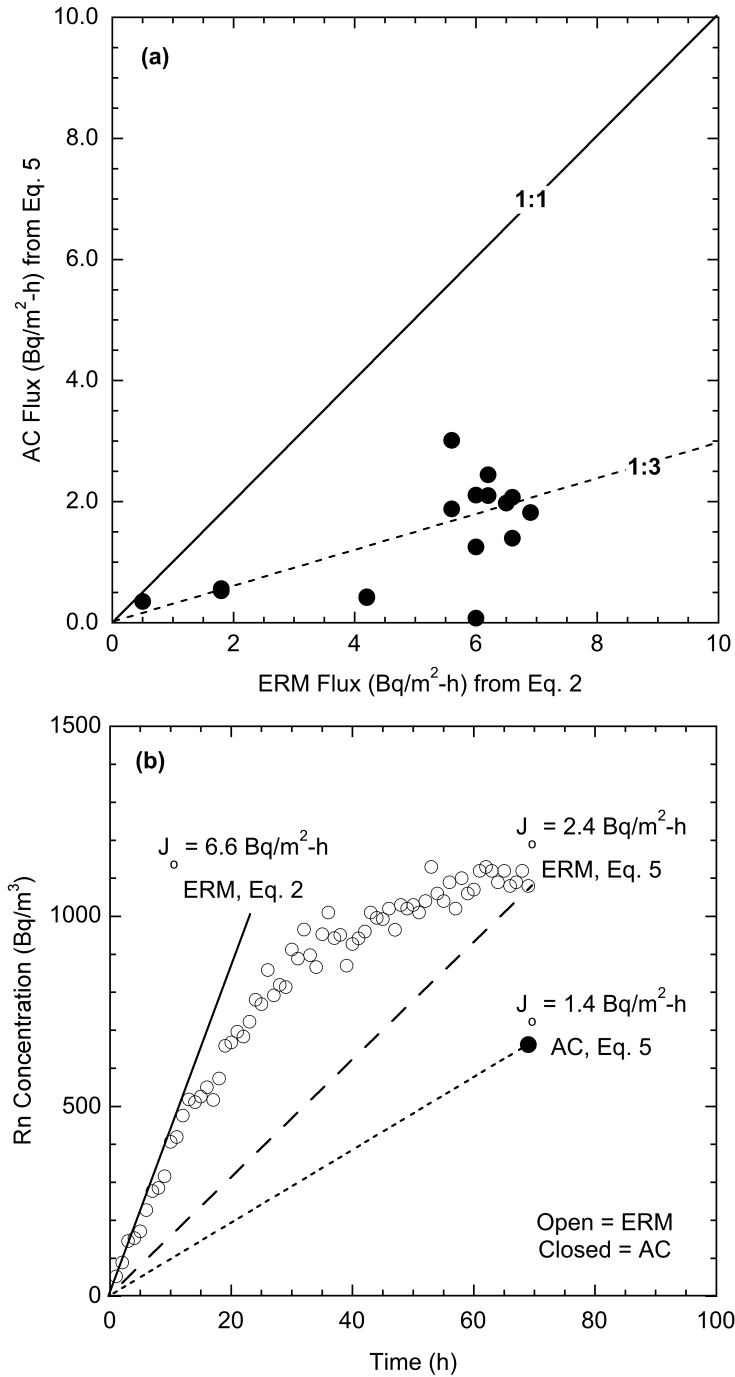


Figure F-9 Rn Fluxes Measured Using AC and Eq. 5 and Using the ERM with Eq. 2: (a) comparison of fluxes measured with AC and ERM for the same chamber and exposure time and (b) fluxes computed from ERM and AC data from 72-h test on concrete source measured with ERM using Eqs. 2 and 5

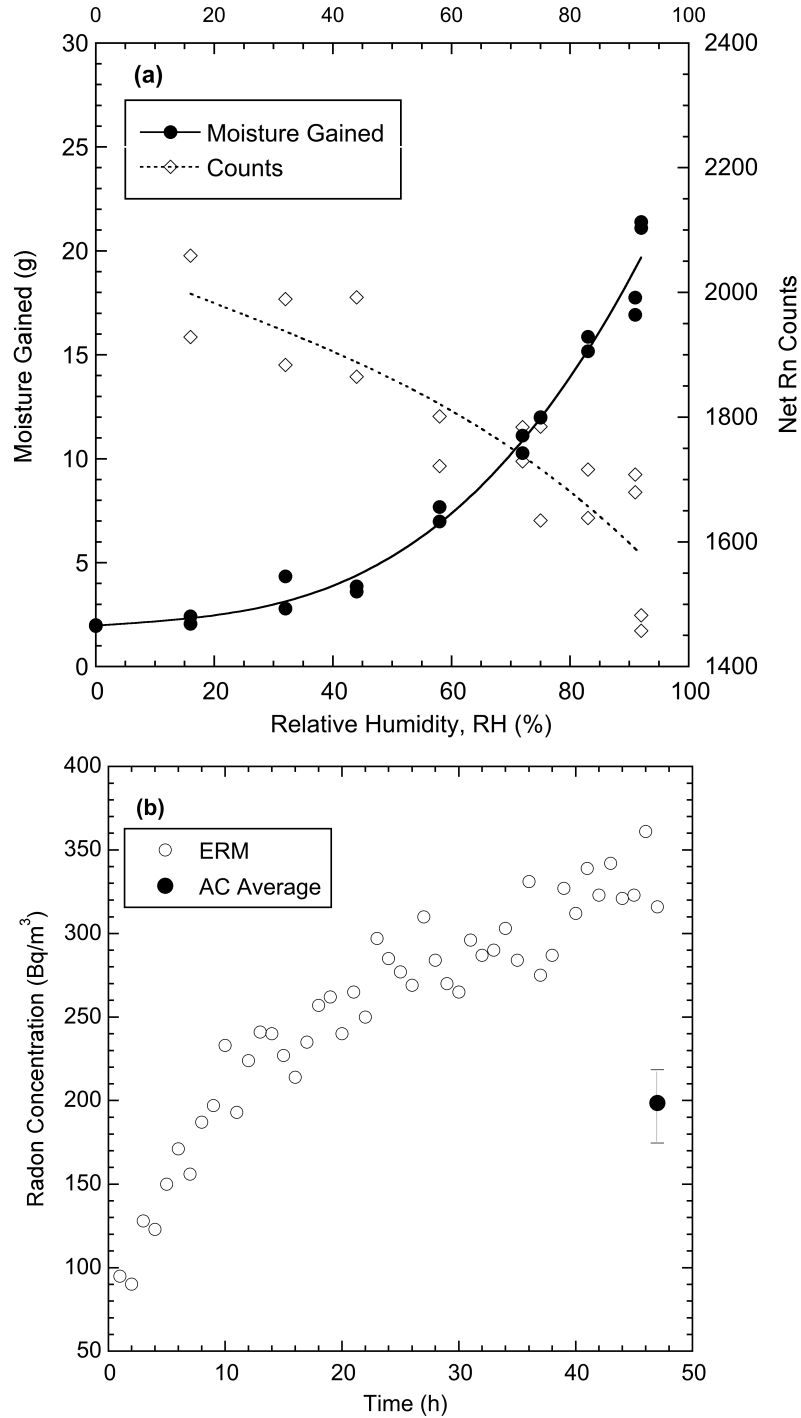


Figure F-10 Effect of Relative Humidity on Moisture Gained by AC and Net Counts from Rn Bound to the AC (a) and Comparison of Rn Concentrations Measured with ERM and AC Canisters Equilibrated in Different Relative Humidity in a Large Flux Chamber with a Granite Source (b)

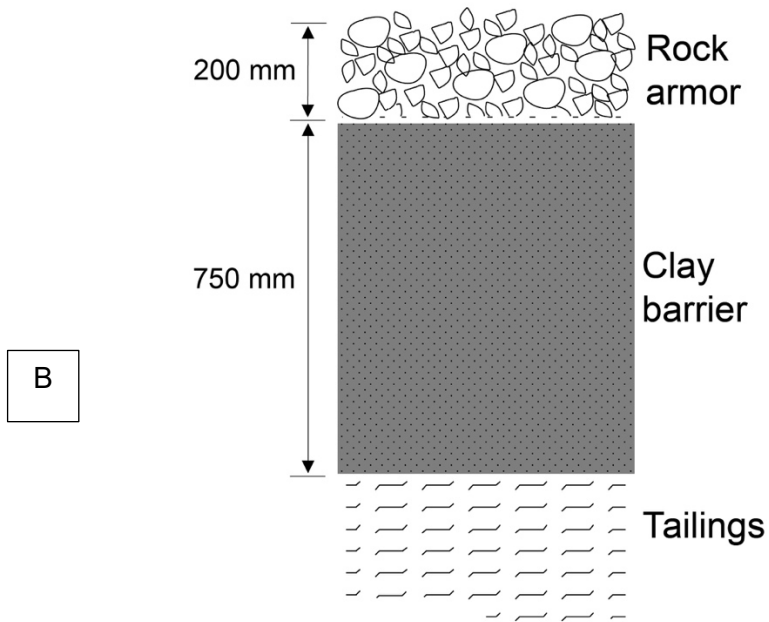
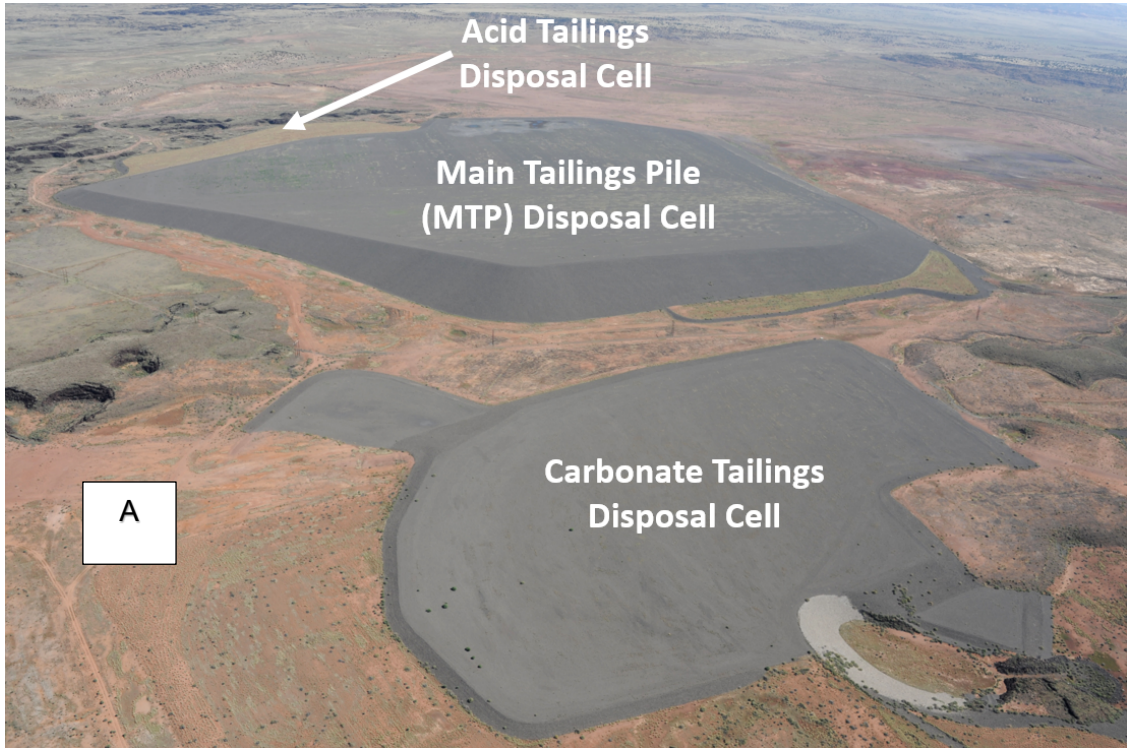


Figure F-11 Main Tailing Pile (MTP) at Bluewater Disposal Facility: Locations of Test Pits (A) and Cover Profile (B)

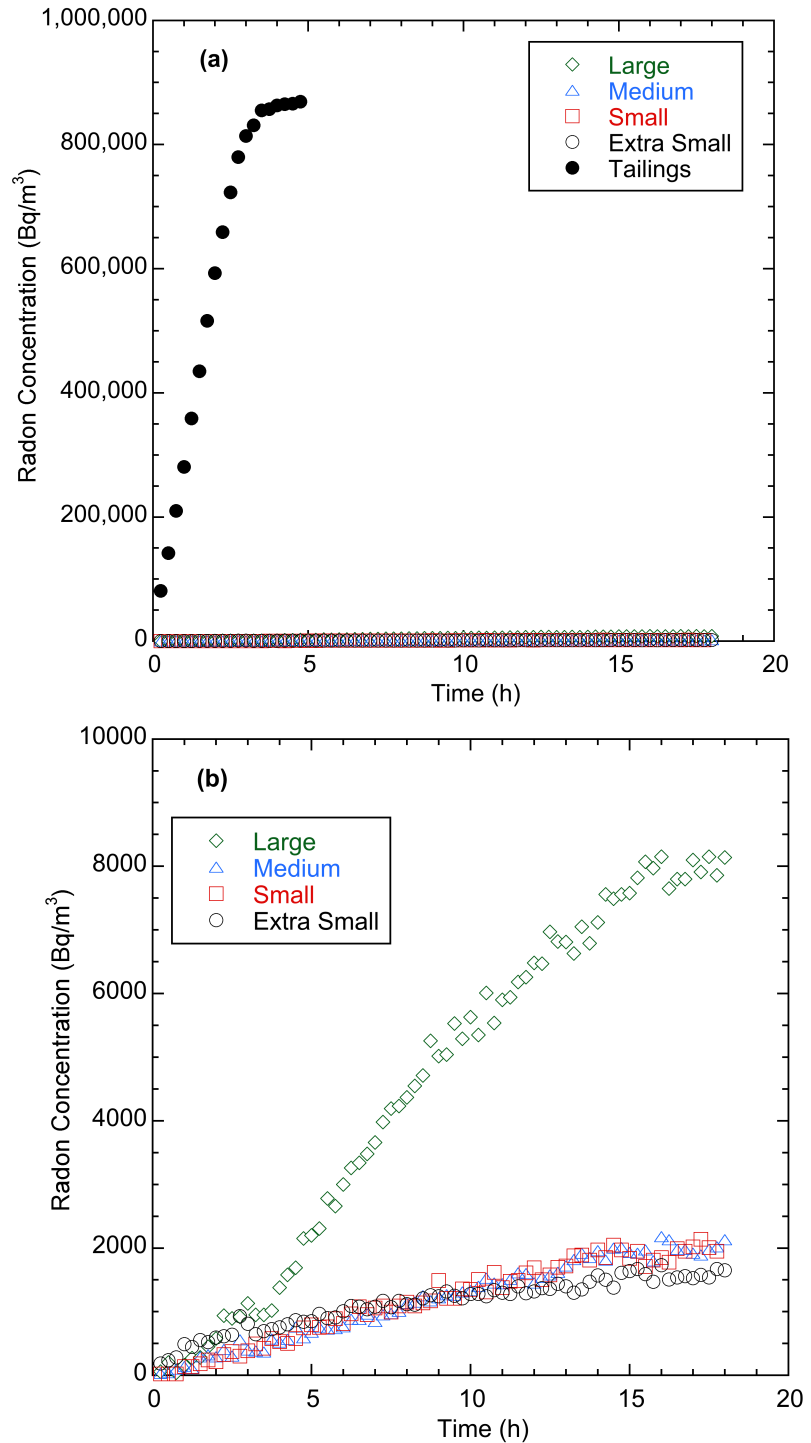


Figure F-12 Rn Buildup Curves Measured in the Field at the Main Tailings Pile at Bluewater Using Chambers of Various Sizes and on the Surface of the Tailings: (A) All Data, Including Rn Barrier Surface and Tailings Surface and (B) Data from Surface of Rn Barrier Only

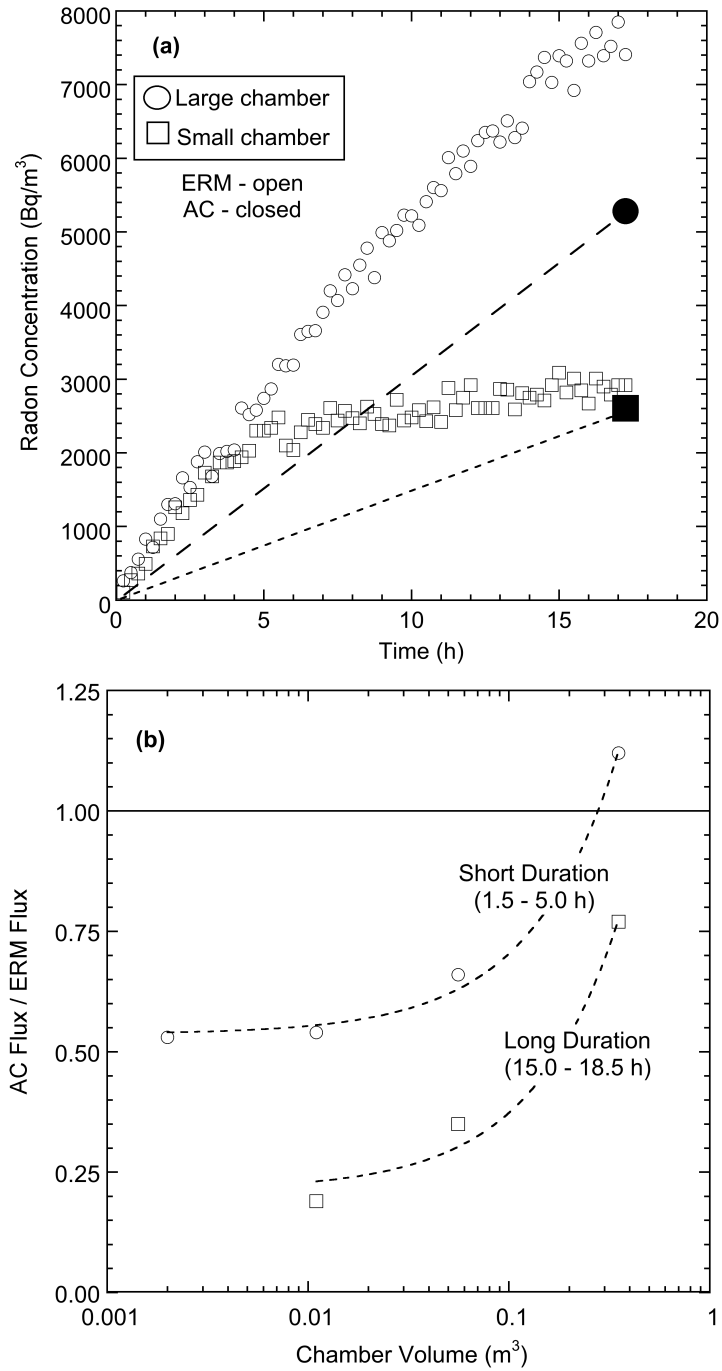


Figure F-13 Rn Concentrations Measured in the Field with ERM and AC with Small and Large Flux Chambers (a) and Ratio of Rn Fluxes Determined from ERM Data (Eq. 2) and AC Data (Eq. 5) as a Function of Chamber Volume for Short and Long Duration Tests (b)

F.5 SUMMARY AND CONCLUSIONS

Experiments were conducted in the laboratory and field to evaluate methods for measuring radon (Rn) flux from Rn barriers constructed over uranium mill tailings. Flux chambers of various size (area, $A = 0.020 \text{ m}^2$ to 2.32 m^2 ; volume to area ratio, $V/A = 0.083$ to 0.347 m) were equipped with activated carbon (AC) canisters and an electronic radon monitor (ERM) with a solid-state alpha detector. Crushed granite and a concrete slab were used as Rn sources in the laboratory. Field measurements were made on the surface of the Rn barrier and directly on the underlying waste at the Bluewater disposal facility near Grants, New Mexico. The following conclusions are drawn based on the findings from the study.

- Average Rn fluxes measured in the laboratory were independent of chamber size, but the flux was more variable for smaller chambers due to less spatial averaging in a smaller chamber. In the field, however, Rn flux recorded by the largest chamber was much higher than with the smaller chambers, suggesting that the smaller chambers did not capture preferential paths for Rn transport. Large chambers are recommended to increase the likelihood of detecting preferential paths.
- Rn fluxes computed by fitting the entire Rn concentration buildup curve from the ERM were slightly lower (86-90%) than Rn fluxes computed from a linear fit to the initial portion of the buildup curve. Either method can be used to determine the Rn flux with comparable accuracy.
- Rn concentrations measured using AC canisters were consistently lower than Rn concentrations measured with the ERM (typically about 60% of the Rn concentration from the ERM), regardless of flux chamber size and AC exposure time ranging (12 to 96 h). Tests at various RH showed that the AC had greater water uptake at higher humidity, and a corresponding reduction in net measured Rn counts. Despite correcting the AC data for adsorbed moisture, the average Rn concentrations measured with AC were about 60% of those measured with the ERM.
- Rn fluxes determined from analysis of the Rn buildup curve measured by the ERM were approximately 3 times higher than Rn fluxes computed from Rn concentrations obtained from AC canisters in the flux chambers in the laboratory and the field. The AC data yielded a lower flux because the Rn concentration was under-estimated and the non-linearity in the buildup curve was not captured. ERMs and large flux chambers are recommended for measuring Rn flux in the field.
- Better agreement was obtained between Rn fluxes computed from Rn buildup curves recorded by an ERM and from AC measurements when a larger flux chamber was used and the test duration was shorter. If AC measurements must be used in the field to measure Rn concentrations, large flux chambers ($A > 2.0 \text{ m}^2$, $V/A > 0.15 \text{ m}$) and short test durations ($t \sim 4 \text{ h}$) are recommended.

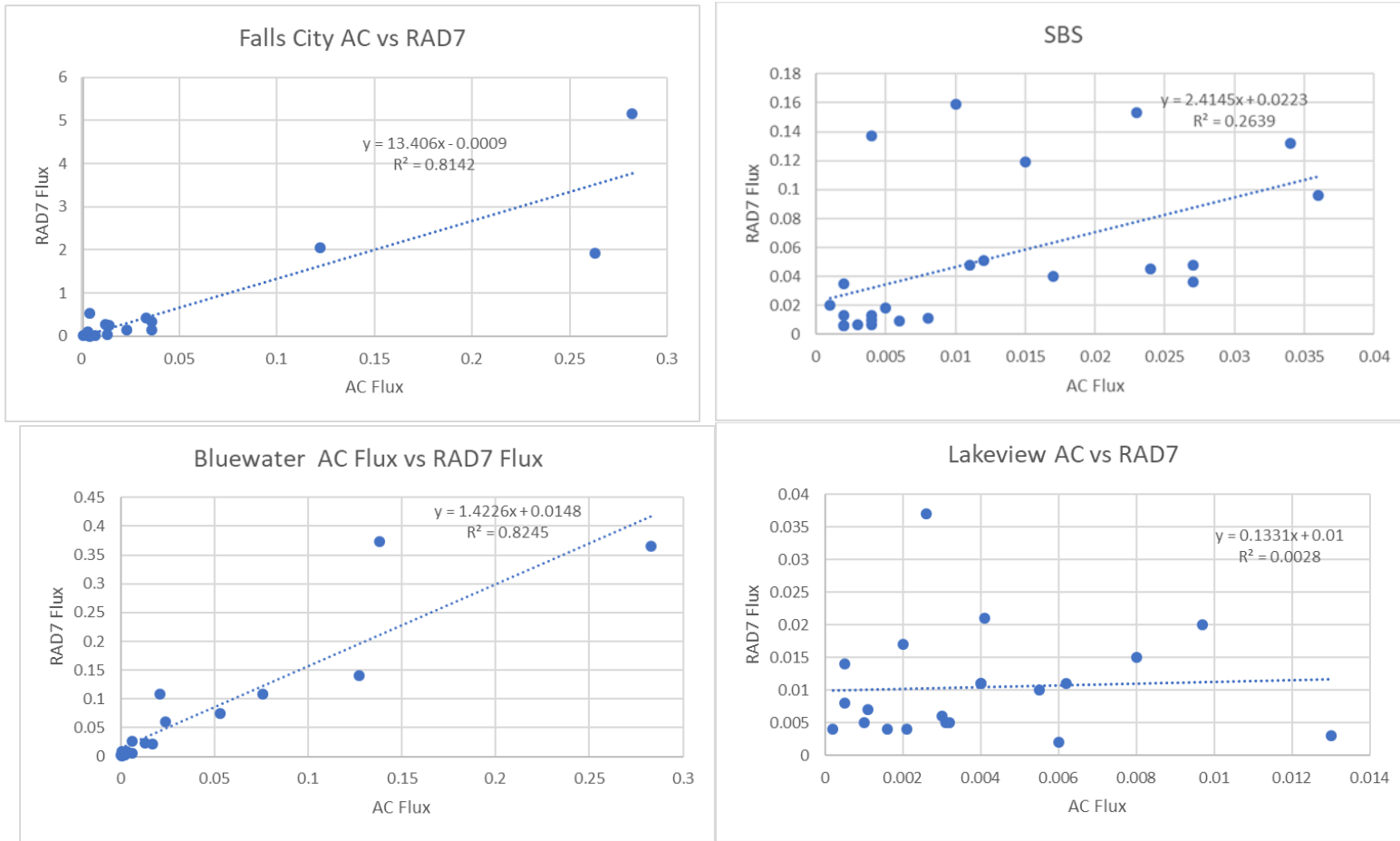


Figure F-14 Fluxes Determined by AC and RAD7 in Field Measurements at Each Site At Least One Factor Impacting the Correlation Between the AC and RAD7 Appears to be Detection Limits for the AC Method

F.6 REFERENCES

- Albrecht, B. and Benson, C. (2001), Effect of Desiccation on Compacted Natural Clays. *J. Geotechnical and Geoenvironmental Engineering*, 127(1), 67-75.
- Albright, W., Benson, C., Gee, G., Abichou, T., McDonald, E., Tyler, S., and Rock, S. (2006), Field Performance of a Compacted Clay Landfill Final Cover at a Humid Site. *J. Geotechnical and Geoenvironmental Engineering*, 132 (11) 1393-1403.
- Albright, W., Benson, C., Gee, G., Abichou, T., Tyler, S., Rock, S. (2006), Field Performance of Three Compacted Clay Landfill Covers, *Vadose Zone J.*, 5(6), 1157-1171.
- Atlantic (1996), Completion Report for Reclamation of the Bluewater Mill Site, Atlantic Richfield Company, Grants, New Mexico.
- Benson, C., Abichou, T., Olson, M., and Bosscher, P. (1995), Winter Effects on the Hydraulic Conductivity of Compacted Clay, *J. Geotech. Eng.*, 121(1), 69-79.
- Benson, C., Albright, W., Fratta, D., Tinjum, J., Kucukkirca, E., Lee, S., Scalia, J., Schlicht, P., Wang, X. (2011), Engineered Covers for Waste Containment: Changes in Engineering Properties and Implications for Long-Term Performance Assessment, NUREG/CR-7028, Office of Research, U.S. Nuclear Regulatory Commission, Washington, DC.
- Benson, C. and Othman, M. (1993), Hydraulic Conductivity of Compacted Clay Frozen and Thawed In Situ, *J. Geotech. Eng.*, 119(2), 276-294.
- Benson, C., Sawangsuriya, A., Trzebiatowski, B., and Albright, W. (2007), Post-Construction Changes in the Hydraulic Properties of Water Balance Cover Soils, *J. Geotech. and Geoenvironmental Eng.*, 133(4), 349-359.
- Chao, C. and Tung, T. (1999), Radon Emanation of Building Material-Impact of Back Diffusion and Difference between One-Dimensional and Three-Dimensional Tests. *Health Physics* 76 (6) 675-681.
- Chao, C., Tung, T., Chan, D. and Burnett, J. (1997), Determination of Radon Emanation and Back Diffusion Characteristics of Building Materials in Small Chamber Tests. *Building and Environment*, 32(4), 355-362.
- Countess, R. (1976), Radon Flux Measurement with a Charcoal Canister. *Health Physics* 31: 455.
- Daoud, W. Z., & Renken, K. J. (1999). Laboratory Measurements of the Radon Gas Diffusion Coefficient for a Fractured Concrete Sample and Radon Gas Barrier Systems. In *1999 International Radon Symposium* (p. 14.0-14.12).
- EPA (1986), *Radon Flux Measurements on Gardiner and Royster Phosphogypsum Piles Near Tampa and Mulberry, Florida*. United States Environmental Protection Agency, Washington, DC.

- Gervino, G., Bonetti, R., Cigolini, C., Marino, C., Prati, D. and Pruiti, L. (2004), Environmental Radon Monitoring: Comparing Drawbacks and Performance of Charcoal Canisters, Alpha Track and E-PERM detectors. *Nuclear Instruments and Methods in Physics Research*, 518, 452-455.
- Grossi, C., Vargas, A., Comacho, A., Lopez-Coto, I., Bolivar, J.P., Xia, Y., Conen, F. (2011), Inter-comparison of different direct and indirect methods to determine radon flux from soil," *Radiation Measurements*, 46(1): 112-118.
- Hutter, A.R., and Knutson, E.O., (1998), "An international inter-comparison of soil gas radon and radon exhalation measurements," *Health Physics*, 74(1): 108-114.
- Khire, M. V., Benson, C. H., & Bosscher, P. J. (1997). Water Balance Modeling of Earthen Final Covers. *Journal of Geotechnical and Geoenvironmental Engineering*, 123(8), 744–754. [https://doi.org/10.1061/\(ASCE\)1090-0241\(1997\)123:8\(744\)](https://doi.org/10.1061/(ASCE)1090-0241(1997)123:8(744))
- Othman, M., Benson, C., Chamberlain, E., and Zimmie, T. (1994), Laboratory Testing to Evaluate Changes in Hydraulic Conductivity Caused by Freeze-Thaw: State-of-the-Art, *Hydraulic Conductivity and Waste Containment Transport in Soils*, STP 1142, ASTM, S. Trautwein and D. Daniel, eds., 227-254.
- Stefani, N. (2016), Field and Laboratory Measurement of Radon Flux and Diffusion for Uranium Mill Tailings Cover Systems, MS Thesis, University of Wisconsin-Madison, Madison, WI, USA.
- Stothoff, S. (2012), Analysis of Mill Tailings Cover Performance, Final Report, US Nuclear Regulatory Commission Contract NRC-41-09-011, Center for Nuclear Waste Regulatory Analyses, San Antonio, TX.
- Sutter, G., Luxmore, R., and Smith, E. (1993), Compacted Soil Barriers at Abandoned Landfill Sites are Likely to Fail in the Long Term. *Journal of Environmental Quality*, 22 (2), 217-226.
- Tuccimei P., Moroni, M. and Norcia, D. (2006), Simultaneous Determination of ^{222}Rn and ^{220}Rn Exhalation Rates from Building Materials Used in Central Italy with Accumulation Chambers and Continuous Solid State Alpha Detectors: Influence of Particle Size, Humidity and Precursors Concentration. *Applied Radiation and Isotopes*, 64, 254-263.
- Ujic, P., Celikovic, I., Kandic, A. and Zunic Z. (2008) Standardization and Difficulties of Thoron Exhalation Rate Measurements Using an Accumulation Chamber. *Radiation Measurements*, 43, 1396-1401.
- UMTRCA (2013), Uranium Mill Tailings Radiation Control Act Sites. Office of Legacy Management, US Department of Energy, Washington, DC.
- Vanmarcke, E. (1983), *Random Fields—Analysis and Synthesis*, MIT Press, Cambridge, MA.
- Vargas, A. and Ortega, X. (2007) Influence of Environmental Changes on Integrating Radon Detectors: Results of and Inter-comparison Exercise. *Radiation Protection Dosimetry*, 123 (4) 529-536.

APPENDIX G

EFFECT OF CHAMBER SIZE ON RADON FLUX MEASUREMENT

G.1 Introduction

An original assumption regarding size of cover defects leading to high Rn emissions was that visually identifiable defects such as cracks would be present in the radon barrier. The idea was then to measure fluxes from those cracks as well as from adjacent areas with no cracks to assess the impact of preferential pathways on Rn flux. Possible defects could include shrinkage cracks, erosion piping, animal burrows (from ants to groundhogs), and channels from dead roots. Diffusion modeling, reported by Kalkwarf and Mayer, 1983 (NUREG/CR-3395), suggested that a collection of defects that would increase Rn fluxes by a factor of two or more would easily be observed visually and would be 2 cm wide, less than one meter apart and penetrate 75% of the cover thickness. However, soil column tests indicated that turbulent flow in the crack, induced by winds blowing across the cover, and drying of the cover near these defects would substantially enhance flux.

Related to the question of defect size is the size of the accumulation chambers, specifically the area exposed to the cover surface. If too small an area is used to measure Rn flux, the measurement may not be representative. For example, if the majority of Rn flux emanating through the Rn barrier is through cracks spaced far apart from one another, there is a chance that a small area flux chamber may not be placed on any defects, obtaining an unrealistically low flux. If pathways controlling Rn flux are very small in scale (small defect, uniform spacing) a small area chamber should suffice and provide the same result as would a chamber with a greater area. The discrepancy exists when the structure controlling the Rn flux is larger in scale. Figure G-1, below provides a simple example of how measurements may be affected by flux chamber area at different scales of soil structure.

With the idea of visible defects in mind, four Rn flux chamber sizes were used to measure fluxes. The chamber shapes and dimensions are shown in Figure G-2. The thought being that systematic differences in flux measurements for different sized chambers would provide information on the size and/or spacing of preferential pathways.

A simple analysis of the Rn flux data collected at the four UMTRCA sites was used to investigate whether or not the area of the flux chamber used in the field significantly affected measurements. For each test pit, a geometric mean flux value was calculated from the combined measurements from that pit (up to 8 measurements from flux chambers with different areas). Then, each individual flux value was divided by the geometric mean flux of that test pit. If the result was equal to one, then the value was equivalent to the mean. If all flux measurements obtained from a test pit were the same, then the value will be one for each of them. It was hypothesized that this ratio would have significant scatter for extra small chambers and would have less scatter as chamber size is increased. Figure G-2 and Table G-1, below, show this ratio for flux measurements from all four UMTRCA sites.

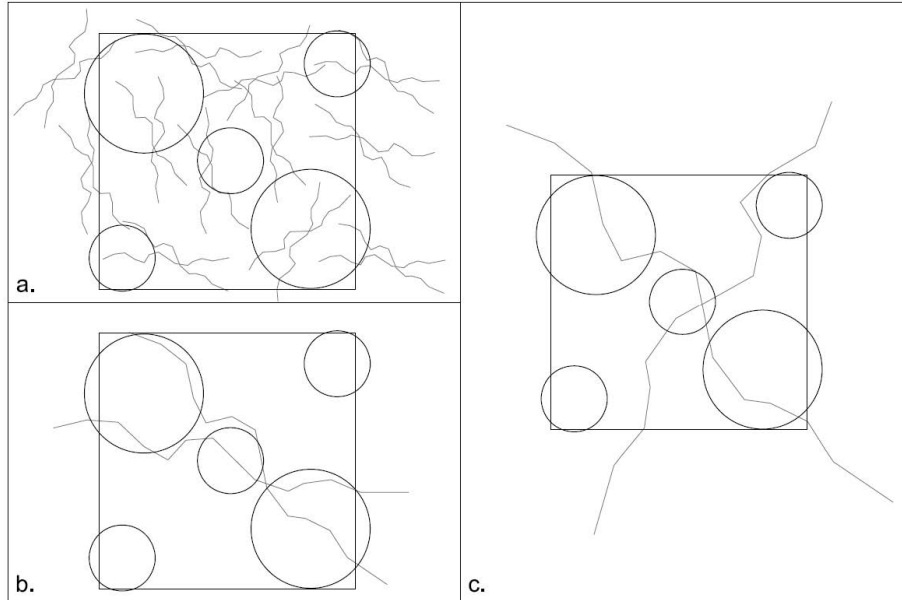


Figure G-1 How Scale of Soil Structure and Sampling Area May Affect Flux Measurements Different sized flux chambers are shown arranged in a uniform pattern superimposed on hypothetical cracks in the Rn barrier. Crack spacing $a < b < c$ (Michaud, 2018)

G.2 Field Measurements and Chamber Size

Table G-1 shows that while the extra small chambers have average flux ratios close to one, there exists significant variability in this observation, as made apparent by the larger standard deviation. The medium chamber area appears to provide flux ratios with the least amount of variability and a ratio close to one, suggesting that flux chambers with an area of 0.26 m² may be large enough to effectively incorporate the scale of the soil structure controlling Rn flux at the four UMTRCA sites visited for this research. It is unclear why the scatter for the large chambers in this study is so large.

It should be noted that flux chambers were placed adjacent to one another in each test pit. The chambers were closely spaced, within a meter or two of each other. Ideally, flux measurements would initially be taken over an area with the smallest chamber size spaced very closely together. This would then be followed by measurements of the same area using the next larger chamber size and so on and so forth. This would provide more confidence that the spatial variation or the soil structure was the main variable in each measurement. For example, the majority of the cracks (or other form of soil structure) in a given test pit may have been completely covered by the large chamber, and the adjacent areas may have been relatively free of structure, or vice versa.

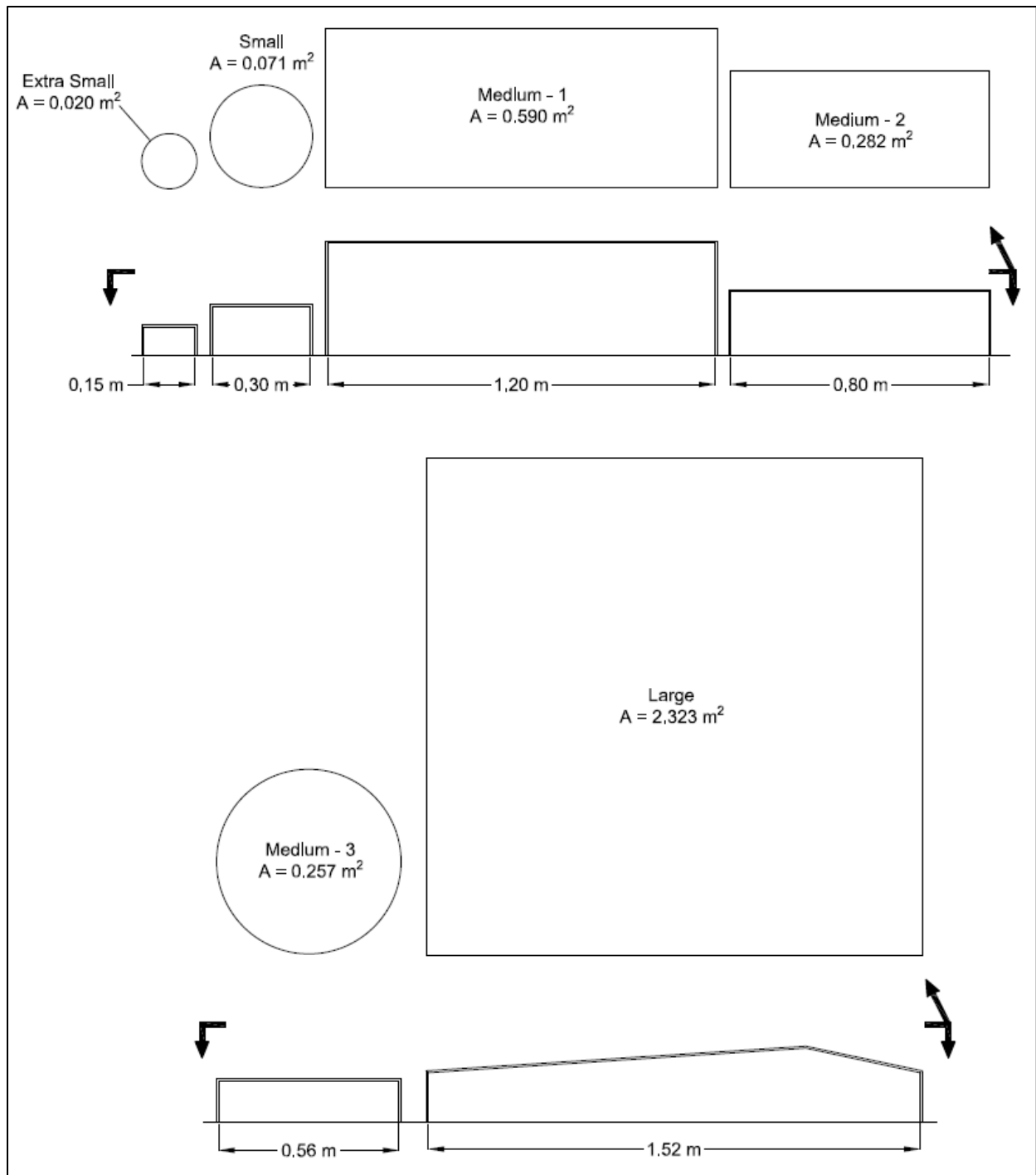


Figure G-2 The Shape and Dimensions of Accumulation Chambers Used in this Project

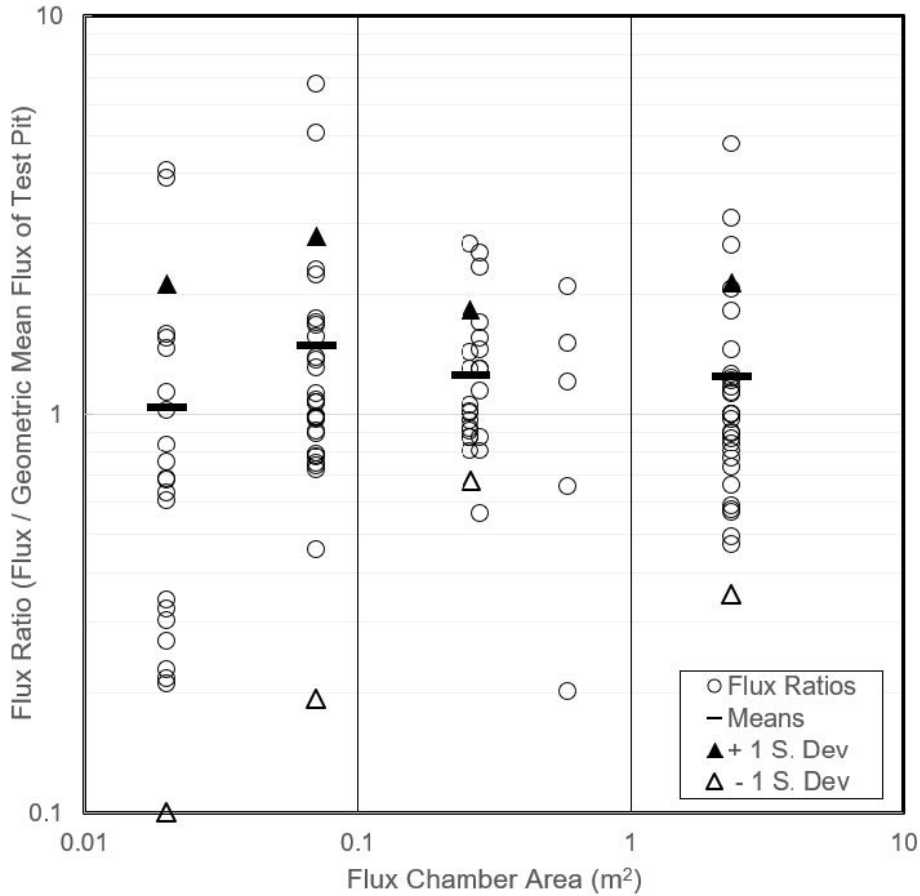


Figure G-3 Rn Fluxes from Each Chamber, Normalized by the Geometric Mean Rn Flux from their Respective Test Pits (from Michaud, 2018)

Table G-1 Summary of Flux Ratios Shown in Figure G-3

Flux Chamber Designation	Chamber area (m ²)	Average Flux Ratio	Std Dev. of Flux Ratio
Extra Small	0.020	1.04	1.07
Small	0.071	1.49	1.29
Medium	0.260	1.25	0.57
Large	2.323	1.24	0.89

The observations made above may not necessarily be true for all UMTRCA sites or for all conditions. It is possible that sites with very small-scale soil structure, or no soil structure at all may not show any dependence on scale as was observed at these four sites. As-built flux chamber measurements are typically obtained using flux chambers with areas similar to the small chambers used in this study. It is likely that at the time of these measurements, the Rn barrier was relatively free of the macrostructure that is observed after decades of service. Therefore, the use of a small area flux chamber may suffice as the diffusion of Rn through the barrier was likely occurring through the micro-scale pore space of the soil.

To determine if development of preferential pathways for Rn transport may be site specific, perhaps related to cover material mineralogy, box and whisker plots were prepared with flux measurements from each site, which are given in Tables G-2 – G-5. Figures G-4 to G-7 are plots for the four sites. In these figures, the horizontal line within each box represents the median flux value from each dataset while the x is the mean. The top (upper quartile, UQ) and bottom (lower quartile, LQ) of the boxes represent the +/- 25% limits of the dataset and the distance between the top and bottom of the boxes represent the interquartile distance (IQD). The whiskers represent the maximum and minimum values that fall within an “acceptable range” which is defined as $UQ + 1.5 \times IQD$ and $LQ - 1.5 \times IQD$. The individual points represent outliers which are either greater or less than the “acceptable range”.

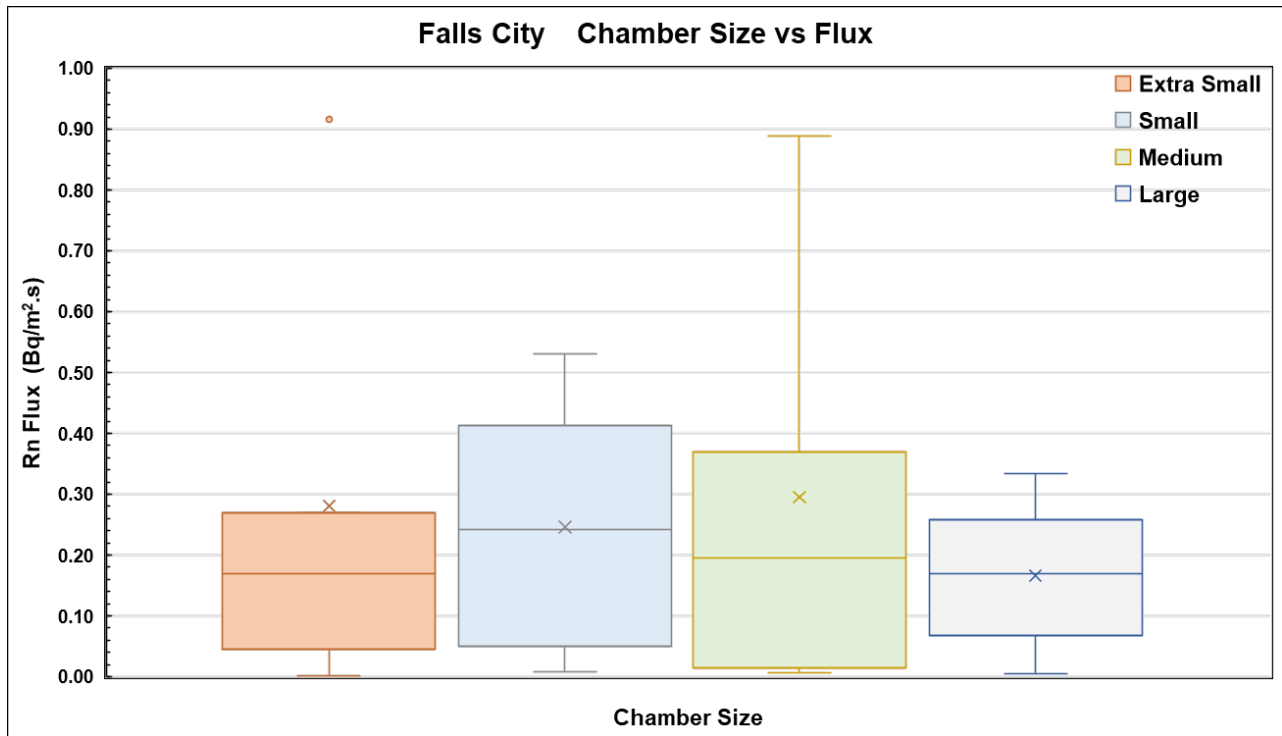


Figure G-4 A Box and Whisker Plot for Falls City Flux Data for Each Size Accumulation Chamber

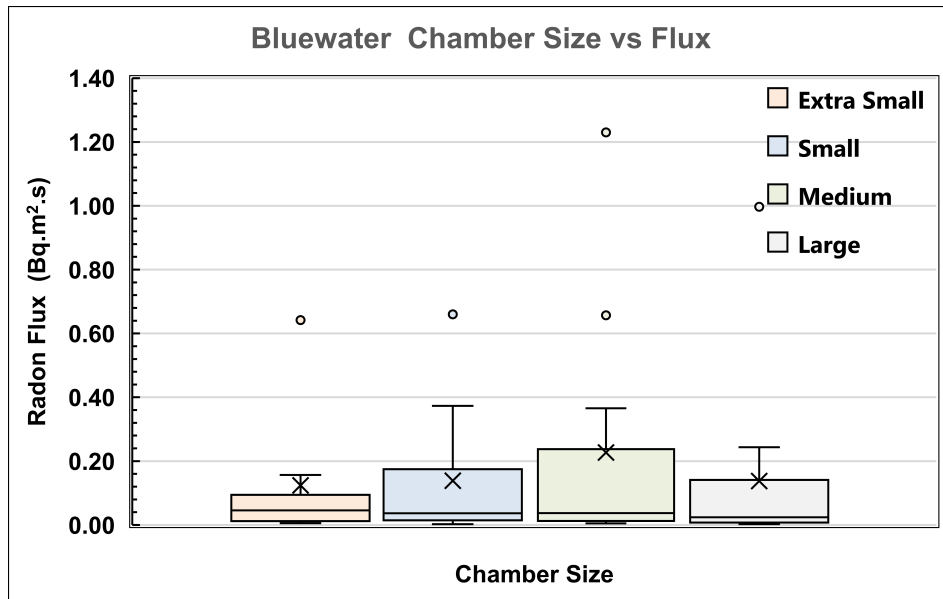


Figure G-5 A Box and Whisker Plot for Bluewater Showing Flux for Each Size Accumulation Chamber

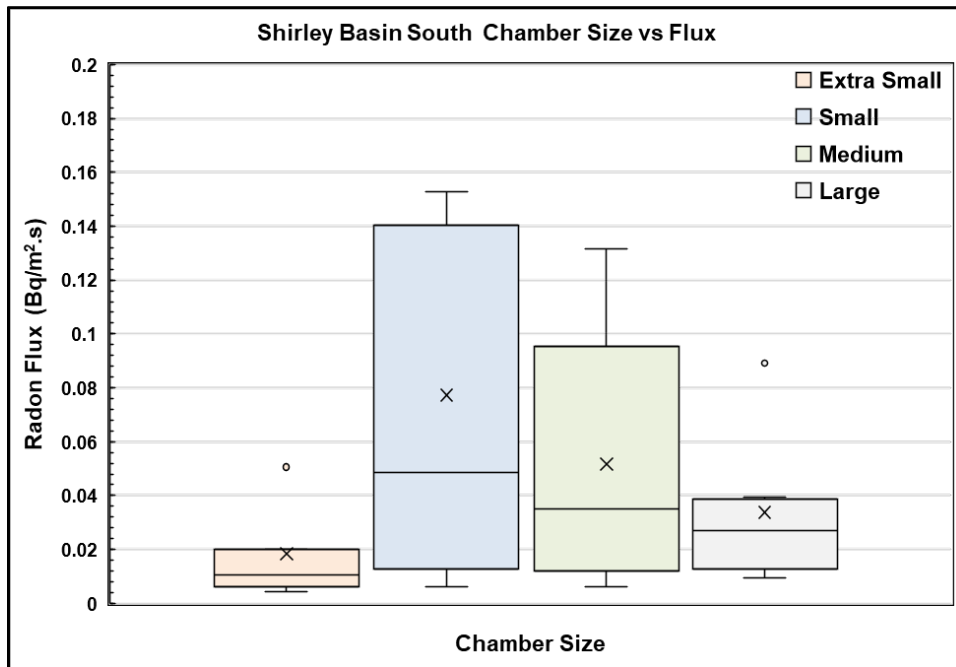


Figure G-6 A Box and Whisker Plot for Shirley Basin South Showing Flux for Each Size Accumulation Chamber

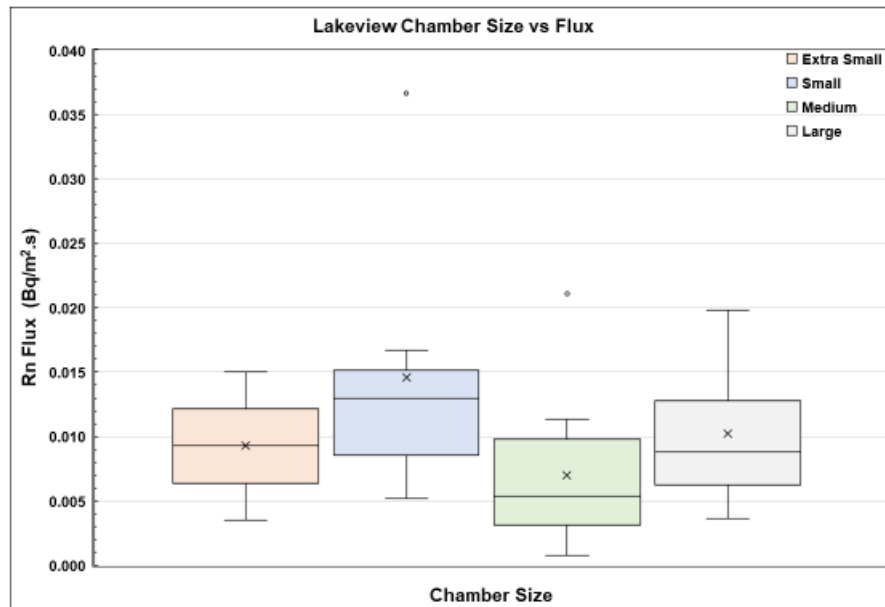


Figure G-7 A Box And Whisker Plot for Lakeview Showing Flux for Each Size Accumulation Chamber Note that the extra small chamber data set consisted only of two measurements

The median, mean, and IQD (box height) for all sizes of chambers for Falls City were similar, suggesting that any preferential pathways were varied enough in size and distribution that chamber size did not matter. This is also the case for the Lakeview site. In this case the plot may simply reflect the very low fluxes because of the low Ra-226 content of the site.

For the Bluewater site, while the median fluxes were all similar, the extra small chambers had a notably smaller IQD than the others. This was especially the case for the Shirley Basin South data set, where the mean, median, and IQD for extra small chambers were well below those of the other chamber sizes, especially the small chambers. Here the median and the upper quartile were seven times lower than those for the small chambers. This strongly suggests that the extra small chambers were small enough that they often missed locations of higher Rn flux. It also means that the defects leading to elevated fluxes were small, with a dimension or spacing less than the 0.15 m diameter of the extra small chambers but large enough that they were often observed by the small chambers with a 0.3 m diameter.

Table G-2 Falls City Rn-222 Flux (Bq/m²•s) in Different Size Chambers

Rn Flux Extra Small	Rn Flux Small	Rn Flux Medium	Rn Flux Large
0.002	0.009	0.007	0.005
0.045	0.013	0.014	0.040
0.169	0.160	0.196	0.150
0.270	0.323	0.370	0.190
0.916	0.443	0.889	0.280
	0.530		0.334

Table G-3 Lakeview Rn-222 Flux (Bq/m²•s) in Different Size Chambers

Rn Flux Extra Small	Rn Flux Small	Rn Flux Medium	Rn Flux Large
0.004	0.017	0.003	0.004
0.015	0.014	0.008	0.020
	0.007	0.006	0.007
	0.037	0.002	0.010
	0.005	0.001	
	0.011	0.004	
	0.013	0.021	
		0.005	
		0.011	

Table G-4 Bluewater Rn-222 Flux (Bq/m²•s) in Different Size Chambers

Rn Flux Extra Small	Rn Flux Small	Rn Flux Medium	Rn Flux Large
0.008	0.002	0.005	0.003
0.040	0.026	0.037	0.003
0.006	0.015	0.037	0.024
0.013	0.037	0.016	0.040
0.642	0.038	0.007	0.140
0.074	0.007	0.021	0.024
0.157	0.057	1.230	0.009
0.051	0.660	0.109	0.997
	0.014	0.009	0.141
	0.373	0.366	0.244
	0.293	0.657	0.005
			0.008
			0.152

Table G-5 Shirley Basin South Rn-222 Flux (Bq/m²•s) in Different Size Chambers

Flux Extra Small	Rn Flux Small	Rn Flux Medium	Rn Flux Large
0.051	0.048	0.045	0.036
0.010	0.048	0.132	0.089
0.020	0.006	0.007	0.011
0.006	0.007	0.006	0.009
0.004	0.153	0.096	0.018
	0.137	0.035	0.040
	0.143	0.013	
	0.013	0.119	

APPENDIX H

FACTORS OF SOIL DEVELOPMENT AND PEDOGENIC PROCESS IN ENGINEERED SURFACE COVERS FOR WASTE CONTAINMENT

H.1 Introduction

This section is divided into two segments: a discussion on factors of soil development, and a review of the qualities and rates of pedogenic processes. A framework of soil development is proposed that incorporates forming factors relevant to engineered surface covers for waste containment, and a conceptual model that describes the co-evolution of soil processes and morphology is presented. Special emphasis is placed on processes that result in morphological development *within* the compacted mineral barrier (CMB, or “radon barrier”) of engineered surface covers in the Uranium Mill Tailings Radiation Control Act (UMTRCA) program. The framework allows for the systematic study of soil change on covers and is accompanied by results from field investigations at four UMTRCA sites in Section 7. Soil surveys that complement this work are reported elsewhere (DOE-a, DOE-b, DOE-c, and DOE-d forthcoming).

All soils, including those engineered for waste containment, are a heterogeneous mixture of reactive primary particles, secondary aggregates, pore space, liquids, gasses, and biota organized across scales at the earth’s surface. Soils are open and dynamic systems that are subject to recurring fluxes of energy and mass with impacts to both short-term function and long-term evolution. As living systems, soils evolve and change by taking freely available energy from the environment (e.g., in the form of sunlight, water, nutrients and other materials), transforming it, and moving toward higher order (i.e., more complex) systems (Lin 2011). As an energy-consuming activity, soil evolution is a dissipative process that results in the self-organization of internal architecture as evident in the emergence of aggregates, pore space, soil horizons, and pedons in natural systems (Targulian and Goryachkin 2004; Lin 2010a; Lin 2010b). The dynamic properties of soil change, and the self-organization of soil morphology through time, gives rise to an abundance of natural soil diversity as seen in the many colors, textures, patterns, and heterogeneities present across the world’s many soils. However, the inevitability of earth surface process, and corresponding pedogenic processes that drive soil change can run counter to conventional engineering efforts that rely on the rigid isolation of wastes through the structural maintenance of compacted barriers common to waste management systems across the planet, including those in the UMTRCA program.

Historically, the dynamic properties of soil development, and the emergence of novel soil morphology, have been underemphasized in the planning of engineered cover systems. Disposal cells for the isolation of uranium mill tailings in the UMTRCA program are expected to control radioactive and other hazardous wastes for up to 1000 years, to the extent reasonably achievable, and, in any case, for at least 200 years (10 CFR 40, Appendix A). Conventional cover systems have largely been designed to resist natural processes, as opposed to working with them, at considerable economic cost (Clarke et al. 2004).

In as little as 5 years post construction, soil processes including bioturbation by plants and animals (Arthur and Markham 1983; Burt and Cox 1993; Link et al. 1995), freeze-thaw cycling (Kim and Daniel 1992; Benson et al. 1995), and desiccation cracking (Montgomery and Parsons

1989; Melchior 1997) have led to the emergence of soil morphology and subsequent alterations to the as-built hydraulic properties of compacted barriers in engineered surface covers (Taylor et al. 2003; Albright et al. 2004; Benson et al. 2011). Field studies that explore connections between cover performance and earth surface processes are rare (Beedlow and Hartley 1984; Burt and Cox 1993; Link et al. 1994; Smith et al. 1997; Waugh et al. 1999; Taylor et al. 2003; Albright et al. 2006a; Fourie and Tibbett 2000; DeJong et al. 2015; Williams 2019). Herein we propose a conceptual framework of soil development and provide linkages to soil processes that result in changes to morphology and performance in engineered surface covers for waste containment.

H.2 A Framework of Soil Development in Engineered Surface Covers

The use of soil-forming factors as a framework to describe soil and ecosystem condition is one of the most significant developments in the field of soil science. The framework allows for the general description and spatial prediction of soils and ecosystems from interactions between a small number of master variables (i.e., state factors) (Buol et al. 2011). The framework describes soil (s) as a function of parent material (p), topographic setting (r), climatic variation (cl), biotic influence (o), and time (t) (Dokuchaev 1886; Jenny 1941). The expression of one factor in relation to the overall condition of a soil can be explored by isolating that single factor and keeping the others constant through the study of soil sequences. Soil-forming factors can be further grouped into flux factors (cl and o) and site factors (p and r). Both flux and site factors are dependent on time (t). Lin 2011 expresses the cumulative effect of flux factors on soil development as conditioned by site factors as Eq. [H.1].

$$s = \int_{t_0}^{t_n} f[cl(t), o(t)]dt \mid p(t), r(t), \dots \quad \text{[H.1]}$$

While traditional pedology has largely focused on soil formation in natural settings over tens of thousands to millions of years, human induced change through disturbance, cultivation, and secondary erosion have considerably accelerated rates of soil change to much shorter time frames of years to decades (i.e., Richter and Markewitz 2001). Efforts to incorporate man-made soil change into models of soil formation were initially proposed by Yaalon and Yaron (1966). Amundson and Jenny (1991) integrated humans into the biotic influence factor (o) through the inclusion of genotype and cultural inheritance. Dudal et al. (2002) suggested that human influence was so significant that it required an independent soil-forming factor all together. Galbraith (2004) includes a well-developed discussion on how industrial and mine soils could be considered taxonomically, and how diagnostic horizons and epipedons in these soils can be approached. Such efforts have not only increased the awareness of anthropogenic impacts to ongoing soil processes, but also provided guidance on how to conceptually place these soils within existing pedological frameworks. However, adequate approaches to address the various nuances associated with the active construction of soil systems for the long-term performance of engineering tasks including waste containment remain underdeveloped.

H.2.1 Factors of Soil Formation in Engineered Surface Covers for Waste Containment

Engineered covers for waste containment are conceptually distinct from both natural soils and the majority of anthropogenically modified soils, in that traditional site factors (p and r) are of human design, sourcing, transport, and installation. Given that engineered covers in the

UMTRCA program are constructed of local soils or engineered soil admixtures, regulated by federal and state law, and actively managed to isolate wastes for up to 1000 years, considerable forces beyond nature play a more disproportionate role in defining soil morphology than existing models of soil formation typically include. As such, a conceptual framework of soil change in engineered covers must adequately incorporate the factors that define soil morphology at design, and through time, in order to have real impact across both applied science and regulatory settings.

Herein we refer to the initial design of an engineered surface cover for waste containment as (de). Collectively, the design of an engineered cover is expressed in Eq. [H.2].

$$de = f[sf_{f[cl, tr, r \dots]}, np_{f[wa, st, tx, mn, ch, ed \dots]}, hc_{f[cp, se, pp, rg, co \dots]}, \dots] \quad [H.2]$$

Engineering design (de) is influenced by a combination of the following: site factors (sf), natural material properties (np), and human cultural factors (hc). Site factors (sf) include historical climate (cl) and surrounding terrain features (tr) that influence overall disposal cell design and geometry, including aspect and slope (r). Natural material properties (np) include waste attributes (wa), cover stratigraphy (st), material texture (tx), material mineralogy (mn), construction heterogeneities (ch), and soil edaphic suitability for plant growth (ed). Human cultural factors (hc) include construction practices (cp), stakeholder engagement (se), political processes (pp), regulations (rg), and cost (co). The dots represent factors that are highly location or project specific such as risks associated with groundwater contamination, ownership disputes or bankruptcies, highly localized politics and regulations, executive orders, voluntary commitments, agreements with non-government organizations, contractual agreements, and risks associated with episodic natural events such as fires, floods or earthquakes.

Ongoing human management (m) can be considered a recurring flux factor along with climate (cl) and organisms (o). Management is dependent on cover condition at the time that an active management strategy was developed ($s_{t(n-1)}$) based on a shared set of human cultural factors as described above and expressed in Eq. [H.3].

$$m = f[s_{t(n-1)}, hc_{f[cp, se, pp, rg, co \dots]}, \dots] \quad [H.3]$$

Collectively, a more representative model of soil development in engineered covers (Ec) is presented in Eq. [H.4]. This model incorporates the cumulative effects of climate, organisms, and management on soil development on the engineered design. Table H.1 summarizes the soil development factors.

$$Ec = \int_{t_0}^{t_n} f[cl(t), o(t), m(t), \dots] dt |_{de(t)} \quad [H.4]$$

Table H-1 Factors of Soil Development in Engineered Surface Covers for Waste Containment

Symbol	Factor	Example variables
<i>s</i>	Soil state	Soil morphology and ecosystem state
<i>cl</i>	Climate	Average temperature, average precipitation
<i>o</i>	Organisms	Flora and fauna
<i>r</i>	Slope and aspect	Degree of incline, direction, length, and geometry of slope
<i>p</i>	Parent material	Mineralogy, micro features, age of materials, natural source
<i>t</i>	Time	Time
Ec	Engineered cover state	Soil morphology and ecosystem state of the engineered cover system
de	Design	Variables included in site (<i>sf</i>), material (<i>np</i>), and human cultural factors (<i>hc</i>)
<i>sf</i>	Site factors	Collectively: climate, terrain, slope and aspect
<i>tr</i>	Terrain	The geomorphology of the surrounding environment impacting flux
<i>np</i>	Natural material properties	Collectively: waste attributes, cover stratigraphy, material texture, material mineralogy, construction heterogeneities, and soil edaphics
<i>wa</i>	Waste attributes	The volume, mineralogy, toxicity, and reactivity of wastes
<i>st</i>	Cover stratigraphy	The collective horizonation of cover layers from waste to surface
<i>tx</i>	Material texture	The clay, silt, sand and gravel fraction
<i>mn</i>	Material mineralogy	The clay mineralogy of barrier and protective materials
<i>ch</i>	Construction heterogeneities	The inclusion of discontinuities in material properties in the barrier or other cover materials
<i>ed</i>	Soil edaphics	The suitability of the material to sustain plant growth
<i>hc</i>	Human cultural factors	Collectively: construction practices, stakeholder engagement, political processes, regulation, and cost
<i>cp</i>	Construction practices	Equipment selection, best management practice, material processing (i.e., pug mill, screening, etc.), addition and degree of water added, and compaction methods
<i>se</i>	Stakeholder engagement	The assortment, and activity, of social groups (local to global) that have a vested interest in the site, and participate in expressing those interests during operation, remediation, closure, or maintenance
<i>pp</i>	Political processes	The development and enforcement of local, state, federal, and international laws by officials; often closely corresponds to stakeholder engagement
<i>rg</i>	Regulations	The specific laws (and amendments) that are the result of stakeholder engagement and political processes
<i>co</i>	Cost	The resources available for construction and maintenance of sites

H.2.2 Construction Design Influences Parent Material and Topographic Relief

The long-term containment of wastes in the UMTRCA program is accomplished through physical isolation by radon barriers designed to limit liquid and gas flux. The term “radon barrier” is used when explicitly referring to CMB’s in UMTRCA covers. These dense and low permeability layers are similar to naturally occurring claypans that form through clay dispersion, downward particle sorting, and pore plugging over long time-periods (Nikiforoff and Alexander 1942; White et al. 1981). To maintain low permeability under diverse environmental conditions, radon barriers are covered with materials that are intended to prohibit degradation from surface processes including freeze-thaw cycling, surface erosion, and plant and animal intrusion.

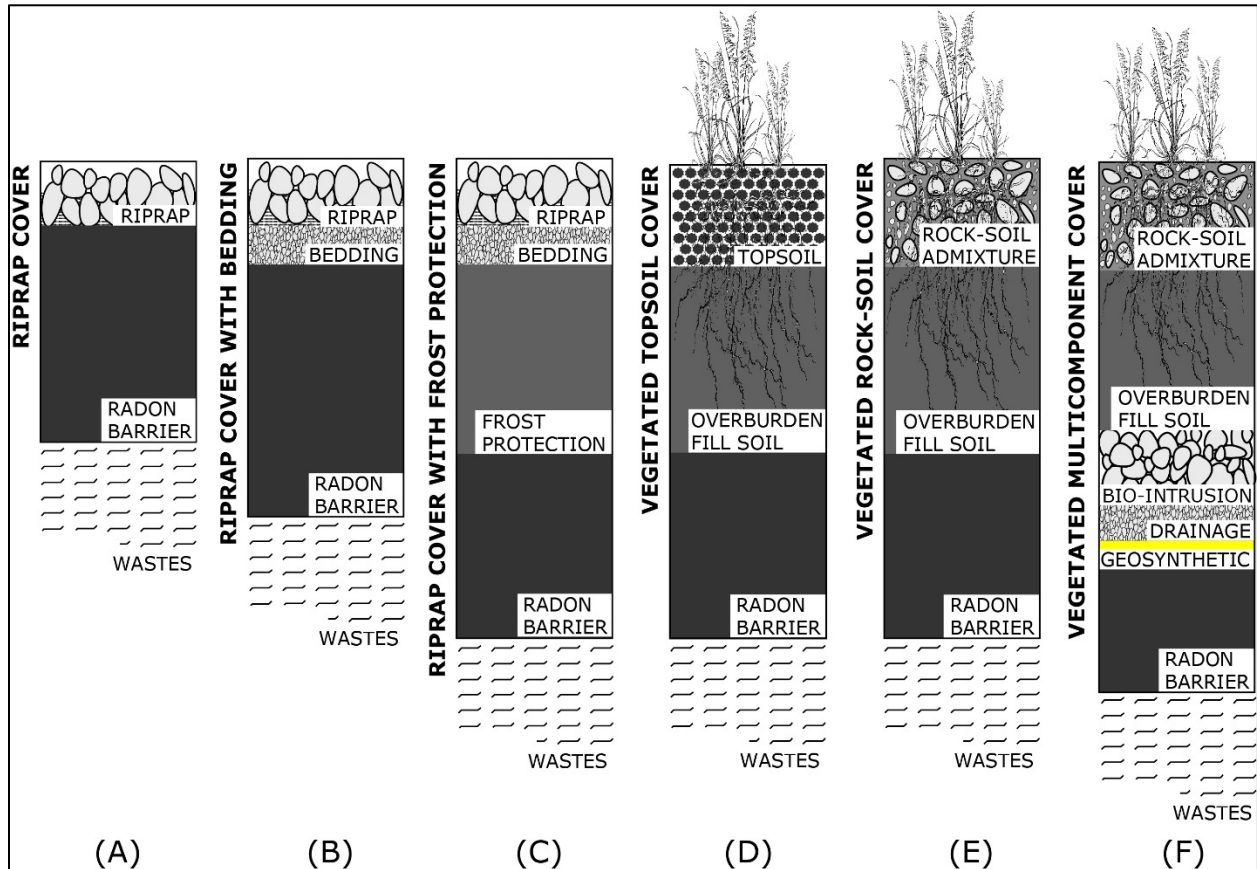


Figure H-1 Stratigraphy of Common UMTRCA Cover Designs at Construction

UMTRCA covers can take many forms (Figure H-1). (A) Rock riprap covers are comprised of a layer of compacted fine sediments (the “radon” barrier) placed directly over wastes and covered by large aggregate rock riprap for erosion protection. (B) Rock riprap covers may also be constructed with a bedding layer of gravels and coarse sands between the radon barrier and the riprap to further control erosion by confining drainage above the radon barrier surface and constraining the removal of barrier materials. (C) In cold environments, a frost protection layer can be included to limit freeze-thaw above the radon barrier. In climates with sufficient precipitation, vegetated covers are common and use a thick layer of overburden fill soil for a

water storage and rooting layer, followed by a topsoil layer; or (D) a rock-soil admixture layer (E) for erosion protection. (F) Vegetated multicomponent covers can include a combination of additional layers such as capillary breaks to increase water storage above the break, reduce downward unsaturated flow, and inhibit barrier drying; lateral drainage layers to reduce infiltration; biointrusion layers to limit animal burrowing; or geotextiles to limit percolation of meteoric water into tailings. Most side slopes in the UMTRCA portfolio employ rock riprap cover designs for erosion protection with very few exceptions. A summary of UMTRCA site-specific design features are presented in DOE 1999a and DOE 1999b.

H.2.2.1 Cultural and Regulatory Drivers Involved in Cover Placement and Design

The initial placement, design, and long-term management of waste covers are dependent on many cultural factors. Such factors occur at global-to-local scales and have impacts to both static and dynamic site attributes. Static attributes can include geographic location, total volume of waste generated, and the year of construction. For radioactive materials, waste activity can also be considered a static attribute that is dependent on ore quality and mill processing conditions. Dynamic attributes can include community engagement, political processes, any changes to regulations through time, and scientific advancements in civil and environmental engineering.

The UMTRCA program is rooted in the geopolitical environment of World War II and the Cold War. Federal U.S. policy supported the development of a domestic uranium mining, milling, and processing economy with the U.S. Atomic Energy Commission (AEC) purchasing all the uranium produced in the western United States until the 1970s. Albrethsen and McGinley (1982) provide a summary history of domestic uranium procurement under AEC contracts. Chenoweth (1997) highlights processes of raw material procurement for the Manhattan Project on the Colorado Plateau. O'Rear (1966) outlines the early history of domestic uranium production and decisions that influenced initial placement of infrastructure. Albrethsen et al. (1986) provide an account of activities undertaken by the formerly named Atomic Energy Commission Grand Junction Operations Office—the entity responsible for managing uranium exploration—government leasing, and AEC uranium purchasing efforts.

As uranium demand waned in the 1970s after AEC procurement contracts expired, mills began closing and many mill owners declared bankruptcy. Tens of millions of cubic yards of uranium mill tailings were left abandoned, and Congress eventually enacted UMTRCA in 1978 to remediate mill sites supported by AEC procurement contracts. An account of the political conditions that led to the drafting of UMTRCA can be found in Mogren (2002). A discussion of the regulatory background with respect to design, performance, and long-term monitoring of UMTRCA sites can be found in Section 2.

The location of uranium mills was the product of a combination of economic factors including proximity to uranium mines, road and rail transport, labor, access to fresh water for processing, land ownership, permitting, local community engagement, federal policy, national security considerations, and profitability (Merritt 1971). The final location of roughly half of the UMTRCA uranium mill tailings disposal cells was not selected because of the specific sites' suitability as an *ideal* long-term storage location for wastes. Under many circumstances, the risk of transporting tailings from mill locations to dedicated offsite storage facilities outweighed the calculated benefits, and disposal facilities were constructed in place. Under some conditions, the locations of legacy mill tailings were deemed unsuitable for long-term containment, and tailings were moved offsite based on alternative site selection criteria (DOE 1989).

The engineering approaches to UMTRCA cover designs developed in the 1980s represented a state-of-the-art understanding of waste containment for the time (DOE 1999a; DOE 1999b). The 200-to-1000-year design life, and scale of the environmental challenge, was unprecedented. To meet these challenges, federal resources were invested in waste cover innovation beginning in the late 1970s at Los Alamos National Laboratory (LANL), Pacific Northwest National Laboratory (PNNL), and Idaho National Laboratory (INL), among others (Fitzner et al. 1979; Winsor and Whicker 1980; McKenzie et al. 1982; Gano and States 1982; Cline et al. 1982; Arthur and Markham 1983; Beedlow and Hartley 1984; Foxx et al. 1984a; Foxx et al. 1984b; Wing 1988). The field of geotechnical engineering has evolved considerably since the 1980s and UMTRCA cover designs have integrated new design and construction approaches through time. Given advances in our understanding of geotechnical design, the integration of knowledge from long-term performance studies, a more informed awareness of material properties and natural processes relevant to landform stability, and improvements in construction practice, it is imperative that the historical conditions at the time of cover design and construction be understood when approaching the study of these systems.

H.2.2.2 Thickness, Compaction, and Depth from Surface

Radon barriers in the UMTRCA program were initially designed to control radon diffusion to the surface. Radium-226 (^{226}Ra) and radon-222 (^{222}Rn) are progeny of uranium-238 (^{238}U) and are present in mill tailings (the “source materials”). ^{222}Rn is a colorless, odorless, radioactive gas with a half-life of 3.8 days. Conceptually, the low gaseous diffusivity of the compacted barrier will attenuate ^{222}Rn . With a low radon barrier diffusion coefficient, ^{222}Rn would decay several half-lives as it travels to the surface, thereby significantly reducing in concentration and mitigating risk to human health. For the control of radon gas, suitable barrier thickness is determined by modeling radon diffusion based on measurements of optimum density and moisture content and, in some cases, lab measurements of radon diffusion in columns (Nielson and Rogers 1982; Rogers et al. 1984; NRC 1989). Wastes with higher activity will require thicker barriers; therefore, waste attributes (wa) exert control over final cover thickness and stratigraphy. Additionally, borrow soils with higher porosity will require a thicker barrier.

After the U.S. Environmental Protection Agency (EPA) published draft groundwater quality standards in 1989, DOE refined the cover design process and placed greater emphasis on designing “low-permeability” radon barriers to maintain the hydraulic isolation of subsurface wastes (DOE 1989). At that time, DOE informally adopted a standard specified in the Resource Conservation and Recovery Act of 1976 (RCRA) for designing low-permeability caps for disposal of hazardous waste in shallow-land burial facilities. RCRA guidance requires a compacted soil layer with a saturated hydraulic conductivity less than 10^{-9} meters per second (m/s) (EPA 1989). DOE design guidance indicated that this low conductivity could be achieved with either highly compacted native soil or bentonite-amended native soil (DOE 1989). The new guidance also provided a framework for selecting and designing cover components based on site-specific needs. This approach gave options for adding components to the original design such as a thick “protection layer” intended to isolate the barrier from surface processes including frost, plant rooting, and animal burrowing.

H.2.2.3 Pore Size Distribution in Compacted Mineral Barriers at Construction

The distribution of pore space in geologic parent materials influences the initial transport of liquids and gasses in young soils and subsequent patterns of change. The mechanisms of parent material deposition in natural landscapes significantly impact pore size distribution. Materials deposited by ice (glacial till) are poorly sorted and contain rock materials broadly scoured across landscapes of sizes ranging from clay particles to boulders. Similarly, materials deposited by gravity at the base of mountains (colluvium) are also poorly sorted. Parent materials deposited by rivers and streams (alluvium) are sorted from larger to smaller particles with distance from the stream. Those sediments deposited in lakes (lacustrine) or oceans (marine) result in well-sorted laminar sheets, while those deposited by the wind (aeolian) are highly sorted and are dominated by silt sized particles.

Soils that are considered suitable for the construction of radon barriers include the Unified Soil Classification System classes CL, CH, SC, and CL-ML (NRC 2003). High plasticity clays are favored to minimize connected pore space, maximize compaction, and thereby limit rates of gas flux and water infiltration. Gravel and remnant soil structure from borrow materials are undesirable; however, they are inevitably found in final CMB's and their occurrence can be influenced through sorting and secondary processing. Sorting occurs when materials are excavated from natural environments, transported in trucks, crushed, and applied. More recent cover construction efforts have included material-processing equipment to increase the plasticity of materials prior to installation (i.e., pug mills). CMB's with 50–75% sand, a broad range of grain size, and a balance of silt and high plastic swelling smectite clays have been considered ideal in terms of crack resistance and low hydraulic conductivity (Kleppe and Olson 1985). Over regulatory time frames (e.g., 200–1000 years) the texture of placed soil materials will not appreciably change and represents a static feature, with few exceptions including the selective transport of fines out of coarser materials, with a high uniformity coefficient through the erosive process of suffusion (DOE forthcoming). The suffusion of fines from engineered sand-bentonite mixtures used for surface CMB's (not liners) has been well documented (see Section H.2.3.5).

Despite best engineering, construction, and management efforts, variation (both across and within sites) exists in the texture of in-service CMB's. Such variability is also common to natural landscapes at the field scale (Iqbal et al. 2005; Mzuku et al. 2005). Hutchings et al. (2001) observed that particle size distribution within an in-service CMB was highly variable and contained numerous localized zones of coarse gravels. Locations that were more sandy or gravelly were also associated with greater numbers of plant roots, indicating that textural discontinuities can serve as initial locations of soil change in CMB's. Similar observations were made in the soil surveys that complement this study (DOE forthcoming).

H.2.2.4 Mineralogy of Compacted Mineral Barriers

The mineralogy of soil parent materials provides the original supply of plant nutrients that are released by weathering, influencing vegetation and soil development from subsequent organic inputs, physical modifications, and chemical transformations (Anderson 1988). Soils formed from mafic rocks, such as basalt, are generally more fertile, with large amounts of calcium, magnesium and phosphorous, compared to those formed from felsic rock, including granite (Harley and Gilkes 2000). Soils formed from ultramafic rocks, such as serpentinite, have poor fertility, and are composed of plant communities that have adapted to nutrient limitations. Soils formed from limestone and dolomite tend to be alkaline, while those formed in sandstones tend to be mildly acidic with a low supply of nutrients. The impact of soil pH on vegetation is varied

with some plants preferring acidic over neutral soils (Marschner 1991). Weathered mancos shale is a commonly used for the construction of CMB's on the Colorado plateau, and the generation of sulfuric acid from mineral weathering can create acidic soils unfavorable for many plants (Potter et al. 1985) in addition to selenium and boron toxicity (Mast et al. 2014); however, endemic vegetation have adapted to exploit such soils (Comstock and Ehleringer 1992). In some cases, acid-generating sulfide clays have been intentionally used for the construction of CMB's in waste covers to deter root growth with notable success (Robinson and Handel 1995).

In practice, CMB's are predominantly made of materials sourced in economic proximity to wastes and are composed of a diverse set of minerals including quartz, feldspar, carbonates, sulfates, 1:1 clay (e.g., illite and kaolinite), and 2:1 clay (i.e., smectite group minerals). Such materials are subject to ongoing chemical transformation in soils at various timescales (Churchman and Lowe 2012). In most settings, the ideal CMB would be composed of smectite group minerals with high swelling potential, a high liquid and plastic limit, very low hydraulic conductivity when compacted wet of optimum, and the capacity to self-heal. Smectites are comprised of layers of negatively charged aluminosilicate sheets held together by charge-balancing counter-ions including Na^+ , K^+ , Mg^{2+} , and Ca^{2+} . In the presence of water, smectite swells through the process of interfoliar cation hydration; however in the absence of water, smectitic clays are very prone to fracture through desiccation and cracking. If protected from surface processes that cause physical, chemical, or biological alteration, and if the barrier maintains saturation in low salinity pore water, compaction can persist for millions of years (Sellin and Leupin 2013). However, maintaining saturation is dependent on other design and climate factors, and complete protection from shrink-swell processes is not realistic in surface CMB's.

H.2.2.5 Engineered Sand-Bentonite Mixtures

The term "sand" in sand-bentonite mixtures is common language and does not necessarily mean that only sand size particles (>0.075 mm) were included in mixtures. Commonly, materials amended with bentonite include some percentage of fines (<0.075 mm); however, they are inadequate to meet design criteria. Engineered sand-bentonites are unnatural materials comprised of a coarse fraction with low plasticity amended with a small percentage of highly plastic sodic clay mineral. Sand-bentonite mixtures have been used as CMB's in situations where suitable natural clayey soils are not readily or economically available (Garlanger et al. 1987; Chapuis 2002; O'Sadnick et al. 1995; Kumar and Yong 2002).

While commonly used for waste liners that remain saturated, sand-bentonites constitute a small percentage (i.e., $<5\%$) of surface CMB's. However, the occurrence in the UMTRCA portfolio is significantly higher with approximately 25% of (current) UMTRCA radon barriers containing bentonite amendment (Lommler et al. 1999). Such mixtures are known to be vulnerable to erosional piping by the washing out of bentonite fines from the coarse soil matrix through suffusion (Marcotte et al. 1994; Barrington et al. 1998; Kaoser et al. 2006). In such systems, as the applied hydraulic pressure of the system increases (e.g., in downslope locations), the removal of bentonite fines also increases resulting in greater hydraulic conductivity of the remaining material and an increased likelihood of erosional piping (Kaoser et al. 2006). As such, DOE design specifications indicate that bentonite-amended radon barriers should not be used on slopes in excess of 4.5 percent unless material testing is pursued to ensure the stability of the layer to erosion (DOE 1989).

Sand-bentonite mixtures are also prone to shrink-swell and desiccation-cracking with hydraulic conductivity increasing by as many as 5 orders of magnitude after three drying cycles (Malusis et al. 2011). Additionally, the high shrink-swell potential in bentonite materials can be significantly altered through cation substitution. Sodium (Na^+)-bentonite (of the nature used for sand-bentonite mixtures) can swell to 8 to 10 times their original volume, while Calcium (Ca^{2+})-bentonite can only swell to twice their initial volume (Egloffstein 1995). Given high cation exchange capacity and weak interlayer bonds, the Na^+ cations initially located between layers in Na^+ -bentonite are easily substituted for Ca^{2+} cations, resulting in lower swelling potential and higher porosity which can influence the suffusion of fines out of sand-bentonite mixtures, particularly those with high uniformity coefficients. Lin and Benson (2000) report that hydraulic conductivity increases under such conditions because cracks, formed during desiccation, do not fully heal when the bentonite is rehydrated. Furthermore, Egloffstein (1995) suggests that even very low Ca^{2+} concentrations between 0.0000025–0.015 mols per liter in pore water can convert Na^+ -bentonite into Ca^{2+} -bentonite, provided enough pore volumes of flow pass through the material. In the desert southwest, soils are commonly high in calcium carbonate (CaCO_3), with aeolian dusts and rainfall further increasing CaCO_3 concentrations (see Section H.3.9.1.) suggesting that sand-bentonite CMB's in the southwest may be prone to cation substitution with impacts to performance.

H.2.2.6 Construction and Material Heterogeneities in Compacted Mineral Barriers

Unlike highly sorted and uniformly manufactured materials including plastic or steel, natural soil materials are dominated by heterogeneities in texture, mineralogy, biotic activity and foreign objects including man-made debris. Within the UMTRCA program, material specifications for acceptable soil texture and soil organic matter content of radon barrier borrow materials have been established to manage heterogeneity within acceptable limits, and material audits are typically performed on every 1000–10,000 cubic meters of material (DOE 1989; NRC 2003). Given the vast surfaces of individual covers in the UMTRCA program (6–200-plus hectare [ha]), cover systems will inevitably contain various material heterogeneities reflecting natural heterogeneities in the landscapes used for material sourcing (Smith et al. 1997). Excavations of in-service radon barriers have shown that soil structures (e.g., peds, clods, aggregates) that were naturally formed in borrow material soil profiles, can be retained during radon barrier compaction despite best management efforts to remove them (Waugh and Smith 1997; DOE forthcoming). The structure and size of remnant soil structure can have considerable impacts to compaction and hydraulic properties of CMB's (Daniel and Benson 1990).

A CMB is a stratigraphy of individual depositional events (i.e., loose lift-and-compaction events) composed of materials that can contain slight morphological variation (given borrow material heterogeneities), and construction variation (given moisture, compaction effort, and equipment selection). Such variations in depth can lead to the emergence of horizontal inter-lift zones of lower bulk density and higher hydraulic conductivity that may result in planes of weakness or continuous preferential flow paths (Bennett and Kimbrell 1991; Benson and Wang 1996). The methods of placement of loose lifts on slopes can occur in parallel (i.e., “to grade”) or horizontal (i.e., “stepped”) deposition and compaction events and require special consideration and more rigorous quality control testing and inspection (Bennett and Kimbrell 1991). Variable hillslope loose lift stratigraphy has been associated with the observance of erosional pipes in a poorly graded sand-bentonite radon barrier at the Mexican Hat, Utah, UMTRCA site (DOE forthcoming).

In addition to physical variations, chemical and biological variations can also be present in CMB's at construction (Schlesinger and Pilmanis 1998). Taylor et al. (2003) observed dead plant roots of varying sizes within an in-service CMB and suggested that they came from borrow materials. Construction debris including wooden stakes, ball bearings, bolts, and various other materials can also be observed in various layers of cover systems (DOE forthcoming).

Human artifacts, relic structures, and material heterogeneities have been hypothesized as initial places of soil change given the inherent variation in physical properties and subsequent matric potential gradients (Burt and Cox 1993; Albright 2006b; Benson et al. 2011). Remnant soil structure, laminar compression planes between lift-and-compaction events, and zones of coarse sands and gravels are commonly found enmeshed with the highest density of fine and very fine roots within in-service CMB's, suggesting that such voids are the preferred locations of root penetration immediately post construction (Taylor et al. 2003). Given textural differences and root establishment, material heterogeneities can also serve as locations for preferential flow. In silty-textured CMB's, or those with a high percentage of dispersive clays, these preferential flow paths may enlarge over time. In such soils, contact erosion or piping may occur under high intensity rain events (see Section H.3.3).

H.2.2.7 Construction Topography

As a constructed landform, topography and relief are initially dependent on engineering design [Eq.H.2]. Relief describes the physical orientation of a landform in relation to relative elevation gain, slope, and aspect. In terrain with variable topography, soil moisture collects at lower points in the landscape with consequences to vegetation abundance and patterning. On a field scale, topography will create microenvironments of drier or wetter locations than average. Additionally, relief and aspect influence the duration of daily and annual solar gain, resulting in hotter or colder microenvironments with impacts to soil reactions and plant productivity. Given solar gain, drier soils are expected on south-facing slopes, which may impact rates of desiccation cracking in CMB's, and subsequent performance for hydrologic and gas control. Consequently, north-facing slopes may remain saturated for longer duration than site average.

The geometry and sharpness of hillslope topography also influences rates of soil drainage, soil depth, and wind velocity. Across several sites in the UMTRCA portfolio, the leeward slopes of rock riprap disposal cells preferentially collect aeolian dust as a result of decreased wind speeds. The establishment of vegetation has been observed to correspond with dust infill on leeward slopes. Drainage, erosion, sediment transport, prolonged saturation, and the collection of soluble salts and carbonate can also be influenced by topography given the preferential movement of water downslope with gravity (DOE forthcoming). Depressions or channels on waste covers serve as low points and can be designed to facilitate drainage or result from the settlement of saturated wastes that dewater over time. Such cover depressions can result in ephemeral lakes (DOE 2014). Topographically varied waste covers that more closely resemble natural drainage systems have also been proposed (Zhang et al. 2018). Prolonged saturation in CMB's occurring in depressions, drainages, or slopes may also have impacts to long-term soil morphology due to decreased rates of desiccation and cracking. Given the inverse relationship between soil moisture and gas diffusivity, low points on cover systems that remain saturated for prolonged time periods also result in lower rates of radon diffusion (see Section 4 and Section 7).

H.2.3 Climate

Climate influences two fundamental inputs to soil formation: precipitation and solar energy (Buol et al. 2011). Water dissolves and transports materials into, within, and out of soils, and directly contributes to plant and animal growth. As precipitation increases, vegetation diversity and abundance generally increase (Jenny 1980). In areas with higher rainfall, plant rooting is more abundant at shallower depths in the soil profile, while plant rooting in arid zones is characterized by deeper and broader rooting given resource limitations and the need to source water over greater lateral distances and depths (Fan et al. 2017).

While average climate conditions can provide guidance on expected vegetation patterning, extreme weather events, including large storms and flood events, can play considerable roles in shaping landscapes, particularly in semiarid and arid regions. On waste covers, such rainfall events can significantly increase the risk of erosion. Probable maximum precipitation (PMP) events are used to calculate surface erosion potential and identify the mean rock riprap diameter (D_{50}) and gradation needed to resist such events as a function of slope and slope length (Maynard et al. 1989; Abt et al. 1991; Abt et al. 1998).

The majority of UMTRCA covers are in relatively dry environments, with 80% of the current sites receiving between 200 and 400 mm of precipitation annually, impacting not only initial cover design, but also long-term performance (Voorhees et al. 1983). Periodicity and timing of precipitation during the year influences vegetation establishment, succession, and persistence, soil water balance, and deep percolation. The melting of snowpack during low evapotranspiration (ET) in spring may contribute most significantly to deep percolation in vegetated waste covers in the western United States. In semiarid zones, monsoonal rainfall during the summer will commonly result in shallow water storage in the root zone before being transpired by the fall. Under vegetated conditions, the duration of seasonal water deficit can also contribute to the formation and patterning of soil fractures from root-induced desiccation and cracking (Kodikara and Costa 2013).

Temperature plays a controlling role in regulating soil physical processes including freeze-thaw and shrink-swell cycling. Temperature also greatly influences the type and abundance of vegetation in an area. As temperatures increase, soil organic carbon and nitrogen tend to decrease resulting in feedbacks to plant productivity (Jenny 1980). Air temperature, humidity, and windspeed are also the primary variables used in calculating potential ET which greatly influences the rates of water movement through soils in semiarid environments.

Rates of chemical reactions in the soil are impacted by temperature, and for every 10°C increase in temperature, the speed of reactions generally increase by 2 to 3 times (Van't Hoff 1884). Reactions including nitrogen mineralization, pH buffering, and respiration have significant impacts on plant growth. Under warmer climate conditions, rates of organic carbon decomposition and nitrogen mineralization increase with consequences to soil quality (Hungate et al. 2003).

The absorption of thermal energy into soils is influenced by surface albedo through variables including vegetation, surface color, and aspect. The dark surfaces of basalt rock riprap common to disposal cells in the UMTRCA program can absorb more heat than vegetated covers, while trees provide the greatest insulation from solar gain. However, if rock riprap is sufficiently deep, rocks (regardless of albedo) can thermally insulate CMB's resulting in higher vapor pressure gradients, reduced evaporation, and increased soil moisture at the CMB-rock riprap boundary (Waugh et al. 2018a). In the northern hemisphere, south-facing slopes will tend

to be warmer and drier than north-facing slopes; therefore CMB's on south-facing slopes may be more prone to desiccation and cracking and reduced vegetative cover.

H.2.4 Vegetation and Soil Development

Soils and organisms interact and evolve together (Jenny 1980). Grassland soils are characterized by deep organic rich surface horizons, mixing by animals including earthworms and rodents, and general horizontal uniformity in soil morphology, at fixed depths, at the field scale (Six et al. 1998). Semiarid and xeric shrubland soils are characterized by patchiness in nutrients, soil morphology, and soil hydraulic properties (Lyford and Qashu 1969; Schlesinger and Pilmanis 1998; Bird et al. 2002). Soils in mixed temperate to subtropical forests have high leaf litter, and higher acidity given the presence of organic acids, resulting in increased mineral weathering and chemical horizonation (McKeague et al. 1983). Given the lifespan of individual trees, forest soils can be characterized by patchiness associated with root development, soil compaction, and episodic windfall and root churning (Pärtel and Wilson 2002).

Engineered surface covers for waste containment are present across all major biomes and vegetation patterning can have significant and irreversible impacts to as built soil engineering properties (Burt and Cox 1993; Link et al. 1994; Smith et al. 1997; Waugh and Richardson 1997; Waugh et al. 1999; Taylor et al. 2003; Albright et al. 2006a; Fourie and Tibbett 2007). With few exceptions, the soil morphology of waste covers in shrubland environments is heterogeneous between profiles, while those waste covers in grassland environments display more uniform soil morphology between profiles (Section 7; DOE forthcoming).

H.2.4.1 Edaphic Conditions of Engineered Surface Covers at Construction

Edaphic condition refers to soil characteristics relevant to plant growth including acidity, aeration, toxicity, and nutrient availability. It is common for the soils in waste covers to contain adverse chemical conditions including metal toxicity, extreme pH values, salinity, and nutrient deficiencies given proximity to heavy industry. Such adverse conditions can influence rates and patterns of root establishment and above ground biomass (Handel et al. 1997). It is widely understood that plants growing in nutrient deficient environments (i.e., low NO_3^-) will develop fast growing taproots with nominal root branching (Wiersum 1958; Drew and Saker 1975; Ericsson 1995). N, P, K, and Fe nutrient deficiencies can affect root branching, root hair production, root diameter, and root growth angle (Forde and Lorenzo 2001). The same trend in root development is found under conditions of Cd, Cr, Cu, Ni, Zn toxicity (Peralta et al. 2001).

The soil atmosphere above buried wastes may also inhibit plant growth. Anoxic conditions of municipal landfill covers are often indurated with methane, carbon dioxide, hydrogen sulfide, ammonia, and other metabolically inhibitory gases (Ham 1979; Handel et al. 1997). Studies conducted by EPA have shown damage to tree roots growing in high concentrations of noxious gases common to municipal landfills (Flower et al. 1977; Flower et al. 1981). Root inhibition by gases generated by decomposing municipal waste can hinder, but not necessarily prevent, the revegetation of closed landfills (Gilman et al. 1981). However, not all hazardous wastes requiring burial (including uranium mill tailings in the UMTRCA program) will produce gases known to be detrimental to vegetation establishment, and if they do, they will only produce them for a short period of time given very low levels of decomposable organic matter in the subsurface (Smith et al. 1997). Given the various adaptations that native plants can make to adjust to native substrates and the immense heterogeneity in metal pollution, nutrient

availability, soil pH, and the composition and concentration of gasses trapped in the subsurface, few generalizations can be made about edaphic restrictions of engineered covers at construction. As such, it remains important to characterize materials used for cover construction during the design process and as a component of long-term cover monitoring.

H.2.4.2 Incorporating Vegetation into Design

The biotic condition of a waste cover is influenced by initial design, ongoing management, and surface changes resulting in more-or-less suitable conditions for plant growth. UMTRCA covers are rarely, if ever, planted with vegetation other than grasses and forbs; however, natural vegetation succession can be permitted depending on site specific waste characteristics, cover design, and site reuse goals as defined in site specific Long-Term Surveillance Plans. In the UMTRCA program, designs have traditionally favored static rock riprap over vegetated designs for reasons including uncertainty in natural succession and unknown performance impacts associated with root development in the radon barrier. When located in climates that can support diverse vegetation, rock riprap covers represent far from equilibrium designs in relation to surrounding natural conditions, and their surfaces have been observed to change more rapidly when compared to vegetated designs (Waugh et al. 2009; DOE forthcoming).

H.2.4.3 Management of Vegetation

In vegetated waste cover designs, grasses and small shrubs are often managed through grazing by cattle or mowing and bailing. Vegetation encroachment on rock riprap surfaces and vegetated covers planted with grasses has been liberally observed across the UMTRCA portfolio and can be costly to manage (Waugh and Smith 1997; Waugh et al. 2007; Waugh et al. 2009). Deep-rooted plants (i.e., long considered a threat to engineering integrity) are often hand cut and treated with herbicide. The economic costs, and the human and environmental health risks associated with indefinite herbicide applications, have resulted in efforts to better understand the long-term impacts of plant rooting on cover systems (DOE 2015; DOE 2016; DOE 2019a).

The establishment of vegetation on rock riprap covers may enhance cover performance through increasing evaporative demand on some sites (Glenn et al. 2001; Waugh et al. 2009; Waugh et al. 2015). Long-term lysimeter studies on an experimental waste cover in Grand Junction, Colorado, show that the establishment of mixed steppe vegetation limits deep percolation of precipitation versus unvegetated controls (Waugh et al. 2018a). After 19 years at the ET cover at the Monticello, Utah, Site deep percolation is limited to between 0.1% and 0.5% of annual precipitation (Benson et al. 2018; Waugh et al. 2018b). Given the high likelihood of vegetation encroachment on conventional rock riprap covers, and the associated benefits of vegetation on water balance, stakeholders are exploring opportunities to transition conventional covers to water balance covers (Waugh et al. 2018a; Waugh et al. 2018b).

Vegetation management decisions can play a considerable role in the development of CMB condition through time. Deep plant rooting may be limited if vegetation is effectively controlled. However, some vegetation, including mesquite, are resistant to all but the most aggressive of management efforts (Streets and Stanley 1938; Herndon 1980). The removal of biomass by haying can also have long-term impacts to carbon deposition and nutrient cycling from reduced plant litter, which can alter long-term vegetation density with implications to surface erosivity (Blanco-Canqui and Lal 2009). Overgrazing can result in a deterioration of plant quality and

increased risk of soil erosion, while properly managed grazing practices can result in increased pasture health, plant rooting, infiltration, and erosion control (Bilotta et al. 2007).

H.2.5 Regulatory Time Frames

Soils change over time given the configuration of other soil forming factors. Time controls the number of cycles through which pedogenic processes can result in morphological change (see Section H.3). Waste covers are unlike many natural soils in that they have a relatively well-defined time = 0 and are engineered to perform functions over a specified time (e.g., the regulatory time frame). The processes that occur within these time frames are most relevant to managers and regulators needing to understand feedbacks associated with earth surface process, soil change, and cover performance. However, longer term changes beyond regulatory time frames, will likely be of considerable interest to future communities living in proximity to aging waste disposal cells.

The time frames associated with maintaining satisfactory waste isolation greatly depend on the type of waste being buried. Disposal cells for municipal waste containment (i.e., household garbage) are generally required to maintain stability for 30–50 years (40 CFR 258), disposal cells for the isolation of uranium mill tailings are expected to maintain stability for 200–1000 years (40 CFR 192.02), low-level radioactive waste disposal facilities are required to maintain stability for 300–500 years (10 CFR Part 61.44), while covers for the isolation of mid- to high-level radioactive wastes are required to achieve long-term stability over 10,000 year timescales (Wing 1988) in accordance with DOE Order 435.1 Pg Chg 1, *Radioactive Waste Management*.

Our understanding of soil change is largely based on the long-term soil record (tens of thousands to millions of years) from chronosequence studies (Stevens and Walker 1970; Huggett 1998). Relatively few pedogenic studies have explored the decadal-to-century-long regulatory timescales relevant to waste covers (Richter 2007; Richter et al. 2007). Substantial changes to as-built CMB morphology have occurred in as little as 5 years after construction from a mix of abiotic and biotic processes (Burt and Cox 1993; Benson et al. 1995; Melchior 1997; Benson et al. 2011). However, few studies have been performed to measure changes that may occur after 25 years from construction representing a significant gap in our understanding of long-term performance. Natural analog soils, formed under similar forming factors to waste covers, have been used to estimate the long-term direction of waste cover change (Waugh et al. 1994a; Waugh et al. 1994b; Waugh et al. 1997). Such studies remain sparse, and a systematic understanding of soil processes and rates of change relevant to regulatory time frames remains underdeveloped.

H.3 Pedogenic Process in Engineered Surface Covers for Waste Containment

Soil-forming factors are not processes, nor are they directly responsible for the development of soil morphology. They are master variables that are used to predict soil properties across landscapes. Soil morphology is maintained, created, and regulated by additions, losses, transformations, and transfers of energy and mass occurring at the earth's surface through space and time (Simonson 1959). Additions can include carbon and nitrogen input from plant materials, aeolian dust, sediment deposition from overland flow, or cow manure as a byproduct from animal foraging. Losses can include organic matter decomposition and volatilization into carbon dioxide, wind or water erosion, the leaching of soluble salts, or the export of biomass from surface management by cutting and bailing. Transformations can include physical

processes of desiccation-cracking or freeze-thaw cycling, pedoturbation by plant roots and animal burrowing, humification of organic carbon into stable aggregates, the weathering of primary minerals into secondary products, or cation substitution in clay minerals. Transfers can include soluble salt and carbonate movement within the profile, the deposition of plant debris in cracks and redistribution by thermal- or moisture-driven mixing, or the leaching of iron and manganese from redox reactions resulting in the formation of gleyic features.

This section first focuses on the initial drivers of soil change in waste covers with emphasis on physical processes including desiccation-cracking, freeze-thaw cycling, clay dispersion, and erosion that can impact the CMB. The impacts associated with secondary processes including plant rooting, bioturbation by animals, and the formation of soil structure are then explored, followed by processes including the accumulation and redistribution of aeolian dust, soil organic carbon, soluble salts, calcium carbonate, oxidation reduction reactions, and the formation of secondary aggregates from broken down CMB and accumulated materials.

H.3.1 Desiccation and Cracking

There are two main mechanisms responsible for the formation of soil structure (1) those processes of aggregation that lead to the binding and stabilization of non-cohesive particles into larger particles and (2) those processes of fragmentation that result in the breakdown of consolidated blocks within cohesive materials (Ghezzehei 2012). The earliest stages of soil development in CMB's are attributed to fracturing from shrink-swell and desiccation-cracking phenomena associated with wetting and drying cycles (e.g., see Yesiller et al. 2000 and Albrecht and Benson 2001, for detailed reviews on the subject). When bulk soils become saturated, the pressure of the system increases due to limited gas movement resulting in the stress induced expansion and reorientation of platy silt and clay particles against rigid, nonreactive, sand particles. As soils dry, pressure recedes causing contraction along planes of weakness and small discontinuities (i.e., structural, textural, or compaction related) in otherwise uniformly conditioned, fine textured materials (Benson and Wang 1996; Hutchings et al. 2001; Taylor et al. 2003). Upon soil rewetting, preferential flow occurs along legacy planes of weakness (Omidi et al. 1996). Some studies proposed that microdefects and air-filled pores act as initial points of crack initiation in fine-textured soils (Frydman 1967; Snyder and Miller 1985; Morris et al. 1992).

Soil texture and mineralogy correspond to the degree of cyclic volume change with fine-textured soils of smectitic mineralogy resulting in the greatest volume change and the strongest degree of structural unit expression upon complete drying (DeJong and Warkentin 1965). Finer-textured soils also tend to have less shear resistance and will break into smaller structural units resulting in increased crack density (Southard and Buol 1988). The speed of soil drying can also greatly influence crack size, with slow and even drying resulting in larger cracks, and fast uneven drying resulting in smaller cracks (Krisdani et al. 2008). Cracking is also more pronounced in high clay soils after prolonged saturation versus intermittent hydration (Kleppe and Olson 1985). In rock riprap waste cover systems, thinner riprap and bedding layers that are in direct contact with underlying CMB's can contribute to increased rates of desiccation versus deeper riprap and bedding layers.

Cracking results in the establishment of preferential flow paths. In dispersive soils, such flow paths may enlarge through time leading to surface rilling or erosional piping (Sherard et al. 1976). Surface desiccation cracks are considered primary contributors to erosional pipe initiation in natural landscapes across much of the western United States (Parker 1963; Parker

and Jenne 1967). As wetting and drying cycles continue through time, emergent fractures in CMB's may become reinforced through the deposition of dissolved solutes and soil organic matter churned from the surface (Blokhuis et al. 1990), which can lead to the establishment of plant roots along fracture planes (Burt and Cox 1993). Taylor et al. (2003) suggests that the infill of coarser illuviated materials into emergent desiccation cracks in the CMB may be responsible for creating conditions suitable for secondary root intrusion at a shallow, planted cover in Northwest Territories, Australia. Depth from ground surface, climate, and the composition of materials placed above the CMB exert significant influence on rates and patterns of initial soil cracking (Benson et al. 1995; Albright et al. 2004; Albright et al. 2006a; Albright et al. 2006b; DOE forthcoming).

H.3.2 Freeze-Thaw Cycling

In frigid climates, fracturing from freeze-thaw cycling can also contribute to the development of irreversible porosity in high clay soils (Edwards and Cresser 1992). In as little as two cycles, rates of hydraulic conductivity can more than triple in clay soils and increase by 100-fold in clays compacted wet of optimum (Kim and Daniel 1992; Benson and Othman 1993). The thermal conductivity of compacted soils is greater than noncompacted soils, with freezing depth and thawing rate higher in compacted soils (Barnett 1937). The amount and type of ground cover greatly influence the rate and depth of both freezing and thawing characteristics. Soils covered with leaf litter and mulch remain warmer, while uncovered soils are more prone to freezing (Kohnke and Werkhoven 1963). Frost duration and depth are also influenced by vegetation type with coniferous woodlands remaining frozen longer and at greater depths, followed by deciduous forests, mixed meadows and grasslands (Post and Dreibelbis 1942; Harris 1972). Recurring cycles of ice nucleation can result in lenticular-platy soil morphology in uniformly textured soils.

The initial moisture content of soils impacts frost characteristics, and dry soils have been shown to freeze faster, and to greater depth, than wet soils (Willis et al. 1961). The concentration of soluble salts can also modify freezing characteristics with higher concentrations of salts decreasing the freezing point of soils (Fuchs et al. 1978). Pore structure and soil texture also contribute to variation in freezing. Ice nucleation first occurs in large soil pores, with sustained lower temperatures being required to freeze water in smaller pores (Larson and Allmaras 1971). Therefore, it can be expected that as-built CMB's will require lower temperatures (or longer times) to freeze as compared to adjacent, noncompacted, natural fine-textured soils with larger pore spaces. However, as CMB's begin to develop pore structure, threats from freezing and thawing may increase.

H.3.3 Soil Erosion and Piping

Soil erosion by water is a critical issue of global concern (Lal 2001; Morgan 2005). Erosional processes can occur at the surface or subsurface. Despite the significance and geographic extent of subsurface erosion (Poesen 2018), most of the research literature has focused on processes of erosion caused by overland flow and incision (Cerdan et al. 2010; Castillo and Gómez 2016). The disproportionate representation in the literature has been attributed to the difficulty in studying subsurface processes (Swanson et al. 1989; Faulkner 2006). Only when a pipe roof collapses are the extent of erosional features revealed (Verachtert et al. 2010; Verachtert et al. 2011).

Erosional soil piping is a significant and widespread process that has been reported across almost all climactic zones (Poesen 2018). In the broadest sense, soil piping involves the formation of linear voids (i.e., pipes) by the concentrated flow of water in the subsurface, which can result in the collapse of the soil surface and the formation of gullies (Jones 2004). Piping is influenced by a combination of site factors including individual storm events and long-term climate; the physical, chemical, and biological properties of soils; landform topography; vegetation type and age; and land use (Bernatek-Jakiel and Poesen 2018).

From the perspective of geotechnical engineering, several of the most destructive forms of erosion to earthen structures can be attributed to soil piping (Richards and Reddy 2007), and a review by Foster et al. (2000) found that 46% of dam failures were associated with erosional piping. Engemoen (2017) examined U.S. Bureau of Reclamation dam failure incidents and estimated that 80% of all document cases of erosional piping in embankments are associated with soils with no or low plasticity ($PI \leq 7$).

Richards and Reddy (2012) describe how the overall quantity and mineralogy of the fines fraction in soil influences the initiation and mode of soil piping, with non-plastic fines reducing required seepage velocity to initiate piping and plastic fines greatly increasing the hydraulic gradient required to initiate piping. Cohesion is not a static property and can be altered by soil processes characterized by additions, losses, transformations, and transfers of energy and mass into and through the soil system over time (Simonson 1959).

Erosional piping has been observed along downslope regions at the UMTRCA cover at the Mexican Hat site (DOE 2019b). Piping was attributed to a combination of suffusion, dispersion, and internal erosion given radon barrier texture dominated by low-cohesion sands, variations in bulk density, and hydraulic conductivity with depth in the radon barrier, dispersive fines located within a poorly graded sandy skeleton in a sand-bentonite mixture, and insufficient (e.g., sandy) fines in the bedding layer (DOE 2020).

H.3.4 Plant Rooting

The physical properties of CMB's can affect plant rooting through direct penetration resistance, limited hydraulic conductivity, nominal plant available water, and restricted gaseous diffusion (Taylor and Brar 1991). The negative impact of soil compaction to plant rooting has been studied extensively (e.g., Unger and Kaspar 1994; Kozłowski 1999). Depending on plant species and soil type, soil bulk density between 1.5–1.8 g cm³ can significantly limit or stop root growth (Heilman 1981; Simmons and Pope 1987; Siegel-Issem et al. 2005; Bengough et al. 2006). The as-built density of a CMB is commonly 1.75 g cm³ (Goldman et al. 1988), which can result in the development of thick and short roots versus long and fine roots (Russell 1977). Initial rooting in high bulk density soils favors emergent cracks to improve access to subsoil moisture, which can lead to localized alterations to chemical, physical, and biological properties relative to the bulk soil (Pierret et al. 1999; Jegou et al. 2001; Pankhurst et al. 2002). In waste covers that incorporate vegetation into design, thick layers of (i.e., noncompacted) overburden soil materials can serve as a favorable medium for roots, with root benching commonly observed at the top edge of the CMB.

In lieu of the physical or chemical limitations imposed on rooting in CMB's at construction, the establishment of vegetation has been liberally observed even on waste covers that do not incorporate overburden or topsoil layers (DOE 1992; Burt and Cox 1993; Waugh and Smith 1997; Hutchings et al. 2001; Taylor et al. 2003; DOE forthcoming). Considering that growth

rates of fine roots can range from a few millimeters to a few centimeters per day (Pierret et al. 2016), root development in CMB's can happen rapidly.

The impact of plant rooting on as-built CMB morphology can be considerable. Plant roots not only accelerate rates of wetting and drying cycles but also promote small scale soil-water heterogeneities and stress imbalances which can result in the propagation of microcracks (Angers and Caron 1998). Root size exerts a proportional influence on crack size with very fine roots and root hairs controlling the formation of the smallest cracks (Dorioz et al. 1993), and crack propagation extending to the outer boundaries of the rooted zone (Mitchell and VanGenuchten 1992). Cracks associated with root-soil desiccation can be as wide as 50 mm depending on soil mineralogy, texture and climate (Ravina 1983), with greater plant biomass generally corresponding to the formation of cracks of greater length and total area (Grevers and Jong 1990).

During drought conditions at Rum Jungle, Northwest Territories, Australia, Taylor et al. (2003) characterized an extensive network of desiccation cracks associated with root mats in CMB's occurring along polygonal blocky structures that were structurally reinforced by dark staining from illuviated organic materials and iron oxidation. Similar features have been observed by others in both dry and humid environments (Waugh and Smith 1997; Albright et al. 2006a). The development of cracks from desiccation in CMB's can also occur when overlying soils are saturated (Hakonson 1986), indicating that the rate of water extraction by roots exceeds the rehydration rate of the underlying CMB (Waugh et al. 2006).

When plant roots expand into nonfractured bulk soils, they exert pressure on surrounding particles resulting in the reinforcement of macropore space through densification (Greacen et al. 1968; Dexter 1987). The localized compaction from densification around living roots can initially reduce infiltration rates, particularly at the surface (Guidi et al. 1985; Bruand et al. 1996); however, when roots die, the resulting macropore cavities are commonly stabilized through decaying organic materials which can lead to increased hydraulic conductivity (Barley 1954; Gish and Jury 1983). Plant root morphology greatly influences long-term infiltration characteristics, with hydraulic conductivity increasing year-over-year under plants with large diameter, long, and straight roots (i.e., alfalfa) (Meek et al. 1989; Meek et al. 1990). The pores formed by most roots are between 25–100 mm in size and are considered macropores (Gibbs and Reid 1988; FitzPatrick 1993; Lin et al. 1999). Such pores play a significant role in preferential flow in unsaturated soils (Beven and Germann 1982). As such, the formation of macropores by roots is a primary contributor of hydraulic properties in undisturbed soils (Edwards et al. 1989), including CMB's for waste containment (Waugh and Smith 1997; Taylor et al. 2003; Waugh et al. 2007).

Given hydrologic impacts associated with natural succession and subsequent plant rooting in CMB's, recent efforts have explored how conventional "low-permeability" covers may be transformed into ET covers to redirect soil-water back into the atmosphere (Waugh et al. 2009). However, a tradeoff exists given that plant roots can increase gas flux by accelerating the drying of barriers and creating preferential pathways for radon gas diffusion at UMTRCA sites (Link et al. 1994; Benson et al. 2018; Section 4).

The observation of dead roots in CMB's has been reported (Hutchings et al. 2001; Taylor et al. 2003; DOE forthcoming); however, the full impact of root turnover on waste cover evolution and performance remains understudied. In addition to impacts on hydraulic properties, the deposition of dead roots into soil contributes to nutrient cycling (Gish and Jury 1983; Aerts et al. 1992), stimulates the growth of bacteria (Rovira 1965), is a growth substrate for fungi (Went and

Stark 1968), provides food for nematodes, arthropods and earthworms (Curry and Schmidt 2007; Bonkowski et al. 2009), and increases aggregate stability (Tisdall and Oades 1982; Oades 1984). Rates of root turnover are highly variable within individual biomes (Yuan and Chen 2010), among plant species located at the same site (Coleman et al. 2000; Withington et al. 2006), and among individuals of the same species in the same field (McCormack et al. 2014). Total root lifespan commonly ranges from days to weeks in both grasslands and forests (Hendrick and Pregitzer 1997; Gill 1998; Arnone et al. 2000; Tingey et al. 2000). In nutrient-limited environments, including those likely present in many compacted barriers, Ryser (1996) suggests that plants decrease rates of root turnover to avoid unrecoverable nutrient losses.

The development of vegetation on waste covers can reduce erosion risk. Plant establishment results in bio-structural erosion control through the combined effects of reducing overland water flow velocity and increased soil shear strength (Gyssels et al. 2005). Root architecture plays a considerable role in regulating slope stabilization and shallow erosion control (Reubens et al. 2007). Vegetation with desirable rooting characteristics including root distribution, length, orientation, diameter, and seasonal root mass variability can be used to construct dynamic slopes for erosion control (Stokes et al. 2009).

H.3.4.1 Time Frames and Patterns of Plant Rooting in Compacted Mineral Barriers

Though variable depending on vegetation and climate, the time frames associated with root establishment within CMB's generally correspond to the thickness of the rock riprap and soil layers above the CMB with thinner layers corresponding to greater rooting risk (Hutchings et al. 2001). Anderson et al. (1993) suggests that a 2 m thick unconsolidated soil layer planted with native perennial shrubs and grasses is enough to isolate perennial grass roots above a CMB at Idaho National Engineering Laboratory (INEL). However, a review of 1084 citations by Foxx et al. (1984a) indicates that 7% of the native vegetation found to grow on fine-textured soils across the western United States have rooting depths in excess of 4.5 m, posing a risk to shallow waste disposal sites (Foxx et al. 1984b). A later systematic review on the role of biointrusion on UMTRCA radon barriers by Link et al. (1994) suggests that soil layers exceeding 2 m may be ineffective at isolating the roots of many grasses, forbes, shrubs, and trees from CMB's over periods longer than 100 years. Furthermore, Schenk and Jackson (2005) concluded that deep roots are most common to seasonally dry, semiarid zones with fine-textured soils, suggesting that the majority of UMTRCA sites in the western United States are in zones most susceptible to deep rooted vegetation.

It is likely that the long-term rooting depth in cover systems is not entirely consistent with native soils. Physical rooting restrictions imposed by initial CMB morphology, low rates of water percolation through CMB's compared to native soils, and the presence of buried wastes that may pose restrictions to vegetative growth, may all contribute to variations in rooting characteristics on covers versus natural soils. An adequate accounting of root patterning in both constructed and native soils is required if soil morphological information from natural analogs is to be accurately used to estimate the long-term conditions of waste cover systems over regulatory lifetimes. The study of analog soils with indurated and cemented soil horizons is likely most informative when making such comparisons.

A review of the literature on plant rooting characteristics of in-service rock riprap and vegetated covers (with emphasis on the UMTRCA portfolio) is presented in Appendix I, and a summary is presented in Figure H-2. Regardless of design or climate, initial plant rooting generally occurs along existing fractures or in areas of material heterogeneity created during construction (e.g.,

areas of thinner rock-riprap, or areas of riprap with greater fines content). After as little as 4 years at a vegetated humid cover, or after 20 years' regardless of cover design or climate, very fine roots are found through the depth of the CMB in most waste cover investigations reported in the literature. Medium to coarse roots generally do not penetrate through the depth of CMB's after several decades of service.

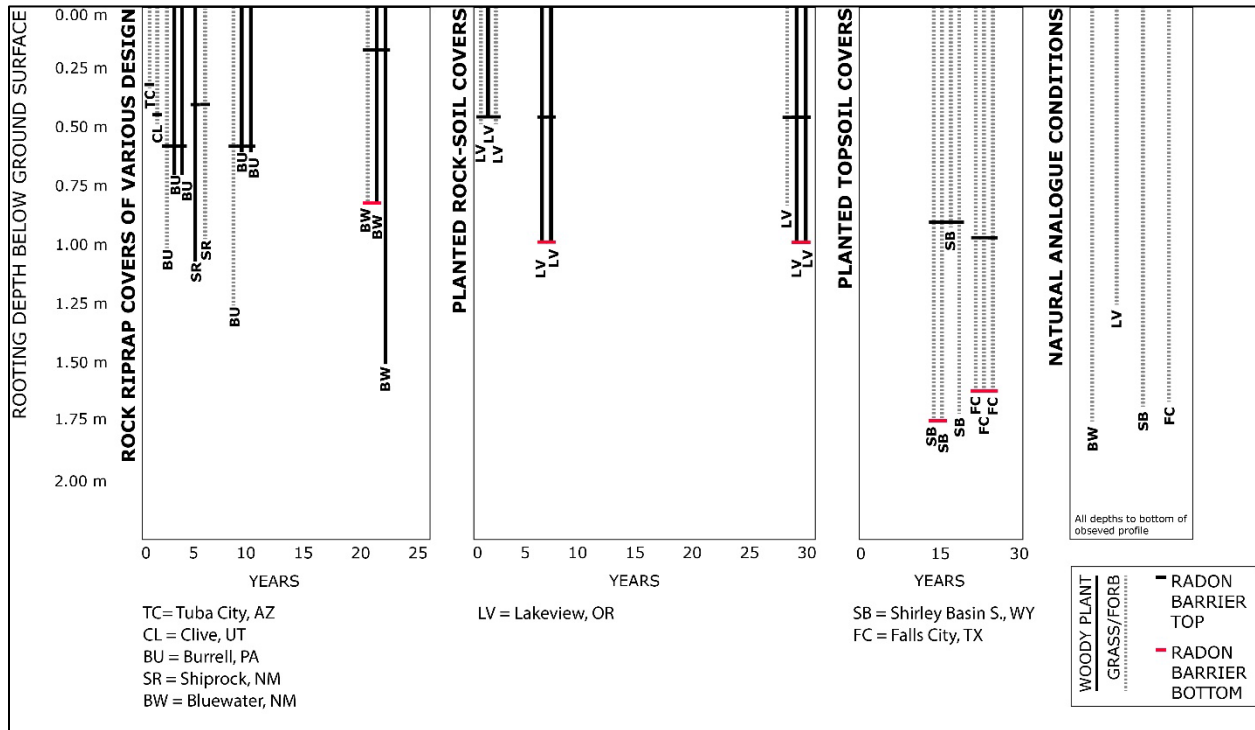


Figure H-2 Plant Rooting Depth Since Time of Construction in UMRCA Covers

H.3.5 Impact of Vegetation Patterning on Soil Condition

The patterning of shrubs in semiarid environments creates “islands of fertility” through the concentration of nutrients (including N, P, and K) localized beneath canopies (Schlesinger and Pilmanis 1998). For *Prosopis velutina* (velvet mesquite) a shrub common to the southwestern United States, plant mortality rates control the longevity of deposited nutrients with localized soil nitrogen and carbon being reduced by 75% 40 years after plant death (McClaran et al. 2008). Bulk density is also generally lower in soils under plants than in open areas between plants in semiarid environments. Aggregate stability at the 250-micrometer scale, C:N ratio, and glomalin are all highest under mesquite (*Prosopis glandulosa* Torr.) compared to sparsely vegetated interspaces (Bird et al. 2002). This corresponds to an average of nearly 3 times greater infiltration rate into soils under plants than in the open area between paloverde (*Cercidium microphyllum*) and creosote bush (*Larrea tridentata*) (Lyford and Qashu 1969). The maintenance of higher hydraulic conductivity soils is attributed to plant rooting and microbial processes that stabilize emergent soil structure through mechanisms including exudation of extracellular polysaccharides and aggregate enmeshment by mycorrhizal fungi (Morales et al.

2010). Such locations serve as biological “hot-spots” in semiarid environments and correspond to higher rates of carbon turnover, nitrogen cycling and biodiversity (Bundt et al. 2001).

H.3.6 Bioturbation by Animals

The establishment of vegetation on waste covers can create habitat for animals (Waugh and Smith 1997). Burrowing and tunneling animals can pose a threat to waste cover performance from direct vertical displacement of wastes (Winsor and Whicker 1980; McKenzie et al. 1982), and secondary drying and cracking of the CMB through wind-induced ventilation from tunnel systems (Vogel et al. 1973) thereby increasing potential rates of water infiltration and gas diffusion (Cadwell et al. 1989; Landeen 1994; Suter et al. 1993). The impact of animal burrowing on UMTRCA covers has long been explored (Gano and States 1982; Cline et al. 1982; Beedlow and Hartley 1984; Bowerman and Redente 1998), resulting in design and long-term management suggestions intended to limit biological intrusion by animals (Hakonson et al. 1982a; Hakonson 1986). An extensive review on the risks associated with bioturbation on waste covers is provided by Bowerman and Redente (1998).

The incidence of documented animal intrusions into DOE waste covers are numerous. At the Grand Junction, Colorado, UMTRCA site, prairie dogs burrowed through interim soil caps and transported mill tailings to the surface (McKenzie et al. 1982). At Hanford, Washington, a large mammal believed to be a coyote or badger burrowed into a waste trench (O'Farrell and Gilbert 1975). At the INL, rodents have excavated through CMB's in excess of 1.2 m thick (Arthur and Markham 1983).

The physical extent of animal burrowing on cover systems can be extensive. At a single burial site at LANL pocket gophers excavated a total of 12,000 kg of soil per ha during a 1-year period, resulting in an estimated 8 m³ void space across an estimated 2.8 m long tunnel network (Hakonson et al. 1982b). Ants are among the most important soil engineers in semiarid areas (Cammeraat and Risch 2008). Harvester ants (*Pogonomyrmex spp.*) can excavate nests that are 1.5 m deep and occur up to 1 m away from the center of the mound (MacKay 1981). Nests from *Pogonomyrmex spp.* were shown to increase rates of infiltration up to 2.5 m away from the center of the mound in clay loams at the INL (Blom et al. 1994). Across the Wye waste repository in the 300 Area at Hanford, Washington, a total of 358 *Pogonomyrmex spp.* colonies were counted, with the total volume of displaced material from single colonies averaging 1774 cm³ per colony, at an annual soil displacement rate of 1 kg per colony, and average excavation depths exceeding 2.3 m (Fitzner et al. 1979). At Rum Jungle, Northwest Territories, Australia, a total of 18 large termite mounds were observed across the 36-ha waste cover. When excavated, extensive termite galleries were found in barriers to the depth of wastes (>60 cm) (Taylor et al. 2003). At moist sites, earthworm burrowing may cause the most significant changes to waste cover soils over time, although little work has been done on their activity within waste covers (Beedlow and Hartley 1984). Earthworms have been observed in several UMTRCA waste covers (DOE forthcoming).


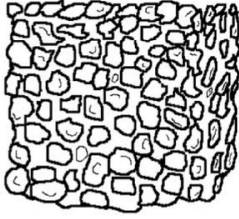
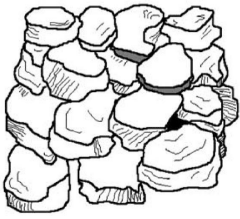

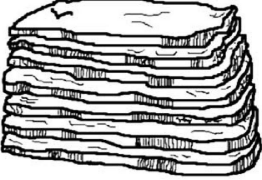
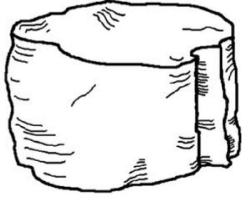
Patterns and intensities of bioturbation by invertebrates and small mammals are greatly influenced by vegetation, climate, and soil type. Most burrowing mammals, in semiarid areas, prefer sparse vegetation in disturbed areas (McCloskey 1976; Fitzner et al. 1979; O'Farrell 1980; Kinlaw 1999), conditions that are common in early successional environments across UMTRCA waste covers on the Colorado Plateau. Daily minimum and maximum temperatures also greatly influence total burrowing depth with deeper burrows being found in zones with temperature extremes (either hot or cold) as animals seek thermal stability (Kinlaw 1999). Soil

texture can also influence burrowing characteristics, with species-to-species variation being considerable. In a xeric shrub community in southeastern Oregon, chipmunk (*Eutamias minimus*) burrowing density was directly related to higher clay percentage, while an inverse relationship was found between pocket mice (*P. parvus*) burrow density and the percentage of clay (Feldhamer 1979). High clay percentage and induration by carbonate (conditions similar to CMB's) have also been found to correspond to greater burrow complexity, total excavation volume and burrow length (Laundre and Reynolds 1993). Additionally, animals with larger body mass are also generally more capable of excavating in soils with larger rock fragment size (Kinlaw 1999).

Large rocks attract burrowing mammals because they serve as protected sites against predation (Smith et al. 1997). The observation of burrows (both active and abandoned) on in-service UMTRCA waste covers has largely favored locations with rock riprap, specifically slopes and along top-deck-side-slope interfaces (DOE forthcoming). A review of factors that affect small mammal habitability on UMTRCA waste covers was compiled by Gano and States (1982); however, studies to determine long-term performance impacts associated with animal burrowing, or expected burrow densities on in-service waste covers have been sparse (DOE 2015; DOE 2016).

H.3.7 Development of Soil Structure

Soil structure broadly encompasses the spatial arrangement of particles in soil and has significant implications to soil function and plant growth (Bronick and Lal 2005). Soil structure exists across a spectrum from single grained, non-cohesive particles (i.e., sand dunes) to massive structures (i.e., monolithic clays with no internal features), with emphasis being placed on collections of particles (i.e., soil aggregates or peds) occurring somewhere in the middle of the spectrum (Ghezzehei 2012; Schoeneberger et al. 2012). A generalized description of major soil structure classes and pathways to development is presented in Figure H-3.

<p align="center">SINGLE GRAIN</p> 	<p align="center">GRANULAR</p> 	<p align="center">BLOCKY</p> 
<p>Composed of largely non-reactive sand size particles of roughly uniform size distribution.</p>	<p>Predominantly the result of biological forces including: earthworms, insects, fungal hyphae, and fine roots.</p>	<p>Developed through cycles of shrink-swell. Size defined by boundaries in homogeneous matrix (i.e. root patterning). Most common to soils with rapid drying.</p>
<p align="center">PRISMATIC</p> 	<p align="center">PLATY</p> 	<p align="center">MASSIVE</p> 
<p>Uniform shrinkage after extended periods of saturation. Most common in uniformly textured soils, enriched with sodium, that slowly dry.</p>	<p>Generally occur through unidirectional compressional forces. Most commonly produced in surface soils compressed by heavy equipment.</p>	<p>Common in fine textured sediments that are slowly sorted and cemented (argillinc), manufactured (clay barriers), or compressed (fragipan).</p>

Images courtesy of the U.S. Department of Agriculture

Figure H-3 Soil Structure and Mechanisms of Formation

H.3.8 Secondary Aggregation of Broken-Down Barrier Materials

Soil aggregation and stabilization are a secondary process that first require CMB's with massive structure (i.e., from compaction) to be broken down by the processes of desiccation-cracking, wetting-drying, fracture, root penetration, and bioturbation by animals, as described in previous sections. Once a CMB turns into a collection of heterogeneous materials of mixed particle and pore sizes, the process of soil aggregation may occur through well characterized pathways (Tisdall and Oades 1982; Six et al. 2004).

The aggregation of soil particles involves several processes that are influenced by initial conditions, climate, mineralogy, soil organic carbon content, flora and fauna, and microorganisms. Aggregation requires the presence of organic binding agents which vary in chemical structure under different forms of vegetation and management (Kay 1990). Tisdall and Oades (1982) classify organic binding agents into three broad categories based on its persistence: (1) polysaccharides (lasting weeks); (2) roots, fungal hyphae, bacteria, and algae (lasting months to several years); and (3) humic materials and polymers (lasting tens to hundreds of years).

Plant rooting in CMB's is likely the primary factor contributing to any observed stabilization of soil aggregates, given additions of soil organic matter through root turnover and the aggregate enmeshment by root associated fungal hyphae (Haynes and Beare 1997; Tisdall and Oades 1979; Tisdall et al. 1997), particularly in semiarid environments (Chaudhary et al. 2009). Microorganisms and root exudates contribute to the production of rhizosphere polysaccharides that can glue individual soil particles together (Watt et al. 1993; Traoré et al. 2000). The soil water regime can also contribute to the formation and stabilization of soil particles on plant roots (Watt et al. 1994), with root associated aggregate strength shown to increase through intense and frequent drying cycles from plant induced ET (Horn and Dexter 1989; Czarnes et al. 2000). In semiarid environments, the emergence of secondary aggregates increases hydraulic conductivity (Bouma and Anderson 1973; Boyle et al. 1989). As structuring increases, CMB's shift from uniformly constructed soils toward dynamic and heterogeneous biological soils. The process of secondary aggregate formation and stabilization is more pronounced in biological soils, and results in the long-term maintenance of emergent soil architecture. The stabilization of soil structure in CMB's will likely increase both hydraulic conductivity and radon diffusion.

H.3.9 Accumulation and Redistribution of Aeolian Dust, Soil Organic Matter, pH, Soluble Salts, and Calcium Carbonate

Given the influence of aeolian dust (Dietze et al. 2012; Turk and Graham 2011), soil organic matter (Oades 1984; Dexter et al. 2008), soluble salts (Gray and Schlocker 1969), and calcium carbonate (Flach et al. 1969) to soil physical properties relevant to hydraulic performance of soils in semiarid environments, an understanding of the rates and qualities of additions, transformations, translocations, and losses of these materials can aid in the long-term forecasting of future waste cover condition and performance.

H.3.9.1 Aeolian Dust

Aeolian deposition is common in semiarid environments where many UMTRCA waste covers are located (Goldstein et al. 2008). In southern Colorado, individual events can deposit up to 2 g/m² dust (Lawrence et al. 2010); however, dust (silt and clay) deposition across the southwest is highly episodic (Reheis and Urban 2011). Rock fragments that occur naturally on desert soil surfaces or as engineered rock riprap, and gravel applied as a mulch by ancient and traditional farmers, have both been shown to accelerate dust accumulation (Goossens 1994; Xiao-Yan and Lian-You 2003). Dust deposition can lead to the formation of new soil horizons (McFadden et al. 1998); change the morphology, hydrology, chemistry, erodibility, fertility, and ecology of desert soil profiles (Dietze et al. 2012); and change the hydraulic conductivity and water storage capacity of soil profiles (Shafer et al. 2007; Reynolds et al. 2006; Turk and Graham 2011). Desert pavements derived from aeolian deposition may have partially hydrophobic surfaces (Belnap 2006). These conditions can lead to increased overland flow velocity and a greater potential for erosion (Rodríguez-Caballero et al. 2012). Additionally, calcium carbonate in dust can accumulate in the underlying soil profile (Van der Hoven and Quade 2002), and nutrients and propagules in the dust can change the composition and productivity of desert ecosystems (Reynolds et al. 2001; Garner and Steinberger 1989). The accumulation of aeolian dusts in rock riprap has been observed on numerous UMTRCA waste covers (Burt and Cox 1993; DOE 2019c).

H.3.9.2 Soil Organic Matter

Organic matter content has a direct relationship with many soil physical and engineering properties. As soil organic matter content increases, bulk density decreases (Curtis and Post 1964; Saini 1966), aggregation and total pore space increase (Kladivko and Nelson 1979; Oades 1984), infiltration capacity and hydraulic conductivity increase (Rawls et al. 1982; Dexter et al. 2008), and water holding capacity increases under higher tensions (Gupta and Larson 1979). Soil organic matter content also corresponds to the presence of soil arthropods and earthworms that further increase pore space through burrowing (Six et al. 2004).

In agricultural soils, the management of organic carbon is desired to improve the physical properties of soils for crop production (Bacon 1929; Bayer 1930). However in CMB's, it is commonly accepted that soil organic matter content runs counter to desired engineering parameters including compaction and hydraulic isolation (Franklin et al. 1973).

In mineral soils, compaction is sensitive to small changes in organic matter, particularly under higher rather than lower moisture contents (Soane 1990); therefore, native soil materials used for the construction of CMB's are selected for low carbon content. Over time, earth surface and pedogenic processes may lead to the accumulation and redistribution of carbon from dust deposition, plant root turnover, leaf litter accumulation, and microbial transformation of organic matter into humic materials. Post construction soils can rapidly accumulate soil organic carbon (Roberts et al. 1988; Bendfeldt et al. 2001; Schafer et al. 1980; Biber et al. 2013), corresponding to increased water holding capacity (Roberts et al., 1988), the evolution of depth dependent soil structure (Schafer et al. 1980; Anderson 1977; Roberts et al. 1988; Biber et al. 2013) and elevated rates of nitrogen cycling (Anderson 1977).

In native vertic soils (high clay soils that are characterized by shrink-swell), increases in soil stability have been linked to higher amounts of the mobile fraction of organic matter, as opposed to total organic carbon content (Cook et al. 1992; Lefroy et al. 1993). Additionally, surface vegetation type has been shown to considerably influence the total mobile carbon fraction of vertic soils (Cook et al. 1992). Given connections between vegetation, mobile organic carbon content, and soil structuring, the management of vegetation on waste covers will likely have long-term impacts to soil structuring and persistence within CMB's.

The accumulation and distribution of soil organic matter in CMB's have received little research attention to date. Given natural heterogeneity in excavated borrow materials that are sourced across broad landscapes during construction, the distribution of organic matter in a CMB may not only be a result of transformations or translocations occurring since construction, but also as built heterogeneity from sourced materials and construction sequence. No data exist to characterize as-built spatial distribution of carbon in CMB's; therefore, direct links between observed soil process, carbon distribution, soil morphology, and performance remain challenging given a lack of confidence in initial CMB condition.

H.3.9.3 Soil pH

Soil pH is the measure of soil acidity or alkalinity and has been referred to as a master soil variable given connections between pH and nearly all soil physiochemical processes (McBride 1994). In addition to direct impact to plant growth, pH also influences microbial activity, metal ion solubility, precipitation and dissolution kinetics, oxidation-reduction, and clay dispersivity (Haynes and Naidu, 1998). Clay particles have greater tendency to flocculate at high pH values and disperse

at low pH values with impacts to soil hydraulic properties (Haynes and Naidu, 1998). In acid soils, aluminum (Al) toxicity, constrains root elongation, and can negatively impact plant growth. In arid regions, elevated sodicity is commonly associated with high dissolved carbonate concentrations in soil solution, and thus high pH. When such arid soils dry, large soil aggregates and fractures tend to form (BoixFayos et al. 2001). In agricultural fields, carbonate (in the form of lime) is commonly applied to soils to neutralize pH resulting in conditions generally more favorable to plant growth, which subsequently results in increased rates of soil organic matter deposition and soil aggregation (Haynes and Naidu 1998). The addition of organic matter tends to lower the pH of soil, thereby enhancing rates of mineral weathering, however cations released during weathering naturally act to neutralize acidity.

H.3.9.4 Soluble Salts

Salts more soluble than gypsum are called *soluble salts*. Most commonly, these salts occur as combinations of the cations Ca^{2+} , Mg^{2+} , Na^+ , and H^+ with the anions CO_3^{2-} , SO_4^{2-} , Cl^- , and NO_3^- and water. The initial sources of salts in waste covers are varied. Salts can accumulate from atmospheric or aeolian deposition in semiarid landscapes, from the transport of salt from the soil materials used in construction, or from passive wicking from waste materials under the CMB. In semiarid and arid areas, the upward movement of contaminated salts from subsurface wastes through evaporative wicking has been identified as a potential vector for waste mobility (Young et al. 1986).

Given high solubility, many salts can remain dissolved in soil water until evaporation. The distribution of soluble salts within in-service CMB's may serve as an indicator of the cumulative water balance within profiles, in addition to the predominant direction of water movement through waste covers. If evaporation exceeds infiltration, salt accumulation will happen near the surface. If infiltration exceeds evaporation, salts precipitate lower in the profile (Turk et al. 2011). The depth distribution of sodium chloride (NaCl), a highly soluble salt, can vary seasonally in a soil profile, occurring near the surface in drier months and low in the profile during monsoons (Jackson et al. 1956), and may serve as a generalized tracer of water balance in waste covers. Similar logic is shared for tracking long-term radon diffusion given lead-210 gradients in radon barrier profiles (Fuhrmann et al. 2019b).

H.3.9.5 Calcium Carbonate

CaCO_3 or calcite is common to soils in semiarid and arid environments. Throughout the western United States, the deposition of atmospheric CaCO_3 , as both dissolved ions in rainwater and solid particulates in dust, can be substantial. Aeolian dusts in southern Nevada and California can contain 10–30% calcite resulting in 1–6.6 grams per meter squared per year ($\text{g/m}^2/\text{yr}$) CaCO_3 (Reheis et al. 1995). In southern New Mexico, aeolian dust can deposit 0.35–1.3 $\text{g/m}^2/\text{yr}$ CaCO_3 , (Gile and Grossman 1979) with rain delivering an additional 1.5 $\text{g/m}^2/\text{yr}$ CaCO_3 (Junge and Werby 1958; Lodge et al. 1968). In central Texas, rain supplies an additional 2.3 $\text{g/m}^2/\text{yr}$ CaCO_3 with no contributions from aeolian dust (Rabenhorst et al. 1984). Given depositional patterns throughout much of the Quaternary Period, appreciable amounts of calcite are naturally present in native soils in the western United States, including those materials used for the construction of waste covers.

The processes responsible for regulating the accumulation of CaCO_3 in soils are varied (Reeves 1976). The precipitation of calcite in soils is driven by several factors including pore space, pH,

CO₂ concentration, temperature, and pressure (Turk et al. 2011). Calcite has a solubility of 0.06g L⁻¹ at 25 °C, pH 8, and P_{CO₂} of 10⁻⁴ Mpa, more soluble than silicate minerals, but much less soluble than many salts including NaCl. The movement of water through the soil profile generally corresponds to the location of calcite precipitation. In many soils, the most favored mode of calcite precipitation is evaporation or transpiration of water until the soil solution is supersaturated with respect to CaCO₃ (Reeves 1976; Klappa 1983). Under such conditions, the depth and position of calcic horizons in natural soils is related to the depth of *effective* leaching. However, this does not mean that all water movement stops at the depth of calcite deposition, only that water does not carry CaCO₃ in solution beyond this depth (Hunter et al. 1990). The presence of textural breaks limiting the capillary movement of water, the effective rooting depth, and the activity of bacteria and fungi have all been shown to correspond to calcite deposition patterns in semiarid and arid environments (Stuart and Dixon 1973; Klappa 1983). The microbial production of calcite and subsequent cementation of soils can be considerable, and stimulated bio-cementation has been proposed to stabilize engineered soils with low shear from erosion (DeJong et al. 2006; Umar et al. 2016).

The investigation of calcic horizons in natural analog soils has been explored as a means to understand long-term water movement in waste covers (Hunter et al 1990; Dwyer 2003) and explore the potential for percolation into tailings using alternative cover designs. However, Hunter et al. (1990) concludes that the depth at which carbonates precipitate as calcic horizons does not indicate the depth below which water flow stops completely, and that unsaturated recharge can occur at depths exceeding calcic horizons.

The creation of pore space through physical and biotic processes dominate the discussion of soil change in CMB's; however, induration and cementation by materials including calcite, may serve to block emergent pore space through time. Cementation by calcite is generally connected with high clay content and the presence of dissolved amorphous silica, as facilitated by calcite induced clay flocculation (McNeal and Coleman 1966). Under such conditions, as individual calcite nodules grow and eventually merge, they can restrict hydraulic conductivity (Gile et al. 1966). After enough cycles of ET and calcite accumulation, pore space can become sufficiently plugged and a thin, hard, dense, and strongly cemented laminar horizon can form restricting the movement of soil water. However, not all calcite precipitation results in soil cementation (Flach et al. 1969). If appreciable amounts of calcite are found in a soil it is recognized as a calcic horizon if it is not cemented, and as a petrocalcic horizon if it is cemented (Soil Survey Staff 2003). Petrocalcic soils are largely concentrated in arid and semiarid landscapes where annual evaporation exceeds infiltration.

Rates of soil cementation by calcite vary widely as a function of soil-forming factors (Leeder 1975; Wright 1990). Stage IV calcite cementation has been observed on surfaces less than a few thousand years old (Hay and Reeder 1978); however, the majority of petrocalcic soils in the western United states have required closer to 100,000 years to form (Machette 1985; Wright 1990). On a young lava flow (i.e., estimated at <7000 years of age) at the Bluewater site, a stage II, noncemented, calcic horizon has formed in a combination of aeolian and fluvial sediments (DOE forthcoming). Natural analogs have been successfully used to measure the hydraulic properties of calcic horizons and compare them to noncalcic soil horizons to determine the potential influence of calcite accumulation on water movement in adjacent waste covers (Hunter et al. 1990).

H.3.9.6 *Reduction and Oxidation*

Under saturated conditions, CMB's can undergo redox processes that result in changes to soil morphology. When soil pore space is filled by water and oxygen is depleted, microbially induced reduction results in the dissolution of redox sensitive compounds including Fe and Mn (hydr)oxides, nitrates, and sulfates resulting in selective losses from anoxic zones. In many fine textured soils, prolonged saturation leads to the reduction of iron from its oxidized (ferric) Fe^{3+} state to its reduced and water soluble (ferrous) Fe^{2+} state. The reduction of iron in soil results in a grey or bluish color (gleying). For CMB's intended to limit gas diffusion, maintaining high soil moisture is advantageous given the inverse relationship between soil moisture and gas diffusion (Nielson and Rogers 1982; Rogers et al. 1984). The observation of gleyic features within in-service CMB's provides evidence that the barrier has (on average) maintained saturated conditions and may serve as an indicator that the barrier has been effective at limiting gas diffusion over time.

H.3.10 Physical Breakdown and Chemical Weathering of Rock Riprap

Rock riprap is commonly applied to waste covers to control erosion. Riprap selection for UMTRCA covers is based on methodologies developed by Foley et al. (1985) and Nelson et al. (1986) that largely focus on rock thickness and gradation characteristics. Riprap gradation is specified to meet minimum or maximum D_{50} (i.e., 50% of the particles are larger or smaller, by weight), for given material thickness, as a function of maximum precipitation events and slope attributes to control flow velocity below erosion risk thresholds (Maynard et al. 1989; Abt et al. 1991a).

Given performance lifetimes, rock riprap must withstand natural weathering processes that lead to rock breakdown to ensure that D_{50} is maintained over time (Lagasse et al. 2006). Rock weathering is attributed to both chemical and physical processes, rock characteristics related to durability, and climatic conditions affecting the rate and degree of weathering (Table H-2). A comprehensive review of topics in geology relevant to weathering processes and rock durability relevant to riprap use in UMTRCA covers is presented by Lindsey et al. (1982).

Weathering can have a significant impact on the durability of in-service rock aggregates (Fookes et al. 1988). Physical weathering processes such as freeze-thaw and salt crystallization along microfractures produced during rock quarrying, material transport, or application to ground surface have the most significant impact to riprap performance. Decreased rock size can result in increased rates of overland flow velocity and erosion risk (Abt et al. 1988; Abt et al. 1991b; Abt and Johnson 1991).

Table H-2 Summary of Factors and Processes Responsible for Riprap Weathering (adapted from Brunsden 1979)

Main Controls		Physical Weathering	Response of Material
Weathering environment Climatic Atmospheric Hydrospheric Local factors e.g., topography, drainage, water table	The physical environment →	Salt crystallization* Freezing and thawing* Wetting and drying* Colloid processes (Organic processes) (Sheeting, unloading, and spalling)* Insolation*	→ Disintegration Rubblization Comminution Volume change Grain size change Surface area change Consolidation
Chemical Weathering			
Lithosphere Lithology Parent rock Structure Climatic Atmospheric	The chemical environment →	Hydration Hydrolysis Solution* Oxidation* Reduction* Carbonation*	→ Unaffected minerals due to lack of time or weak agents Decomposition, recombination, and cation-exchange reactions
Hydrospheric Crystal structure		Chelation Fixation	Leaching Dissolved ions

* Indicates processes considered most applicable to engineering timescales

Chemical weathering is most significant in hot and wet climates and varies as a function of parent rock lithology. The use of sandstone, limestone (or dolomite), mixed river cobble, and basalt riprap are common to UMTRCA covers. The chemical weathering products of each rock type are diverse (e.g., Lindsey et al. 1982) and can have impacts to the soil chemical environment of waste covers and the engineering properties of CMB's. Limestone and dolomite weathering releases significant amounts of CaCO₃ with impacts to pH, clay dispersion, and cementation (see Section H.3.8.5). Many forms of basalt contain easily weatherable olivine and volcanic glass that can result in the generation of silica dioxide (SiO₂). Pedogenic silicates (including opal-A) can result in soil aggregate stabilization and soil cementation, even under relatively low silica concentrations (Turk et al. 2011), with impacts to soil hydraulic properties. Silicate solubility increases under high pH (>9) and temperature (Drees et al. 1989), conditions common to the semiarid and arid southwestern United States. Root produced organic acids also correspond to elevated silica dissolution (Turk et al. 2011), and rates of pedogenic silicate stabilization of soil aggregates in CMB materials are expected to increase as plants establish on rock riprap covers.

H.3.11 Soil Process and Time

Time plays a central role in the development of soil given recurring pedogenic processes that accumulate as morphological expressions (Lin 2010a). Targulian and Krasilnikov (2007) provide a framework for categorizing soil processes that corresponds to the observation of soil morphology in chronosequence studies. The framework describes the characteristic times that specific pedogenic processes result in alterations to a soil body over 1 to 1-million-year timescales. A conceptual framework that captures the relative contribution of specific soil processes relevant to regulatory time frames in the UMTRCA program is proposed (Figure H-4). Four time periods are adapted from Caldwell and Reith (1993). Short-term is the roughly 0-10 year period dominated by physical processes post construction; medium-term is the roughly 10-

200 year period dominated by biological processes and active maintenance; long-term is the roughly 200-1000 year period characterized by passive maintenance; very long-term is the roughly 1000-10,000 year period when the waste cover is in equilibrium with the environment.

With few exceptions, short-term soil processes have been widely observed in the months immediately following waste cover construction (Kim and Daniel 1992; Benson et al. 1995; Melchior 1997) and are dominated by desiccation and cracking, freeze-thaw cycling, consolidation, and erosion. Medium-term processes take place on annual and decade scales (Burt and Cox 1993; Link et al. 1995; Waugh et al. 1999) and are dominated by bioturbation by plants and animals. Given the inability to observe 100-plus year-old waste cover systems, relationships between anticipated additions, transfers, transformations and losses to soil morphology are derived from trends observed in natural soils (e.g., Targulian and Krasilnikov 2007). Long-term and very long-term processes emphasize the accumulation and redistribution of materials with impacts to aggregate structuring, pore-clogging, and horizonation, and can be informed through the study of natural analogs.

For those waste covers that cannot support vegetation (because of climate, cover design, aggressive vegetation management, or site-specific limitations) and if those surfaces are covered with rock riprap for erosion control, short-term soil processes may dominate indefinitely. Very hot and very dry sites may fit in this category. The formation of soil morphology in arid environments is generally a very slow process occurring over hundreds of thousands of years (Wells et al. 1985), and episodic events (such as large rainstorms) play a significant role in the development of soil morphology, specifically through erosion (Cable and Huxman 2004; Schwinning et al. 2004). One would expect such episodic events to contribute significantly to soil change in these unvegetated, arid environments. Over sufficiently long timescales, the accumulation and redistribution of mobile elements (including dust and carbonate from rainfall) may eventually lead to the formation of young desert pavements in arid and semi-arid environments.

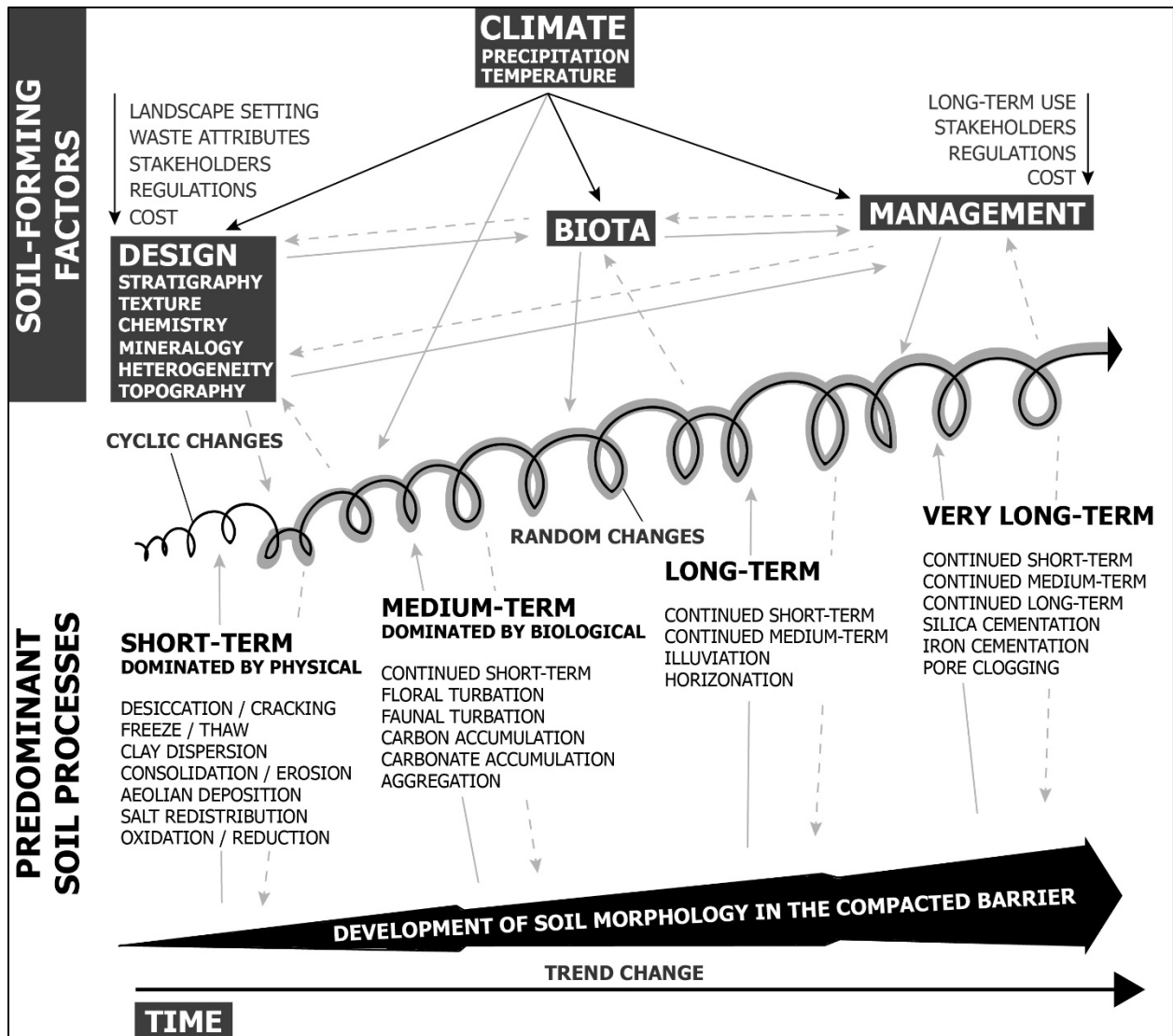


Figure H-4 Site Factors, Soil Process, and Morphological Development in Compacted Mineral Barriers¹

¹Conceptual model of the coevolution of soil process and morphology in CMB's for waste containment is based on Lin (2010a). Solid black arrows represent the dominant direction of influence. Solid gray arrows represent interactions. Dashed arrows represent a feedback between factors, change, soil processes, and morphology. Time frames for the incremental evolution of soil process are based on Targulian and Krasilnikov (2007) and the field investigation that complements this study (Section 7; DOE forthcoming).

H.4 Section Summary

Soils are open and dynamic systems that are subject to recurring fluxes of energy and mass with impacts to both short-term function and long-term evolution. Historically, the dynamic properties of soil development, and the emergence of novel soil morphology, have been under emphasized in the planning of engineered cover systems intended for the long-term containment of wastes. Conventional cover systems have largely been designed to resist natural processes, as opposed to working with them. In as little as 5-years post construction, soil processes including bioturbation by plants and animals have resulted in significant and irreversible changes to as-built barrier morphology with impacts to long-term engineered performance. These changes have been observed to occur unevenly across space and time.

Herein a conceptual framework of soil development in engineered surface covers for waste containment has been proposed. The framework accounts for pedogenic processes that alter soil morphology, and engineered performance, over time. Special emphasis is placed on processes that result in morphological development *within* the compacted radon barrier of waste covers in the UMTRCA program. The framework allows for the systematic study of soil change in these systems.

H.5 References

- Abrol, I.P., J.S.P. Yadav, and F.I. Massoud, 1988. *Salt-Affected Soils and Their Management*, No. 39, Food and Agriculture Organization of the United Nations.
- Abt, S.R., R.J. Wittier, J.F. Ruff, D.L. LaGrone, M.S. Khattak, J.D. Nelson, N.E. Hinkle, and D.W. Lee, 1988. "Development of Riprap Design Criteria by Riprap Testing in Flumes: Phase II," NUREG/CR-4651, 2, U.S. Nuclear Regulatory Commission, Washington, D.C.
- Abt, S.R., K. High, and J. McBee, 1991a. "Refined Cap Design for Uranium Tailings Sites," *Journal of Energy Engineering*, 117(2), 71–86.
- Abt, S.R., J.F. Ruff, and R.J. Wittler, 1991b. "Estimating Flow Through Riprap," *Journal of Hydraulic Engineering*, 117(5), 670–675.
- Abt, S.R., and T.L. Johnson, 1991. "Riprap Design for Overtopping Flow," *Journal of Hydraulic Engineering*, 117(8), 959–972.
- Abt, S.R., T.L. Johnson, C.I. Thornton, and S.C. Trabant, 1998. "Riprap Sizing at Toe of Embankment Slopes," *Journal of Hydraulic Engineering*, 124(7), 672–677.
- Aerts, R., C. Bakker, and H. De Caluwe, 1992. "Root Turnover as Determinant of the Cycling of C, N, and P in a Dry Heathland Ecosystem," *Biogeochemistry*, 15(3), 175–190.
- Albrecht, B.A., and C.H. Benson, 2001. "Effect of Desiccation on Compacted Natural Clays," *Journal of Geotechnical and Geoenvironmental Engineering*, 127(1), 67–75.

- Albrethsen, H., and F.E. McGinley, 1982. *Summary History of Domestic Uranium Procurement Under U.S. Atomic Energy Commission Contracts*, GJBX-220(82), U.S. Department of Energy, Grand Junction Area Office, Colorado.
- Albrethsen, A., W.L. Chenoweth, and F. McGinley, 1986. "A Summary History of the Activities of the Grand Junction Office of the AEC, ERDA, and DOE," Self-published white paper, Grand Junction, Colorado.
- Albright, W.H., C.H. Benson, G.W. Gee, A.C. Roesler, T. Abichou, P. Apiwantragoon, B.F. Lyles, and S.A. Rock, 2004. "Field Water Balance of Landfill Final Covers," *Journal of Environmental Quality*, 33(6), 2317–2332.
- Albright, W.H., C.H. Benson, G.W. Gee, T. Abichou, E.V. McDonald, S.W. Tyler, and S.A. Rock, 2006a. "Field Performance of a Compacted Clay Landfill Final Cover at a Humid Site," *Journal of Geotechnical and Geoenvironmental Engineering*, 132(11), 1393–1403.
- Albright, W.H., C.H. Benson, G.W. Gee, T. Abichou, S.W. Tyler, and S.A. Rock, 2006b. "Field Performance of Three Compacted Clay Landfill Covers," *Vadose Zone Journal*, 5(4), 1157–1171.
- Amundson, R., and H. Jenny, 1991. "The Place of Humans in the State Factor Theory of Ecosystems and their Soils," *Soil Science*, 151(1), 99–109.
- Anderson, D.W., 1977. "Early Stages of Soil Formation on Glacial Till Mine Spoils in a Semi-Arid Climate," *Geoderma*, 19(1), 11-19.
- Anderson, D.W., 1988. "The Effect of Parent Material and Soil Development on Nutrient Cycling in Temperate Ecosystems," *Biogeochemistry*, 5(1), 71–97.
- Anderson, J.E., R.S. Nowak, T.D. Ratzlaff, and O.D. Markham, 1993. "Managing Soil Moisture on Waste Burial Sites in Arid Regions," *Journal of Environmental Quality*, 22, 62–69.
- Angers, D.A. and J. Caron, 1998. "Plant-Induced Changes in Soil Structure: Processes and Feedbacks," *Biogeochemistry*, 42(1-2), 55–72.
- Arnold J.A., J.G. Zaller, E. Spehn, G. Hirschel, P. Niklaus, C. Korner, 2000. "Dynamics of Root Systems in Native Grasslands: Effects of Elevated Atmospheric CO₂," *New Phytologist*, 147, 73–85.
- Arthur, W.J., III and O.D. Markham, 1983. "Small Mammal Soil Burrowing as a Radionuclide Transport Vector at a Radioactive Waste Disposal Area in Southeastern Idaho," *Journal of Environmental Quality*, 12, 117-122.
- Bacon, C.A., 1929. "Some Physical Aspects of Organic Matter," *Agricultural Engineering*, 10, 83–85.
- Barley, K.P., 1954. "Effects of Root Growth and Decay on the Permeability of a Synthetic Sandy Loam," *Soil Science*, 78(3), 205–210.
- Barnett, R.J., 1937. "Ground Cover Affects Frost Penetration," *Transactions of the Kansas Academy of Science*, 40, 203–207.

- Barrington, S.F., K. El Moueddeb, J. Jazestani and M. Dussault, 1998. The Clogging of Non-Woven Geotextiles with Cattle Manure Slurries," *Geosynthetics International*, 5(3), 309–325.
- Bayer, L.D., 1930. "The Effect of Organic Matter upon Several Physical Properties of Soils," *American Society of Agronomy Journal*, 22, 703–708.
- Beedlow, P.A., and J.N. Hartley, 1984. *Long-Term Protection of Uranium Mill Tailings*, DOE/UMT-0218; PNL-4984, Pacific Northwest Laboratory, Richland, Washington.
- Bell, F.G., and D. J. H. Walker, 2000. "A Further Examination of the Nature of Dispersive Soils in Natal, South Africa," *Quarterly Journal of Engineering Geology and Hydrogeology*, 33(3), 187–199.
- Belnap, J., 2006. "The Potential Roles of Biological Soil Crusts in Dryland Hydrologic Cycles," *Hydrological Processes*, 20, 3159–3178.
- Bendfeldt, E.S., J.A. Burger, and W.L. Daniels, 2001. "Quality of Amended Mine Soils After Sixteen Years," *Soil Science Society of America Journal*, 65(6), 1736-1744.
- Bengough A.G., M.F. Bransby, J. Hans, S.J. McKenna, T.J. Roberts, and T.A. Valentine, 2006. "Root Responses to Soil Physical Conditions; Growth Dynamics from Field to Cell," *Journal of Experimental Botany*, 57, 437–447.
- Bennett, R.D., and A.F. Kimbrell, 1991. "Recommendations to the NRC for Soil Cover Systems over Uranium Mill Tailings and Low-Level Radioactive Wastes: Construction Methods for Sealing Penetrations in Soil Covers," NUREG/CR-5432-VOL. 3, U.S. Nuclear Regulatory Commission.
- Benson, C.H., and M.A. Othman, 1993. Hydraulic Conductivity of Compacted Clay Frozen and Thawed In Situ," *Journal of Geotechnical Engineering*, 119(2), 276–294.
- Benson, C.H., T.H. Abichou, M.A. Olson, and P.J. Bosscher, 1995. "Winter Effects on Hydraulic Conductivity of Compacted Clay," *Journal of Geotechnical Engineering*, 121(1), 69–79.
- Benson, C.H., and X. Wang, 1996. "Field Hydraulic Conductivity Assessment of the NCASI Final Cover Test Plots," *Environmental Geotechnics*, 96–9, Department of Civil and Environmental Engineering, University of Wisconsin, Madison, Wisconsin.
- Benson, C.H., W.H. Albright, D.O. Fratta, J.M. Tinjum, E. Kucukkirca, S.H. Lee, J. Scalia, P.D. Schlicht, and X. Wang, 2011. *Engineered Covers for Waste Containment: Changes in Engineering Properties and Implications for Long-Term Performance Assessment*, Vol. 1 NUREG/CR-7028, Nuclear Regulatory Commission Report.
- Benson, C.H., W.H. Albright, W.J. Waugh, and M.M. Davis, 2018. "Field Hydrologic Performance of Earthen Covers for Uranium Mill Tailings Disposal Sites on the Colorado Plateau," Long-Term Stewardship Conference, August 20–23, 2018, U.S. Department of Energy Office of Legacy Management, Grand Junction, Colorado.
- Bernatek-Jakiel, A., and J. Poesen, 2018. "Subsurface erosion by soil piping: Significance and research needs," *Earth-Science Reviews*, 185, 1107–1128.

- Beven, K., and P. Germann, 1982. "Macropores and Water Flow in Soils," *Water Resources Research*, 18(5), 1311–1325.
- Biber, P., S. Seifert, M.K. Zaplata, W. Schaaf, H. Pretzsch, and A. Fischer, 2013. "Relationships Between Substrate, Surface Characteristics, and Vegetation in an Initial Ecosystem," *Biogeosciences*, 10, 8283–8303.
- Bilotta, G.S., R.E. Brazier, and P.M. Haygarth, 2007. "The Impacts of Grazing Animals on the Quality of Soils, Vegetation, and Surface Waters in Intensively Managed Grasslands," *Advances in Agronomy*, 94, 237–280.
- Bird, S.B., J.E. Herrick, M.M. Wander, and S.F. Wright, 2002. "Spatial Heterogeneity of Aggregate Stability and Soil Carbon in Semi-Arid Rangeland," *Environmental Pollution*, 116(3), 445–455.
- Blanco-Canqui, H., and R. Lal (2009). "Crop Residue Removal Impacts on Soil Productivity and Environmental Quality." *Critical Reviews in Plant Science*, 28(3), 139-163.
- Blokhuis, W.A., M.J. Kooistra, and L.P. Wilding, 1990. "Micromorphology of Cracking Clayey Soils (Vertisols)," *Developments in Soil Science*, 19, 123–148, Elsevier.
- Blom, P.E., J.B. Johnson, B. Shafii, J. and Hammel, 1994. "Soil Water Movement Related to Distance from Three *Pogonomyrmex salinus* (Hymenoptera: Formicidae) Nests in South-Eastern Idaho," *Journal of Arid Environments*, 26, 241–255.
- Boix-Fayos, C., A. Calvo-Cases, and A.C. Imeson, M.D. Soriano-Soto, 2001. "Influence of Soil Properties on the Aggregation of some Mediterranean Soils and the Use of Aggregate Size and Stability as Land Degradation Indicators," *Catena*, 44, 47–67.
- Bonkowski, M., C. Villenave, and B. Griffiths, 2009. "Rhizosphere Fauna: The Functional and Structural Diversity of Intimate Interactions of Soil Fauna with Plant Roots," *Plant and Soil*, 321(1-2), 213–233.
- Bouma, J., and J.L. Anderson, 1973. "Relationships Between Soil Structure Characteristics and Hydraulic Conductivity," *Field Soil Water Regime*, 77–105.
- Bowerman, A.G., and E.F. Redente, 1998. "Biointrusion of Protective Barriers at Hazardous Waste Sites," *Journal of Environmental Quality*, 27(3), 625–632.
- Boyle, M., W.T. Frankenberger, and L.H. Stolzy, 1989. "The Influence of Organic Matter on Soil Aggregation and Water Infiltration," *Journal of Production Agriculture*, 2(4), 290–299.
- BSI (British Standards Institution), 1990. *Methods of Test for Soils for Civil Engineering Purposes: Part 5: Compressibility, Permeability and Durability Tests*, 1377 (5), London.
- Bronick, C.J. and R. Lal, 2005. "Soil Structure and Management: A Review," *Geoderma*, 124(1-2), 3–22.
- Bruand, A., I. Cousin, B. Nicoulaud, O. Duval, and J.C. Begon, 1996. "Backscattered Electron Scanning Images of Soil Porosity for Analyzing Soil Compaction Around Roots," *Soil Science Society of America Journal*, 60(3), 895–901.

- Brunsdon, D., 1979. "Weathering," *In: Embleton, C., and J., Thomas (eds) Process in Geomorphology*, Edward Arnold, London, England.
- Bundt, M., F. Widmer, M. Pesaro, J. Zeyer and P. Blaser, 2001. "Preferential Flow Paths: Biological 'Hot Spots' in Soils," *Soil Biology and Biochemistry*, 33(6), 729–738.
- Buol, S.W., R.J. Southard, R.C. Graham, and P.A. McDaniel, 2011. "Soil Genesis and Classification," Sixth Edition, John Wiley & Sons.
- Burt, C.J., and S.W. Cox, 1993. "An Assessment of Plant Biointrusion on Six UMTRA Project Disposal Cells," Waste Management Conference 1993, Working Towards a Cleaner Environment, Tuscon, Arizona.
- Cable, J.M. and T.E. Huxman, 2004. "Precipitation Pulse Size Effects on Sonoran Desert Soil Microbial Crusts," *Oecologia*, 141(2), 317–324.
- Cadwell, L.L., L.E. Eberhardt, and M.A. Simmons, 1989. *Animal Intrusion Studies for Protective Barriers: Status Report for FY 1988*, PNL-6869, Pacific Northwest Laboratory, Richland, Washington.
- Caldwell, J.A., C. Reith, 1993. *Principals and Practice of Waste Encapsulation*. Lewis Publishers, Michigan, United States.
- Cammeraat, E.L.H. and A.C. Risch, 2008. "The Impact of Ants on Mineral Soil Properties and Processes at Different Spatial Scales," *Journal of Applied Entomology*, 132(4), 285–294.
- Castillo, C., and J.A. Gómez, 2016. "A Century of Gully Erosion Research: Urgency, Complexity and Study Approaches," *Earth-Science Reviews*, 160:300–319, <https://doi.org/10.1016/j.earscirev.2016.07.009>.
- Cerdan, O., G. Govers, Y. Le Bissonnais, K. Van Oost, J. Poesen, N. Saby, A. Gobin, A. Vacca, J. Quinton, K. Auerswald, A. Klik, F.J.P.M. Kwaad, D. Raclot, I. Ionita, J. Rejman, S. Rousseva, T. Muxart, M.J. Roxo, and T. Dostal, 2010. "Rates and Spatial Variations of Soil Erosion in Europe: A Study Based on Erosion Plot Data," *Geomorphology*, 122, 167–177, <https://doi.org/10.1016/j.geomorph.2010.06.011>.
- Chapuis, R.P., 2002. "Full-Scale Hydraulic Performance of Soil–Bentonite and Compacted Clay Liners," *Canadian Geotechnical Journal*, 39(2), 417–439, DOI:10.1139/t01-092.
- Chaudhary, V.B., M.A. Bowker, T.E. O'Dell, J.B. Grace, A.E. Redman, M.C. Rillig, and N.C. Johnson, 2009. "Untangling the Biological Contributions to Soil Stability in Semiarid Shrublands," *Ecological Applications*, 19(1), 110–122.
- Chenoweth, W.L., 1997. "Raw Materials Activities of the Manhattan Project on the Colorado Plateau," *Nonrenewable Resources*, Vol. 6, No. 1.
- Churchman, G.J., and D.J. Lowe, 2012. "Alteration, Formation, and Occurrence of Minerals in Soils," *Handbook of Soil Sciences*, 1, 20-1.

- Clarke, J.H., M.M. MacDonell, E.D. Smith, R.J. Dunn, and W.J. Waugh, 2004. "Engineered Containment and Control Systems: Nurturing Nature," *Risk Analysis: An International Journal*, 24(3), 771-779.
- Cline, J. F., F.G. Burton, D.A. Cataldo, W.E. Skiens, and K.A. Gano, 1982. *Long-Term Biobarriers to Plant and Animal Intrusions of Uranium Tailings*, DOE/UMT-0209, September, Pacific Northwest Laboratory.
- Coleman, M.D., R.E. Dickson, and J.G. Isebrands, 2000. "Contrasting Fine-Root Production, Survival and Soil CO₂ Efflux in Pine and Poplar Plantations," *Plant and Soil*, 225, 129–139.
- Comstock, J.P. and J.R. Ehleringer, 1992. "Plant Adaptation in the Great Basin and Colorado Plateau," *The Great Basin Naturalist*, 195–215.
- Cook, G.D., H.B. So, and R.C. Dalal, 1992. "Structural Degradation of Two Vertisols under Continuous Cultivation," *Soil and Tillage Research*, 24(1), 47–64.
- Curry, J.P. and O. Schmidt, 2007. "The Feeding Ecology of Earthworms—A Review," *Pedobiologia*, 50(6), 463–477.
- Curtis, R.O. and B.W. Post, 1964. "Estimating Bulk Density from Organic-Matter Content in Some Vermont Forest Soils," *Soil Science Society of America Journal*, 28, 285–286.
- Czarnes, S., P.D. Hallett, A.G. Bengough, and I.M. Young, 2000. "Root-and Microbial-Derived Mucilages Affect Soil Structure and Water Transport," *European Journal of Soil Science*, 51(3), 435–443.
- Daniel, D.E., and C.H. Benson, 1990. "Water Content-Density Criteria for Compacted Soil Liners," *Journal of Geotechnical Engineering*, 116(12), 1811–1830.
- Dietze, M., S. Bartel, M. Lindner, and A. Kleber, 2012. "Formation Mechanisms and Control Factors of Vesicular Soil Structure," *Catena*, 99, 83–96.
- DeJong, E., and B.P. Warkentin, 1965. "Shrinkage of Soil Samples with Varying Clay Content," *Canadian Geotechnical Journal*, 2(1), 16–22.
- DeJong, J.T., M.B. Fritzges, and K. Nüsslein, 2006. "Microbially Induced Cementation to Control Sand Response to Undrained Shear," *Journal of Geotechnical and Geoenvironmental Engineering*, 132(11), 1381–1392.
- DeJong, J., M. Tibbett, and A. Fourie, 2015. "Geotechnical Systems that Evolve with Ecological Processes," *Environmental Earth Sciences*, 73(3), 1067–1082.
- Dexter, A.R., 1987. "Compression of Soil Around Roots," *Plant and Soil*, 97, 401–406.
- Dexter, A.R., G. Richard, D. Arrouays, E.A. Czyż, C. Jolivet, and O. Duval, 2008. "Complexed Organic Matter Controls Soil Physical Properties," *Geoderma* 144(3-4), 620–627.

- DOE (U.S. Department of Energy), 1989. *Technical Approach Document*, Rev. 2, UMTRA-DOE/AL 050425.0002, Uranium Mill Tailings Remedial Action Program, Albuquerque, New Mexico.
- DOE (U.S. Department of Energy), 1992. *Vegetation Growth Patterns on Six Rock-Covered UMTRA Project Disposal Cells*, UMTRA-DOE/AL-400677.0000, Albuquerque, New Mexico.
- DOE (U.S. Department of Energy), 1999a. *Uranium Mill Tailings Remedial Action Surface Project 1979-1999, End of Project Report*, DOE/AL/62350-500, Albuquerque, New Mexico.
- DOE (U.S. Department of Energy), 1999b. *Uranium Mill Tailings Surface Project 1978-1998, Disposal Cell Design Summary Report*, DOE/AL/62350-501, Albuquerque, New Mexico.
- DOE (U.S. Department of Energy), 2014. *Site Status Report: Groundwater Flow and Contaminant Transport in the Vicinity of the Bluewater, New Mexico, Disposal Site*, LMS/BLU/S11381, Office of Legacy Management.
- DOE (U.S. Department of Energy), 2015. *Technical Task Plan 003: Long-Term Cover Performance*, LMS/S12624, Office of Legacy Management.
- DOE (U.S. Department of Energy), 2016. *2016–2025 Strategic Plan*, DOE/LM-1477, Office of Legacy Management, Washington D.C.
- DOE (U.S. Department of Energy), 2019a. *Uptake of Elements of Concern by Plants Growing on UMTRCA Disposal Cell Covers*, LMS/S27283, ESL-RPT-2019-02, Office of Legacy Management.
- DOE (U.S. Department of Energy), 2019b. *Side Slope Cover Depressions Evaluation Report, Mexican Hat, Utah*, LMS/HAT/S14765, Office of Legacy Management, Grand Junction, CO.
- DOE (U.S. Department of Energy), 2019c. *Aeolian Deposition in the Rock Riprap Cover, Field Work Plan Bluewater Disposal Site, New Mexico*, LMS/BLU/S25466, Office of Legacy Management.
- DOE (U.S. Department of Energy), DOE-a – d, In Preparation.
- DOE (U.S. Department of Energy), 2020. *Erosional Piping Characterization and Data Report, Mexican Hat, Utah, Disposal Cell*, LMS/HAT/S29391, Office of Legacy Management.
- DOE Order 435.1 Pg Chg 1, *Radioactive Waste Management*, U.S. Department of Energy, January 9, 2007.
- Dokuchaev, V.V., 1886. "Report to the Provincial Zensvto (local authority) of Nizhnii-Novgorod (now Gorki), No. 1," *Main Phases in the History of Land Assessment in European Russia, with Classification of Russian Soils*.
- Dorioz, J. M., M. Robert, and C. Chenu, 1993. "The Role of Roots, Fungi and Bacteria on Clay Particle Organization. An Experimental Approach," *Geoderma*, 179–194.

- Drees, R.L., L.P. Wilding, N.E. Smeck, and A.L. Senkayi, 1989. "Silica in Soils: Quartz and Disordered Silica Polymorphs," *Minerals in Soil Environments*, 1, 913–974.
- Drew, M.C. and L.R. Saker, 1978. "Nutrient Supply and the Growth of the Seminal Root System in Barley: III. Compensatory Increases in Growth of Lateral Roots, and in Rates of Phosphate Uptake in Response to a Localized Supply of Phosphate," *Journal of Experimental Botany*, 29(2), 435–451.
- Dudal, R., F.O. Nachtergaele, and M.F. Purnell, 2002. "The Human Factor of Soil Formation," *17 World Congress of Soil Science*, Bangkok, Thailand, August 14–21, 2002.
- Dwyer, S.F., 2003. *Water Balance Measurements and Computer Simulations of Landfill Covers*, Doctoral dissertation, University of New Mexico.
- Edwards, A.C., and M.S. Cresser, 1992. "Freezing and Its Effect on Chemical and Biological Properties of Soil," *Advances in Soil Science*, 59–79, Springer, New York, New York.
- Edwards, W.M., M.J. Shipitalo, L.B. Owens, and L.D. Norton, 1989. "Water and Nitrate Movement in Earthworm Burrows Within Long-Term No-Till Cornfields," *Journal of Soil and Water Conservation*, 44(3), 240–243.
- Egloffstein, T., 1995. "Properties and Test Methods to Assess Bentonite Used in Geosynthetic Clay Liners," *Geosynthetic Clay Liners*, Balkema, Rotterdam, The Netherlands, 51–72.
- Elges, H.F.W.K., 1985. "Dispersive Soils: Problem Soils in South Africa-State of the Art," *Civil Engineer in South Africa*, 27(7), 347–353.
- Engemoen, W.O., 2017. "Latest Compilation of Internal Erosion Incidents at Bureau of Reclamation Dams," Proceeding of the 37th Annual USSD Conference, United States Society on Dams, Anaheim, California, 433–450.
- EPA (U.S. Environmental Protection Agency), 1989. *Technical Guidance Document: Final Covers on Hazardous Waste Landfills and Surface Impoundments*, EPA/530-SW-89-047, Office of Solid Waste and Emergency Response, U.S. Environmental Protection Agency, Washington, D.C.
- Ericsson, T., 1995. "Growth and Shoot: Root Ratio of Seedlings in Relation to Nutrient Availability," *Nutrient Uptake and Cycling in Forest Ecosystems*, 205–214, Springer, Dordrecht.
- Fan, Y., G. Miguez-Macho, E.G. Jobbágy, R.B. Jackson, and C. Otero-Casal, 2017. "Hydrologic Regulation of Plant Rooting Depth," *Proceedings of the National Academy of Sciences*, 114(40), 10572–10577.
- Faulkner, H., 2006. "Piping Hazard on Collapsible and Dispersive Soils in Europe," In: Boardman, J., Poesen, J. (Eds.), *Soil Erosion in Europe*, John Wiley & Sons, Ltd, Chichester, pp. 537–562. <https://doi.org/10.1002/0470859202>.
- Feldhamer, G., 1979. "Vegetative and Edaphic Factors Affecting Abundance and Distribution of Small Mammals in Southeast Oregon," *The Great Basin Naturalist*, 39, 207–218.

- Fitzner, R.E., K.A. Gano, W.H. Rickard, and L.E. Rogers, 1979. *Characterization of the Hanford 300 Area Burial Grounds. Task IV. Biological Transport*, PNL-2774, Battelle Pacific Northwest Labs., Richland, Washington.
- FitzPatrick, E.A., 1993. *Soil Microscopy and Micromorphology*, 158, Chichester, John Wiley & Sons.
- Flach, K.W., W.D. Nettleton, L.H. Gile, and J.G. Cady, 1969. "Pedocementation: Induration by Silica, Carbonates, and Sesquioxides in the Quaternary," *Soil Science*, 107(6), 442–453.
- Flower, F.B., I. Leone, and W. Gilman, 1977. *Vegetation Kills in Landfill Environs*, EPA/600/9–77–026, U.S. Environmental Protection Agency, Cincinnati, Ohio.
- Flower, F.B., E.F. Gilman, and I.A. Leone, 1981. "Landfill Gas, What It Does to Trees and How Its Injurious Effects May Be Prevented," *Journal of Arboriculture*, 7(2), 43–52.
- Foley, M.G., C.S. Kimball, D.A. Myers, and J.M. Doesburg, 1985. *Selection and Testing of Rock for Armoring Uranium Tailings Impoundments*, NUREG/CR–3747, Pacific Northwest Labs. Richland, Washington.
- Fookes, P.G., C.S. Gourley, and C. Ohikere, 1988. "Rock weathering in engineering time," *Quarterly Journal of Engineering Geology and Hydrogeology*, 21(1), 33–57.
- Forde, B., and H. Lorenzo, 2001. "The Nutritional Control of Root Development," *Plant and Soil*, 232, 51–68.
- Foster, M., R. Fell, and M. Spannagle, 2000. "A Method for Assessing the Relative Likelihood of Failure of Embankment Dams by Piping: Reply," *Canadian Geotechnical Journal*, 37, 1025–1061, <https://doi.org/10.1139/t01-109>.
- Fourie, A.B., and M. Tibbett, 2007. *Post-Mining Landforms: Engineering a Biological System*, keynote lecture, Fourie A.B., Tibbett M., Wiertz J. (eds), Second International Seminar on Mine Closure, October 2007, Santiago, Chile, pp. 3–12.
- Fox, T.S., G.D. Tierney, and J.M. Williams, 1984a. *Rooting Depths of Plants Relative to Biological and Environmental Factors*, LA-10254-MS, Los Alamos National Laboratory, New Mexico.
- Fox, T.S., G.D. Tierney, and J.M. Williams, 1984b. *Rooting Depths of Plants on Low-Level Waste Disposal Sites*, LA--10253-MS, Los Alamos National Laboratory, New Mexico.
- Franklin, A.G., L.F. Orozco, and R. Semrau, 1973. "Compaction and Strength of Slightly Organic Soils," *Journal of Soil Mechanics & Foundations*, American Society of Civil Engineers, 99 (SM7), 541–557.
- Frydman S., 1967. "Triaxial and Tensile Strength Tests on Stabilized Soil", *Proceedings of the Third Asian Regional Conference on Soil Mechanics and Foundation Engineering*, Haifa, Israel.

- Fuchs, M., G.S. Campbell, and R. Papendick, 1978. "An Analysis of Sensible and Latent Heat Flow in a Partially Frozen Unsaturated Soil," *Soil Science Society of America Journal*, 42, 379–385.
- Fuhrmann, M., C.H. Benson, W.J. Waugh, H. Arlt, and M.M. Williams, 2019a. *Proceedings of the Radon Barriers Workshop*, NUREG/CP-0312, U.S. Nuclear Regulatory Commission, Washington, D.C.
- Fuhrmann, M., A. Michaud, M. Salay, C.H. Benson, W.J. Likos, N. Stefani, W.J. Waugh, and M.M. Williams, 2019b. "Lead-210 Profiles in Radon Barriers, Indicators of Long-Term Radon-222 Transport," *Applied Geochemistry*, 110, 104434.
- Galbraith, J.M., 2004. "Proposed Changes to Soil Taxonomy that May Affect Mine Soil Classification," 2004 National Meeting of the American Society of Mining and Reclamation, American Society of Mining and Reclamation.
- Gano, K.A. and J.B. States, 1982. *Habitat Requirements and Burrowing Depths of Rodents in Relation to Shallow Waste Burial Sites*, PNL-4140, May, Pacific Northwest National Laboratory.
- Garlanger, J.E., F.K. Cheung, and S.T. Bishar, 1987. "Quality Control Testing for a Sand Bentonite Liner," *Geotechnical Practice for Waste Disposal '87*, R. D. Woods, Geotech. Spec. Publ. No. 13, ASCE, New York, 488–499.
- Garner, W., and Y. Steinberger, 1989. "A Proposed Mechanism for the Formation of 'Fertile Islands' in the Desert Ecosystem," *Journal of Arid Environments*, 16, 257–262.
- Gerber, F. A., and H.J. Harmse, 1987. "Proposed Procedure for Identification of Dispersive Soils by Chemical Testing," *Civil Engineer in South Africa*, 29(10), 397–399.
- Ghezzehei, T. A., 2012. "Soil Structure," *Handbook of Soil Sciences*, 2, 1–17.
- Gibbs, R.J., and J.B. Reid, 1988. "A Conceptual Model of Changes in Soil Structure Under Different Cropping Systems," *Advances in Soil Science*, 123–149, Springer, New York, New York.
- Gile, L.H., F.F. Peterson, and R.B. Grossman, 1966. "Morphological and Genetic Sequences of Carbonate Accumulation in Desert Soils," *Soil Science*, 101(5), 347–360.
- Gile, L.H. and R.B. Grossman, 1979. *The Desert Project Soil Monograph: Soils and Landscapes of a Desert Region Astride the Rio Grande Valley near Las Cruces, New Mexico*, Lincoln, Nebraska, U.S. Department of Agriculture, Soil Conservation Service.
- Gill, R.A., 1998. "Biotic Controls over the Depth Distribution of Soil Organic Matter," PhD thesis, Colorado State University, Colorado.
- Gilman, E.F., I.A. Leone, and F.B. Flower, 1981. *Critical Factors Controlling Vegetation Growth on Completed Sanitary Landfills*, EPA-600/2-81-164, U.S. Environmental Protection Agency, Cincinnati, Ohio.

- Gish, T.J., and W.A. Jury, 1983. "Effect of Plant Roots and Root Channels on Solute Transport," *Transactions of the ASAE*, 26(2), 440–0444.
- Glenn, E.P., W.J. Waugh, J.D. Moore, C. McKeon, and S. Nelson, 2001. "Evaluation of Revegetation Methods at an Abandoned Uranium Mill Site on the Colorado Plateau, Arizona," *Journal of Environmental Quality*, 30, 1154–1162.
- Goldman, L.J., L.I. Greenfield, A.S. Damle, G.L. Kingsbury, C.M. Norheim, and R.S. Truesdale, 1988. "Design, Construction, and Evaluation of Clay Liners for Waste Management Facilities," EPA/530-SW-86-007-F, Risk Reduction Engineering Laboratory, U.S. Environmental Protection Agency, Cincinnati, Ohio.
- Goldstein, H.L., R.L. Reynolds, M.C. Reheis, J.C. Yount, and J.C. Neff, 2008. "Compositional Trends in Aeolian Dust Along a Transect Across the Southwestern United States," *Journal of Geophysical Research Atmospheres*, 113, F02S02.
- Goossens, D., 1994. "Effect of Rock Fragments on Eolian Deposition of Atmospheric Dust," *Catena*, 23, 167–189.
- Gray, D.H., and J. Schlocker, 1969. "Electrochemical Alteration of Clay Soils," *Clays and Clay Minerals*, 17(5), 309–322.
- Greacen, E.L., D.A. Farrell, and B. Cockroft, 1968. "Soil Resistance to Metal Probes and Plant Roots," *Transactions of the 9th Congress of the International Society of Soil Science*, Adelaide, 1, 769–779.
- Grevers, M.C.J., and E.D. Jong, 1990. "The Characterization of Soil Macroporosity of a Clay Soil under Ten Grasses Using Image Analysis," *Canadian Journal of Soil Science*, 70(1), 93–103.
- Guidi, G., G. Poggio, and G. Petruzzelli, 1985. "The Porosity of Soil Aggregates from Bulk Soil and from Soil Adhering to Roots," *Plant and Soil*, 87(2), 311–314.
- Gupta, S., and W.E. Larson, 1979. "Estimating Soil Water Retention Characteristics from Particle Size Distribution, Organic Matter Percent, and Bulk Density," *Water Resources Research*, 15(6), 1633–1635.
- Gyssels, G., J. Poesen, E. Bochet, and Y. Li, 2005. "Impact of Plant Roots on the Resistance of Soils to Erosion by Water: A Review," *Progress in Physical Geography*, 29(2), 189–217.
- Hakonson, T.E., J.F. Cline, and W.H. Rickard, 1982a. "Biological Intrusion Barriers for Large-Volume Waste-Disposal Sites," LA-UR-82-2971, Los Alamos National Laboratory.
- Hakonson, T.E., J.L. Martinez, and G.C. White, 1982b. "Disturbance of a Low-Level Waste Burial Site Cover by Pocket Gophers," *Health Physics*, 42(6), 868–871.
- Hakonson, T.E., 1986. *Evaluation of Geologic Materials to Limit Biological Intrusion into Low-Level Radioactive Waste Disposal Sites*, LA--10286-MS, Los Alamos National Laboratory, February.

- Ham, R.K., 1979. *Recovery, Processing, and Utilization of Gas from Sanitary Landfills* Vol. 1, Environmental Protection Agency, Office of Research and Development, Municipal Environmental Research Laboratory.
- Handel, S.N., G.R. Robinson, W.F. Parsons, and J.H. Mattei, 1997. "Restoration of Woody Plants to Capped Landfills: Root Dynamics in an Engineered Soil," *Restoration Ecology*, 5(2), 178–186.
- Harley, A.D. and R.J. Gilkes, 2000. "Factors Influencing the Release of Plant Nutrient Elements from Silicate Rock Powders: A Geochemical Overview," *Nutrient Cycling in Agroecosystems*, 56(1), 11–36.
- Harmse, H.J., 1980. "Dispersiewe Gronde: Hul Ontstaan, Identifikasie Enstabilisasie," *Ground Profile*, April, 22:10.
- Harris, A.F., 1972. "Infiltration Rate as Affected by Soil Freezing Under Three Cover Types," *Soil Science Society Proceedings*, 36, 489–492.
- Hay, R.L. and R.J. Reeder, 1978. "Calcretes of Olduvai Gorge and the Ndolanya Beds of Northern Tanzania," *Sedimentology*, 25, 649–73.
- Haynes, R.J., and M.H. Beare, 1997. "Influence of Six Crop Species on Aggregate Stability and Some Labile Organic Matter Fractions," *Soil Biology and Biochemistry*, 29(11-12), 1647–1653.
- Haynes, R.J., and R. Naidu, 1998. "Influence of Lime, Fertilizer and Manure Applications on Soil Organic Matter Content and Soil Physical Conditions: A Review," *Nutrient Cycles in Agroecosystems*, 51, 123–137.
- Heilman, P., 1981. "Root Penetration of Douglas-fir Seedlings into Compacted Soil," *Forest Science*, 27, 660–666.
- Hendrick R.L and K.S. Pregitzer, 1997. "The Relationship Between Fine Root Demography and the Soil Environment in Northern Hardwood Forests," *Ecoscience*, 4: 99–105.
- Herndon, E.B., 1980. "Herbicide Effects on Mesquite Cut Stumps, Research Highlights, Noxious Brush and Weed Control," *Texas Range and Wildlife Management*, 11, 62.
- Horn, R., and A.R. Dexter, 1989. "Dynamics of Soil Aggregation in an Irrigated Desert Loess," *Soil and Tillage Research*, 13(3), 253–266.
- Huggett, R.J., 1998. "Soil Chronosequences, Soil Development, and Soil Evolution: A Critical Review," *Catena*, 32(3-4), 155–172.
- Hungate, B.A., J.S. Dukes, M.R. Shaw, Y. Luo and C.B. Field, 2003. "Nitrogen and Climate Change," *Science*, 302(5650), 1512–1513.
- Hunter, C.R., A.J. Busacca, and W.J. Waugh, 1990. "A Feasibility Study of Modeling Pedogenic Carbonates in Soils and Sediments at the U.S. Department of Energy's Hanford Site," PNL-7413, Pacific Northwest National Laboratory, Richland, Washington.

- Hutchings, T.R., A.J. Moffat, and R.A. Kemp, 2001. "Effects of Rooting and Tree Growth of Selected Woodland Species on Cap Integrity in a Mineral Capped Landfill Site," *Waste Management & Research*, 19(3), 194–200.
- Hutchings, T.R., D. Sinnett, A.J. Peace, and A.J. Moffat, A. 2006. "The Effect of Woodland Growth on a Containment Landfill Site in Hertfordshire, United Kingdom," *Urban Forestry & Urban Greening*, 5(4), 169-176.
- Iqbal, J., J.A. Thomasson, J.N. Jenkins, P.R. Owens, and F.D. Whisler, 2005. "Spatial Variability Analysis of Soil Physical Properties of Alluvial Soils," *Soil Science Society of America Journal*, 69(4), 1338–1350.
- Jackson, E.A., G. Blackburn, and A.R.P. Clarke, 1956. "Seasonal Changes in Soil Salinity at Tintinara, South Australia," *Australian Journal of Agricultural Research*, 7(1), 20–44.
- Jegou D., S. Schrader, H., Diestel, and D. Cluzeau, 2001. "Morphological, Physical and Biochemical Characteristics of Burrow Walls Formed by Earthworms," *Applied Soil Ecology*, 17, 165–174.
- Jenny, H., 1941. "Factors of Soil Formation," *Soil Science*, 52(5), 415.
- Jenny, H., 1980. *The Soil Resource: Origin and Behavior*, 37, Springer-Verlag, New York.
- Jones, J.A.A., 2004. "Pipe and Piping," In: Goudie, A.S. (Ed.), *Encyclopedia of Geomorphology*, Routledge, London, 784–788.
- Junge, C.E., and R.T. Werby, 1958. "The Concentration of Chloride, Sodium, Potassium, Calcium, and Sulfate in Rain Water over the United State," *Journal of Meteorology*, 15, 417–425.
- Kaoser S., S. Barrington, M. Elektorowicz, and T. Ayadat, 2006. "The Influence of Hydraulic Gradient and Rate of Erosion on Hydraulic Conductivity of Sand-Bentonite Mixtures," *Soil and Sediment Contamination: An International Journal*, 15(5), 481–496.
- Kay, B.D., 1990. "Rates of Change of Soil Structure under Different Cropping Systems," *Advances in Soil Science* 12, 1–52, Springer, New York, New York.
- Kim, W.H. and D.E. Daniel, 1992. "Effects of Freezing on Hydraulic Conductivity of Compacted Clay," *Journal of Geotechnical Engineering* 118(7), 1083-1097.
- Kinlaw, A.L., 1999. "A Review of Burrowing by Semi-Fossorial Vertebrates in Arid Environments," *Journal of Arid Environments*, 41(2), 127–145.
- Kladivko, E.J. and D.W. Nelson, 1979. "Changes in Soil Properties from Application of Anaerobic Sludge," *Journal of the Water Pollution Control Federation*, 325–332.
- Klappa, C.F., 1983. "A Process Response Model for the Formation of Pedogenic Calcretes," In R.C.L. Wilson (ed.), *Residual Deposits: Surface Related Weathering Processes and Materials*. Geological Society of London Special Publication No. 11, Blackwell Scientific Publications, Oxford, England.

- Kleppe, J.H., and R.E. Olson, 1985. "Desiccation Cracking of Soil Barriers," *Hydraulic Barriers in Soil and Rock*, ASTM International.
- Kodikara, J. and S. Costa, 2013. "Desiccation Cracking in Clayey Soils: Mechanisms and Modelling," *Multiphysical Testing of Soils and Shales*, 21–32, Springer-Verlag Berlin Heidelberg.
- Kohnke, H., and C.H. Werkhoven, 1963. "Soil Temperature and Soil Freezing as Affected by an Organic Mulch," *Soil Science Society of America Journal*, 27, 13–17.
- Kozlowski, T.T. 1999. "Soil Compaction and Growth of Woody Plants," *Scandinavian Journal of Forest Research*, 14(6), 596–619.
- Krisdani, H., H. Rahardjo, and E.C. Leong, 2008. "Effects of Different Drying Rates on Shrinkage Characteristics of a Residual Soil and Soil Mixtures," *Engineering Geology*, 102(1-2), 31–37.
- Kumar, S., and W.L. Yong, 2002. "Effect of Bentonite on Compacted Clay Landfill Barriers," *Soil and Sediment Contamination: An International Journal*, 11(1), 71–89.
- Lagasse, P.F., P.E. Clopper, L.W. Zevenbergen, and J.F. Ruff, 2006. *Riprap Design Criteria, Recommended Specifications, and Quality Control*, National Cooperative Highway Research Program, Report 568, Transportation Research Board, Washington D.C.
- Lal, R., 2001. "Soil Degradation by Erosion," *Land Degradation & Development* 12, 519–539, <https://doi.org/10.1002/ldr.472>.
- Landeen, D.S., 1994. *The Influence of Small Mammal Burrowing Activity on Water Storage at the Hanford Site*, WHC-EP—0730, Westinghouse Hanford Co.
- Larson, W.E., and R.R. Allmaras, 1971. "Management and Natural Force as Related to Compaction," *Compaction of Agricultural Soils*, Barnes, K.K., Carleton, W.M., Taylor, H.M., Throckmorton, R.I., Vanden Berg, G. (eds), *American Society of Agricultural Engineers*, 367–427, St. Joseph, Michigan.
- Laundre, J.W. and T.D. Reynolds, 1993. "Effects of Soil Structure on Burrow Characteristics of Five Small Mammal Species," *Great Basin Naturalist*, 53, 358–366.
- Lawrence, C.R., T.H. Painter, C.C. Landry, and J.C. Neff, 2010. "Contemporary Geochemical Composition and Flux of Aeolian Dust to the San Juan Mountains, Colorado, United States," *Journal of Geophysical Research: Biogeosciences*, 115(G3).
- Leeder, M.R., 1975. "Pedogenic Carbonates and Flood Sediment Accretion Rates: A Quantitative Model for Alluvial Arid-Zone Lithofacies," *Geological Magazine*, 112(3), 257–270.
- Lefroy, R.D., G.J. Blair, and W.M. Strong, 1993. "Changes in Soil Organic Matter with Cropping as Measured by Organic Carbon Fractions and ¹³C Natural Isotope Abundance," *Plant and Soil*, 155(1), 399–402.

- Lin, H.S., K.J. McInnes, L.P. Wilding, and C.T. Hallmark, 1999. "Effects of Soil Morphology on Hydraulic Properties I. Quantification of Soil Morphology," *Soil Science Society of America Journal*, 63(4), 948-954.
- Lin, H.S., 2010a. "Linking Principles of Soil Formation and Flow Regimes," *Journal of Hydrology*, 393(1-2), 3-19.
- Lin, H.S., 2010b. "Earth's Critical Zone and Hydopedology: Concepts, Characteristics, and Advances," *Hydrology and Earth System Sciences*, 14(1), 25.
- Lin, H.S., 2011. "Three Principles of Soil Change and Pedogenesis in Time and Space," *Soil Science Society of America Journal*, 75(6), 2049-2070.
- Lin, L.C., and C.H. Benson, 2000. "Effect of Wet-Dry Cycling on Swelling and Hydraulic Conductivity of GCLs," *Journal of Geotechnical and Geoenvironmental Engineering*, 126(1), 40-49.
- Lindsey, C.G., L.W. Long, and C.W. Begej, 1982. *Long-term Survivability of Riprap for Armoring Uranium-Mill Tailings and Covers: A Literature Review*, NUREG/CR-2642, Pacific Northwest Laboratory, Richland, Washington.
- Link, S.O., J.L. Downs, and W.J. Waugh, 1994. *The Role of Plants on Isolation Barrier Systems*, (No. PNL-SA-24159; CONF-941124-18) Pacific Northwest Laboratory, Richland, Washington.
- Link, S.O., L.L. Cadwell, K.L. Petersen, M.R. Sackschewsky, and D.S. Landeen, 1995. *The Role of Plants and Animals in Isolation Barriers at Hanford*, PNL-10788, Pacific Northwest Laboratory, Richland, Washington.
- Lodge, Jr. J.P., J.B. Pate, W. Basbergill, G.S. Swanson, K.C. Hill, E. Lorange, and A.L. Lazrus, 1968. *Chemistry of United States Precipitation. Final report on the National Precipitation Sampling Network*, Boulder, Colorado, National Center for Atmospheric Research.
- Lommler, J.C., P.K. Chen, E. Artiglia, F.B. Guros, B. Bridgeman, S. Cox, 1999. "DOE UMTRA Project Disposal Cell Design Summary," Waste Management Conference, February 28 – March 4, 1999, Tucson, Arizona.
- Lyford, F.P., and H.K. Qashu, 1969. "Infiltration Rates as Affected by Desert Vegetation," *Water Resources Research*, 5(6), 1373-1376.
- Machette, M.N., 1985. "Calcific Soils of the Southwestern United States," *Soils and Quaternary geology of the southwestern United States, Geological Society of America Special Paper*, 203, 1-21.
- Mackay, W.P., 1981. "A Comparison of the Nest Phenologies of Three Species of Pogonomyrmex Harvester Ants (Hymenoptera: Formicidae)," *Psyche: A Journal of Entomology*, 88(1-2), 25-74.

- Malusis, M.A., S. Yeom, and J. C. Evans, 2011. "Hydraulic Conductivity of Model Soil–Bentonite Backfills Subjected to Wet–Dry Cycling," *Canadian Geotechnical Journal*, 48(8), 1198–1211.
- Marcotte D., J.C. Marron, and M. Fafard, 1994. "Washing of Bentonite in Laboratory Hydraulic Conductivity Tests," *Journal of Environmental Engineering*, 120(3), 691–698.
- Marschner, H., 1991. "Mechanisms of Adaptation of Plants to Acid Soils," *Plant and Soil*, 134(1), 1–20.
- Mast, M.A., T.J. Mills, S.S. Paschke, G. Keith, and J.I. Linard, 2014. "Mobilization of Selenium from the Mancos Shale and Associated Soils in the Lower Uncompahgre River Basin, Colorado," *Applied Geochemistry*, 48, 16–27.
- Maynard, S.T., J.F. Ruff, and S.R. Abt, 1989. "Riprap Design," *Journal of Hydraulic Engineering*, 115(7), 937–949.
- McBride, M.B., 1994. *Environmental Chemistry of Soils*, Oxford University Press, New York.
- McClaran, M.P., J. Moore-Kucera, D.A. Martens, J. van Haren, and S.E. Marsh, 2008. "Soil Carbon and Nitrogen in Relation to Shrub Size and Death in a Semi-Arid Grassland," *Geoderma*, 145(1), 60–68.
- McCloskey, R.T., 1976. "Community Structure in Sympatric Rodents," *Ecology* 57(4), 728–739.
- McCormack, M.L., T.S. Adams, E.A. Smithwick, and D.M. Eissenstat, 2014. "Variability in Root Production, Phenology, and Turnover Rate Among 12 Temperate Tree Species," *Ecology*, 95(8), 2224–2235.
- McFadden, L.D., E.V. McDonald, S.G. Wells, K. Anderson, J. Quade, and S.L. Forman, 1998. "The Vesicular Layer of Desert Soils: Genesis and the Relationship to Climate Change and Desert Pavements Based on Numerical, Modeling, Carbonate Translocation Behavior, and Stable Isotope and Optical Dating Studies," *Geomorphology* 24: 101–145.
- McKeague, J.A., F. DeConinck, and D.P. Franzmeier, 1983. "Spodosols," *Developments in Soil Science*, 11, 217–252.
- McKenzie, D.H., L.L. Cadwell, L.E. Eberhardt, W.E. Kennedy Jr., R.A. Peloquin, and M.A. Simmons, 1982. *Relevance of Biotic Pathways to the Long-term Regulation of Nuclear-Waste Disposal, Topical report on reference western arid low-level sites*, NUREG/CR-2675-Vol. 2; PNL-4241-Vol. 2, Pacific Northwest Laboratory, Richland, Washington.
- McNeal, B. L., and N.T. Coleman, 1966. "Effect of Solution Composition on Soil Hydraulic Conductivity 1," *Soil Science Society of America Journal* 30(3), 308–312.
- Meek, B.D., E.A. Rechel, L.M. Carter, and W.R. DeTar, 1989. "Changes in Infiltration Under Alfalfa as Influenced by Time and Wheel Traffic," *Soil Science Society of America Journal*, 53(1), 238–241.

- Meek, B.D., W.R. DeTar, E.R. Rechel, L.M. Carter, and D. Rolph, 1990. "Infiltration Rate as Affected by an Alfalfa and No-Till Cotton Cropping System," *Soil Science Society of America Journal*, 54(2), 505–508.
- Melchior, S., 1997. "In-Situ Studies of the Performance of Landfill Caps (Compacted Soil Liners, Geomembranes, Geosynthetic Clay Liners, Capillary Barriers)," *Land Contamination and Reclamation*, 5(3), 209–216.
- Merritt, R.C., 1971. *The Extractive Metallurgy of Uranium*, Colorado School of Mines Research Institute, Golden, Colorado.
- Mitchell, A.R., and M.T. VanGenuchten, 1992. "Shrinkage of Bare and Cultivated Soil," *Soil Science Society of America Journal*, 56(4), 1036–1042.
- Mitchell, J.K., and K. Soga, 2005. *Fundamentals of Soil Behavior, Third Edition*, Hoboken, New Jersey, John Wiley & Sons.
- Mogren, E.W., 2002. "Warm Sands: Uranium Mill Tailings Policy in the Atomic West," *Environmental History* Vol. 8, No.1, University of New Mexico Press, Albuquerque, New Mexico.
- Montgomery, R., and L. Parsons, 1989. "The Omega Hills Final Cover Test Plot Study: Three Year Data Summary," *1989 Annual Meeting of the National Solid Waste Management Association, Washington, DC*.
- Morales, V.L., J.Y. Parlange, and T.S. Steenhuis, 2010. "Are Preferential Flow Paths Perpetuated by Microbial Activity in the Soil Matrix? A Review," *Journal of Hydrology*, 393(1-2), 29–36.
- Morgan, R.P.C., 2005. *Soil Erosion and Conservation*, 3rd ed., Blackwell Publishing, the United Kingdom.
- Morris P.H., J. Graham, and D.J. Williams, 1992. "Cracking in Drying Soils", *Canadian Geotechnical Journal*, 29, 262–277.
- Mzuku, M., R. Khosla, R. Reich, D. Inman, F. Smith, and L. MacDonald, 2005. "Spatial Variability of Measured Soil Properties Across Site-Specific Management Zones," *Soil Science Society of America Journal*, 69(5), 1572–1579.
- Nelson, J.D., S.R. Abt, R.L. Volpe, C. Van Zyl, N.E. Hinkle, and W.P. Staub, 1986. *Methodologies for Evaluating Long-Term Stabilization Designs of Uranium Mill Tailings Impoundments*, NUREG/CR-4620. Colorado State University, Fort Collins, Colorado.
- Nielson, K.K., and V.C. Rogers, 1982. *A Mathematical Model for Radon Diffusion in Earthen Materials*, NUREG/CR-2765; PNL-4301; RAE-18-2, Rogers and Associates Engineering Corporation, Salt Lake City, Utah.
- Nikiforoff, C.C., and L.T. Alexander, 1942. "The Hardpan and the Claypan in a San Joaquin Soil," *Soil Science*, 53(3), 157–172.

- NRC (U.S. Nuclear Regulatory Commission), 1989. *Calculation of Radon Flux Attenuation by Earthen Uranium Mill Tailings Covers*, Regulatory Guide 3.64, June.
- NRC (U.S. Nuclear Regulatory Commission), 2003. *Final Standard Review Plan for the Review of a Reclamation Plan for Mill Tailings Sites Under Title II of the Uranium Mill Tailings Radiation Control Act of 1978*, NUREG-1620, Rev.1.
- Oades, J.M., 1984. "Soil Organic Matter and Structural Stability: Mechanisms and Implications for Management," *Plant and Soil*, 76, 319–337.
- O'Farrell, M.J., 1980. Spatial Relationships of Rodents in a Sagebrush Community," *Journal of Mammalogy* 61(4), 589–605.
- O'Farrell, T.P. and R. O. Gilbert, 1975. "Transport of Radioactive Materials by Jackrabbits on the Hanford Reservation," *Health Physics*, 29, 9–15.
- Omid, G.H., J.C. Thomas, and K.W. Brown, 1996. "Effect of Desiccation Cracking on the Hydraulic Conductivity of a Compacted Clay Liner," *Water, Air, and Soil Pollution*, 89(1-2), 91–103.
- O'Rear, N.B., 1966. *Summary and Chronology of The Domestic Uranium Program*. U.S. Atomic Energy Commission, TM-187. U.S. Department of Energy, Grand Junction Office, Colorado.
- O'Sadnick, D.L., B.E. Simpson, and G.K. Kasel, 1995. "Evaluation and Performance of a Sand/Bentonite Liner," *Geoenvironment 2000*, Y. B. Acar and D. E. Daniel, Geotech. Spec. Publ. No. 46, ASCE, New York, 688–701.
- Paige-Green, P, 2008. "Dispersive and Erodible Soils – Fundamental Differences," SAIEG/ SAICE Problem Soils Conference, Midrand, November 2008, pp. 59–67.
- Pankhurst C.E., A., Pierret, B.G. Hawke, and J.M. Kirby, 2002. "Microbiological and Chemical Properties of Soil Associated with Macropores at Different Depths in a Red-Duplex Soil in NSW Australia," *Plant and Soil*, 238, 11–20.
- Parker, G.G, 1963. "Piping, A Geomorphic Agent in Landform Development of the Drylands," *International Association of Scientific Hydrology Publication*, 65, 103–113.
- Parker, G.G., and E.A. Jenne, 1967. "Structural Failure of Western Highways Caused by Piping," *Highway Research Record*, 203, 56–76.
- Pärtel, M. and S.D. Wilson, 2002. "Root Dynamics and Spatial Pattern in Prairie and Forest," *Ecology*, 83(5), 1199–1203.
- Peralta, J.R., J.L. Gardea-Torresdey, K.J. Tiemann, E. Gomez, S. Arteaga, E. Rascon, and J.G. Parsons, 2001. "Uptake and Effects of Five Heavy Metals on Seed Germination and Plant Growth in Alfalfa (*Medicago Sativa* L.)," *Bulletin of Environmental Contamination and Toxicology*, 66(6), 727–734.

- Pierret A., C.J. Moran and C.E. Pankhurst, 1999. "Differentiation of Soil Properties Related to the Spatial Association of Wheat Roots and Soil Macropores," *Plant and Soil*, 211, 51–58.
- Pierret, A., J.L. Maeght, C. Clément, J.P. Montoroi, C. Hartmann, and S. Gonkhamdee, 2016. "Understanding Deep Roots and their Functions in Ecosystems: An Advocacy for more Unconventional Research," *Annals of Botany*, 118(4), 621–635.
- PL 95-604. "Uranium Mill Tailings Radiation Control Act of 1978," Public Law.
- Poesen, J., 2018. "Soil Erosion in the Anthropocene: Research Needs," *Earth Surface Processes and Landforms* 43:64–84, <https://doi.org/10.1002/esp.4250>.
- Post, F.A., and F.R. Dreibelbis, 1942. "Some Influences of Frost Penetration and Microclimate on the Water Relationships of Woodland, Pasture and Cultivated soils," *Soil Science Society of America*, 7, 95–104.
- Potter, L.D., R.C. Reynolds Jr., and E.T. Louderbough, 1985. "Mancos Shale and Plant Community Relationships: Field Observations," *Journal of Arid Environments*, 9(2), 137–145.
- Rabenhorst, M.C., L.P. Wilding, and C.L. Girdner, 1984. "Airborne Dusts in the Edwards Plateau Region of Texas," *Soil Science Society of America Journal*, 48(3), 621–627.
- Ravina, I., 1983. "The Influence of Vegetation on Moisture and Volume Changes," *Geotechnique*, 33(2), 151-157.
- Rawls, W.J., D.L. Brakensiek, and K.E. Saxton, 1982. "Estimation of Soil Water Properties," *Transactions of the ASAE*, 25(5), 1316–1320.
- Reeves, G.M., I. Sims, and J.C. Cripps, Eds, 2006. "Clay Materials Used in Construction," *Geological Society*, London.
- Reheis, M.C., J.C. Goodmacher, J.W. Harden, L.D. McFadden, T.K. Rockwell, R.R. Shroba, E.M. Taylor, and J.M. Sowers, 1995. "Quaternary Soils and Dust Deposition in Southern Nevada and California," *Geological Society of America Bulletin*, 107(9), 1003–1022.
- Reheis, M.C., and F.E. Urban, 2011. "Regional and Climatic Controls on Seasonal Dust Deposition in the Southwestern U.S.," *Aeolian Research*, 3(1), 3-21.
- Reubens, B., J. Poesen, F. Danjon, G. Geudens, and B. Muys, 2007. "The Role of Fine and Coarse Roots in Shallow Slope Stability and Soil Erosion Control with a Focus on Root System Architecture: A Review," *Trees*, 21(4), 385–402.
- Reynolds, R.L., J. Belnap, M. Reheis, P. Lamothe, and F. Luiszer, 2001. "Aeolian Dust in Colorado Plateau Soils: Nutrient Inputs and Recent Change in Source," *Proceedings of the National Academy of Sciences*, 98, 7123–7127.
- Reynolds, R.L., M.C. Reheis, J.C. Neff, H. Goldstein, and J.C. Yount, 2006. "Late Quaternary Eolian Dust in Surficial Deposits of a Colorado Plateau Grassland: Controls on Distribution and Ecologic Effects," *Catena*, 66, 251–266.

- Richards, K.S., and K.R. Reddy, 2007. "Critical Appraisal of Piping Phenomena in Earth Dams," *Bulletin of Engineering Geology and the Environment*, 66(4), 381–402.
- Richards, K.S., and K.R. Reddy, 2012. "Experimental investigation of initiation of backward erosion piping in soils," *Géotechnique*, 62(10):933–942.
- Richter, D.D., and D. Markewitz, 2001. "Understanding Soil Change: Soil Sustainability over Millennia, Centuries, and Decades," Cambridge University Press.
- Richter, D.D., 2007. "Humanity's Transformation of Earth's Soil: Pedology's New Frontier," *Soil Science*, 172(12), 957–967.
- Richter, D.D., M. Hofmockel, M. A. Callahan Jr., D.S. Powlson, and P. Smith, 2007. "Long-Term Soil Experiments: Keys to Managing Earth's Rapidly Changing Ecosystems," *Soil Science Society of America Journal*, 71(2), 266–279.
- Roberts, J.A., W.L. Daniels, J.A. Burger, and J.C. Bell, 1988. "Early Stages of Mine Soil Genesis as Affected by Topsoiling and Organic Amendments," *Soil Science Society of America Journal*, 52(3), 730–738.
- Robinson, G.R., and S.N. Handel, 1995. "Woody Plant Roots Fail to Penetrate a Clay-Lined Landfill: Management Implications," *Environmental Management*, 19, 57–64.
- Rodríguez-Caballero, E., Y. Cantón, S. Chamizo, A. Afana, and A. Solé-Benet, 2012. "Effects of Biological Soil Crusts on Surface Roughness and Implications for Runoff and Erosion," *Geomorphology*, 145, 81–89.
- Rogers, V.C., K.K. Nielson, and D.R. Kalkwarf, 1984. *Radon Attenuation Handbook for Uranium Mill Tailings Cover Design*, NUREG/CR-3533; PNL-4878; RAE-18-5, Rogers and Associates Engineering Corporation, Salt Lake City, Utah.
- Rovira, A.D., 1965. "Interactions Between Plant Roots and Soil Microorganisms," *Annual Reviews of Microbiology*, 19(1), 241–266.
- Russell, R.S., 1977. *Plant Root Systems: Their Function and Interaction With the Soil*, McGraw-Hill Book Company (UK) Limited, London.
- Ryan P., 1985. "Rum Jungle Rehabilitation Project, Review of Revegetation Operations and Monitoring," October 1984–August 198, Conservation Commission of the Northern Territory: Darwin, Australia.
- Ryan P., 1986. "Rum Jungle Rehabilitation Project, Summary of Revegetation Monitoring and Recommendations, Conservation Commission of the Northern Territory: Darwin, Australia.
- Ryser, P., 1996. "The Importance of Tissue Density for Growth and Lifespan of Leaves and Roots: A Comparison of Five Ecologically Contrasting Grasses," *Functional Ecology*, 10, 717–723.
- Saini, G.R., 1966. "Organic Matter as a Measure of Bulk Density of Soil," *Nature*, 210, 1295–1296.

- Schafer, W.M., G.A. Nielsen, and W.D. Nettleton, 1980. "Mine Spoil Genesis and Morphology in a Spoil Chronosequence in Montana," *Soil Science Society of America Journal*, 44(4), 802–807.
- Schenk, H.J., and R.B. Jackson, 2005. "Mapping the Global Distribution of Deep Roots in Relation to Climate and Soil Characteristics," *Geoderma*, 126(1-2), 129–140.
- Schlesinger, W.H., and A.M. Pilmanis, 1998. "Plant-Soil Interactions in Deserts," *Plant-Induced Soil Changes: Processes and Feedbacks* 169–187, Springer Netherlands, Dordrecht, Netherlands.
- Schoeneberger, P.J., D.A. Wysocki, and E.C. Benham, (Eds.), 2012. *Field Book for Describing and Sampling Soils*, Government Printing Office.
- Schwinning, S., O.E. Sala, M.E. Loik, and J.R. Ehleringer, 2004. "Thresholds, Memory, and Seasonality: Understanding Pulse Dynamics in Arid/Semi-Arid Ecosystems," *Oecologia*, 14, 191–193.
- Sellin, P., and O.X. Leupin, 2013. "The Use of Clay as an Engineered Barrier in Radioactive-Waste Management—A Review," *Clays and Clay Minerals*, 61(6), 477–498.
- Shafer, D.D., M.H. Young, S.F. Zitzer, T.G. Caldwell, and E.V. McDonald, 2007. "Impacts of Interrelated Biotic and Abiotic Processes during the Past 125,000 Years of Landscape Evolution in the Northern Mojave Desert, Nevada," *Journal of Arid Environments*, 69, 633–657.
- Sherard, J.L., L.P. Dunnigan, and R.S. Decker, 1976. "Identification and Nature of Dispersive Soils," *Journal of Geotechnical and Geoenvironmental Engineering*, 102 (Proc. Paper No. 12052).
- Sherard, J.L., L.P. Dunnigan, and R.S. Decker, 1977. "Some Engineering Problems with Dispersive Clays," *Dispersive Clays, Related Piping, and Erosion in Geotechnical Projects*, 623, 2.
- Siegel-Issem, C.M., J.A. Burger, R.F. Powers, F. Ponder, and S.C. Patterson, 2005. "Seedling Root Growth as a Function of Soil Density and Water Content," *Soil Science Society of America Journal*, 69, 215–226.
- Simmons, G.L., and P.E. Pope, 1987. "Influence of Soil Compaction and Vesicular-Arbuscular Mycorrhizae on Root Growth of Yellow-Poplar and Sweet Gum Seedlings," *Canadian Journal of Forest Research*, 17, 970–975.
- Simonson, R.W., 1959. "Outline of a Generalized Theory of Soil Genesis," *Soil Science Society of America Journal*, 23(2), 152–156.
- Six, J., E.T. Elliott, K. Paustian, and J.W. Doran, 1998. "Aggregation and Soil Organic Matter Accumulation in Cultivated and Native Grassland Soils," *Soil Science Society of America Journal*, 62(5), 1367–1377.

- Six, J., H. Bossuyt, S. Degryze, and K. Denef, 2004. "A History of Research on the Link Between (Micro) Aggregates, Soil Biota, and Soil Organic Matter Dynamics," *Soil and Tillage Research*, 79(1), 7–31.
- Smith, E.D., R.J. Luxmoore, and G.W. Suter, 1997. "Natural Physical and Biological Processes Compromise the Long-Term Performance of Compacted Clay Caps," *Barrier Technologies for Environmental Management*, National Research Council, Washington, D.C., National Academy Press.
- Snyder V.A., and R.D. Miller, 1985. "Tensile Strength of Unsaturated Soils", *Soil Science Society of America Journal*, 49, 58–65.
- Soane, B.D., 1990. "The Role of Organic Matter in Soil Compactibility: A Review of Some Practical Aspects," *Soil and Tillage Research*, 16(1-2), 179–201.
- Soil Survey Staff, 2003. *Keys to Soil Taxonomy, Ninth Edition*, U.S. Department of Agriculture, Natural Resources Conservation Service.
- Southard, R.J., and S.W. Buol, 1988. "Subsoil Saturated Hydraulic Conductivity in Relation to Soil Properties in the North Carolina Coastal Plain," *Soil Science Society of America Journal*, 52(4), 1091–1094.
- Stevens, P.R., and T.W. Walker, 1970. "The Chronosequence Concept and Soil Formation," *The Quarterly Review of Biology*, 45(4), 333–350.
- Stokes, A., C. Atger, A.G. Bengough, T. Fourcaud, and R.C. Sidle, 2009. "Desirable Plant Root Traits for Protecting Natural and Engineered Slopes Against Landslides," *Plant and Soil*, 324(1-2), 1–30.
- Streets, R.B., and E.B. Stanley, 1938. "Control of Mesquite and Noxious Shrubs on Southern Arizona Grassland Ranges," College of Agriculture, University of Arizona, Tucson, Arizona.
- Stuart, D.M., and R.M. Dixon, 1973. "Water Movement and Caliche Formation in Layered Arid and Semiarid Soils," *Soil Science Society of America Journal*, 37, 323–324.
- Sumner, M.E. 1993. "Sodic Soils-New Perspectives," *Australian Journal of Soil Research*, 31(6), 683–750.
- Suter, G., R. Luxmoore, and E. Smith, 1993. "Compacted Soil Barriers at Abandoned Landfill Sites Are Likely to Fail in the Long Term," *Journal of Environmental Quality*, 22(2), 217–226.
- Swanson, M.L., G.M. Kondolf, and P.J. Boison, 1989. "An Example of Rapid Gully Initiation and Extension by Subsurface Erosion: Coastal San Mateo County, California," *Geomorphology*, 2(4):393–403.
- Targulian, V.O. and S.V. Goryachkin, 2004. "Soil Memory: Types of Record, Carriers, Hierarchy and Diversity," *Revista Mexicana de Ciencias Geológicas*, 21(1), 1-8.

- Targulian, V.O. and P.V. Krasilnikov, 2007. "Soil System and Pedogenic Processes: Self-Organization, Time Scales, and Environmental Significance," *Catena*, 71(3), 373–381.
- Taylor, G., A. Spain, A. Nefiodovas, G. Timms, V. Kuznetsov, and J. Bennett, 2003. "Determination of the Reasons for Deterioration of the Rum Jungle Waste Rock Cover," *Australian Centre for Mining Environmental Research, Brisbane*.
- Taylor, H., and G.S. Brar, 1991. "Effect of Soil Compaction on Root Development," *Soil and Tillage Research*, 19(2-3), 111–119.
- Tingey, D.T., D.L. Phillips, and M.G. Johnson, 2000. "Elevated CO₂ and Conifer Roots: Effects on Growth, Life Span, and Turnover," *New Phytologist*, 147: 87–103.
- Tisdall, J.M., and J.M. Oades, 1979. "Stabilization of Soil aggregates by the Root Systems of Ryegrass," *Soil Research*, 17(3), 429–441.
- Tisdall, J.M. and J. Oades, 1982. "Organic Matter and Water-Stable Aggregates in Soils," *European Journal of Soil Science*, 33(2), 141–163.
- Tisdall, J.M., S.E. Smith, and P. Rengasamy, 1997. "Aggregation of Soil by Fungal Hyphae," *Soil Research*, 35(1), 55–60.
- Traoré, O., V. Groleau-Renaud, S. Plantureux, A. Tubeileh, and V. Boeuf-Tremblay, 2000. "Effect of Root Mucilage and Modelled Root Exudates on Soil Structure," *European Journal of Soil Science*, 51(4), 575–581.
- Turk, J.K., O.A. Chadwick, and R.C. Graham, 2011. "Pedogenic Processes. In P.M. Huang et al. (eds.)," *Handbook of Soil Science* CRC Press, Boca Raton, Florida.
- Turk, J.K., and R.C. Graham, 2011. "Distribution and Properties of Vesicular Horizons in the Western United States," *Soil Science Society of America Journal*, 75, 1449–1461.
- Umar, M., K.A. Kassim, and K.T.P Chiet, 2016. "Biological Process of Soil Improvement in Civil Engineering: A Review," *Journal of Rock Mechanics and Geotechnical Engineering*, 8(5), 767–774.
- Unger, P.W., and T.C. Kaspar, 1994. "Soil Compaction and Root Growth: A Review," *Agronomy Journal*, 86(5), 759–766.
- USDA (U.S. Department of Agriculture), 2012. *Field Book for Describing and Sampling Soils*, version 3.0, Natural Resource Conservation Service.
- Vacher C.A., R.J. Loch, and S.R. Raine, 2004. *Identification and Management of Dispersive Mine Spoils*, Final Report for Australian Centre for Mining Environmental Research, Kenmore Queensland, June.
- Van der Hoven, S.J. and J. Quade, 2002. "Tracing Spatial and Temporal Variations in the Sources of Calcium in Pedogenic Carbonates in a Semiarid Environment," *Geoderma*, 108: 259–276.
- Van't Hoff, J.H., 1884. *Etudes de Dynamique Chimique*, Vol. 1, Muller.

- Verachtert, E., M. Van Den Eeckhaut, J. Poesen, and J. Deckers, 2010. "Factors Controlling the Spatial Distribution of Soil Piping Erosion on Loess-Derived Soils: A Case Study from Central Belgium," *Geomorphology*, 118(3–4):339–348.
- Verachtert, E., W. Maetens, M. Van Den Eeckhaut, J. Poesen, and J. Deckers, 2011. "Soil Loss Rates Due to Piping Erosion," *Earth Surface Processes and Landforms*, 36, 1715–1725, <https://doi.org/10.1002/esp.2186>.
- Vogel, S., C.P. Ellington, and D.L. Kilgore, 1973. "Wind-Induced Ventilation of the Burrow of the Prairie-Dog, *Cynomys ludovicianus*," *Journal of Comparative Physiology*, 85(1), 1–14.
- Voorhees, L.D., M.J. Sale, J.W. Webb, and P.J. Mulholland, 1983. *Long-Term Stabilization of Uranium Mill Tailings*, CONF-830523–8, Environmental Sciences Division, Oak Ridge National Laboratory.
- Watt, M., M.E. McCully, and C.E. Jeffree, 1993. "Plant and Bacterial Mucilages of the Maize Rhizosphere: Comparison of their Soil Binding Properties and Histochemistry in a Model System," *Plant and Soil*, 151(2), 151–165.
- Watt, M., M.E. McCully, and M.J. Canny, 1994. "Formation and Stabilization of Rhizosheaths of *Zea mays* L.(Effect of Soil Water Content)," *Plant Physiology*, 106(1), 179–186.
- Waugh, W.J., J.C. Chatters, G.V. Last, B.N. Bjornstad, S.O. Link, and C.R. Hunter, 1994a. *Barrier Analogs: Long-Term Performance Issues, Preliminary Studies, and recommendations*, No. PNL-9004. Pacific Northwest Laboratory, Richland, Washington.
- Waugh, W.J., K.L. Petersen, S.O. Link, B.N. Bjornstad, and G.W. Gee, 1994b. "Natural Analogs of the Long-Term Performance of Engineered Covers," 379–409, In G.W. Gee and N.R. Wing (eds.), *In-Situ Remediation: Scientific Basis for Current and Future Technologies*, Battelle Press, Columbus, Ohio.
- Waugh, W.J., and G.N. Richardson, 1997. "Ecology, Design, and Long-Term Performance of Surface Barriers: Applications at a Uranium Mill Tailings Site," *Barrier Technologies for Environmental Management*, National Research Council, National Academy Press, Washington, D.C.
- Waugh, W.J. and G.M. Smith, 1997. *Effects of Root Intrusion on the Burrell, Pennsylvania, Uranium Mill Tailings Disposal Site*, GJO–97–5–TAR, U.S. Department of Energy, Grand Junction Office, Grand Junction, Colorado.
- Waugh, W.J., G.M. Smith, and M.K. Kastens, 1997. "Analog of the Long-Term Performance of Vegetated Rocky Slopes for Landfill Covers," *Tailings and Mine Waste 1997*, 291–300.
- Waugh, W.J., S.J. Morrison, G.M. Smith, M. Kautsky, T.R. Bartlett, C.E. Carpenter, and C.A. Jones, 1999. *Plant Encroachment on the Burrell, Pennsylvania, Disposal Cell: Evaluation of Long-Term Performance and Risk*, GJO-99-96-TAR, Environmental Sciences Laboratory, U.S. Department of Energy, Grand Junction, Colorado.
- Waugh, W.J., P.S. Mushovic, and A.W. Kleinrath, 2006. "Lysimeter Tests for an ET Cover Design at Monticello, Utah," *Unsaturated Soils 2006*, 801–812.

- Waugh, W.J., G. Smith, B. Danforth, G. Gee, V. Kothari, and T. Pauling, 2007. "Performance Evaluation of the Engineered Cover at the Lakeview, Oregon, Uranium Mill Tailings Site," Proceedings of the Waste Management 2007 Symposium, Tucson, Arizona.
- Waugh, W.J., C.H. Benson, and W.H. Albright, 2009. "Sustainable Covers for Uranium Mill Tailings, USA: Alternative Design, Performance, and Renovation," Proceedings of 12th International Conference on Environmental Remediation and Radioactive Waste Management, Liverpool, United Kingdom.
- Waugh, W.J., W.H. Albright, C.H. Benson, G.M. Smith, and R.P. Bush, 2015. "Evaluation of Soil Manipulation to Prepare Engineered Earthen Waste Covers for Revegetation," *Journal of Environmental Quality*, 44(6):1911-22.
- Waugh, W.J., W.H. Albright, C.H. Benson, D.C. Dander, M. Fuhrmann, C.N. Joseph, W.J. Likos, D.A. Marshall, A.M. Michaud, A. Tigar, and M.M. Williams, 2018a. "Evaluating the Ecology and Performance of Conventional and Evapotranspiration Covers for Uranium Mill Tailings Disposal Cells," Proceedings of Ecological Society of America 2018, August 5–10, 2018, New Orleans, Louisiana.
- Waugh, W.J., W.H. Albright, C.H. Benson, C.N. Joseph, D.A. Marshall, and A.D. Tigar, 2018b. "Are Natural Processes Transforming Conventional Disposal Cell Covers into Evapotranspiration Covers? Should We Enhance Beneficial Processes?" Long-Term Stewardship Conference, August 20–23, 2018, U.S. Department of Energy Office of Legacy Management.
- Wells, S. G., J.C. Dohrenwend, L.D. McFadden, B.D. Turrin, and K.D. Mahrer, 1985. "Late Cenozoic Landscape Evolution on Lava Flow Surfaces of the Cima Volcanic Field, Mojave Desert, California," *Geological Society of America Bulletin*, 96(12), 1518–1529.
- Went, F.W. and N. Stark, 1968. "The Biological and Mechanical Role of Soil Fungi," *Proceedings of the National Academy of Sciences of the United States of America*, 60(2), 497.
- White, E.M., F.R. Gartner, and R. Butterfield, 1981. "Range Claypan Soil Improvement: Response from Furrowing and Ripping in Northwestern South Dakota," *Rangeland Ecology & Management/Journal of Range Management Archives* 34(2), 119–125.
- Wiersum, L.K., 1958. "Density of Root Branching as Affected by Substrate and Separate Ions," *Acta Botanica Neerlandica* 7, 174–190.
- Williams, M.M., 2019. *Pedogenic Process in Engineered Soils for Radioactive Waste Containment*, Dissertation for Doctor of Philosophy, University of California, Berkeley.
- Willis, W.O., C.W. Carlson, I. Alessi, and H.I. Haas, 1961. "Depth of Freezing and Spring Run Off as Related to Full Soil-Moisture Levels," *Canadian Journal of Soil Science*, 41:115–123.
- Wing, N.R., 1988. *Protective Barrier and Warning Marker System Development Plan*, WHC-EP-0169. Westinghouse Hanford Co., Richland, Washington.

- Winsor, T.F., and W.F. Whicker, 1980. "Pocket Gophers and Redistribution of Plutonium in Soil," *Health Physics*, 39(2), 257–262.
- Withington, J.M., P.B. Reich, J. Oleksyn, and D.M. Eissenstat, 2006. "Comparisons of Structure and Life Span in Roots and Leaves Among Temperate Trees," *Ecological Monographs*, 76, 381–397.
- Wright, V.P., 1990. *A Micromorphological Classification of Fossil and Recent Calcic and Petrocalcic Microstructures*, Proceedings of International Working Meeting on Soil Micromorphology, San Antonio, Texas, 1988.
- Xiao-Yan, L. and L. Lian-You, 2003. "Effect of Gravel Mulch on Aeolian Dust Accumulation in the Semiarid Region of Northwest China," *Soil and Tillage Research*, 70, 73–81.
- Yaalon, D.H., and B. Yaron, 1966. "Framework for Man-Made Soil Changes—An Outline of Metapedogenesis," *Soil Science*, 102(4), 272-277.
- Yesiller, N., C.J. Miller, G. Inci, and K. Yaldo, 2000. "Desiccation and Cracking Behavior of Three Compacted Landfill Liner Soils," *Engineering Geology*, 57(1-2), 105–121.
- Young, J.A., L.L. Cadwell, H.D. Freeman, and K.A. Hawley, 1986. *Long-Term Surveillance and Monitoring of Decommissioned Uranium Processing Sites and Tailings Piles*, United States Nuclear Regulatory Commission, NUREG CR-4504.
- Yuan, Z.Y. and H. Chen, 2010. "Fine Foot Biomass, Production, Turnover Rates, and Nutrient Contents in Boreal Forest Ecosystems in Relation to Species, Climate, Fertility, and Stand Age: Literature Review and Meta-Analyses," *Critical Reviews in Plant Sciences*, 29, 204–221.
- Zhang, Z.F., N. Bugosh, T. Tesfa, M.J. McDonald, and J.A. Kretzmann, 2018. "Conceptual Model for Hydrology-Based Geomorphic Evapotranspiration Covers for Reclamation of Mine Land," *Journal American Society of Mining and Reclamation*, 7(2), 61-88.

APPENDIX I TABLES OF ROOTING CHARACTERISTICS AT UMTRCA SITES

Table I-1 Review of Rooting Characteristics Found in Rock Riprap Covered Barriers for Waste Containment

Location	Climate zone	Species	Age of Cover (yrs)	Design thickness of barrier	Rooting depth, root class ^a , and % of barrier with roots	Depth and material above barrier	Rooting description	Reference
Green River, UT, USA	Hot, semiarid, mixed grassland	Russian thistle	2	90 cm	none 0%	45 cm Rock riprap / bedding	Dust deposited in rock voids. Only plant on cell growing in deposits. Roots confined to this material.	Burt and Cox (1993)
Tuba City, AZ, USA	Hot, semiarid, mixed grassland	Russian thistle	2	110 cm	<2.5 cm vf 2.2%	30 cm Rock riprap / bedding	Dust deposited in rock voids. Most roots growing in this material. Plants growing in zones with thinner rock armor than average.	Burt and Cox (1993)
South Clive, UT, USA	Hot, semiarid, mixed grassland	<i>Halogeton ssp.</i>	2	210 cm	<5 cm vf 2.4%	45 cm Rock riprap / bedding	Dust deposited in rock voids. Most roots growing in this material.	Burt and Cox (1993)
Burrell, PA, USA	Temperate, humid, woodland	Tree-of-heaven (<i>Ailanthus altissima</i>)	4	90 cm	≥ 10 cm m / f 11.1%	60 cm Rock riprap / bedding	Coarse/medium roots confined to bedding layer. Fine roots in barrier.	Burt and Cox (1993)
Burrell, PA, USA	Temperate, humid, woodland	American sycamore (<i>Plantanus occidentalis</i>)	4	90 cm	≥ 10 cm m / f 11.1%	60 cm Rock riprap / bedding	Coarse/medium roots confined to bedding layer. Fine roots in barrier.	Burt and Cox (1993)
Burrell, PA, USA	Temperate, humid, woodland	Box elder (<i>Acer negundo</i>)	4	90 cm	≥ 10 cm m / f 11.1%	60 cm Rock riprap / bedding	Coarse/medium roots confined to bedding layer. Fine roots in barrier.	Burt and Cox (1993)

^aRoot size descriptions in the tables are based on USDA (2012). vf = very fine (<1mm diameter); f = fine (1 to <2 mm); m = medium (2 to <5 mm); co = coarse (5 to <10 mm); vc = very coarse (≥ 10 mm).

Table I-1 Review of Rooting Characteristics Found in Rock Riprap Covered Barriers for Waste Containment (continued)

Location	Climate zone	Species	Age of Cover (yrs)	Design thickness of barrier	Rooting depth, root class ^a , and % of barrier with roots	Depth and material above barrier	Rooting description	Reference
Burrell, PA, USA	Temperate humid, woodland	Japanese knotweed (<i>Fallopia japonica</i>)	4	90 cm	15 cm m / f 46 cm f / vf 51.1%	60 cm Rock riprap / bedding	Taproot stops and spreads at top of clay barrier. m/f roots to 15 cm. f/vf along fractures to 46 cm.	Burt and Cox (1993)
Burrell, PA, USA	Temperate humid, woodland	Giant mullen (<i>Verbascum thapsus</i>)	4	90 cm	<10 cm f / vf 11.1%	60 cm Rock riprap / bedding	Roots largely confined to bedding layer.	Burt and Cox (1993)
Shiprock, NM, USA	Hot, semi-arid, mixed grassland	Salt cedar (<i>Tamarix pentandra</i>)	4	200 cm	10 - 71 cm 35.5%	40 cm Rock riprap / bedding	Large lateral roots at 15cm, fine roots to 71 cm. Along fractures.	Burt and Cox (1993)
Shiprock, NM, USA	Hot, semi-arid, mixed grassland	Summer cyprus (<i>Kochia sieversiana</i>)	6	200 cm	≥ 56 cm 28%	40 cm Rock riprap / bedding	<i>None given</i>	Burt and Cox (1993)
Burrell, PA, USA	Temperate humid, woodland	Japanese knotweed (<i>Fallopia japonica</i>)	9	90 cm	>60 cm f / vf 66.6%	60 cm Rock riprap / bedding	Taproot spreads at top of clay barrier. f/vf along fractures. Matting of f/vf horizontally along compression planes.	Waugh and Smith (1997)
Burrell, PA, USA	Temperate humid, woodland	Sycamore (<i>Platanus spp</i>)	9	90 cm	<5 cm vf 5.5%	60 cm Rock riprap / bedding	vc/c/m roots clogging drainage layer. Minimal vf rooting in top section or barrier.	Waugh and Smith (1997)

Table I-1 Review of Rooting Characteristics Found in Rock Riprap Covered Barriers for Waste Containment (continued)

Location	Climate zone	Species	Age of Cover (yrs)	Design thickness of barrier	Rooting depth, root class ^a , and % of barrier with roots	Depth and material above barrier	Rooting description	Reference
Burrell, PA, USA	Temperate, humid, woodland	Staghorn sumac (<i>Rhus typhina</i>)	9	90 cm	<5 cm vf 5.5%	60 cm Rock riprap / bedding	vc/c/m roots clogging drainage layer. Minimal vf rooting in top section or barrier.	Waugh and Smith (1997)
Burrell, PA, USA	Temperate, humid, woodland	Black locust (<i>Robinia pseudoacacia</i>)	9	90 cm	<5 cm vf 5.5%	60 cm Rock riprap / Bedding	vc/c/m roots clogging drainage layer. Minimal vf rooting in top section or barrier.	Waugh and Smith (1997)
Bluewater, NM, USA	Hot, semiarid, mixed grassland	Squirreltail grass (<i>Elymus elymoides</i>)	21	60 cm	>60 cm 3vf 100%	20 cm Rock riprap	3vf roots in bulk soil through depth of barrier. Root matting in fractures.	DOE (forthcoming)
Bluewater, NM, USA	Hot, semiarid, mixed grassland	Fourwing Saltbush (<i>Atriplex canescens</i>)	21	60 cm	>60 cm 3vf 100%	20 cm Rock riprap	c/m/f/vf roots to depth of 40 cm. m/f/vf roots along fractures through depth of barrier.	DOE (forthcoming)

Table I-2 Review of Rooting Characteristics Found in Vegetated Topsoil and Composite Barriers for Waste Containment

Location	Climate zone	Species	Age of Cover (yrs)	Design thickness of barrier	Rooting depth, root class ^a , and % of barrier with roots	Depth and material above barrier	Rooting description	Reference
Lakeview, OR, USA	Cool, semiarid, sagebrush steppe	Cheatgrass (<i>Bromus tectorum</i>)	2	80 cm	<5 cm f / vf 6.3%	45 cm Rock riprap / topsoil mix / gravel	<i>None given</i>	Burt and Cox (1993)
Lakeview, OR, USA	Cool, semiarid, sagebrush steppe	Big sagebrush (<i>Artemisia tridentata</i>)	2	80 cm	none 0%	45 cm Rock riprap / topsoil mix / gravel	Taproot stops at interface of radon barrier, tertiary roots spread laterally.	Burt and Cox (1993)
Lakeview, OR, USA	Cool, semiarid, sagebrush steppe	Tall wheatgrass (<i>Agropyron spp.</i>) Western wheatgrass (<i>Pascopyrum smithii</i>) Sheep fescue (<i>Festuca ovina</i>)	3	80 cm	<5 cm f / vf 6.3%	45 cm Rock riprap / topsoil mix / gravel	<i>None given</i>	Burt and Cox (1993)
Lakeview, OR, USA	Cool, semiarid, sagebrush steppe	Big sagebrush (<i>Artemisia tridentata</i>) Valley lupine (<i>Lupinus microcarpus</i>)	3	80 cm	5 cm f / vf 6.3%	45 cm Rock riprap / topsoil mix / gravel	Taproot stops at interface of radon barrier, tertiary roots spread laterally. Some in barrier.	Burt and Cox (1993)
Rum Jungle, NT, Australia	Humid, subtropical, woodland	<i>eucalyptus spp</i>	3	30 cm	15 cm m / f >30 cm f / vf 100%	45 cm Sandy clay loam / gravely sand	co/m roots travel horizontally along planes of weakness in compacted lift layers. f/vf roots travel vertically along fractures through the barrier and into wastes.	Ryan (1985); (1986)

Table I-2 Review of Rooting Characteristics Found in Vegetated Topsoil and Composite Barriers for Waste Containment (continued)

Location	Climate zone	Species	Age of Cover (yrs)	Design thickness of barrier	Rooting depth, root class ^a , and % of barrier with roots	Depth and material above barrier	Rooting description	Reference
Rum Jungle, NT, Australia	Humid, subtropical, woodland	<i>Acacia holosericea</i>	3	30 cm	5 cm m / f >30 cm f / vf 100%	45 cm Sandy clay loam / gravely sand	Majority of roots in unconsolidated soils above barrier. f/vf roots travel along fractures through clay barrier and into wastes.	Ryan (1985); (1986)
Albany, GA, USA	Warm, humid, mixed grassland	Mixed Bermuda and rye grasses	4	45 cm	45 cm vf 100%	15 cm Sandy clay loam	Well-formed blocky and laminar aggregates to 60 cm depth. Rooting around aggregate edges. Roots typically exist along fractures but occur in bulk soil, as well. Crack and rooting density decrease with depth.	Albright et al. (2006)
Hamburg, Germany	maritime temperate	Mixed pasture of: <i>Lotus corniculatus</i> , <i>Cirsium ssp.</i> , <i>Rumex ssp.</i> , <i>Armoracia rusticana</i>	8	60 cm	60 cm vf 100%	100 cm Topsoil / geotextile / sandy drainage layer	Plant roots have massively intruded and completely grown through the soil liner. Soil was hard, brittle, and very dry with 2mm wide cracks.	Melchior (1997)
Lakeview, OR, USA	Cool, semiarid, sagebrush steppe	Rubber rabbitbrush (<i>Ericameria nauseosa</i>)	8	45 cm	45cm vf, f 100%	45 cm Rock riprap / topsoil mix / gravel	Taproot stops at interface of radon barrier, tertiary roots spread laterally. f/vf roots travel vertically along fractures into barrier.	Waugh et al. (1997)

Table I-2 Review of Rooting Characteristics Found in Vegetated Topsoil and Composite Barriers for Waste Containment (continued)

Location	Climate zone	Species	Age of Cover (yrs)	Design thickness of barrier	Rooting depth, root class ^a , and % of barrier with roots	Depth and material above barrier	Rooting description	Reference
Lakeview, OR, USA	Cool, semiarid, sagebrush steppe	Big sagebrush (<i>Artemisia tridentata</i>)	8	45 cm	45cm vf, f 100%	45 cm Rock riprap / topsoil mix / gravel	Taproot stops at interface of radon barrier, tertiary roots spread laterally. f/vf roots travel vertically along fractures into barrier.	Waugh et al. (1997)
Lakeview, OR, USA	Cool, semiarid, sagebrush steppe	Antelope bitterbrush (<i>Purshia tridentata</i>)	8	45 cm	45cm vf, f 100%	45 cm Rock riprap / topsoil mix / gravel	Taproot stops at interface of radon barrier, tertiary roots spread laterally. f/vf roots travel vertically along fractures into barrier.	Waugh et al. (1997)
Hertfordshire, UK	Temperate maritime, woodland	Black alder (<i>Alnus glutinosa</i>)	10	100 cm	6 - 30 cm 30%	57 - 71 cm Overburden	Fine/medium. Along fractures.	Hutchings et al. (2001)
Hertfordshire, UK	Temperate maritime, woodland	Corsican pine (<i>Pinus nigra var. maritima</i>)	10	100 cm	1 - 2 cm 2%	55 - 70 cm Overburden	Fine. Minor intrusion along top barrier interface.	Hutchings et al. (2001)
Hertfordshire, UK	Temperate maritime, woodland	Sycamore maple (<i>Acer pseudoplatanus</i>)	10	100 cm	0 - 3 cm 3%	62 - 65 cm Overburden	Fine. Minor intrusion along top barrier interface.	Hutchings et al. (2001)
Hertfordshire, UK	Temperate maritime, woodland	Black alder (<i>Alnus glutinosa</i>)	15	100 cm	> 45 cm 45%	55 - 85 cm Overburden	<i>None given</i>	Hutchings et al. (2006)

Table I-2 Review of Rooting Characteristics Found in Vegetated Topsoil and Composite Barriers for Waste Containment (continued)

Location	Climate zone	Species	Age of Cover (yrs)	Design thickness of barrier	Rooting depth, root class ^a , and % of barrier with roots	Depth and material above barrier	Rooting description	Reference
Rum Jungle, NT, Australia	Humid, subtropical, woodland	mixed tussock grassland	18	30 cm	15 cm m / f >30 cm f / vf 100%	45 cm Sandy clay loam / gravely sand	Most f/vf roots located along the cracks between polygon faces of emergent soil structure. Some in bulk soil. Root density decreases with depth.	Taylor et al. (2003)
Rum Jungle, NT, Australia	Humid, subtropical, woodland	<i>Acacia auriculiformis</i>	18	30 cm	5 cm m >30 cm f / vf 100%	45 cm Sandy clay loam / gravely sand	Majority of roots in unconsolidated soils above barrier. f/vf roots travel along fractures through barrier and into wastes. Root density decreases with depth.	Taylor et al. (2003)
Rum Jungle, NT, Australia	Humid, subtropical, woodland	<i>eucalyptus ssp.</i>	18	30 cm	10 cm co / m >30 cm f / vf 100%	45 cm Sandy clay loam / gravely sand	Dense vc/co/m rooting in the unconsolidated soils above barrier. co/m roots in top section of barrier, f/vf roots travel along fractures through barrier and (≥ 5cm) into wastes. Root density decreases with depth.	Taylor et al. (2003)

Table I-2 Review of Rooting Characteristics Found in Vegetated Topsoil and Composite Barriers for Waste Containment (continued)

Location	Climate zone	Species	Age of Cover (yrs)	Design thickness of barrier	Rooting depth, root class ^a , and % of barrier with roots	Depth and material above barrier	Rooting description	Reference
Falls City, TX, USA	Humid	Yellow bluestem (<i>Bothriochloa ischaemum</i> var. <i>songarica</i>) Honey mesquite (<i>Prosopis glandulosa</i>)	22	65 cm	8 cm co / f 12.3%	100 cm Topsoil / clay overburden	co and f roots travel 8 cm into barrier	DOE (forthcoming)
Falls City, TX, USA	Humid	Yellow bluestem (<i>Bothriochloa ischaemum</i> var. <i>songarica</i>)	22	65 cm	65 cm vf 100%	100 cm Topsoil / clay overburden	vf roots travel through depth of barrier in the bulk soil fraction.	DOE (forthcoming)
Shirley Basin South, WY, USA	Frigid semiarid	Russian bunchgrass	16	85 cm	85 cm f 100%	85 cm Topsoil / sandy overburden	f roots travel through depth of barrier in the bulk soil fraction.	DOE (forthcoming)
Lakeview, OR, USA	Cool, semiarid, sagebrush steppe	Rubber rabbitbrush (<i>Ericameria nauseosa</i>) Western wheatgrass (<i>Pascopyrum smithii</i>) Sheep fescue (<i>Festuca ovina</i>)	29	45 cm	45 cm vf, f 100%	45 cm Rock riprap / topsoil mix / gravel	F and vf roots travel through depth of barrier along fractures.	DOE (forthcoming)
Lakeview, OR, USA	Cool, semiarid, sagebrush steppe	Antelope bitterbrush (<i>Purshia tridentata</i>) Western wheatgrass (<i>Pascopyrum smithii</i>) Sheep fescue (<i>Festuca ovina</i>)	29	45 cm	45cm vf, f 100%	45 cm Rock riprap / topsoil mix / gravel	F and vf roots travel through depth of barrier along fractures and in bulk soil.	DOE (forthcoming)

APPENDIX J

MORPHOLOGICAL DEVELOPMENT SCORING SYSTEM VALUES

J.1 Soil Morphology Scoring System

For each soil horizon, records were made for morphological properties, including profile thickness, horizon/material thickness, boundary, Munsell color system, pedality/structure (size, shape and grade, consistence), root morphology per unit area (abundance, diameter, class), the shape and size of void structures or animal excavations, rupture resistance, descriptions of inclusions, and other anomalous morphology in accordance with the U.S. Department of Agriculture (USDA) Natural Resource Conservation Service *Field Book for Describing and Sampling Soils*, version 3.0 (USDA 2012). Soil structure (Table J.1), soil grade (Table J.2), root size (Table J.3), root quantity (Table J.4), and rupture resistance (Table J.5) descriptions from USDA (2012) are provided to aid in figure and data interpretation. Soil moisture was determined gravimetrically (gravimetric water content percentage [GWC%]) by Stefani (2016) and Michaud (2018), and a model that relates GWC% to suction was used to group soils by water class state (USDA 2012) in the following classes: saturated (>30%), wet (20–30%), moist (10–20%), dry (7–10%), and very dry (<7%).

The detailed characterization of (visible) interpedal, intrapedal, transpedal macropore space (size, type, and quantity) was adapted from Lin et al. (1999a). Pore size was based on radius (for cylindrical pores) or width (for planar pores) in six classes: very fine (<0.5 mm), fine (0.5–1 mm), medium (1–2.5 mm), coarse (2.5–5 mm), very coarse (5–10 mm), and extremely coarse (>10 mm). Pore type corresponds to the general shape, continuity, and connectivity of pores across three classes: vughs (small spherical or elliptical cavities), channels (cylindrical and elongated), or planar fractures. Quantity of pores was visually recorded across the soil surface to charts of pore areal percentages as modified from USDA (2012) across five classes: very few (<0.25%), few (0.25–0.5%), common (0.5–2%), many (2–5%), and very many (>5%).

Table J-1 Soil Structure and Size Classifications

Size Class	Code	Criteria for Structural Unit Size (mm)		
		Granular (gr), platy (pl)	Columnar (cpr), prismatic (pr), wedge (wg)	Angular blocky (abk), subangular blocky (sbk), lenticular (lp)
Very fine	vf	<1	<10	<5
Fine	f	1 to <2	10 to <20	5 to <10
Medium	m	2 to <5	20 to <50	10 to <20
Coarse	co	5 to <10	50 to <100	20 to <50
Very coarse	vc	≥10	100 to <500	≥50
Extremely coarse	ec		≥500	

Table J-2 Soil Grade Classifications

Grade	Code	Criteria
Structureless	0	No discrete units observable in place or in hand samples
Weak	1	Units are barely observable in place or in a hand sample
Moderate	2	Units well-formed and evident in place or in a hand sample
Strong	3	Units are distinct in place (undisturbed soil) and separate cleanly when disturbed

Table J-3 Root Size

Size class	Code	Root Diameter	Soil Area Assessed
Very fine	vf	<1 mm	1 cm ²
Fine	f	1 to <2 mm	1 cm ²
Medium	m	2 to <5 mm	10 cm ²
Coarse	co	5 to <10 mm	10 cm ²
Very coarse	vc	≥10 mm	1 m ²

Table J-4 Root Quantity

Grade	Code	Criteria
Few	1	<1 per area of soil assessed 0.2 to <1 per area of soil assessed <0.2 per area of soil assessed
Common	2	1 to <5 per area of soil assessed
Many	3	≥5 per area of soil assessed

Table J-5 Rupture Resistance

Measured At Field Moist Soil Water State		Specimen Fails Under
Class	Code	
Very friable/friable	VFR/FR	Very slight to slight force with fingers, <20 N
Firm/very firm	FI/VFI	Moderate to strong force with fingers, 20–80 N
Extremely firm/slightly rigid	EF/SR	Hand or foot pressure with body weight, 80–800 N
Rigid/very rigid	R/VR	Blow by hammer, 800 N ≤ 3 J

Abbreviations: cm² = square centimeters, m² = square meters, N = newtons, J = joules

J.2 Soil Morphological Development Score (SMDS)

The point system developed by Lin et al. (1999a) was used to provide a quantitative measure of the morphological attributes in the radon barriers (e.g., moisture, texture, pedality, porosity, and rooting), referred to as the soil morphological development score (SMDS). Lin et al. (1999a) assumed a hypothetical structureless clay as the reference soil. This reference soil was assumed to contain no macropores or roots and to exist in a fully swollen and saturated state. The reference soil is comparable to the intended condition of a radon barrier where the compaction process has eliminated all structure in the soil. Lin et al (1999a) assigned points to each morphological feature based on the impact of that feature on hydraulic conductivity relative to the reference soil. Lin et al. (1999a) assigned the points using a “one-at-a-time” search method to obtain an optimal correlation with measured infiltration rates (Shoup 1982; McCuen and Snyder 1986). Points for morphological soil classes are in Table J.6.

Points were assigned using the definitions from Lin et al. (1999a) to each feature in each horizon that was apparent in the radon barrier and in the natural analogue. Horizons frequently corresponded to lift-and-compaction interfaces within the radon barrier. For pedality, macroporosity, and root density, which have multiple descriptors (e.g., ped grade, ped size, and ped shape), the score for the feature was computed as the product of the pertinent descriptors using Equations J.1, as described in Lin et al (1999a):

$$\text{Pedality} = (\text{ped grade}) \times (\text{ped size}) \times (\text{ped shape}) \quad (\text{J.1a})$$

$$\text{Macroporosity} = (\text{pore quantity}) \times (\text{pore size}) \times (\text{pore type}) \quad (\text{J.1b})$$

$$\text{Root density} = (\text{root quantity}) \times (\text{root size}) \quad (\text{J.1c})$$

The individual scores for the morphological feature were then summed to produce the SMDS for the horizon using Equation J.2:

$$\text{SMDS} = (\text{texture})+(\text{pedality})+(\text{macroporosity})+(\text{root density})+(\text{water content}) \quad (\text{J.2})$$

A total radon barrier SMDS (t SDMS) was calculated to evaluate how soil morphology has affected D_{Rn} by summing the SMDS for each horizon (Equations 7.1) based on their relative contribution of each horizon to the thickness of the radon barrier. A t SMDS was also calculated for the natural analogues, as constrained to the horizons at the same depth as the radon barrier. A partial SMDS (p SDMS) was calculated to evaluate how soil morphology has affected K_{sat} by constraining scoring to the depth and thickness of the block monolith sample.

Tables J.7–10 present categorized Soil Morphological Development Score values for each of the sites investigated in this study

Table J-6 Points for Soil Morphological Classes (Lin et al. 1999a)

Morphological Feature ^a	Descriptor	Class	Points
Texture	No additional descriptors	Clay	1
		Silty clay	2
		Sandy clay	3
		Silty clay loam	4
		Clay loam	5
		Sandy clay loam	6
		Loam	10
		Silt loam	13
		Sandy loam	15
		Silt	19
		Loamy sand	24
Sand	27		
Pedality	Ped grade	Massive	0
		Weak	1
		Moderate	5
		Strong	25
		Single grain	50
	Ped size	Very coarse	1
		Coarse / medium	3
		Fine / very fine	18
	Ped shape	Massive	0
		Platy	1
		Prismatic	10
		Blocky	10
		Granular / single grain	30
Macroporosity ^b	Quantity	Very few	1
		Few	3
		Common	10
		Many	28
		Very many	60
	Size	Very fine	1
		Fine	9
		Medium	49
		Coarse	60
		Very coarse	70
		Extremely coarse	75
	Type	Vugh	1
		Channel	8
Fracture		10	
Packing void		25	
Root Density	Quantity	Few / very few	1
		Common	16
		Many	25
	Root size	Very coarse	1
		Coarse / medium	13
		Fine / very fine	43
Water Content ^a	No additional descriptors	Saturated	1
		Wet	3
		Moist	7
		Dry	30
		Very dry	65

^a Soil morphology described using standard soil survey procedures (USDA 2012).

^b Method for pore size and shape characterization described in Lin et al (1999a)

^c Gravimetric water content was related to saturation by water class state in USDA (2012): saturated (>30%), wet (20–30%), moist (10–20%), dry (7–10%), very dry (<7%).

Table J- 7 Falls City, Texas Morphological Development Scoring System Values

Profile ID	Barrier Horizon	Horizon Thickness (cm)	Grav. Water GWC %	Texture	Pedality			Macroporosity			Root Density		SMDS	Profile SMDS
					Grade	Size	Shape	Quantity	Size	Type	Quantity	Size		
1	Rn 1.a	8	32% 1	SiC	w	f	b	vf	f	f	vf vf vf	co f vf	462	135
				2	1	18	10	1	18	10	1 1 1	13 43 43		
	Rn 1.b	54	36% 1	SiC	w	m	b	vf	vf	f	vf	vf	86	
				2	1	3	10	1	1	10	1	43		
2	Rn 1.a	10	38% 1	SiC	m	f	b	vf	vf	f	vf	vf	956	253
				2	5	18	10	1	1	10	1	43		
	Rn 1.b	42	38% 1	SiC	w	m	b	vf	vf	f	vf	vf	86	
				2	1	3	10	1	1	10	1	43		
4	Rn 1.a	22	32% 1	SiC	m	f	b	f	f	f	vf	vf	1485	847
				2	5	18	10	3	18	10	1	43		
	Rn 1.b	23	32% 1	SiCL	w	f	b	vf	vf	f	vf	vf	238	
				4	1	18	10	1	1	10	1	43		
5	Rn 1.a	6	37% 1	SiCL	-	n/a	-	n/a	n/a	n/a	n/a	n/a	5	5
				4	0	0	0	0	0	0	0	0		
	Rn 2.b	31	39% 1	SiCL	-	n/a	-	n/a	n/a	n/a	n/a	n/a	5	
				4	0	0	0	0	0	0	0	0		
6	Rn 1.a	19	44% 1	SiCL	-	n/a	-	vf	vf	f	vf f/c	f vf	402	198
				4	0	0	0	1	1	10	1 8	43 43		
	Rn 1.b	10	42% 1	SiCL	-	n/a	-	n/a	n/a	n/a	f	vf	48	
				4	0	0	0	0	0	0	1	43		
	Rn 1.c	16	40% 1	SiCL	-	n/a	-	n/a	n/a	n/a	f	vf	48	
				4	0	0	0	0	0	0	1	43		
AN-1	A	28	21% 3	SiC	m	f	b	f f	f vf	f v	f f c m m	vc co m f vf	3551	2940
				2	5	18	10	3 3	9 1	10 1	1 1 16 25 25	1 13 13 43 43		
	Btk1	33	30% 1	SiC	m	f	b	f f	f vf	f v	f c m m	co m f vf	3547	
				2	5	18	10	3 3	9 1	10 1	1 16 25 25	13 13 43 43		
	Btk2	29	30% 1	C	w	vc	b	vf vf	vf vf	f v	f f m m	co m f vf	2279	
				1	1	1	10	1 1	1 1	10 1	1 1 25 25	13 13 43 43		
	Btk3	36	34% 1	C	w	vc	b	vf vf	vf vf	f v	f c m	m f vf	1879	
				1	1	1	10	1 1	1 1	10 1	1 16 25	13 43 43		
	2Btk/Cr	26	38% 1	C	m	f	b	f	f	f	f c m	m f vf	2948	
				1	5	18	10	3	9	10	1 16 25	13 43 43		

9-1

Falls City, Texas

Table J-8 Bluewater, New Mexico Morphological Development Scoring System Values

Profile ID	Barrier Horizon	Horizon Thickness (cm)	Grav. Water GWC %	Pedality				Macroporosity			Root Density		SMDS	Profile SMDS
				Texture	Grade	Size	Shape	Quantity	Size	Type	Quantity	Size		
1	Rn 1	20	11% 7	SCL 6	w 1	m 3	pl 1	vf 1	vf 1	v 1	vf 1	vf 43	60	31
	Rn 2	14	12% 7	SCL 6	n/a 0	n/a 0	n/a 0	n/a 0	n/a 0	n/a 0	n/a 0	n/a 0	13	
	Rn 3	33	11% 7	SL 15	n/a 0	n/a 0	n/a 0	n/a 0	n/a 0	n/a 0	n/a 0	n/a 0	22	
2.A (1.0 m)	Rn 1	15	8% 30	SL 15	s 25	f 18	b 10	f 3	f 9	f 10	c 16	vf 43	5503	1158
	Rn 2	23	11% 7	SCL 6	m 5	m 3	b 10	c 10	vf 1	f 10	f 1	vf 43	306	
	Rn 3	21	14% 7	C 1	w 1	m 3	b 10	f 3	vf 1	f 10	f 1	vf 43	111	
2.B (0.0 m)	Rn 1	11	4% 65	SL 15	s 25	vf 18	b 10	c f 10 3	f vf 9 1	f v 10 1	c m 16 25	f vf 43 43	7246	2516
	Rn 2	23	9% 30	SCL 6	m 5	f 18	b 10	c 10	vf 1	f 10	m 25	vf 43	2111	
	Rn 3	36	20% 3	C 1	m 5	m 3	b 10	c 10	vf 1	f 10	m 25	vf 43	1332	
3	Rn 1.a	12	7% 30	SL 15	m 5	f 18	b 10	f 3	vf 1	v 1	f c 1 16	f vf 43 43	1679	551
	Rn 1.b	8	9% 30	SCL 6	m 5	f 18	b 10	n/a 0	n/a 0	n/a 0	vf 1	vf 43	979	
	Rn 1.c	18	8% 30	SCL 6	w 1	co 3	b 10	n/a 0	n/a 0	n/a 0	n/a 0	n/a 0	66	
	Rn 2	16	9% 30	SCL 6	n/a 0	n/a 0	n/a 0	n/a 0	n/a 0	n/a 0	n/a 0	n/a 0	36	
4	Rn 1.a	7	5% 65	SL 15	m 5	f 18	b 10	f 3	vf 1	v 1	vf 1	vf 43	1026	134
	Rn 1.b	12	9% 30	SL 15	w 1	vc 1	b 10	f 3	vf 1	v 1	vf 1	vf 43	101	
	Rn 2	22	11% 7	SCL 6	w 1	vc 1	b 10	n/a 0	n/a 0	n/a 0	n/a 0	n/a 0	23	
	Rn 3	28	11% 7	SCL 6	n/a 0	n/a 0	n/a 0	n/a 0	n/a 0	n/a 0	n/a 0	n/a 0	13	

Table J-8 Bluewater, New Mexico Morphological Development Scoring System Values (continued)

Profile ID	Barrier Horizon	Horizon Thickness (cm)	Grav. Water GWC %	Pedality				Macroporosity			Root Density		SMDS	Profile SMDS	
				Texture	Grade	Size	Shape	Quantity	Size	Type	Quantity	Size			
5.A (0.0 m)	Rn 1	25	6% 65	SCL	s	m	b	m c	f vf	f v	c m m m	co m f vf	6034	2861	
				6	25	3	10	28 10	9 1	10 1	16 25 25 25	13 13 43 43			
				SL	w	co	b	c vf	vf vf	f v	c f f f	co m f vf			
	Rn 2.a	15	6% 65	15	1	3	10	10 1	1 1	10 1	16 1 1 1	13 13 43 43	518		
				SL	w	vc	b	vf	vf	f	n/a	n/a			
	Rn 2.b	16	5% 65	15	1	1	10	1	1	10	0	0	100		
				SL	w	vc	b	vf	vf	f	n/a	n/a			
	5.B (1.5 m)	Rn 1	15	5% 65	SCL	s	m	b	m c	f vf	f v	c c c	m f vf		4935
					6	25	3	10	28 10	9 1	10 1	16 16 16	13 43 43		
Rn 2.a		23	8% 30	SCL	w	co	b	c vf	vf vf	f v	f f f	m f vf	266		
				6	1	3	10	10 1	1 1	10 1	1 1 1	13 43 43			
Rn 2.b		21	7% 30	SCL	w	vc	b	c	vf	f	n/a	n/a	146		
				6	1	1	10	10	1	10	0	0			
MP2 ^a	Rn 1.a	20	5% 65	SCL	s	vf	b	vm f	f vf	f v	c f	f vf	10705		
				6	25	18	10	60 3	9 1	10 1	16 1	43 43			
	Rn 1.b	19	6% 65	SCL	s	vf	b	vm f	f vf	f v	c f	f vf	10705		
Rn 2.a	29	6% 65	L	s	vf	b	vm f	f vf	f v	c	vf	10676			
7	Rn 1.a	24	5% 65	SCL	m	m	b	f f	f vf	f v	c c c c	co m f vf	2286		
				6	5	3	10	3 3	9 1	10 1	16 16 16 16	13 13 43 43			
	Rn 1.b	12	5% 65	SCL	w	co	b	n/a	n/a	n/a	f f c c	co m f vf	1503		
				6	1	3	10	0	0	0	1 1 16 16	13 13 43 43			
	Rn 2	37	6% 65	SCL	w	co	b	n/a	n/a	n/a	f f f f	co m f vf	213		
				6	1	3	10	0	0	0	1 1 1 1	13 13 43 43			
	Rn 3	36	8% 30	SCL	w	vc	b	n/a	n/a	n/a	n/a	n/a	n/a	46	
				6	1	1	10	0	0	0	0	0			
	Rn 4	33	9% 30	SCL	w	vc	b	n/a	n/a	n/a	n/a	n/a	n/a	46	
				6	1	1	10	0	0	0	0	0			
Rn 5	34	9% 30	SCL	n/a	n/a	n/a	n/a	n/a	n/a	n/a	n/a	n/a	36		
			6	0	0	0	0	0	0	0	0				
Rn 6	36	11% 7	SCL	n/a	n/a	n/a	n/a	n/a	n/a	n/a	n/a	n/a	13		
			6	0	0	0	0	0	0	0	0				
Rn 7	23	13% 7	SCL	n/a	n/a	n/a	n/a	n/a	n/a	n/a	n/a	n/a	13		
			6	0	0	0	0	0	0	0	0				

^a MP-2 is an ant mound profile. Given destructive nature of sampling, we could not conduct morphology of TP-6 and take K_{sat} and radon flux measurements

Table J-8 Bluewater, New Mexico Morphological Development Scoring System Values (continued)

Profile ID	Barrier Horizon	Horizon Thickness (cm)	Grav. Water GWC %	Pedality				Macroporosity			Root Density		SMDS	Profile SMDS	
				Texture	Grade	Size	Shape	Quantity	Size	Type	Quantity	Size			
Bluewater, New Mexico	8	Rn 1	22	8% 30	SCL 6	s 5	f 18	b 10	vf vf 1 1	vf vf 1 1	f v 10 1	f 1	vf 43	990	487
		Rn 2	21	9% 30	SCL 6	m 5	f 18	b 10	vf 1	vf 1	f 10	f 1	vf 43	989	
		Rn 3	37	9% 30	SCL 6	m 5	vc 1	b 10	n/a 0	n/a 0	n/a 0	n/a 0	n/a 0	86	
		Rn 4	16	13% 7	SCL 6	n/a 0	n/a 0	n/a 0	n/a 0	n/a 0	n/a 0	n/a 0	n/a 0	63	
	AN-3	Bt 1	21	6% 65	SCL 6	s 25	vf 18	b 10	m c m 28 10 28	f f f 9 9 9	f c v 10 8 1	f f m m 1 1 25 25	co m f vf 13 13 43 43	10239	5205
		Bt 2	29	6% 65	SCL 6	s 25	f 18	b 10	c c c 10 10 10	f f f 9 9 9	f c v 10 8 1	f f m m 1 1 25 25	co m f vf 13 13 43 43	8457	
		Btk	39	7% 30	SCL 6	m 5	m 3	b 10	c c c 10 10 10	f f f 9 9 9	f c v 10 8 1	f f c m 1 1 16 25	co m f vf 13 13 43 43	3685	
		Btm	12	9% 30	SCL 6	w 1	m 3	b 10	vf 1	vf 1	f 10	f c c 1 16 16	m f vf 13 43 43	1465	
		CB	33	9% 30	CL 5	s 25	f 18	b 10	c f 10 3	f vf 9 1	f v 10 1	f c 1 16	f vf 43 43	6169	
		2 Btk	36	9% 30	SCL 6	s 25	f 18	b 10	c f 10 3	f vf 9 1	f v 10 1	c 16	vf 43	6127	
	AN-6	B	32	NM 65	C 1	s 25	vf 18	b 10	vm f m 60 3 28	f f f 9 9 9	f c v 10 8 1	f f c m 1 1 16 25	co m f vf 13 13 43 43	12223	7439
		Bk	26	NM 65	CL 5	s 25	vf 18	b 10	vm f 60 3	f vf 9 1	f v 10 1	f f m 1 1 25	m f vf 13 43 43	11104	
CBk		34	NM 30	CL 5	n/a 0	n/a 0	n/a 0	n/a 0	n/a 0	n/a 0	f f f 1 1 1	m f vf 13 43 43	134		

Table J-9 Shirley Basin South, Wyoming Morphological Development Scoring System Values

Profile ID	Barrier Horizon	Horizon Thickness (cm)	Grav. Water GWC %	Pedality				Macroporosity			Root Density		SMDS	Profile SMDS		
				Texture	Grade	Size	Shape	Quantity	Size	Type	Quantity	Size				
Shirley Basin South, WY	DC-2	Rn 1	12	21% 3	SC 3	n/a 0	n/a 0	n/a 0	n/a 0	n/a 0	n/a 0	c 16	vf 43	694	202	
		Rn 2	16	24% 3	C 1	n/a 0	n/a 0	n/a 0	n/a 0	n/a 0	n/a 0	vf 16	vf 43	47		
		Rn 3	12	26% 3	C 1	n/a 0	n/a 0	n/a 0	n/a 0	n/a 0	n/a 0	1 1	vf 43	47		
		Rn 4	8	28% 3	C 1	n/a 0	n/a 0	n/a 0	n/a 0	n/a 0	n/a 0	n/a 0	n/a 0	4		
	DC-3	Rn 1.a	6	25% 3	C 1	n/a 0	n/a 0	n/a 0	vf 1	vf 1	f 10	vvf 0.5	vf 43	36	7	
					C 1	n/a 0	n/a 0	n/a 0	n/a 0	n/a 0	n/a 0	n/a 0	n/a 0	4		
		Rn 2	13	31% 1	C 1	n/a 0	n/a 0	n/a 0	n/a 0	n/a 0	n/a 0	n/a 0	n/a 0	2		
					C 1	n/a 0	n/a 0	n/a 0	n/a 0	n/a 0	n/a 0	n/a 0	n/a 0	4		
		Rn 4	16	28% 3	C 1	n/a 0	n/a 0	n/a 0	n/a 0	n/a 0	n/a 0	n/a 0	n/a 0	n/a 0		4
					C 1	n/a 0	n/a 0	n/a 0	n/a 0	n/a 0	n/a 0	n/a 0	n/a 0	n/a 0		4
	Rn 5	6	29% 3	C 1	n/a 0	n/a 0	n/a 0	n/a 0	n/a 0	n/a 0	n/a 0	n/a 0	n/a 0	4		
	DC-4	Rn 1	16	30% 1	C 1	n/a 0	n/a 0	n/a 0	n/a 0	n/a 0	n/a 0	c 16	vf 43	690	156	
		Rn 2	16	26% 3	C 1	n/a 0	n/a 0	n/a 0	n/a 0	n/a 0	n/a 0	vf 1	vf 43	47		
					C 1	n/a 0	n/a 0	n/a 0	n/a 0	n/a 0	vf 1	vf 43	47			
		Rn 4	15	24% 3	C 1	n/a 0	n/a 0	n/a 0	n/a 0	n/a 0	n/a 0	vvf 0.5	vf 43	26		
					C 1	n/a 0	n/a 0	n/a 0	n/a 0	n/a 0	vvf 0.5	vf 43	26			
Rn 6		7	23% 3	C 1	n/a 0	n/a 0	n/a 0	n/a 0	n/a 0	n/a 0	vvf 0.5	vf 43	26			

6-f

Table J-9 Shirley Basin South, Wyoming Morphological Development Scoring System Values (continued)

	Profile ID	Barrier Horizon	Horizon Thickness (cm)	Grav. Water GWC %	Texture	Pedality			Macroporosity			Root Density		SMDS	Profile SMDS
						Grade	Size	Shape	Quantity	Size	Type	Quantity	Size		
Shirley Basin South, WY	DC-5	Rn 1	19	32% 1	C 1	n/a 0	n/a 0	n/a 0	n/a 0	n/a 0	n/a 0	vvf 0.5	vf 43	24	24
		Rn 2	12	31% 1	C 1	n/a 0	n/a 0	n/a 0	n/a 0	n/a 0	n/a 0	vvf 0.5	vf 43	24	
		Rn 3	22	32% 1	C 1	n/a 0	n/a 0	n/a 0	n/a 0	n/a 0	n/a 0	vvf 0.5	vf 43	24	
	DC-6	Rn 1	18	28% 3	C 1	n/a 0	n/a 0	n/a 0	n/a 0	n/a 0	n/a 0	vvf 0.5	vf 43	26	26
		Rn 2	19	26% 3	C 1	n/a 0	n/a 0	n/a 0	n/a 0	n/a 0	n/a 0	vvf 0.5	vf 43	26	
		Rn 3	20	26% 3	C 1	n/a 0	n/a 0	n/a 0	n/a 0	n/a 0	n/a 0	vvf 0.5	vf 43	26	
	AN-4	Btk 2	15	NM 3	C 1	w 1	vc 1	b 10	vf 1	vf 1	f 10	c m 16 25	f vf 43 43	1787	703
		Bx 1	14	NM 3	C 1	n/a 0	n/a 0	n/a 0	vf 1	vf 1	f 10	c 16	vf 43	702	
		Bx 2	47	NM 3	C 1	n/a 0	n/a 0	n/a 0	vf 1	vf 1	f 10	f/c 8	vf 43	358	

Table J-10 Lakeview, Oregon Morphological Development Scoring System Values

Profile ID	Barrier Horizon	Horizon Thickness (cm)	Grav. Water GWC %	Pedality				Macroporosity			Root Density		SMDS	Profile SMDS	
				Texture	Grade	Size	Shape	Quantity	Size	Type	Quantity	Size			
Lakeview, OR	DC-2 under	Rn 1	10	32% 1	L 10	m 5	m 3	b 10	f f 3 3	vf vf 1 1	f v 10 1	f m m m 1 25 25 25	co m f vf 13 13 43 43	2682	2350
		Rn 2	9	31% 1	SL 15	m 5	m 3	b 10	f f 3 3	vf vf 1 1	f v 10 1	f m m m 1 25 25 25	co m f vf 13 13 43 43	2687	
		Rn 3	7	27% 3	L 10	w 1	co 3	b 10	vf 1	vf 1	f 10	f c m 1 16 25	m f vf 13 43 43	1829	
		Rn 4	7	28% 3	SL 15	m 5	m 3	b 10	f 3	vf 1	f 10	c m 16 25	f vf 43 43	1961	
	DC-2 (1.0 m)	Rn 1	11	NM 3	L 10	w 1	co 3	b 10	f f 3 3	vf vf 1 1	f v 10 1	vf f f c 1 1 1 16	co m f vf 13 13 43 43	833	615
		Rn 2	9	NM 3	SL 15	m 5	f 3	b 10	f f 3 3	vf vf 1 1	f v 10 1	f f c 1 1 16	m f vf 13 43 43	945	
		Rn 3	8	NM 3	L 10	w 1	co 3	b 10	n/a 0	n/a 0	n/a 0	n/a 0	n/a 0	43	
		Rn 4	14	NM 3	L 10	m 5	m 3	b 10	n/a 0	n/a 0	n/a 0	n/a 0	n/a 0	163	
	DC-2 (2.5 m)	Rn 1	11	NM 3	L 10	w 1	m 3	b 10	f f 3 3	vf vf 1 1	f v 10 1	f f c 1 1 16	m f vf 13 43 43	833	522
		Rn 2	9	NM 3	SL 15	w 1	m 3	b 10	f f 3 3	vf vf 1 1	f v 10 1	f f c 1 1 16	m f vf 13 43 43	825	
		Rn 3	8	NM 3	L 10	n/a 0	n/a 0	n/a 0	n/a 0	n/a 0	n/a 0	vf 1	vf 43	56	
		Rn 4	14	NM 3	L 10	n/a 0	n/a 0	n/a 0	n/a 0	n/a 0	n/a 0	n/a 0	n/a 0	13	
DC-4 (bare)	Rn 1	37	51% 1	Si 19	n/a 0	n/a 0	n/a 0	n/a 0	n/a 0	n/a 0	n/a 0	n/a 0	20	20	
DC-4 (grass)	Rn 1	10	37% 1	Si 19	n/a 0	n/a 0	n/a 0	n/a 0	n/a 0	n/a 0	f/c 8	vf 43	364	111	
	Rn 2	28	45% 1	Si 19	n/a 0	n/a 0	n/a 0	n/a 0	n/a 0	n/a 0	n/a 0	n/a 0	20		

Table J-10 Lakeview, Oregon Morphological Development Scoring System Values (continued)

Profile ID	Barrier Horizon	Horizon Thickness (cm)	Grav. Water GWC %	Texture	Pedality			Macroporosity			Root Density		SMDS	Profile SMDS	
					Grade	Size	Shape	Quantity	Size	Type	Quantity	Size			
Lakeview, OR	DC-5	Rn 1	10	29%	Si	m	co	b	c	f	f	c	vf	960	444
				3	19	5	3	10	10	1	10	16	43		
		Rn 2	10	30%	Si	m	co	b	c	9	f	c	vf	960	
				3	19	5	3	10	10	1	10	16	43		
	Rn 3	13	28%	L	w	m	b	vf	vf	f	vf	vf	96		
	Rn 4	15	28%	L	n/a	n/a	n/a	n/a	n/a	n/a	vf	vf	56		
				3	10	0	0	0	0	0	0	1	43		
	DC-10	Rn 1	10	32%	Si	m	m	b	c	vf	f	f m	f vf	1388	1086
				1	19	5	3	10	10	1	10	1 25	43 43		
		Rn 2	10	46%	Si	m	co	b	c	vf	f	f m	f vf	1388	
				1	19	5	3	10	10	1	10	1 25	43 43		
	Rn 3	8	39%	L	w	vc	b	n/a	n/a	n/a	c	vf	709		
	Rn 4	8	30%	L	w	vc	b	n/a	n/a	n/a	c	vf	709		
				1	10	1	1	10	0	0	0	16	43		
				1	10	1	1	10	0	0	0	16	43		
	DC-11 (0.0 m)	Rn 1	16	29%	Si	m	m	b	f	f	f	f c c m	co m f vf	2186	2090
3				19	5	3	10	3	1	10	1 16 16 25	13 13 43 43			
Rn 2		11	17%	Si	m	m	b	f	vf	f	f c c m	co m f vf	2190		
			7	19	5	3	10	3	1	10	1 16 16 25	13 13 43 43			
Rn 3	10	27%	L	m	m	b	vf	vf	f	c m	f vf	1936			
Rn 4	7	30%	L	m	m	b	n/a	n/a	n/a	c m	f vf	1926			
			3	10	5	3	10	0	0	0	16 25	43 43			
DC-12 (0.0 m)	Rn 1	11	35%	Si	s	m	b	vf	vf	f	f c	f vf	1511	560	
			1	19	25	3	10	1	1	10	1 16	43 43			
	Rn 2	11	31%	Si	m	m	b	vf	vf	f	f c	f vf	911		
			1	19	5	3	10	1	1	10	1 16	43 43			
Rn 3	12	30%	L	m	co	b	vf	vf	f	n/a	n/a	171			
Rn 4	19	37%	L	w	co	b	vf	vf	f	n/a	n/a	51			
			1	10	1	3	10	1	1	10	0	0			

Table J-10 Lakeview, Oregon Morphological Development Scoring System Values (continued)

Profile ID	Horizon	Horizon Thickness (cm)	Grav. Water GWC %	Texture	Pedality			Macroporosity			Root Density		SMDS	Profile SMDS	
					Grade	Size	Shape	Quantity	Size	Type	Quantity	Size			
Lakeview, OR	DC-12 (1.0 m)	Rn 1	11	NM 1	Si 19	m 5	m 3	b 10	vf 1	vf 1	f 10	c 16	vf 43	868	253
		Rn 2	11	NM 1	Si 19	m 5	m 3	b 10	vf 1	vf 1	f 10	vf 1	vf 43	223	
		Rn 3	12	NM 1	L 10	w 1	co 3	b 10	vf 1	vf 1	f 10	n/a 0	n/a 0	51	
		Rn 4	19	NM 1	L 10	w 1	co 3	b 10	n/a 0	n/a 0	n/a 0	n/a 0	n/a 0	41	
	DC-13	Rn 1	11	24% 3	L 10	m 5	m 3	b 10	f 3	f 9	f 10	vf c 1 16	f vf 43 43	1207	372
		Rn 2	11	25% 3	L 10	m 5	co 3	b 10	f 3	vf 1	f 10	vf c 1 16	f vf 43 43	924	
		Rn 3	6	28% 3	Si 19	w 1	co 3	b 10	vf 1	vf 1	f 10	vf 1	vf 1	105	
		Rn 4	4	25% 3	Si 19	w 1	co 3	b 10	vf 1	vf 1	f 10	n/a 0	n/a 0	62	
		Rn 5	34	42% 1	Si 19	n/a 0	n/a 0	n/a 0	n/a 0	n/a 0	n/a 0	n/a 0	n/a 0	20	
	AN-2	Bt.1	34	NM 3	Si 19	s 25	f 18	b 10	c c c 10 10 10	f f f 9 9 9	f c v 10 8 1	c m m m 16 25 25 25	co m f vf 13 13 43 43	8915	5366
		Bt.2	28	NM 3	Si 19	m 5	m 3	b 10	f f 3 3	vf vf 1 1	c v 8 1	f c m m 1 16 25 25	co m f vf 13 13 43 43	2570	
		B/Cr	15	NM 3	L 10	m 5	m 3	b 10	vf vf 1 1	vf vf 1 1	c v 8 1	f c m m 1 16 25 25	co m f vf 13 13 43 43	2543	

BIBLIOGRAPHIC DATA SHEET

(See instructions on the reverse)

NUREG/CR-7288
Volume 2

2. TITLE AND SUBTITLE

Evaluation of In-Service Radon Barriers over Uranium Mill Tailings
Disposal Facilities , Appendices

3. DATE REPORT PUBLISHED

MONTH

YEAR

March

2022

4. FIN OR GRANT NUMBER

5. AUTHOR(S)

M. Williams, M. Fuhrmann, N. Stefani, A. Michaud, W. Likos, C. Benson,
W. Waugh

6. TYPE OF REPORT

Technical

7. PERIOD COVERED (Inclusive Dates)

2019-2021

8. PERFORMING ORGANIZATION - NAME AND ADDRESS (If NRC, provide Division, Office or Region, U. S. Nuclear Regulatory Commission, and mailing address; if contractor, provide name and mailing address.)

Geological Engineering, University of Wisconsin-Madison, 1415 Engineering Drive, Madison, WI 53706 USA

9. SPONSORING ORGANIZATION - NAME AND ADDRESS (If NRC, type "Same as above", if contractor, provide NRC Division, Office or Region, U. S. Nuclear Regulatory Commission, and mailing address.)

Division of Risk Analysis, Office of Nuclear Regulatory Research, U. S. Nuclear Regulatory Commission

10. SUPPLEMENTARY NOTES

11. ABSTRACT (200 words or less)

Earthen final covers over uranium mill tailings and associated wastes were investigated at four sites that had been in service for approximately 20 years: Falls City in Texas, Bluewater in New Mexico, Shirley Basin South in Wyoming, and Lakeview in Oregon. Test pits were excavated, radon fluxes were measured, soil morphological observations made, and samples were collected to determine saturated hydraulic conductivity, soil water characteristic curves, Pb-210 concentrations, and related properties. Saturated hydraulic conductivity of the Rn barriers at three of the four sites typically fell within values of 1.0×10^{-7} to 5.0×10^{-6} m/s, regardless of depth or thickness of the cover or radon barrier. One Rn barrier was an exception, with some hydraulic conductivities as low as 10^{-11} m/s. A slight increase over as-built Rn flux was evident for some of the barriers, but site-wide flux comparisons to as-built values are inappropriate because of different sampling and analytical methods used between current and site closure surveys. These higher fluxes are attributed to soil structure induced by root activity and insect burrowing in the Rn barrier, as well as higher Rn diffusion coefficients associated with lower water saturation in areas influenced by root water uptake. A method to use Pb-210 concentration profiles to quantify long-term (decades) Rn-222 fluxes was developed.

12. KEY WORDS/DESCRIPTORS (List words or phrases that will assist researchers in locating the report.)

UMTRCA, radon barriers, hydraulic conductivity, radon flux, Rn diffusion coefficient,
soil morphology, uranium mill tailings, mill tailings covers, Pb-210, Rn-222

13. AVAILABILITY STATEMENT

unlimited

14. SECURITY CLASSIFICATION

(This Page)

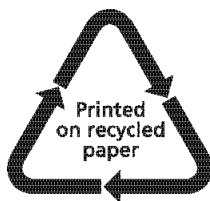
unclassified

(This Report)

unclassified

15. NUMBER OF PAGES

16. PRICE



Federal Recycling Program



UNITED STATES
NUCLEAR REGULATORY COMMISSION
WASHINGTON, DC 20555-0001

OFFICIAL BUSINESS



@NRCgov

**NUREG/CR-7288
Volume 2**

Evaluation of In-Service Radon Barriers over Uranium Mill Tailings Disposal Facilities

March 2022